

The Effect of Work Related Mechanical Stress on the Peripheral Temperature of the Hand

Ricardo Ângelo Rosa Vardasca

A submission presented in partial fulfilment of the requirements of the University of Glamorgan/Prifysgol Morgannwg for the degree of Doctor of Philosophy



Medical Imaging Research Unit
Department of Computing and Mathematical Sciences
Faculty of Advanced Technology
University of Glamorgan/Prifysgol Morgannwg
Wales, United Kingdom

July 2010

Directors of study:

Dr. Peter Plassmann

Supervisors:

Dr. Carl D. Jones

Prof. E. Francis J. Ring

Certificate of Research

This is to certify that, except where specific reference is made, the work presented in this thesis is the result of investigation undertaken by the candidate.

Candidate.....
(Ricardo Vardasca)

Director of Studies
(Dr. Peter Plassmann)

Declaration

This is to certify that neither this thesis or any part of it has been presented or is being currently submitted in candidature for any other degree other than the degree of Doctor of Philosophy of the University of Glamorgan.

Candidate

(Ricardo Vardasca)

Dedicated to

*My family: Parents MARIA and ÂNGELO, brothers TIAGO and TOMÉ,
and grandmothers MARIA and EULÁLIA.*

The memory of my grandfathers MARTIM and PEDRO.

Acknowledgements

Foremost I would like to thank my director of studies, Dr. Peter Plassmann, for his supervision, motivation and helpful guidance throughout the duration of this research project. I profoundly acknowledge his patience, careful oversight, concern and understanding for inspiring me to the focus of this work and accomplishment of this thesis.

I would like to express my gratitude to my second supervisors, Dr. Carl Jones and Prof. Francis Ring, whose constant discussion, medical guidance, incessant advising, continuous motivation and constructive criticism has helped to increase the quality of this work.

I want to praise Mr. Usama Bajwa and my brother Mr. Tomé Vardasca for the collaborative work that had a relevant contribution to improve this project.

Furthermore I would like to thank Prof. Kurt Ammer for his interesting discussions, advice and medical guidance that were of significant importance for the execution of this work. I want also to thank Prof. Michael Griffin, from the Institute of Sound and Vibration Research unit at University of Southampton, for his advice in terms of the development of vibration provocation tests. I want also to express my gratitude to the Swansea Metropolitan University for the opportunity of measuring the amount of vibration from the device used in the tests and for providing me with the opportunity to perform the provocation tests using a high resolution cooled infrared camera essential for comparison of results using different recording devices.

Gratitude to all the volunteers that helped me in this work, providing me their availability, interest and precious time, without whose it would have been impossible to accomplish this project.

Thanks are due to the Faculty of Advanced Technology at University of Glamorgan for funding this project, providing me with financial support and allowing me to learn and explore new knowledge.

My gratitude to Dr. Rafael Caldeirinha for his motivation, without him I would never have gone to the University of Glamorgan. He was the first to believe in my capabilities and also the person who suggested to attend this university after completing my studies in Portugal within the framework of the Erasmus exchange agreement he had established.

Finally I want to express a special thank to my family for their encouragement, moral and financial support and apologise to them for my long absence during the time of completing this work.

Abstract

The evolution and developments in modern industry have resulted a wide range of occupational activities, some of which can lead to industrial injuries. Due to the activities of occupational medicine, much progress has been made in transforming the way that operatives perform their tasks. However there are still many occupations where manual tasks have become more repetitive, contributing to the development of conditions that affect the upper limbs. Repetitive Strain Injury is one classification of those conditions which is related to overuse of repetitive movement. Hand Arm Vibration Syndrome is a subtype of this classification directly related to the operation of instruments and machinery which involves vibration.

These conditions affect a large number of individuals, and are costly in terms of work absence, loss of income and compensation. While such conditions can be difficult to avoid, they can be monitored and controlled, with prevention usually the least expensive solution. In medico-legal situations it may be difficult to determine the location or the degree of injury, and therefore determining the relevant compensation due is complicated by the absence of objective and quantifiable methods.

This research is an investigation into the development of an objective, quantitative and reproducible diagnostic procedure for work related upper limb disorders. A set of objective mechanical provocation tests for the hands have been developed that are associated with vascular challenge. Infrared thermal imaging was used to monitor the temperature changes using a well defined capture protocol. Normal reference values have been measured and a computational tool used to facilitate the process and standardise image processing.

These objective tests have demonstrated good discrimination between groups of healthy controls and subjects with work related injuries but not individuals, $p < 0.05$, and are reproducible. A maximum value for thermal symmetry of $0.5 \pm 0.3^\circ\text{C}$ for the whole upper limbs has been established for use as a reference.

The tests can be used to monitor occupations at risk, aiming to reduce the impact of these conditions, reducing work related injury costs, and providing early detection. In a medico-legal setting this can also provide important objective information in proof of injury and ultimately in objectively establishing whether or not there is a case for compensation.

Resumo

A evolução e desenvolvimentos na indústria moderna resultaram numa extensiva gama de actividades profissionais, algumas das quais podem conduzir a doenças ocupacionais. Devido a actividades da medicina profissional, muito progresso foi feito transformando a forma como os operadores executam as suas tarefas. No entanto ainda há muitas ocupações onde tarefas manuais se tornaram mais repetitivas, contribuindo para o desenvolvimento de condições que afectam os membros superiores. *Repetitive Strain Injury* é uma das classificações destas condições e está relacionada com o sobreuso de movimentos repetitivos. *Hand Arm Vibration Syndrome* é um subtipo desta classificação directamente relacionada com a operação de instrumentos e maquinaria que envolve vibração.

Estas condições afectam um número grande de indivíduos, e são dispendiosas em termos de dias de ausência de trabalho, perda de rendimento e compensações. Enquanto tais condições podem ser difíceis de evitar, elas podem ser monitorizadas e controladas, sendo a prevenção a solução menos cara. Em situações médico-legais pode ser difícil determinar o grau de doença, e consequentemente a determinação da correspondente compensação devido à ausência de métodos objectivos e quantitativos.

Esta pesquisa é uma investigação no desenvolvimento de um procedimento diagnóstico objectivo, quantitativo e reproduzível para as doenças ocupacionais que afectam os membros superiores. Um conjunto de testes objectivos de provocação das mãos foi desenvolvido e é associado a um desafio vascular. A técnica de imagens térmicas de infravermelhos foi utilizada para monitorizar o processo que usa um protocolo de captura bem definido. Valores de referência foram medidos e uma ferramenta computacional foi utilizada para facilitar o processo de uniformizar o processamento de imagem.

Estes testes objectivos demonstraram boa discriminação entre grupos de controlo suadáveis e grupos de sujeitos com lesões ocupacionais mas não entre indivíduos, $p < 0.05$, e são reproduzíveis. Um valor máximo de simetria térmica de $0.5 \pm 0.3^\circ\text{C}$ foi estabelecido como referência para todos os membros superiores.

Estes testes podem ser usados para monitorizar ocupações de risco, reduzindo o impacto destas condições, levando a uma redução dos custos relacionados com doenças ocupacionais, e fornecendo a sua descoberta precoce. Numa situação médico-legal isto pode fornecer também informação objectiva importante como prova de lesão e por fim verificar a necessidade de haver compensação.

Table of Contents

1 – Introduction.....	1
1.1. Background.....	1
1.2. Prevalence	2
1.3. Legal considerations.....	4
1.4. The case for early detection.....	5
1.5. Current diagnostic approach.....	5
1.6. Research to date	6
1.7. Aim.....	7
1.8. Objectives.....	7
1.9. Proposed methodology.....	8
1.10. Contribution to knowledge.....	9
1.11. Structure of the thesis.....	10
2 – Literature Review.....	12
2.1. Hands.....	12
2.1.1. Anatomy.....	12
2.1.2. Physiology.....	25
2.2. Mechanical Stress.....	33
2.3. Hand-Arm Syndrome.....	34
2.3.1. – Repetitive Strain Injury (RSI).....	35
2.3.2. – Hand-Arm Vibration Syndrome (HAVS).....	43
2.4. RSI related questionnaires.....	54
2.5. Thermography.....	54
2.5.1. Physical principles.....	55
2.5.2. Infrared cameras.....	59
2.5.3. Thermography in medicine.....	65
2.5.4. Importance of standardisation.....	66
2.5.5. Proposed standard medical thermographic protocols.....	67
2.5.6. Quality assurance in a thermal imaging system.....	68
2.5.7. Software for medical thermography.....	69
2.5.8. Non-invasive alternatives for medical thermography.....	70
2.6. Thermal physiology reference data.....	72
2.7. Hand vascular test.....	75
2.8. Image processing.....	79
2.8.1. Introduction.....	79
2.8.2. Image enhancing techniques.....	82
2.8.3. Features extraction.....	83
2.8.4. Template matching.....	86
2.8.5. Interpolation techniques.....	87
2.8.6. Feature based registration.....	87
2.8.7. Conclusion.....	94
3 – Methodology.....	95
3.1. Image capture protocol.....	95
3.2. Online RSI Questionnaire.....	99
3.3. Image analysis experiments.....	100
3.3.1 Experiment 1: Suitability of body views.....	101
3.3.2 Experiment 2: Suitability of standardised body views	106
3.4. Statistical Methods.....	109

3.5. Pilot stress tests.....	111
3.5.1. Keyboard provocation test, KPT.....	111
3.5.2. Vibration provocation test, VPT.....	121
3.6. Objective provocation tests.....	130
3.6.1. Keyboard provocation test, KPT.....	134
3.6.2. Vibration provocation test, VPT.....	137
3.6.3. Mouse provocation test, MPT.....	138
3.6.4. Cold stress test, CST.....	141
3.6.5. Inter-camera assessment test.....	144
3.7. Image processing developments.....	144
3.7.1. Image enhancement.....	145
3.7.2. Edge detection.....	146
3.7.3. Interpolation methods.....	149
3.7.4. Barycentric warp model.....	151
3.8. Summary.....	156
4 – Experimental Results.....	158
4.1. Online RSI Questionnaire.....	158
4.2. Reference data	164
4.3. Objective provocation tests.....	166
4.3.1. Keyboard provocation test.....	167
4.3.2. Vibration provocation test.....	173
4.3.3. Mouse provocation test.....	178
4.3.4. Cold Stress Test.....	183
4.3.5. Cold stress test evaluation methods comparison	187
4.3.6. Inter-camera assessment test.....	194
4.4. Image processing developments.....	194
4.4.1. Image enhancement.....	194
4.4.2. Edge detection.....	199
4.4.3. Interpolation methods.....	204
4.4.4. Barycentric warp model.....	206
4.5. Summary.....	208
5 – Discussion.....	210
5.1 - Capture protocol.....	210
5.2 - Incidence of occupational conditions in a sample population.....	211
5.3 - Medical reference data.....	212
5.4 - Image processing developments.....	213
5.4.1 - Image enhancement.....	214
5.4.2 - Edge detection.....	214
5.4.3 - Interpolation methods.....	215
5.4.4 - Barycentric warp model.....	216
5.5 - Objective provocation tests.....	216
6 – Conclusion.....	219
6.1. Meeting the aim.....	219
6.2. Proposed future work	220
References.....	221
Webliography.....	233
Appendices.....	235

List of Figures

Fig. 1: Hand Arm Syndrome diagram with its main proponents.....	1
Fig. 2: Investigation plan for the characterisation of hand injuries in a sample population.....	8
Fig. 3: Phase diagram for the development of a Hand-Arm Syndrome diagnosis procedure with different stages of investigation on the right.....	9
Fig. 4: Diagram of thesis structure.....	11
Fig. 5: Definition of hand anatomical terms.....	12
Fig. 6: Bones of the hand (right hand in dorsal view), Webliography[1].....	13
Fig. 7: Bone joints of the hand (right hand in dorsal view), Webliography[2].....	14
Fig. 8: Extrinsic muscles of the hand (right hand palmar view), Webliography[3].....	15
Fig. 9: Intrinsic muscles of the hand (on left: right hand in dorsal view, on right: left hand in palmar view), Webliography[4].....	16
Fig. 10: Ligaments of the hand (left hand in dorsal view), Webliography[5].....	18
Fig. 11: Roots of the nerves of the hand on the spine, Webliography[6].....	19
Fig. 12: Regions of each nerve of the hand (right hand on both palmar and dorsal views), Webliography[7].....	19
Fig. 13: Dermatomes of the hand, Webliography[21].....	21
Fig. 14: Arteries of the hand (right hand palmar view and right hand dorsal view), Webliography[8].	22
.....	22
Fig. 15: Veins of the hand (right dorsal hand), Webliography[9].....	22
Fig. 16: Sub-layers of the epidermis (Palm of the hand), Webliography[10].....	24
Fig. 17: Skin structure and layers, Webliography[11].....	25
Fig. 18: Sensors of the hand skin, Webliography[12].....	27
Fig. 19: Microcirculation diagram, Webliography[13].....	28
Fig. 20: Human body thermoregulation diagram according to Houdas and Ring.....	29
Fig. 21: Mechanisms of heat loss, Webliography[14].....	31
Fig. 22: Hand Arm Syndrome hierarchy.....	35
Fig. 23: Components of a vibration wave, (South, 2004).....	47
Fig. 24: HAVS partial exposure calculation chart (South, 2004).....	49
Fig. 25: Griffin's method of scoring areas of the fingers affected by blanching, (Mansfield, 2005). 51	51
Fig. 26: The electromagnetic spectrum, Webliography[15].....	55
Fig. 27: Herschel's apparatus on discovering infrared radiation, Webliography[16].....	56
Fig. 28: Planck's radiation law, Webliography[17].....	57
Fig. 29: Wien's displacement law, Webliography [18].....	57
Fig. 30: Stefan-Boltzmann function, Webliography[19].....	58
Fig. 31: Stefan-Boltzmann equation, Webliography[20].....	58
Fig. 32: Mean Thermal Areas (MTA) method to assess hands cold stress test recovery.....	76
Fig. 33: The thermal gradient index scale for grading the severity of Raynaud's phenomenon (Ring, 1995).....	77
Fig. 34: One approach to quantification - estimating mean temperature difference between fingers to dorsal hand F-D (Ring, 1995).....	77
Fig. 35: Mean Thermal Gradient (MTG) method to assess hands cold stress test recovery.....	78
Fig. 36: Mean Thermal Profile (MTP) method to assess hands cold stress test recovery.....	78
Fig. 37: Steps involved in digital imaging processing, Webliography[21].....	80
Fig. 38: Point correspondence between source and destination triangles using barycentric coordinates.....	93
Fig. 39: Example of a live overlay mask.....	98
Fig. 40: FLIR A40 IR camera on laboratory stand.....	98

Fig. 41: Architecture of the online questionnaire application for data collection and analysis.....	100
Fig. 42: Statistics editor of CThERM software package to analyse AOIs.....	102
Fig. 43: Both Hands Dorsal regional view, AOI evaluating hand thermal symmetry (a threshold value was used to ignore background temperature).....	102
Fig. 44: Left Arm Anterior regional view, AOI evaluating arm and forearm thermal symmetry.....	102
Fig. 45: Right Arm Anterior regional view, AOI evaluating arm and forearm thermal symmetry.....	103
Fig. 46: Right Arm Dorsal regional view, AOI evaluating arm and forearm thermal symmetry.....	103
Fig. 47: Left Arm Dorsal regional view, AOI evaluating arm and forearm thermal symmetry.....	103
Fig. 48: Total Body Anterior view, AOI evaluating limbs thermal symmetry, not suitable for hands and feet.....	103
Fig. 49: Total Body Dorsal view, AOI evaluating limbs thermal symmetry, not suitable for hands and feet.....	104
Fig. 50: Both Hands Anterior regional view, AOI evaluating wrist thermal symmetry.....	104
Fig. 51: Left Arm Anterior regional view, AOI evaluating elbow thermal symmetry.....	104
Fig. 52: Right Arm Anterior regional view, AOI evaluating elbow thermal symmetry.....	104
Fig. 53: Right Arm Dorsal regional view, AOI evaluating elbow thermal symmetry.....	105
Fig. 54: Left Arm Dorsal regional view, AOI evaluating elbow thermal symmetry.....	105
Fig. 55: Chest Anterior regional view, AOI (red and blue) evaluating shoulder thermal symmetry.....	105
Fig. 56: Upper Back regional view, AOI evaluating shoulder thermal symmetry.....	105
Fig. 57: A standard mask defined by (red) anatomical control points overlaid onto a thermal image on an elbow.....	106
Fig. 58: Mask control points manually adjusted to fit the thermal image outline.....	107
Fig. 59: The captured elbow shape produced in the step shown in fig. 57 (left) is now warped into the standard mask shape.....	107
Fig. 60: Reference AOI model defined by anatomical markers and the AOI formed by triangles (17 AOIs for each hand).....	108
Fig. 61: Reference AOI model for the left arm in anterior view and the right arm in dorsal view (2 AOIs formed by triangles).....	108
Fig. 62: Reference AOI model for the right arm in anterior view and the left arm in dorsal view (2 AOIs formed by triangles).....	108
Fig. 63: One hand typing the other one still.....	112
Fig. 64: Perpendicular position of the camera.....	112
Fig. 65: The pilot Keyboard Provocation Test diagram.....	113
Fig. 66: Areas of Interest for keyboard pilot test.....	114
Fig. 67: Thermograms from a capture sequence of a keyboard stress investigation.....	115
Fig. 68: Average mean temperatures over time on exercising the right hand, keeping the left hand still.....	116
Fig. 69: Average mean temperatures over time on exercising the left hand, keeping the right hand still.....	116
Fig. 70: Hand Thermal Symmetry (Right hand typing and left hand still).....	117
Fig. 71: Hand Thermal Symmetry (Left hand typing and right hand still).....	117
Fig. 72: Hand Thermal Symmetry (Right AOI – Left AOI) characterisation of hand AOI when stressing right hand.....	119
Fig. 73: Hand Thermal Symmetry (Left AOI – Right AOI) characterisation of hand AOI when stressing left hand.....	119
Fig. 74: Forearm Thermal Symmetry (Right AOI – Left AOI) characterisation of forearm AOI when stressing right hand.....	120
Fig. 75: Forearm Thermal Symmetry (Left AOI – Right AOI) characterisation of forearm AOI when stressing left hand.....	120

Fig. 76: The vibration test equipment: on top the vertical vibration motor, underneath the frequency counter, frequency generator and at the bottom the audio amplifier.....	122
Fig. 77: A volunteer holding the vibrating device with the fingertips of one hand, position used for the pilot test (holding the device with just one hand) - rejected.....	123
Fig. 78: Hands positioned at 90° angle to the camera.....	123
Fig. 79: The laser vibrometer measuring the vibration magnitude from the vibration device, the posture for the real objective test (holding the device with all fingertips).....	123
Fig. 80: Laser vibrometer output, the laser measures the acceleration of the vibrating device in several points.....	124
Fig. 81: Vibration magnitude exposure calculation chart, the red line shows the correspondence between weighted acceleration (36 m/s ²) and 'daily' partial vibration (2.5 m/s ²) exposure and exposure time (2 minutes).....	124
Fig. 82: The pilot Vibration Provocation Test diagram.....	125
Fig. 83: Average mean temperature on exposing the right hand to vibration keeping left still, just hands were exposed.....	126
Fig. 84: Average mean temperature on exposing the left hand to vibration keeping right still, just hands were exposed.....	126
Fig. 85: Mean temperature difference from baseline, right hand vibrating and left hand still, just hands were exposed.....	126
Fig. 86: Mean temperature difference after left hand vibrating and right hand still, just hands were exposed.....	127
Fig. 87: Hand Thermal Symmetry (Right AOI – Left AOI) characterisation of hand AOI when stressing right hand with vibration.....	128
Fig. 88: Hand Thermal Symmetry (Right AOI – left AOI) characterisation of hand AOI when stressing left hand with vibration.....	128
Fig. 89: Forearm Thermal Symmetry (Right AOI – Left AOI) characterisation of forearm AOI when stressing right hand with vibration.....	129
Fig. 90: Thermal Symmetry (Right AOI – left AOI) characterisation of forearm AOI when stressing left hand with vibration.....	129
Fig. 91: The virtual keyboard application.....	135
Fig. 92: Pseudocode of the virtual keyboard application.....	136
Fig. 93: The Keyboard Provocation Test diagram.....	136
Fig. 94: The Vibration Provocation Test diagram.....	137
Fig. 95: The Mouse Provocation Test application.....	139
Fig. 96: The mouse provocation application algorithm pseudocode.....	140
Fig. 97: Digram of the Mouse Provocation Test.....	140
Fig. 98: The Cold Stress Test diagram.....	142
Fig. 99: Flowchart of the application to evaluate the three assessment methods of CST.....	143
Fig. 100: The scenario of the medical thermal images noise improvement experiment.....	146
Fig. 101: The scenario of the medical thermal images boundaries detection experiment.....	149
Fig. 102: C# application for Testing image interpolation methods.....	150
Fig. 103: The interpolation comparison methods in medical thermal images scenario.....	151
Fig. 104: Geometrical 'anatomical regions' based model of the hand.....	152
Fig 105: Adjustable control points overlaying the thermal image of the hands.....	154
Fig. 106: Barycentric coordinates correspondence system with Cartesian coordinates.....	154
Fig. 107: Pseudo-code of the triangular barycentric warping method.....	155
Fig. 108: Triangular barycentric warping method flowchart.....	156
Fig. 109: Gender distribution of the questionnaire respondents.....	158
Fig. 110: Overall respondents per hand occupational condition pathological state.....	159
Fig. 111: The gender distribution of the respondents per hand occupational condition pathological	

state.....	160
Fig. 112: The gender distribution of the questionnaire respondents that indicated 'severe symptoms' of hand occupational conditions.....	160
Fig. 113: The age group distribution of the questionnaire respondents per gender that indicated 'severe symptoms' of hand occupational conditions.....	161
Fig. 114: The BMI distribution of the questionnaire respondents per gender that indicated 'severe symptoms' of hand occupational conditions.....	161
Fig. 115: The characterisation by occupation of the respondents per gender that indicated 'severe symptoms' of hand occupational conditions.....	162
Fig. 116: The characterisation of smoking habits of the respondents per gender that indicated 'severe symptoms' of hand occupational conditions.....	162
Fig. 117: The computer keyboard weekly exposure time of the respondents per gender that indicated 'severe symptoms' of hand occupational conditions.....	163
Fig. 118: The computer mouse weekly exposure time of the respondents per gender that indicated 'severe symptoms' of hand occupational conditions.....	163
Fig. 119: Right hand mean temperature difference from baseline when recovering from KPT.....	169
Fig. 120: Left hand mean temperature difference from baseline when recovering from KPT.....	169
Fig. 121: Hand thermal symmetry difference from baseline when recovering from KPT.....	170
Fig. 122: Hand DIPs thermal symmetry difference when recovering from KPT.....	171
Fig. 123: An example comparative set of standardised images between a control subject and a clinically confirmed subject with RSI.....	172
Fig. 124: Right hand mean temperature difference from baseline when recovering from VPT.....	174
Fig. 125: Left hand mean temperature difference when recovering from VPT.....	174
Fig. 126: Hand thermal symmetry difference from baseline when recovering from VPT.....	175
Fig. 127: Hand DIPs thermal symmetry difference when recovering from VPT.....	176
Fig. 128: An example comparative set of standardised images between a control subject and a clinically confirmed subject with HAVS.....	176
Fig. 129: Right hand mean temperature difference from baseline when recovering from MPT.....	179
Fig. 130: Left hand mean temperature difference from baseline when recovering from MPT.....	180
Fig. 131: Hand thermal symmetry difference from baseline when recovering from MPT.....	181
Fig. 132: Hand DIPs thermal symmetry difference when recovering from MPT.....	181
Fig. 133: Right hand mean temperature difference from baseline when recovering from CST.....	184
Fig. 134: Left hand mean temperature difference from baseline when recovering from CST.....	184
Fig. 135: Hand thermal symmetry difference from baseline when recovering from CST.....	185
Fig. 136: Hand DIPs thermal symmetry difference when recovering from CST.....	185
Fig. 137: Screen shot of the application to evaluate the different methods of assessing a CST.....	187
Fig. 138: Chart representation of the calculated thermal indexes of the 3 assessment methods.....	188
Fig. 139: Table with the calculated thermal indexes of the 3 assessment methods.....	188
Fig. 140: Thermal indexes per method after KPT.....	189
Fig. 141: Thermal indexes per method after VPT.....	190
Fig. 142: Thermal indexes per method after MPT.....	191
Fig. 143: Thermal indexes per method after CST.....	192
Fig. 144: Example of resulting images from application of the image enhancing filters.....	195
Fig. 145: The average values of mean temperature comparing the results obtained from each algorithm with the original image.....	196
Fig. 146: Temperature differences in average values from the resulting images from filter applications to the original image in terms of maximum, minimum and mean temperatures and standard deviation.....	196
Fig. 147: Signal to Noise Ratio comparison between the noise filtered images and the original.....	197
Fig. 148: Root Mean Square Error comparison between the noise filtered images and the original.....	

.....	198
Fig. 149: Cross Correlation Coefficient comparison between the noise filtered images and the original.....	198
Fig. 150: Original captured image in grayscale.....	199
Fig. 151: Optimal outline drawn by hand.....	200
Fig. 152: Edge detection without noise pre-processing.....	201
Fig. 153: Edge detection with noise pre-processing.....	202
Fig. 154: Difference between optimum edge length and algorithmically produced edges with and without noise pre-processing.....	203
Fig. 155: Original image loaded from database.....	204
Fig. 156: resultant image from application of Nearest Neighborhood interpolation technique.....	204
Fig. 157: resultant image from application of the Bilinear interpolation method.....	204
Fig. 158: resultant image from application of the bi-cubic interpolation technique.....	205
Fig. 159: Difference in mean temperature between the original and the result of interpolation methods, shows that the less affected algorithm is the Nearest Neighbourhood.....	205
Fig. 160: Difference in standard deviation between the original and the result of interpolation methods, shows that the interpolation algorithm that less affects the standard deviation is the bi-cubic.....	206
Fig. 161: Resultant image of barycentric triangulation warping.....	207
Fig. 162: Comparison between non-standardised and standardised thermal images of the hands.....	207

List of Tables

Table 1: Degrees of injury in RSI (Peddie and Rosenberg, 1997).....	40
Table 2: The continuum of RSI (Helliwell and Taylor, 2004).....	40
Table 3: Taylor-Palmear scale (Gemne et al., 1987).....	50
Table 4: Vascular stages of the Stockholm Workshop scale for HAVS.....	50
Table 5: Sensory-neural stages of the Stockholm Workshop scale for HAVS.....	51
Table 6: Reference values of bilateral thermal symmetry of AOI using thermal imaging (from previous studies).....	75
Table 7: Reported problems from the individuals of the symptoms and the confirmed groups.....	132
Table 8: Volunteers participating in the four Provocation Test (KPT=Keyboard, VPT=Vibration, MPT=Mouse, CST=Cold Stress Test), the '----' represent the volunteers that have not performed the test.....	133
Table 9: Operational characteristics of three infrared imager systems.....	144
Table 10: Size (in pixels) of the AOIs of the hand model.....	152
Table 11: Thermal asymmetry values (mean temperature absolute differences and standard deviations) for upper limbs and joints in regional and total body views for dorsal and anterior perspectives using the first analytical approach.....	164
Table 12: Thermal asymmetry values obtained using the second analytical approach.....	165
Table 13: Statistical analysis of the AOIs used in the first approach of obtaining thermal symmetry values.....	165
Table 14: Statistical analysis results of the AOIs used in the second thermal symmetry method. ...	166
Table 15: HAS stage groups mean temperatures over the KPT.....	167
Table 16: KPT volunteers characterisation in speed typing and miss-typing.....	168
Table 17: Z-test values comparing groups results for hand AOI in the KPT (HS-Highly significant, S-Significant, NS-Non Significant).	172
Table 18: Z-test values comparing groups results for hand AOI thermal symmetry in the KPT (HS-Highly significant, S-Significant, NS-Non Significant).....	173
Table 19: HAS stage groups mean temperatures over the VPT.....	173
Table 20: Z-test values comparing groups results for hand AOI in the VPT(HS-Highly significant, S-Significant, NS-Non Significant)	177
Table 21: Z-test values comparing groups results for hand AOI thermal symmetry in the VPT (HS-Highly significant, S-Significant, NS-Non Significant).....	177
Table 22: MPT volunteers characterisation in number of mouse clicks and pixels traversed.....	178
Table 23: HAS stage groups mean temperatures over the MPT.....	179
Table 24: Z-test values comparing groups results for hand AOI in the MPT test (HS-Highly significant, S-Significant, NS-Non Significant).....	182
Table 25: Z-test values comparing groups results for hand AOI thermal symmetry in the MPT (HS-Highly significant, S-Significant, NS-Non Significant).....	183
Table 26: HAS stage groups mean temperatures over the CST.....	183
Table 27: Z-test values comparing groups results for hand AOI in the CST (HS-Highly significant, S-Significant, NS-Non Significant).....	186
Table 28: Z-test values comparing groups results for hand AOI thermal symmetry in the CST (HS-Highly significant, S-Significant, NS-Non Significant).....	187
Table 29: Z-test results from relationship between groups after KPT vascular assessment (HS-Highly significant, S-Significant, NS-Non Significant).....	190
Table 30: Z-test results from relationship between groups after VPT vascular assessment (HS-Highly significant, S-Significant, NS-Non Significant).....	191

Table 31: Z-test results from relationship between groups after VPT vascular assessment, (HS-Highly significant, S-Significant, NS-Non Significant).....	192
Table 32: Z-test results from relationship between groups after CST(HS-Highly significant, S-Significant, NS-Non Significant)	193
Table 33: Identified cases of hypothermia per method and provocation test.....	193
Table 34: Classification of the performance of the image enhancer filters, the recommended methods are in green and the non recommended in red.	199
Table 35: Comparison of the number of outline pixels, in the closeness to optimal only the images pre-processed with noise removal were considered.....	203
Table 36: The Interclass correlation statistics of the hand AOI before and after standardisation....	208

Glossary

AC – Alternating Current
AOI – Areas of Interest
ACTH – Corticotropin
BMI - Body Mass Index
C – Celsius
CCC – Cross-Correlation Coefficient
CNS – Central Nervous System
CRH – Corticotropin-releasing Hormone
CST – Hands Cold Stress Test
CSV – Comma Separated Values
CTHERM - University of Glamorgan Medical Thermal Imaging Software Package
DC – Direct Current
DIP – Distal Inter Phalanx
DSS – Department of Social Security
EMG - Electromyography
EU – European Union
FPA – Focal Plane Array
GB – Great Britain
Ge – Germanium
HAS – Hand Arm Syndrome
HAVS – Hand Arm Vibration Syndrome
HPA – Hypothalamic-pituitary-adrenal
HSE – Health & Safety Executive
IFOV – Instantaneous Field of View
IIAC – Industrial Injuries Advisory Council
IIS – Industrial Injuries Scheme
InSb – Indium Antimonide
KPT – Keyboard Provocation Test
MCT – Mercury Cadmium Telluride
MDF – Medium Density Fibreboard
MIP – Middle Intra Phalanx

MPT – Mouse Provocation Test
MRC – Medical Research Council
MRI – Magnetic Resonance Imaging
MRTD - Minimum Resolvable Temperature Difference
MTA – Mean Thermal Area
MTG – Mean Thermal Gradient
MTP – Mean Thermal Profile
NETD - Noise Equivalent Temperature Difference
PD – Prescribed Disease
PIP – Proximal Intra Phalanx
PNS – Peripheral Nervous System
PPG – Photoplethysmography
PtSi – Platinum Silicide
QWIP – Quantum Well Infrared Photodetectors
RMSE – Root Mean Square Error
RP – Raynaud's Phenomenon
RSI – Repetitive Strain Injury
RSIA – Repetitive Strain Injury Association
SAS – Sympathoadrenal system
Si – Silicon
SNR – Signal to Noise Ratio
SNS – Sympathetic Nervous System
SRF – Slit Response Function
TA – Thermal Aesthesiometry
TUC – Trade Union Congress
UK – United Kingdom
ULD – Upper Limb Disorder
US - United States
VPT – Vibration Provocation Test
VTT – Vibration Threshold Test
VWF – Vibration White Finger
WRULD – Work Related Upper Limb Disorders

1 – Introduction

In this section an informative overview of the research topic is presented outlining its practical and theoretical value. In addition this section presents the importance, the previous approaches to the problem and the motivation to perform the current work. It introduces the aims and objectives of this work and outlines the contribution to knowledge it claims to make. This chapter ends with information about the organisation of the thesis.

1.1. Background

The evolution and changes of modern places of work add new activities to those classically associated with repetitive and strain causing manual tasks. Computer mouse users, workers using pneumatic hammers, machine operators, typists and many others are at risk of developing one of the two main forms of so called Hand Arm Syndrome (HAS). HAS is not a disease in itself but a summative term describing a variety of clinical phenomena related to upper limb disorders. The two main proponents of the syndrome are Hand Arm Vibration Syndrome (HAVS) and Repetitive Strain Injury (RSI) (Fig. 1) - both work related upper limb occupational disorders caused by over use of tools, instruments or machinery. Within the scope of the this work, RSI is defined as an occupational syndrome caused by repetitive tasks and affecting the upper limbs. HAVS is an occupational condition that affects upper limbs and results from overuse of vibrating tools. Methods for assessing symptoms of HAS are needed for the prevention of further injuries, avoiding work absence and minimising health related costs and legal consequences.

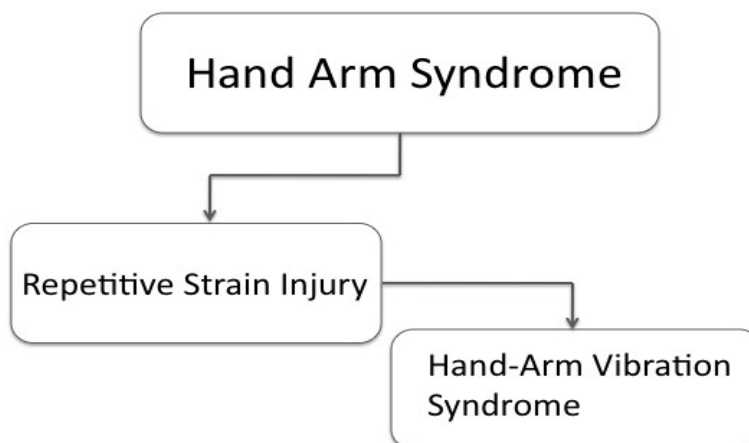


Fig. 1: Hand Arm Syndrome diagram with its main proponents.

Work Related Upper Limb Disorders (WRULD) are damages to body structures such as bones, muscles, joints, tendons, ligaments, nerves and the local blood circulation system that are consequences of work and its environment. The risk factors of this type of conditions are the work environment (e.g. poor workplace layout, excessive heat or cold and high levels of noise), individual factors (e.g. physical capability, lack of experience and life habits) and organisational and psychological factors (e.g. monotony, time pressure, lack of control over tasks performed and limited social interaction). The symptoms of WRULD may take a long period of time to develop and normally manifest as pain, discomfort, numbness and tingling sensations. In more severe cases, affected subjects may also experience swelling of the joints, decreased grip strength and a change in skin colour of the hands and fingers. There are European Union (EU) legislation directives that regulate the work environment in order to prevent this condition, although due to negligence or ignorance they are not always applied (EASHW, 2007).

The European Agency for Safety and Health at Work reported that about two thirds of EU workers are exposed to repetitive arm and hand movements and a quarter to vibrating tools (EFLWC, 2005). This is a significant amount and in a wide range of jobs the development of WRULDs is almost inevitable and consequently now the most common form of occupational disease in the EU with about 45% having the highest incidence of all occupational diseases (Eurostat, 2004).

The condition causes personal suffering, loss of income and cost to business and national economies. A total cost of WRULD in the EU between 0.5% and 2% of gross national product was estimated (EASHW, 1999).

1.2. Prevalence

The first known recognition of pain and disability related to repetitive movement was made in 1713 by the Italian physician Bernardo Ramazzini, who observed that clerks suffered from a condition caused by an incessant movement of the hands and arms always in the same direction. The first recognition in the United Kingdom was made in 1908 with the “telegraphist's cramp” (Sleator et al., 1998). The first reporting of a condition caused by use of vibration tools was in 1911 by Loriga, who identified vascular spasms in Italian miners who operated pneumatic tools (Loriga, 1911).

As in the EU, musculoskeletal disorders are the most common occupational disease in UK.

A survey on self-reported work related diseases in 2004/05 (Jones et al., 2006) showed that an estimated 375,000 people (about 0.87% of the population) in Great Britain (GB) suffered from WRULD caused or made worse by the workplace, this value coincides with those quoted by previous similar studies at 2001/02 and 2003/04. From this value of incidence, an estimated 25% (0.29% of whole GB population) of sufferers had become aware of their condition in the past 12 months. The same report (Jones, 2006) showed an estimate of 4.7 million working days (full day equivalents) were lost through this category of conditions caused or made worse by work activities. This equates to an annual loss of 0.20 day per worker every year (Sleator et al., 1998).

In 1995/96 a Health & Safety Executive (HSE) survey estimated that 506,000 people in the UK were affected by WRULD. The prevalence was around 30% higher in women than in men, increasing with age. 38% of the respondents attributed their conditions to repetitive tasks, 37% to manual handling, 23% to work posture and 10% to physical work. The same study estimated that 36,000 men in the UK suffered from HAVS. From those affected by HAVS, two thirds reported difficulties in picking up small objects and all reported use of hand held power tools as the cause of their condition (Sleator et al., 1998).

A 1999 research report by the HSE found that the prevalence of self-reported symptoms of musculoskeletal disorders in the upper limbs was 17% in general industries (Buckle and Devereux, 1999). According to the Trade Union Congress 'Safety Report Survey' of 2003 the percentage of employers in Wales concerned about upper limb disorders in the workplace was 38% (RSIA, 2007).

A paper in 1994 (Bird and Nicholson, 1994) stated that WRULDs were estimated to cost British industry £1 billion per year. Five years later another paper (David, 1999) suggested that WRULDs are the leading cause of work absence and job resignation with approximate costs of £1.25 billion per year. Every day in the UK, 6 people leave their jobs in consequence of a RSI condition. The costs to UK industry are likely to be between £5 and £20 billion annually. One larger employer found that the average cost of retiring an employee on medical grounds due to RSI was £40,000 (RSIA, 2007).

A HSE study in 1986 found that around 19,000 British workers were at risk of HAVS, and for 10,000 of these the risk was high (Kyriakides, 1988). 1,400 new cases were assessed by the Department of Social Security (DSS) in 1993/94 but only 1,100 received a benefit payment in April 1994 (HSE, 1995). It was thought that there were around 12,000 British sufferers of HAVS who were in employment at the time (Hodgson et al., 1993). Sufferers will often make a claim for compensation from their employers, and settlements are generally around £2,000, although sums in excess of £50,000 were paid out (HSE, 1995). The survey findings suggested that 20% of HAVS

sufferers took sick leave an annual average of 12 days each because of their condition (Hodgson et al., 1993).

In the United States (US) almost one third of all acute injuries involve upper extremities. According to a 1995 “National Health Interview Survey” it is estimated that each year 18 million causes of WRULD occur and cause a visit to a physician. Acute WRULD is responsible for about 32 million days of restricted activity and almost 10 million days of work absence in a year. The same statistics indicate that about 615,000 hospitalisations occur as a consequence of those conditions and of these 587,000 result in surgical procedures. In 1995 the estimated cost of WRULDs per year in the US was estimated to be around \$19 billion. The same study has shown that workers' compensation from these injuries increased linearly from 1980's (Kelsey, 1997). A paper in 2003 (Peper, 2003) estimated that in the US RSI injuries contribute to about 26% of all workplace injuries, the same document estimates that in the year 2000 a value in the range between \$45 and \$60 billion was spent in work compensation due to RSI injuries.

In Sweden three out of five office workers have symptoms of RSI (Buckle and Devereux, 1999). In Australia 60% of children using laptops in school experienced discomfort. 40% of Dutch university students have an RSI condition (RSIA, 2007). In India a study was carried out on 200 Information Technology professionals who operate daily computers on a daily basis. 77.5% of them reported musculoskeletal symptoms. This study suggested the necessity of prevention measures and a periodic appraisal of health for workers in these areas (Suparna et al., 2005).

1.3. Legal considerations

The development of RSI frequently causes sufferers to take their employers to court in order to claim compensation. An early example in the UK of such a claim is Sarah Munson, a journalist at the Portsmouth News, who was awarded £11,371 in compensation on 31st of October 1993 despite the fact that RSI did not figure in any medical dictionary at the time (The Independent, 1993). Another example of a successful court claim are five former Midland Bank workers who were awarded £50,000 each in compensation in May 1998 in spite of the fact that RSI was not recognised by UK employers at the time (BBC, 1998).

As in RSI, HAVS sufferers went to court in order to claim compensation. An example is that of eight former employees of North West Water who were awarded a total of £1.2 million

compensation in August 2000. The company admitted negligence (BBC, 2000). Six other British Gas workers were awarded £430,000 compensation at a Manchester court in 1999 because of HAVS (BBC, 2000). Another typical example of a successful claim for HAVS injury was in 2004 when Stock-on-Tees Borough Council had to pay £350,000 compensation for WRULD (Archer Solicitors, 2004).

The examples above demonstrate that it should be less expensive to avoid WRULD than to do nothing. When avoidance is not possible, control and frequent monitoring of workers' health could prevent or at least diminish the impact of the condition and the likelihood of litigation.

1.4. The case for early detection

In RSI and HAVS early recognition and early treatment mean quick recovery. The early identification of RSI is difficult because it includes a large range of conditions. The American College of Rheumatology has suggested the usage of Medical Imaging modalities to assess this conditions (Van Tulder, 2007). This would provide more detailed and objective information that could be used for a more correct diagnosis and respective indicative treatment and for assessing the treatment progress. An American physician, Pascarelli, suggests, in his book (Pascarelli, 1997), the use of medical thermography as a diagnostic aid mainly due to its simplicity in obtaining an objective record with the aid of a computer, but stated that more research is needed in image processing to improve the technique.

1.5. Current diagnostic approach

The current diagnostic procedure for both RSI and HAVS syndromes is similar. Starting with the medical record of the patient and focusing on the pathophysiological history, a questionnaire and a pain pictogram are used where the patient indicates pain on a scale from 1 to 10. After reviewing this information physical examinations follow in order to identify symptoms and pathologies. This is done subjectively, relying on the clinician's perception and on the patient's claim. The lack of an objective and repeatable measures is evident.

1.6. Research to date

Some research exists to explain the diffusivity of WRULD. Fry (Fry and Dennet, 1988) proposed that muscle overuse leads to a painful condition with changes in muscle fibres. Neurogenic theories suggest that nerves are sensitised by mechanical irritation and traction due to overuse. It causes the nerve to become less tolerant for compression and stretching. Since early WRULD presents few physical signs, the major problem in achieving a diagnosis is the lack of sensitive objective measurements. A study in 1997 (Sharma, 1997) suggested that temperature measurements by infrared imaging using mechanical challenges to the hands could possibly be used as a diagnostic tool in order to evaluate non-specific hand-arm pain and to monitor progress during treatment. The author suggested that future work is needed to confirm this finding. Another study (Greening and Lynn, 1998) that measured vibration thresholds in sensory nerves had shown that patients with WRULD have objective signs of minor polyneuropathy.

A review study performed in 2000 aiming to understand the causes of RSI conditions (Szabo and King, 2000) showed that is often difficult in litigation cases to prove the degree of the injury. Two years later a Swedish scientist (Lundström, 2002) suggest that the lack of normative data and the absence of standard methods to assess the HAS pathology limits its identification. The same author refers that quantitative sensory tests are very dependant on the subject's perception and its sensitivity, specificity and reliability are still unknown.

In 2003 a pilot study (Peper et al., 2003) investigating discomfort measurements in computer operators through "point and type" tests and electromyography, concluded that symptomatic subjects presented more muscular electrical activity than controls performing the same test. The same study concluded that further investigations involving other monitoring techniques were required.

Van Tulder, a Dutch scientist, affirmed (Van Tulder et al., 2007) that major parts of the RSI diagnosis are based on the medical history and physical subjective examinations, however some electrodiagnostic tests such as electromyography are used, although its diagnostic accuracy has not been proven according to Van Tulder.

Another author in 2008 (Augusto et al., 2008) suggested that subjective examinations in assessing RSI conditions are insufficient, objective methods are needed to recognise injury characteristics and to be used on evaluating the treatments.

An investigation in Serbia, observing the vascular changes in HAVS patients through

thermal images (Jankovic et al., 2008), showed that the vascular provocation used was not completely satisfactory, there is a need for further development methods to identify more characteristics in the patient's condition. The same study concluded that thermography demonstrated to be useful in the differential diagnostic tests because of its ability to provide the opportunity for assessing the entire hand simultaneously.

Harada, a Japanese investigator, affirmed that there is no single objective test with satisfactory diagnostic ability for HAVS (Harada, 2008). The same author suggested that for a reliable objective diagnostic indication on the vascular aspect of HAVS, cold stress tests are recommended to evaluate HAVS patients, however a standardised evaluation approach is required.

The absence of objective, quantitative and reproducible diagnostic procedures for Work Related Upper Limb Disorders enhances the difficulties in assessing the injury state and thus the choice of adequate treatment. In legal situations it would quantify the degree of injury thereby providing the opportunity for attributing a fair compensation.

1.7. Aim

It is aim of this work to design, implement and assess an objective, quantitative and reproducible diagnostic procedure for Work Related Upper Limb Disorders (WRULD).

1.8. Objectives

In order to achieve the above aim, the following objectives will be addressed:

1. Standard infrared image capture protocol: design and assessment of the capture protocol to record medical thermal images of the hands.
2. Online hand injury incidence questionnaire: design, implementation and assessment of both questionnaire suitability and results.
3. Hand temperature reference data: design, implementation and assessment of data suitability and results.
4. Mechanical stress provocation tests: design and perform objective, standardised tests and assess the results.

5. Comparison and results assessment of different techniques available in image processing on thermal images such as: enhancement, objects boundaries discovery and interpolation.
6. Standard reference method for thermal image analysis of hands: design, implementation and results assessment.

1.9. Proposed methodology

The proposed solution to achieve the above objectives consists of two independent but related investigations with different methodologies. The first investigation characterises the incidence of hand injuries in a sample population through an online questionnaire (Fig. 2). The second, more complex investigation consists of the development of a standard thermal image capture protocol for hands., including a range of mechanical stress provocation tests, image capture and a standardised methods and analysis tools that use image processing techniques to produce quantitative and statistical data (Fig. 3).

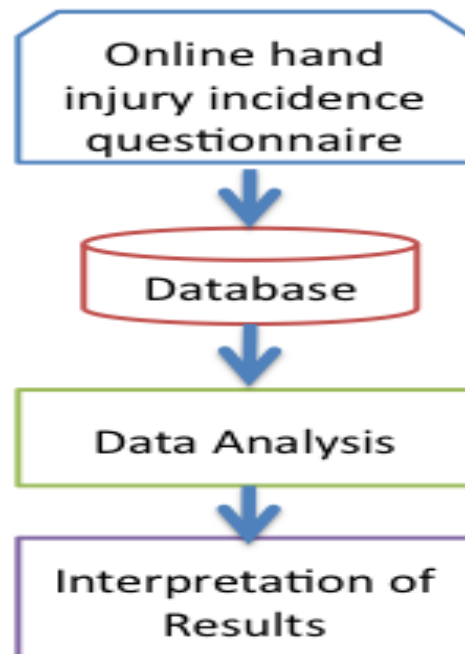


Fig. 2: Investigation plan for the characterisation of hand injuries in a sample population.

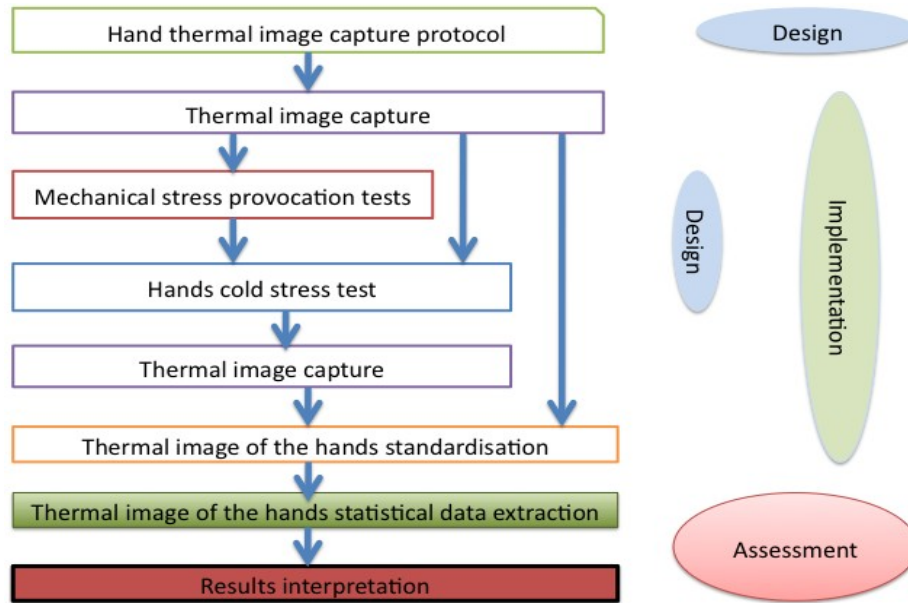


Fig. 3: Phase diagram for the development of a Hand-Arm Syndrome diagnosis procedure with different stages of investigation on the right.

1.10. Contribution to knowledge

This work claims the following contributions to knowledge:

In the design phase:

- The development of a protocol to capture thermal images of hands.
- A new definition for the thermal symmetry of the human body.
- The development of objective mechanical stress provocation tests to assess hand injuries.
- The development of a reference anthropometric geometrical model of hands.

In the implementation stage:

- A comparison of image enhancement techniques for thermal medical images.
- A comparison of edge detection techniques for thermal medical images of hands.
- A comparison of interpolation techniques for thermal medical images.
- The development of a novel warping technique based on triangulation and barycentric coordinates that preserves the true temperature values within defined areas of interest in a predefined model.

In the assessment phase:

- A set of reference values for thermal symmetry of the upper limbs and joints in healthy subjects.
- A second set of thermal symmetry values and mean temperature variation after mechanical provocation and vascular stress tests for healthy and WRULD affected subjects.
- A comparison of three methods that assess the recovery of hands from a cold stress test.
- Identification and quantification of inter- and intra- user measurement errors and variance data for different camera models in standardised image capture and analysis.

1.11. Structure of the thesis

This document is separated into six sections:

This introduction describes the background, motivation, relevance, aims, objectives and contribution to knowledge of present research.

1. The next section, a literature review, demonstrates the anatomical and physiological characterisation of the hands, the nature of the syndromes and their respective prevalences, causes, characterisations and shortcomings of current diagnostic methods. It also describes the technique of thermal imaging and its use in medicine and its alternatives including imaging processing techniques that can be used to improve medical imaging analysis.
2. The third section outlines the methodology used in this research project including the design of experiments and tests and methods of analysis.
3. In the Results section the results of experiments and tests are presented and interpreted.
4. The fifth section discusses the significance of findings and analyses error sources. It also sets the results into the context of other projects and methods.
5. The final part of this document is the Conclusion, where the main results of this project are emphasised and the case for the claimed contribution to knowledge is made. It also provides an outlook into future work.

The diagram in fig. 4 visualises the above structure and outlines the links between different parts of this document.

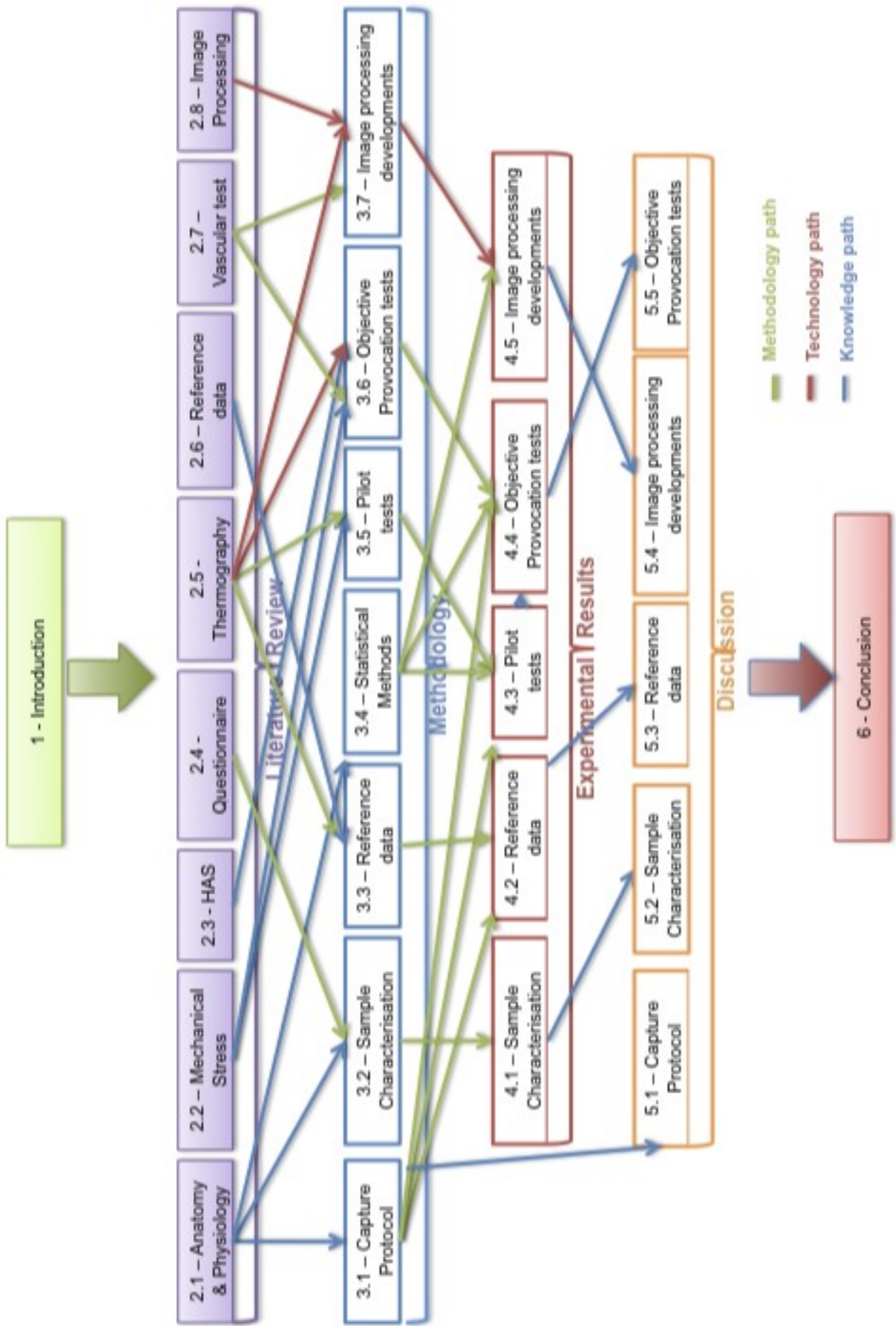


Fig. 4: Diagram of thesis structure.

2 – Literature Review

2.1. Hands

In the context of this work 'hands' are defined to extend from the wrist to the fingertips. Each hand has one thumb and four fingers: (from lateral to medial) are described as little, ring, middle and index. In this subsection relevant information about these extremities is included to increase understanding of how they perform and how they can be affected in a pathological condition. The internal anatomy of the hand is described, its physiology in terms of movement, sensor-motor system, microcirculation and the temperature regulation of the hand is briefly reviewed to elucidate those factors that are of importance in the context of Hand Arm Syndrome.

2.1.1. Anatomy

Since this work frequently cites anatomical terms they are briefly outlined below in sections 2.1.1.1 to 2.1.1.8.

Hands are regarded as having two surfaces, a palmar (anterior) and dorsal (posterior), and two borders, radial (in the medial border of the hand) and ulnar (in the lateral border of the hand) as shown in fig. 5. The palm of the hand is constituted of three areas: thenar (overlies the thumb metacarpal), midpalm (overlies the three middle metacarpals) and hypothenar (overlies the little finger metacarpal) (Jones, 2006).

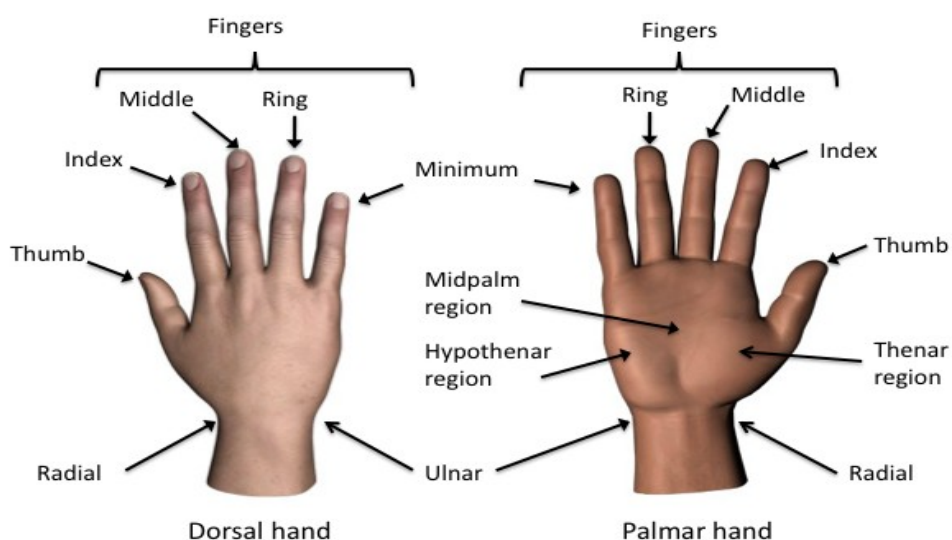


Fig. 5: Definition of hand anatomical terms.

The constitution of the structure of the hand is formed of bones and associated joints, blood vessels (arteries and veins), muscles, nerves, tendons, ligaments, skin, hair and nails (Jameson, 1998).

2.1.1.1. Bones

Each hand is composed of 27 bones (fig. 6): 8 carpal bones are organised in two rows in the wrist that articulate the hand with the radius and ulna (bones of the forearm), 5 metacarpals in the palm, one in each direction of the correspondent finger and thumb and connecting to them; and 14 phalangeal bones that form the fingers and thumb: three in each finger and the remaining two in the thumb. The carpal bones are on the proximal row from lateral to medial: scaphoid, lunate, triquetral and pisiform; and on the distal row in same direction: trapezium, trapezoid, capitate and hamate. The palmar bones, the metacarpals, receive their name from each corresponding finger, each with a head and a shaft. Each finger has 3 phalanges, the proximal, the middle and the distal that carry the nails. The thumb has the proximal and distal phalanges only but no middle phalange (Jones, 2006).

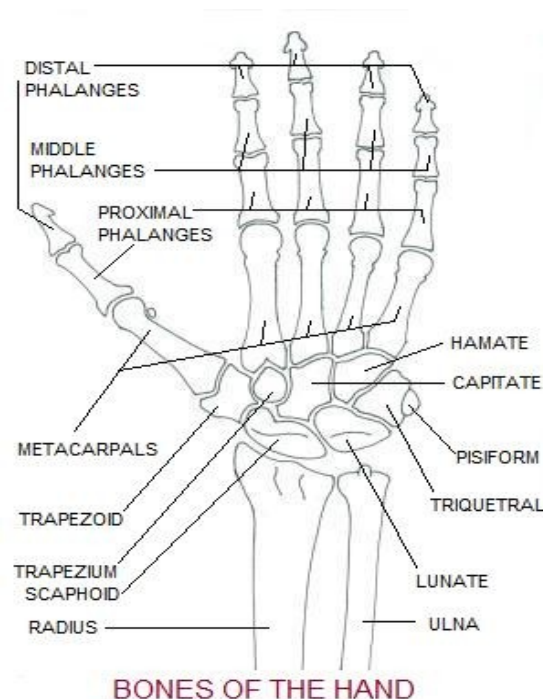


Fig. 6: Bones of the hand (right hand in dorsal view), Webliography[1].

The bones have an integral role in HAS, connecting with other bones through their rounded and flattened surfaces at their farthest ends to form joints where the bones meet. These joints are

covered on their surface with soft cartilage material that acts as a muffler to the bones and aids joint movement. When cartilage is damaged the joints can become painful, and in serious cases leads to arthritis, one of the more severe results of RSI (Jameson, 1998).

2.1.1.2. Joints

Joints are important in the interconnection of bones forming the articulation, which in the hand is very complex and delicate. A major part of the operations performed by hands does depend on this articulation. There are three types of joints present in the hand, the intraphalangeal joints that interconnect the phalanges, the metacarpophalangeal joints which combine metacarpals with phalanges and carpometacarpal joints which link carpal bones with the metacarpals as shown in fig. 7. The carpometacarpal joints are the most flexible, they are responsible for the flexion/extension movement and also radial and ulnar deviation movements. Metacarpophalangeal joints with exception of the thumb, have a very limited independent motion (Jones, 2006).

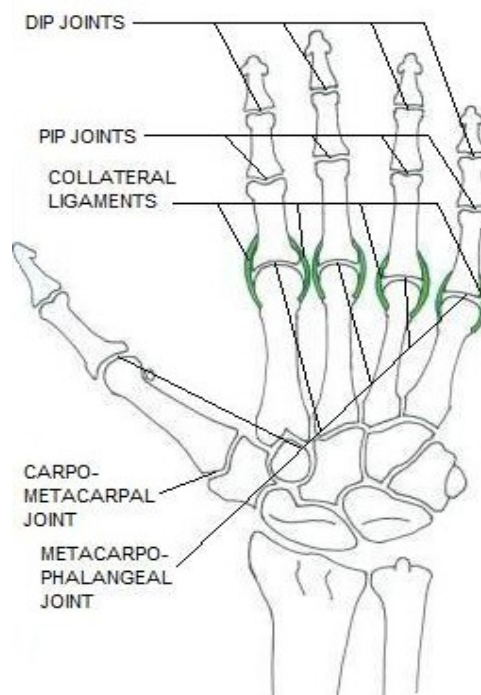


Fig. 7: Bone joints of the hand (right hand in dorsal view), Webliography[2].

The joints are surrounded by joint capsules, which consist of synovial membranes on the inside and tough fibrous membranes on the outside. These capsules control the joint motion range and aid to lubricate the joint surface by secretion of synovial fluid. An inflammation in these

capsules can be a result of RSI, causing pain, discomfort and swelling (Jameson, 1998).

2.1.1.3. Muscles

Muscles are tissues that contain cells which are contractible by nature. That characteristic allows the bones to which the muscles are attached to move. They can be categorised in two groups, the extrinsic (arise outside of the structure they are attached to) and the intrinsic (fully contained in the structure they are attached to). There are 29 muscles that control hand movements, 15 are extrinsic and 14 intrinsic. The extrinsic muscles are divided into two types: flexor and extensor, as shown in fig. 8. The intrinsic muscles, as shown in fig. 9, are divided into four groups: three tenar muscles, three hypothenar eminences and four lumbrical muscles, these are unique muscles in the human body because they originate from tendons instead of bone. (Jones, 2006).

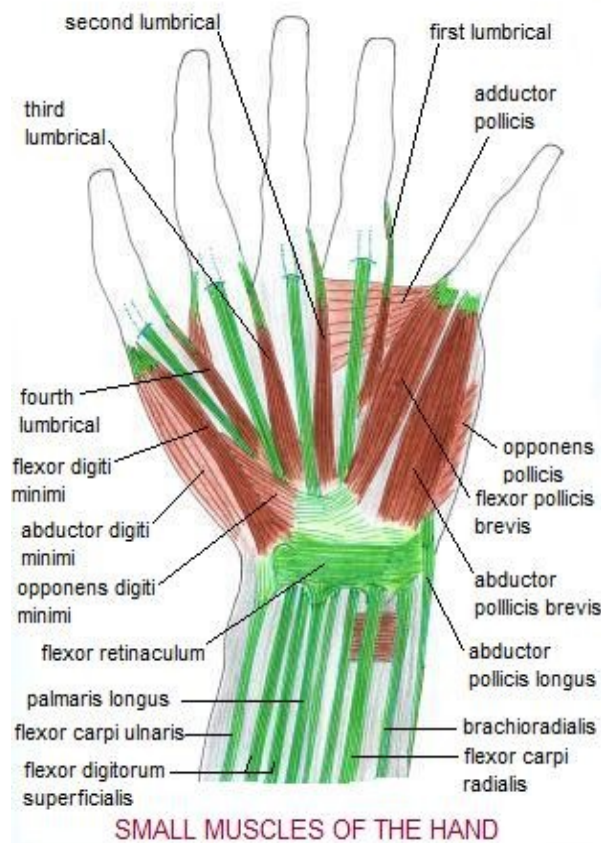


Fig. 8: Extrinsic muscles of the hand (right hand palmar view), Webliography[3].

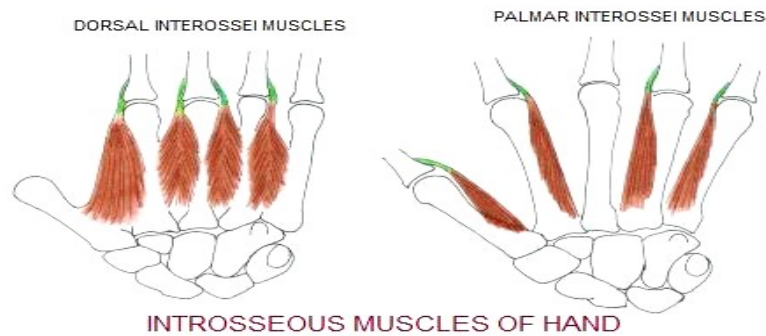


Fig. 9: Intrinsic muscles of the hand (on left: right hand in dorsal view, on right: left hand in palmar view), Webliography[4].

Muscles are amongst the structures most frequently affected by HAS since repetitive movements restrict normal blood flow to these tissues. This also affects the exchange of oxygen between blood and the muscular cells. The decrease of oxygen in the muscles evokes a pain response, inflammation and formation of scar tissue. This situation leads to a loss in muscle contract ability, rise of muscle weakness and sudden muscle fatigue. In a prolonged circumstance this degenerative process caused by HAS may lead to a chronic condition (Jameson, 1998).

2.1.1.4. Tendons

Tendons connect the muscles to the bones (Jameson, 1998). Hand tendons origin in the muscles of the forearm and traverse the carpal tunnel at the wrist to reach the hand where they move the hand and fingers. The finger tendons traverse laterally over the metacarpal bones and the phalanges. They are supplied with blood at the wrist and the metacarpals by the muscles and at the fingers by arterioles. Tendons are independent of each other, although they can collaborate in movements (Nichols, 1960).

Tendons are fine tubular extensions of the muscles that allow them to attach to bones. These muscle-tendon junctions together with tendon-bone junctions are the two areas most likely to be affected by HAS. The overuse of muscles of the upper limbs causes injury to the tendons' attachment at the periosteum (outer layer of the bone). This causes pain and swelling that can be felt over the bones' surface. In severe cases changes over bone surfaces can be identified in x-ray images (Jameson, 1998).

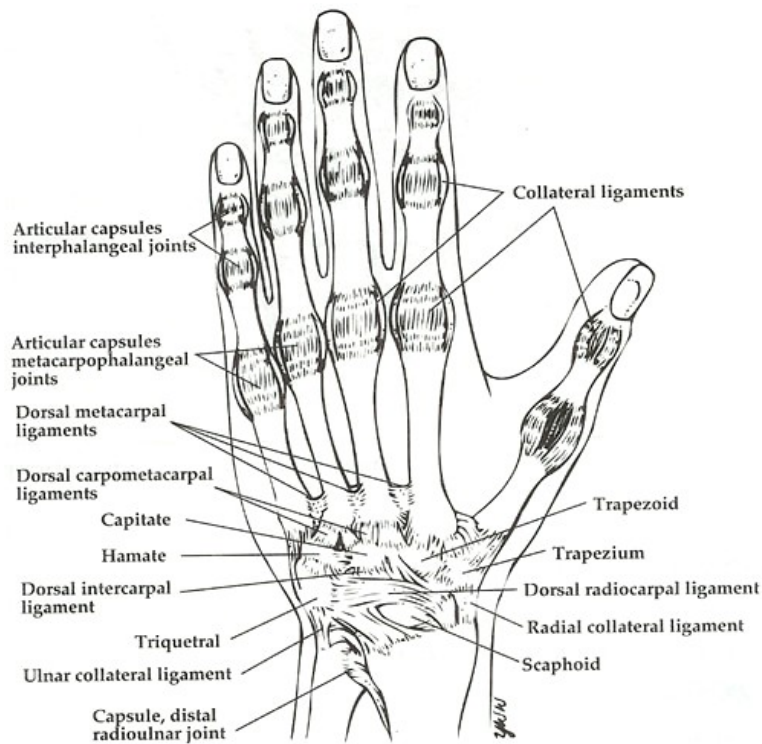
The retinaculum is a structure that guides the tendon from its insertion point at the wrist to

the correspondent finger. When traversing this structure the tendon is wrapped by a sheath of material called the synovial membrane, which secretes a viscous fluid (called synovial fluid). The main function of this fluid is to protect the tendon from friction and to aid its movements underneath the retinaculum. In the case of HAS, the synovial membrane can thicken affecting tendon movement, becoming swollen and thickened in the process. This causes pain and inflammation (which in turn is associated with increased temperature that may aid its detection via infrared imaging) until the stress is withdrawn (Jameson, 1998).

2.1.1.5. Ligaments

Ligaments are fibrous materials that act like semi-elastic bands. They function as a means of joining bones to form joints. The three more important ligaments (fig. 10) of the hand are: the collateral ligaments (found on either side of each finger joint, that prevents abnormal sideways flexion), the volar plates (to connect the proximal and middle phalanx on the palmar side of the joint, and prevent the proximal joint from excess flexion) and the transverse carpal ligament (located around the wrist and encloses the carpal tunnel holding all carpal bones, muscles, tendons, nerves, veins, arteries that compose the wrist)(Jameson, 1998).

In HAS, ligaments play an integral part, not because they tend to become injured, but due to their function to cover or enclose several nerve structures that can contribute to nerve entrapment syndromes. However in HAS it is possible for the ligaments to be injured, this normally occurs only in strenuous work such as carpentry or in other occupations that involve heavy mechanical labour. Ligament injuries are slow to heal, and can take from six months to a year to full recovery. This is caused by the minimal blood supply to the ligaments. Sufferers of HAS with sprained ligaments may experience pain for large periods of time (Jameson, 1998).



Dorsal view of the radiocarpal, intercarpal, and carpometacarpal articulations

Fig. 10: Ligaments of the hand (left hand in dorsal view), Webliography[5].

2.1.1.6. Nerves

Nerves supply the muscles and all other body tissues with information in the form of impulses from and to the brain. They control muscular contraction as well as local body movement and reactions. The nervous system is divided into two subsystems: The central nervous system (CNS) in the brain, and the autonomous or peripheral nervous system (PNS) present in the spinal cord (attached to the brain and all other parts of the body). The hand is innervated by 4 main nerves which include sensor and motor components (fig. 11). These nerves are: posterior antebrachial cutaneous, radial, median and ulnar (Jameson, 1998).

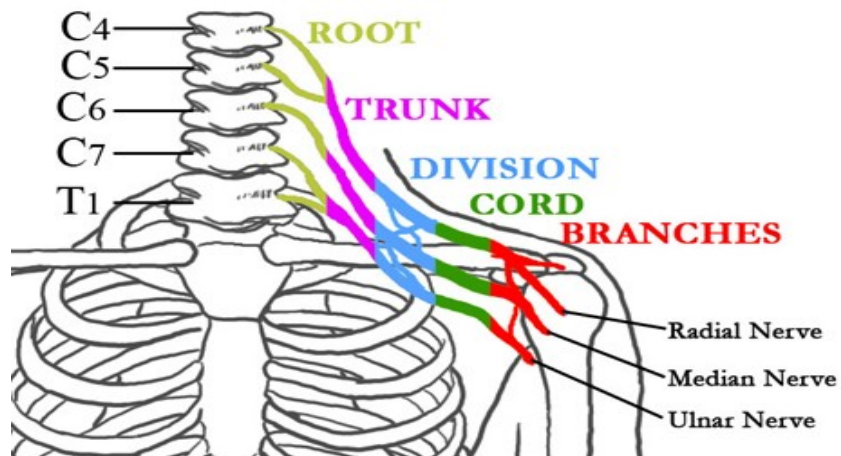


Fig. 11: Roots of the nerves of the hand on the spine, Webliography[6].

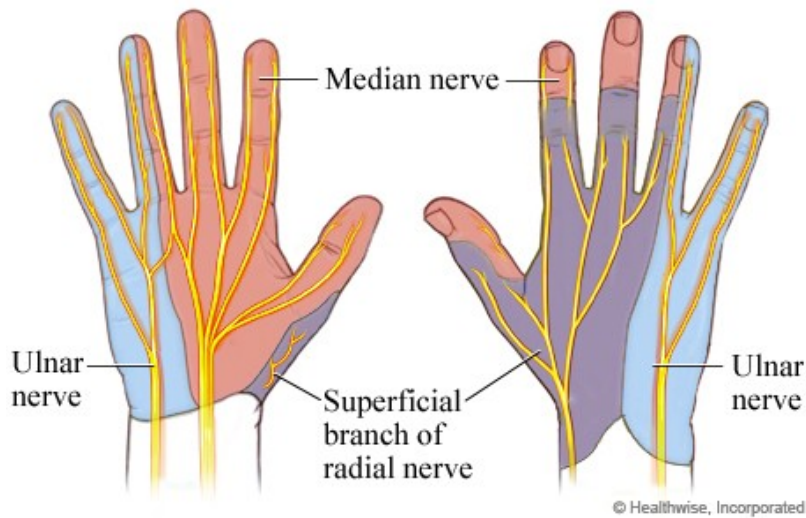


Fig. 12: Regions of each nerve of the hand (right hand on both palmar and dorsal views), Webliography[7].

The posterior antebrachial cutaneous nerve innervates the dorsum skin of the wrist and is connected to the spinal nerve roots C4-T1 (fig. 11) (Tortora and Grabowski, 2003).

The radial nerve (fig. 12) is responsible for innervating the wrist extensors which control the position of the hand and stabilise the fixed unit. It has its origin at the posterior cord of the brachial plexus (fig. 11) (C6-8). The radial nerve innervates the radial three quarters of the dorsum of the hand and the dorsal surface of the thumb and also supplies sensibility to the dorsal surfaces of the index and middle fingers and to the radial side of the ring finger (Jones, 2006).

The median nerve (fig. 12) innervates the muscles involved in the fine precision and pinch functions of the hand. It originates at the lateral and medial cords of the brachial plexus (fig. 11) (C5-T1) and provides motor and sensor capabilities to the anterior surfaces of the thumb, index and middle fingers and the radial side of the ring finger. Dorsal branches of this nerve serve to supply the dorsal aspect of the index and middle fingers distal to the proximal interphalangeal joint and the radial half of the ring finger (Jones, 2006).

The ulnar nerve (fig. 12) drives the muscles involved in the power grasping function of the hand. It has its origin at the medial cord of the brachial plexus (fig. 11) (C8-T1). This nerve innervates the little finger and the ulnar half of the ring finger on the palmar surface; at the dorsal aspect of the hand, the ring and little finger metacarpals, the dorsum of the little finger and the dorso-ulnar half of the ring finger (Jones, 2006).

Regarding hand function, the most important nerve is the median which carries information from the larger area of the palmar surface of the hand, and innervates the intrinsic muscles that control the thumb (Jones, 2006).

HAS often implicates injuries to the Peripheral Nervous System, although the Central Nervous System also plays an important role. Impulses for muscle contraction in the fingers start in the brain and flow downward to the arms passing through the spinal cord, where the CNS communicates with the PNS, and arrive at the hand and fingers. The peripheral nerves are responsible for sending impulses to the organs and receive sensory information from them including the skin. Some of these nerves are engaged in sympathetic and parasympathetic functions. Nerves belonging to the sympathetic nervous system which emerge from the middle-back spinal region cause muscle tension, the release of adrenaline, decrease of digestive function, increased breathing and heart rate. Opposite reactions such as slower breathing, slower heart rate and increased digestive function are caused by the parasympathetic nervous system, from the brain and spinal region near the tailbone (Jameson, 1998).

People in stressful jobs are usually found to have an increased and prolonged sympathetic response. This makes them more susceptible to HAS conditions. The sympathetic response induced muscle tension can cause fatigue of muscles and chronic mechanical stress. Compression of the peripheral nerves may occur at various sites between neck and the upper limbs. It is possible for a nerve to become trapped in more than one location at same time. Among HAS sufferers it is common to find multiple entrapment sites. Nerve impulses are considerably attenuated in situations where the nerve is being compressed at more than one site (Jameson, 1998). Prior to muscle weakness becoming apparent, gradually increasing degrees of numbness and tingling sensations are signs of progressive impairment of nerve conduction. Nerve compression can cause injury of

sympathetic fibres resulting in dryness of the skin and poor circulation to the extremities (Werner and Andary, 2002).

Dermatomes are areas of skin mainly supplied by a single posterior spinal nerve root. In fig. 13 is shown the hand skin areas with the corresponding nerve root. The thumb posterior and anterior skin areas are supplied by the C6 nerve root, the index and middle finger skin areas by the C7 and the remain fingers areas by the C8 nerve root (Casey et al., 1993).

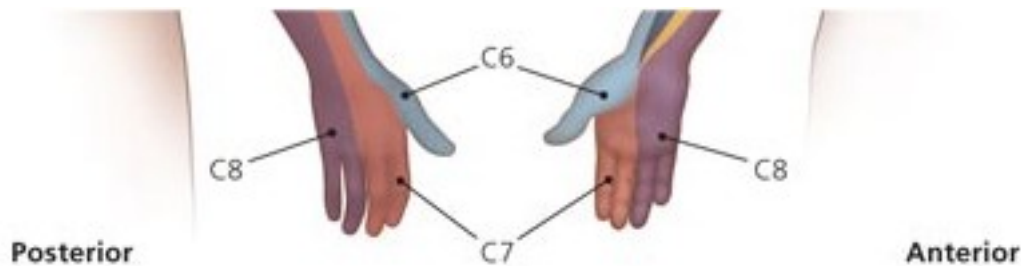


Fig. 13: Dermatomes of the hand, Webliography[21]

In the context of this work hand dermatomes are relevant to identify neurological reactions to mechanical provocation.

It is, however, the interaction of nerves with the blood supply to the hand that is at the core of this work. This aspect is explained in greater detail in the following section.

2.1.1.7. Blood vessels, veins and arteries

The hand has one of the richest and complex vascular networks of the human body (Jameson, 1998).

Hands are fed by two main arteries that carry oxygen-rich blood from the heart to the tissues, the radial (middle side) and ulnar (lateral side) (fig. 14). Both are branches of the brachial artery, which supplies the upper limbs from the aorta artery. After reaching the hand via the carpal tunnel at the wrist, both arteries form two palmar branches, the superficial and the deep palmar branches that respectively contribute to the superficial and deep palmar arches. From these arches the digital arteries, two for each finger, are formed (Nichols, 1960).

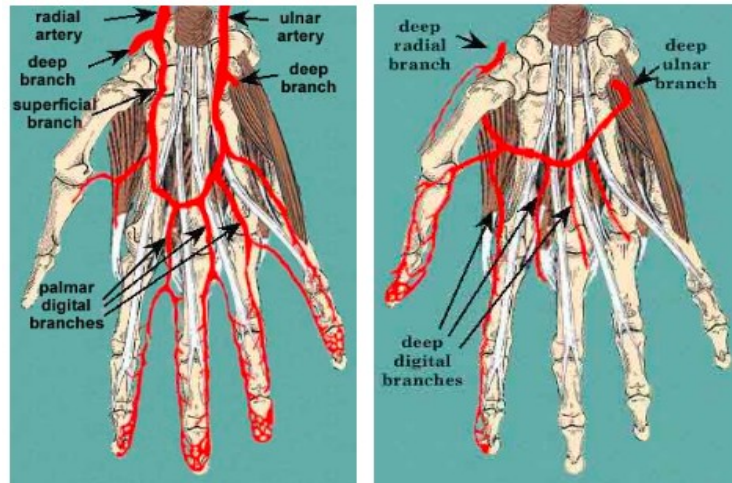


Fig. 14: Arteries of the hand (right hand palmar view and right hand dorsal view), Webliography[8].

Two main veins carry oxygen-deficient blood back to the heart (fig. 15) the cephalic (median) and basilic (lateral). Both will merge into the brachial vein at the forearm. There is a dorsal venous arch, resultant from the digital veins, two for each finger, that ends at the cephalic and basilic veins (Nichols, 1960).

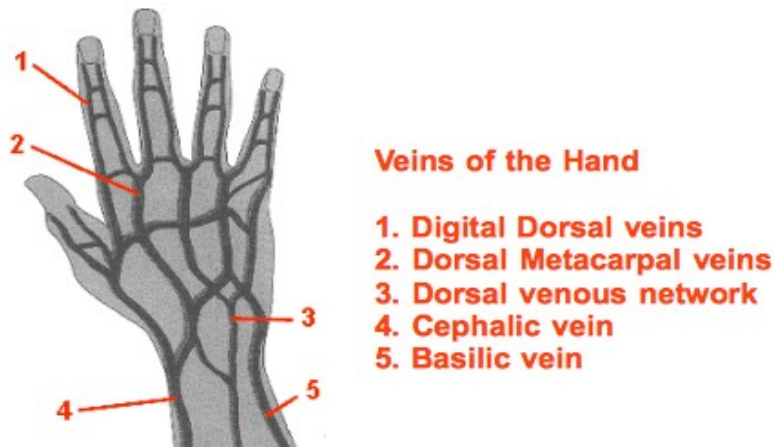


Fig. 15: Veins of the hand (right dorsal hand), Webliography[9].

In HAS conditions bleeding of small capillaries and veins may occur due to direct injury. A pressure increase within the cells causing oxygen deprivation may also occur due to a leakage of

fluid to the surrounding areas outside the cells. This decrease of oxygen supply to the cell structures may cause the cells to die (Jameson, 1998).

Inflammation due to direct pressure causing nerve compression and/or swollen tissues causes a decline in blood flow to the nerve. As a consequence there is less oxygen available to the nerve cells which results in degeneration of myelin. Myelin thinning affects the speed and wave form of the nerve impulse. In a prolonged situation of nerve compression and reduced blood flow, the axon, which is responsible for transmitting impulses to the tissues will start to degenerate. These symptoms are not noticed immediately as the nerves consist of thousands of axons. Only after a considerable number of axons have died the symptoms will appear. It is relevant to note that axons are very slow at regenerating, if they have that capability at all. This is one of the reasons why HAS must be diagnosed at an early stage and treatment should be initiated immediately otherwise irreparable harm to the nerve cells with long term disability will be the consequence. It is believed that in HAS affected patients with an over-productive sympathetic nervous system this can cause the blood vessels to constrict and dilate inappropriately, and thus constituting a condition that is known as Raynaud's phenomenon (Jameson, 1998).

Since blood supply to the hands directly affects their temperature an abnormal reaction of the nervous system to stimuli, may be noticeable by monitoring hand skin temperature. In order to understand this causal relationship the next section introduces the layer between superficial blood vessels and the outside world: the skin.

2.1.1.8. Skin

Skin differs on both sides of the hand, at the dorsum it is thin, soft, hairy and pliable and on the palmar side it is thick and hairless, with unique characteristics for special functions (Jones, 2006).

Skin is constituted of three layers: epidermis, dermis and hypodermis (Tortora and Grabowski, 2003).

The outer layer is the epidermis, it is a protective wrap over the body structures, constituted of stratified squamous epithelium with an underlying basal lamina. It is this layer by its own characteristics that makes the skin waterproof. The thickness of the epidermis at the hand varies from 0.5mm on the dorsal region to the 1.2mm on the palmar. This layer does not have any blood vessel cells, the deepest sublayers are nourished through diffusion from blood capillaries that extend from the upper layers of the dermis (Tortora and Grabowski, 2003).

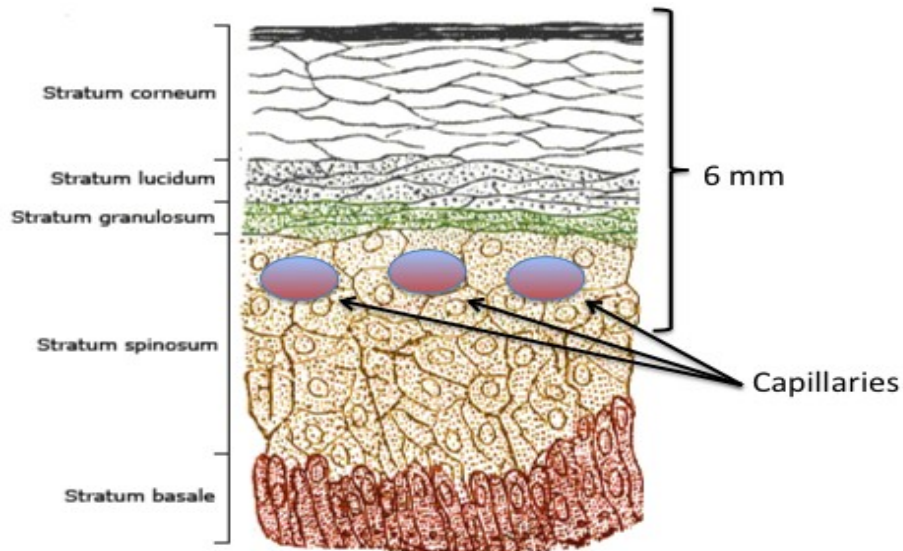


Fig. 16: Sub-layers of the epidermis (Palm of the hand), *Webliography*[10].

The middle tier of the dermis has enfolded glands, nerves, blood vessels and hair follicles (the latter are not present on palmar skin). This layer is composed of two sublayers: the papillary region and the reticular region. The papillary region (fig. 16) is placed on the superficial chunk of the dermis (20%) and consists of areolar connective tissue with elastic fibers, it contains dermal papillae that accommodate capillaries, corpuscles of touch and free nerve endings (Tortora and Grabowski, 2003) Using infrared imaging, circulatory activity can be monitored up to 6mm inside of body, therefore peripheral capillary activity can be recorded using this technique.

The inner layer of the skin is the hypodermis (fig. 17), although it is not considered to be a part of the skin. It attaches the skin to underlying bone and muscle and supplies it with blood vessels and nerves (Jones, 2006).

The skin has several functions, those relevant to this work are: sensation detection (due to the nerve endings that react to temperature, touch, pressure, vibration, and tissue injury), temperature regulation and evaporation control (Tortora and Grabowski, 2003).

Skin has different pigmentation, which explains the different skin colour of the humans. In all other attributes and features the hand remains similar (Smith and Burns, 1999).

Skin becomes thinner with age, is more easily damaged and loses the ability to heal due to a fall in elasticity, decrease in blood flow and lower glandular activity (Tortora and Grabowski, 2003).

An important property of the skin in the context of this work is, due to the measurement of infrared radiation emitted by the skin, is its emissivity (the relative power of its surface to emit heat by radiation) that is usually at a characteristic value of 0.98. This means that the human skin is a poor thermal reflector but has a high ability to both absorb and emit radiated energy (Hardy, 1934).

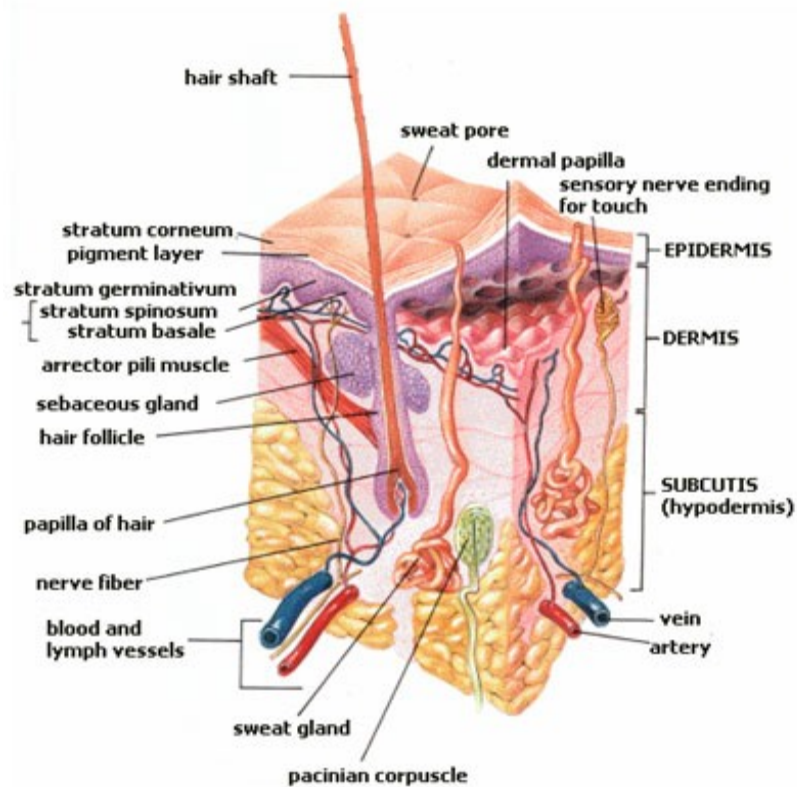


Fig. 17: Skin structure and layers, Webliography[11].

2.1.2. Physiology

In this section the physiology of the hand is presented, the characterisation of the sensory system of the hand, the microcirculation with its important role for thermoregulation.

2.1.2.1. Sensor System

The hand sensory system has a relevant role in thermoregulation of the hand. This system is important for the activation or suppression of an answer from the autonomous nervous system. The acclimatisation period described in section 3.1 is an example of how ambient constant temperature habituation and contact avoidance with other materials are significant.

The hand is an important source of information, it is equipped with different sensors that transmit sensor-motor data to the brain through the nervous system. These sensors can be exteroceptive (perceiving sense from outside the body) or interoceptive (perceiving sense from within the body) (Jones, 2006). The different sensors that can be found in the human hand are

mechanoreceptors, thermoreceptors, nociceptors, muscle receptors and joint receptors (fig. 18). Mechanoreceptors however are directly related to tactile sensation and act on mechanical stimuli. Touching, hearing and equilibrium are examples of sensation perceived by these sensors. (Jones, 2006).

Thermoreceptors provide thermal information of objects from thermoreceptive afferent units in the skin. Hands provide two different types of thermoreceptors: cold receptors and warm receptors, with cold receptors being in the majority and located closer to the skin surface. The density of these receptors per square centimetre on the dorsal hand is 7 for cold sensors and 0.5 for warm. Cold receptors respond to skin temperature decreases over a range of 5-43°C and become more active at skin temperature of 25°C. Contrastingly, the warm receptors discharge signals at skin increasing temperatures reaching a maximum at 45°C. Between 30°C and 36°C no thermal sensation is noted, although both types are spontaneously triggered. During daily activities hand can vary in skin temperature between 20°C and 40°C, normally remaining between 30°C and 35°C. When hand skin temperature is sensed over 45°C or below 13°C these sensors transmit a sensation of pain to the brain. On the palmar hand these sensors are innervated by the median nerve. Warm sensors conduct much faster (1-2m/s) than cold sensors (10-20m/s). This identifies them as unmyelinated fibers in opposition to the cold receptors that are small-diameter myelinated fibers (Jones, 2006) The thermoreceptors of the skin can perceive a temperature difference of 0.01°C this, however, may take up 10 seconds (Widmeier et al., 2004).

Nociceptors mediate pain sensations and are selectively sensitive to high-intense stimulation of several different energy forms such as electrical, mechanical, chemical or thermal. These receptors are continually relaying impulses to the brain. The density of these receptors per square centimetre on the dorsal hand is 188. Muscle receptors provide to the central nervous system the information about muscle length and force. Joint receptors reflect the location of stresses during limb movements (Jones, 2006).

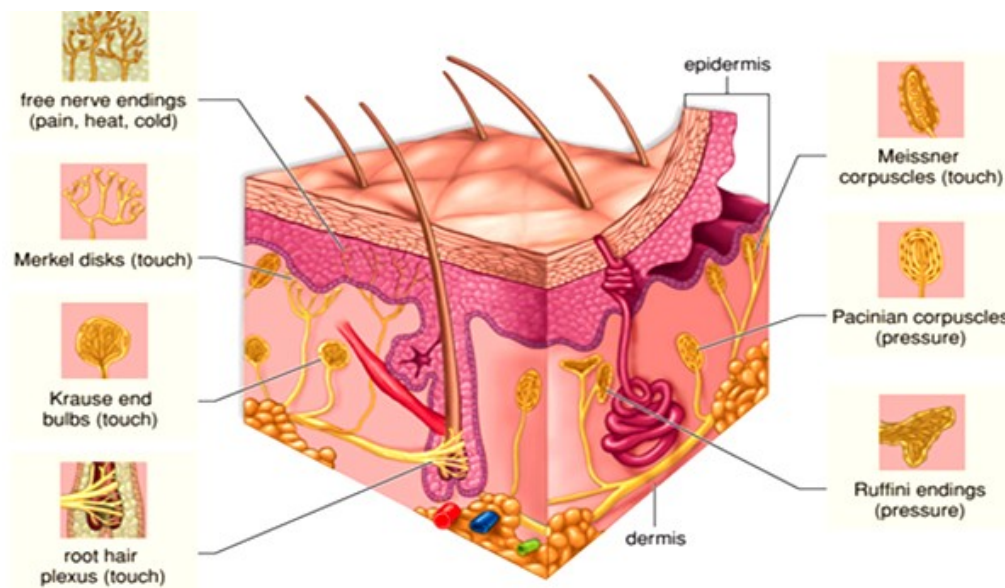


Fig. 18: Sensors of the hand skin, Webliography[12].

2.1.2.2. Microcirculation

Microcirculation is the name given to the smallest blood vessels (<100µm in diameter) in the vasculature. The components of the thermoregulation system are arterioles (arterial side), capillaries and venules (venous side) (fig. 19). Arterioles are small diameter blood vessels with thin muscular walls. These elements are the primary site of vascular resistance, they obtain autonomic nervous system innervation and also regulate their diameter according to a response to various circulating hormones. In a healthy vascular system these elements are relaxed. The increase of total peripheral resistance of the arterioles may lead to hypertension. This is important in this work because this resistance affects directly affects the peripheral temperature. Arterioles are composed of vascular smooth muscle and endothelium, that have direct communication between them. Endothelium is a thin layer of cells that forms the interior surface of blood vessels. These cells are involved in several vascular aspects such as the control of blood pressure by vasoconstriction or vasodilatation. The endothelium produces nitric oxide and any deregulation in this function may be a sign of a pathological state, which may be reflected in the peripheral temperature. The arterioles provide blood to the capillaries, which are the body's smallest blood vessels (5-10µm in diameter). They connect arterioles and venules and provide the interchange of water, oxygen, carbon dioxide, heat, chemical substances and many other nutrients between blood and neighbouring cells that

constitute tissues.

There are three types of capillaries: continuous, fenestrated and sinusoidal. Metarterioles allow direct communication between arterioles and venules, and have an important role in bypassing the blood flow through the capillaries. The regulation of blood flow into capillaries is provided by precapillary sphincters that answer to nitric oxide. The blood flow influences the peripheral temperature, which is transferred to the external environment through infrared emission. This emission can be recorded by an infrared imaging system and used to monitor pathological states indicated by deficient nitric oxide regulation. Venules are small blood vessels that endorse deoxygenated blood to return from the capillaries to the larger veins and from these back to the heart to be re-oxygenated by the lungs (Tortora and Grabowski, 2003).

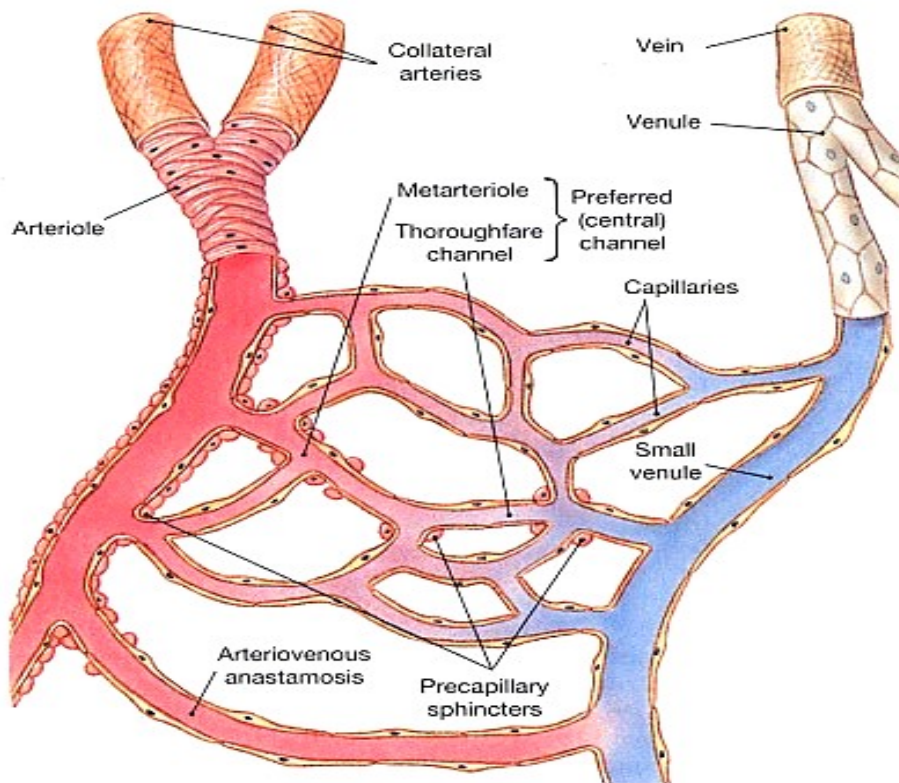


Fig. 19: Microcirculation diagram, Webliography[13].

The principal functions of microcirculation can be summarised firstly as the transportation of blood cells and substances such as oxygen and glucose to and from the cells and secondly as the regulation of blood pressure, fluid tissues and body temperature (Tortora and Grabowski, 2003).

The full process of thermoregulation is summarised in the next section.

2.1.2.4. Thermoregulation

It is known that the temperature of the hand varies according to the surrounding environment. At a constant environmental temperature of 30°C it varies on average between 32.9°C and 34.8°C, in a cool environment (20-25°C) it can vary from 24°C to 32.9°C and in hot conditions (35-40°C) it can arrive to a maximum of 35.9°C (Houdas and Ring, 1982).

Thermoregulation is the capacity of a body to maintain and regulate its temperature within a limited range of values. In humans the core temperature must be constant, around 37°C, to maintain normal organ activity. The temperature within the body can be regulated by autonomic and behavioural means, as shown Fig. 20, where the red flux represents the heat transfer path and the green the signal path (Houdas and Ring, 1982).

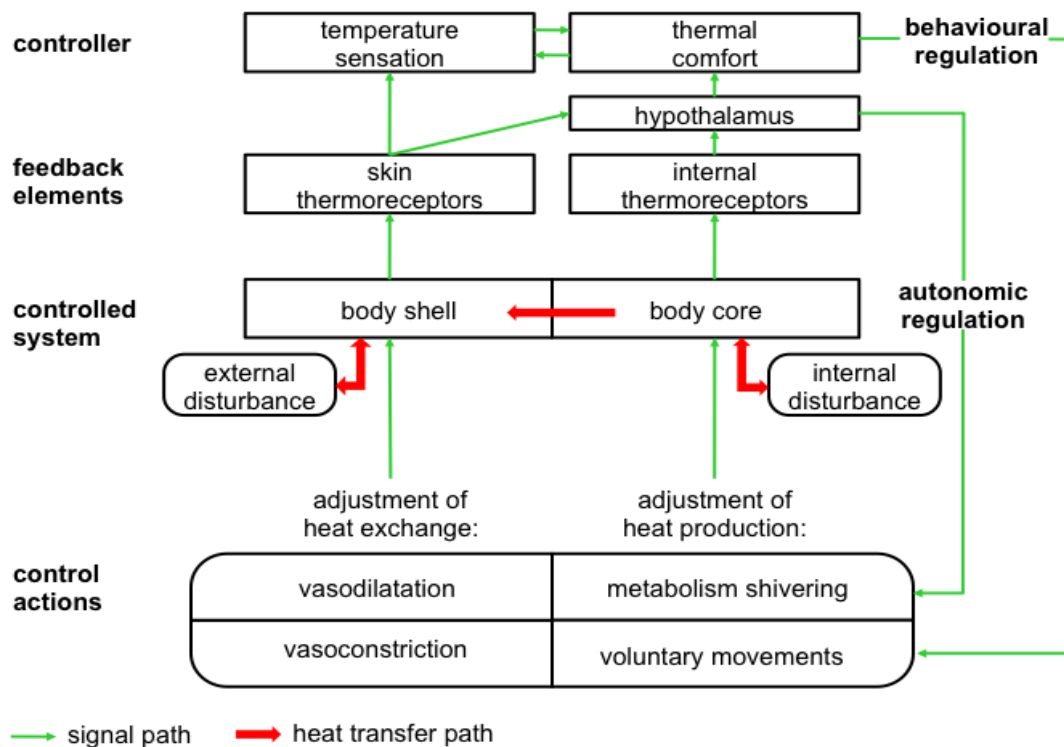


Fig. 20: Human body thermoregulation diagram according to Houdas and Ring.

Thermoreceptors are spread throughout the human body, internally sensing the temperature close to the organs and peripherally sensing the shell temperature under the dermis. Any variation of temperature values is communicated via the nervous system to the body central temperature controller, that is a group of neurons in the anterior part of the hypothalamus, known as the preoptic area. It is this area that receives nervous impulses from the thermoreceptors, mucous membranes

and other areas of the hypothalamus. Neurons from the preoptic area generate impulses at high frequency when blood temperature increases and at lower frequency when blood temperature decreases. These impulses propagate to two other parts of the hypothalamus known as the heat-losing centre and the heat-promoting centre, that when stimulated by the preoptic area set into activity a series of responses that lower or rise body temperature correspondingly. When the sensory system acknowledges a decrease in core temperature nervous impulses are sent to the preoptic area, which in turn activates the heat-promoting centre through hormones production activating the heat gain mechanisms such as: vasoconstriction (decrease on warm blood flow), shivering (muscle contractions and stretching), and a slow increase of metabolism rate. If a core temperature increase is perceived the thermoreceptors will sent nervous signals to the preoptic area, which generates hormones that inhibits the heat-promoting centre and activates the heat-losing centre, which in turn activates the body temperature decrease mechanisms such as vasodilatation and sweat glands stimulation that activate perspiration through sympatethic nervous system (Tortora and Grabowski, 2003).

The task of preserving normal body temperature presupposes an exchange of thermal energy to the surrounding environment at the same rate as it is produced by metabolic reactions (Tortora and Grabowski, 2003).

According to Tortotra and Gabowski (2003) heat can be transferred to the external environment through four mechanisms shown in Fig. 21:

- **Conduction**, where heat exchange occurs between materials or substances that are in direct contact with each other. In a unclothed resting state about 3% of body heat is dissipated via conduction .
- **Convection**, where transfer of heat happens by the movement of a fluid or gas between areas of different temperature. Contact with cold or warm water or being close to a working fan are good examples of this type of heat exchange. At a steady state the amount of percentage of heat removed from a unclothed human body by convection is about 15%.
- **Radiation** transfers heat in the form of infrared rays between two objects without physical contact. A body looses heat by radiating more infrared waves than it absorbs from cooler objects, however when surrounded by warm objects the opposite happens. In a unclothed steady state about 60% of heat loss occurs by radiation.
- **Evaporation**, which occurs when heat transforms a liquid into a gas. About 70% of the human body is composed of water, a certain amount of water is lost through the skin,

mucous membranes and breath. The amount of evaporation is directly related to the relative humidity of the air. The higher the relative humidity the lower the evaporation rate. In a situation of 100% relative humidity heat may be gained by the body through condensation of water on the skin as fast as heat is lost by evaporation. Under resting conditions the unclothed human body loses 22% of heat by evaporation.

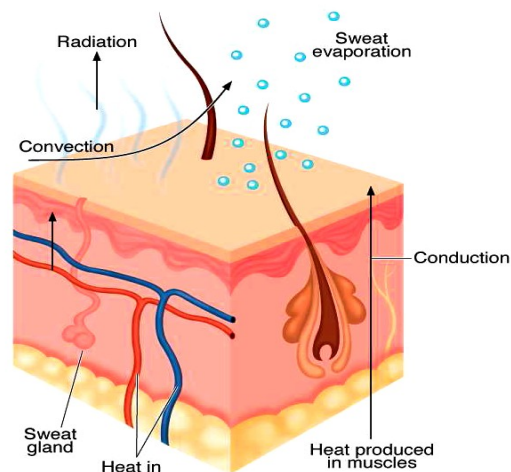


Fig. 21: Mechanisms of heat loss, Webliography[14].

The human body is very sensitive to temperature variation, it is known that for normal activity the core temperature varies between 36°C and 37.5°C, outside of that interval some functional activities start to be compromised. More than 7°C variation from the lower or upper limit can be fatal (Tortora and Grabowski, 2003).

Depending on the surrounding environment, the temperature of the skin is between 1°C and 6°C lower than the body core temperature. In order to prevent the core temperature to deviate from normal values the human body has thermal effectors, which are able to react to a need for core temperature increase or decrease (Tortora and Grabowski, 2003).

Factors such as age, body mass index and gender affect this thermoregulation, and this is a reason why they should be taken into consideration in this work. Children and adolescents have a higher metabolic rate due to the reactions present in their body as a consequence of normal growth. Older people may have lost the capability of the vasomotor system, have a very slow metabolic rate due to the ageing of cells and a reduced production of perspiration. Subjects with large body mass are less affected by heat exchange with the environment than people with small body mass. Women, due to their menstrual cycle, present core temperature oscillations between 0.2 to 0.4°C (Tortora and Grabowski, 2003).

The blood flowing in the veins and arteries of the hand is of lower temperature than in other regions of the body. This phenomenon is explained by the blood in the brachial artery being cooled by cold blood returning to the heart from the hand by way of deep veins in close proximity to the vessels – an arrangement that resembles a counter-flow heat exchanger. The method used in the hand to conserve heat consists in most of the venous blood returning from the distal section being diverted to deep tissues and therefore being heated by the blood passing through the main artery trunk. For dissipating heat the venous blood circumvents this heat trap in the form of the warmed blood passing through the main artery, being deflected initially by arteriovenous anastomoses into the superficial system of cutaneous and subcutaneous veins where the heat is then lost to the external environment (Abramson, 1967).

Since skin is a predominant organ in the hand, and since (compared to muscle tissue) only a small amount of blood is required to satisfy the oxygen requirements of the tissues of the hand, the circulation plays a majority role in thermoregulation. High cutaneous blood flow in the hand due to vasodilatation results in an increase in skin temperature. This alters the temperature gradient between the body and its environment, and produces accelerated heat loss from the skin. In a warm environment the amount of cooling of the blood as it passes through the hand is minimal, the increase in blood flow occurs without much loss of heat. Heat loss by evaporation in the hands, however, can be considerable. Due to the large number of sweat glands being located on the palmar skin of the hands and feet, large amounts of heat are lost by sweating, and as a result the extremities can have a lower surface temperature than other regions of the body. Consequently there are greater fluctuations in thermal responses to alterations in environmental temperature, especially in the fingertips. Hand microcirculation therefore plays an important role in thermoregulation through a rich sympathetic innervation of the small vessels that facilitate heat dissipation or conservation. *Temperature regulation in the hands is mainly accomplished by vasoconstriction and vasodilatation of the cutaneous blood vessels* (Abramson, 1967).

Common causes of increased temperature values of the hands can be: arthritis, trauma, infection, reactive hyperemia (caused by cold stress, warm stress and alcohol), tenosynovitis, dermatitis, bone fracture, rheumatoid algodystrophy and osteoarthritis. The opposite effect, decreased temperatures of the hands, can have as common causes: neurogenic lesions, arterial occlusion, diabetes, effects of smoking, old skin lesions (scar tissue), vasoplastic disorders, acrocyanosis, diabetic neuropathy, arteriosclerosis, disseminated lupus, carpal tunnel syndrome, Sudek's algodystrophy, dermatomyositis, scleroderma and vasospasms from smoking (Houdas and Ring, 1982).

Many of the above conditions are associated with HAS and the changes in surface

temperature and temperature regulations patterns may allow clinicians to assess their presence and severity.

2.2. Mechanical Stress

In the context of this work mechanical stress is defined as a disruption of normal homeostasis due to a mechanical challenge or task. It can be described by the reactions of the body to forces of a detrimental nature such as infections and various abnormal states that tend to disrupt its normal physiological equilibrium. Its diagnosis is complex, multifactorial and often uncertain. According to Noble (2002) currently there are three measures are clinically used for its identification: questionnaires, biochemical measures and psychological measures:

- When exposed to general stress stimuli, the body responds physiologically by increasing the activity of the hypothalamic-pituitary-adrenal (HPA) axis and the sympathoadrenal system (SAS). Stress gives rise to a number of characteristic behavioural responses. There are several different questionnaires available to quantify the level, since this is always a subjective method.
- In biochemical measures hormones are of interest. The hypothalamus releases the corticotropin-releasing hormone (CRH) and it acts on the adrenal cortex, liberating corticotropin (ACTH) and increasing the secretion of corticosteroid hormones that can be measured in various body fluids such as urine, saliva or blood.
- In measuring the physiologically response to stress, the sympathetic nervous system (SNS) is important because its activity can be used as relevance indicator. During stress response the autonomous nervous system is activated instantaneously and the balance between the sympathetic and parasympathetic components is quickly disrupted. With the sympathetic nervous activity predominant, non-invasive techniques clinically used to assess stress by physiological measures are: heart rate, heart rate variability, blood pressure, blood pressure product and electrodermal activity. All these measures require baseline and pre-stress measurements for proper interpretation.

Prolonged and repeated exposure to mechanical stress can, via the mechanisms outlined above, cause conditions such as HAS which is outlined in the following section.

2.3. Hand-Arm Syndrome

This section of the literature review outlines the medical background of a range of conditions summarised under the term Hand Arm Syndrome (HAS) as far as it is required for the understanding of this project which focuses on work related aspects of HAS only. It is not intended to be a comprehensive review of HAS.

A hand injury scoring system has been developed and proposed by Campbell and Kay (1996) to give an answer to the absence of objective tools for grading the severity of injuries that affect the hand. Their proposed system allows all types of injuries that affect the hands to be classified and subsequently compared in terms of severity.

In order to analyse separately the hand distal to the carpal anatomical components four categories were suggested: integument, skeletal, motor and neural. Each of these categories is examined in detail to cover all possible injury patterns and assigned a numerical grade according to its notable importance (table 2 of Appendix 3). The final hand injury severity score is then calculated according to the result of completing table 1 of Appendix 3 by using individual weighting factors of table 3 of Appendix 3 against the values obtained from the information of table 2 of the same Appendix (3). This is done for each finger of the subject. Finally the hand injury is classified in factors according to the obtained score (see table 4 of Appendix 3). In Campbell's study the final hand injury severity score has shown a significant correlation with the absence time of work caused due to hand injuries ($p < 0.002$). Campbell suggests that in order for scoring systems to be functional and descriptive there are factors that must be considered such as handedness, occupation, treatment and patient psychological profile. He states that a descriptive system simply outlines the exact structural damage at the time of injury, whereas in order to be more specific and of prognostic value a large number of hand injuries is needed. Although he considers that this scoring system for hand injury is a descriptive system to classify injuries into categories, it was considered to be the first stage in the evolution of a quantitative measurement of hand conditions.

The following reviews are structured into two sections, one for the general group of symptoms summarised under the label Repetitive Strain Injury (RSI) and a second one for one of its best understood sub-conditions, the Hand Arm Vibration Syndrome (HAVS). Other sub-conditions of RSI such as Carpal Tunnel Syndrome are very complex, can have other (non-work related genesis) and are generally not as well understood as HAVS. Fig. 22 outlines this hierarchy.

In each section the causes and symptoms of the syndromes are briefly explained. The emphasis of the review is on highlighting the deficiencies of current diagnostic methods and to

introduce potential avenues for improvement. These avenues will then be explored further in the following ‘Discussion’ section.

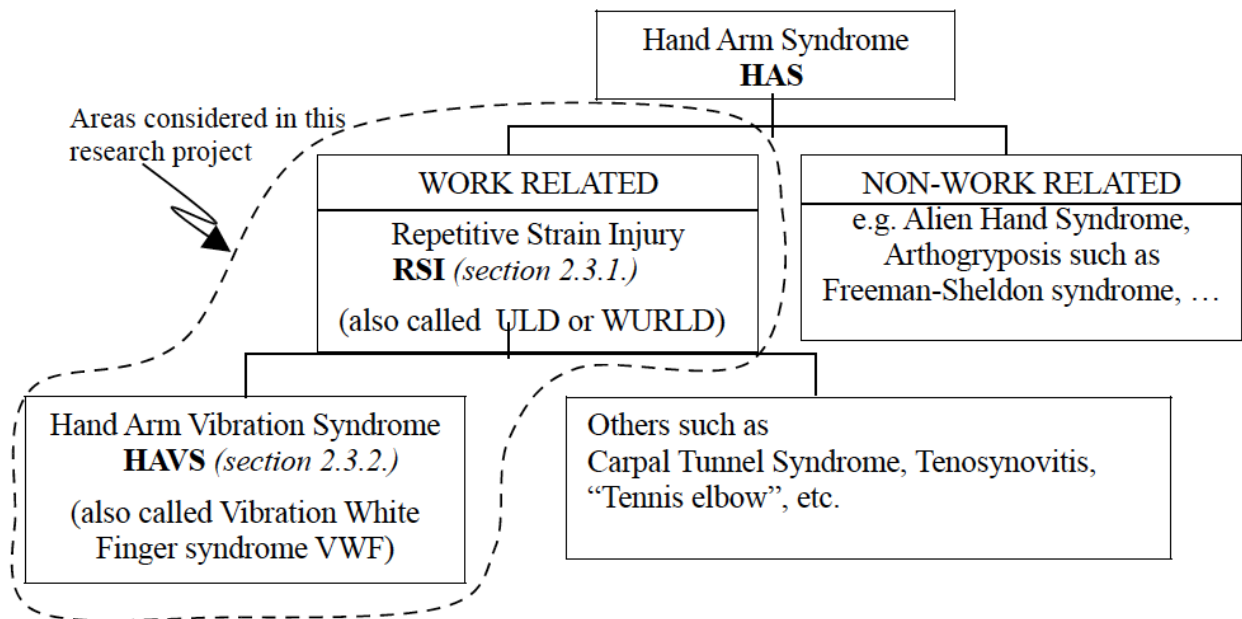


Fig. 22: Hand Arm Syndrome hierarchy.

2.3.1. – Repetitive Strain Injury (RSI)

RSI is also known as ‘cumulative trauma disorder’ or ‘occupational overuse syndrome’, it is one of a loose range of conditions due to repetitive occupational tasks and/or wrong posture affecting muscles, tendons and nerves in the upper extremities and upper back provoking chronic pain and discomfort in affected subjects. RSI can be classified into several sub-syndromes or disorders, one of them is HAVS, that will be studied particularly in this research, other muscle, tendon, nerve syndromes and disorders and cervical radiculopathies are also included in the RSI classification (Pascarelli and Quilter, 1994) but are not considered here.

RSI was first been documented 300 years ago, the first reports of a repetitive phenomenon affecting the human upper limbs were made in occupations involving clerical work and telegraphy (Physiotherapy, 1999). In technically developed countries the highest increase of RSI conditions was in the late 1970’s, mostly from the use of typewriters. With computers and consequent automation of work, this trend has continued for almost 30 years. Alongside technological advances and developments of specialised service industries the number of exposed workers continues to

grow every year (Physiotherapy, 1999).

In the UK the Government Department of Health does not accept the use of the term RSI, claiming that it is invalid as a diagnosis and that it can be misleading. The current term used is Upper Limb Disorder (ULD) or Work Related Upper Limb Disorder (WRULD), but in public media the term RSI is frequent encountered. However, in the UK RSI/ULD/WRULD as a clinical condition is recognised as a serious problem and actions have been taken: an awareness-raising campaign was started and booklets were produced under existing legislation by the government (Den Held and Cockburn, 2000).

2.3.1.1. - Prevalence of RSI

A survey on self-reported work-related illness estimated that around half a million people in the UK suffer from a work-related musculoskeletal condition affecting the upper limbs or the neck. The authors concluded that the only current monitoring system for RSI used in all EU countries is that of subjectively surveying workers. There is no other common method in use to access the syndrome or its degree of severity (Den Held and Cockburn, 2000).

According to an HSE survey, absenteeism due to RSI conditions related complaints cost 5 million working days in the UK in 1995. There are substantial numbers of claims with subsequent legal processes, the precise number, however, is unknown. The Department of Social Security (DSS) compensation recovery service recorded over 400 claims related to RSI in the year ending 31 March 1999. The Employment Relations and Union Services Health & Safety report of 1999 refers to around 2500 civil claims that are pursued by people with RSI every year, a large number of these are settled out-of-court, often for significant sums between £30,000 and £85,000 (Physiotherapy, 2001). The UK government policy on RSI specifies general duties for all employers under the Health and Safety Act of 1974 to assess and reduce risks and to ensure the health and safety of employees but there is no quantitative goal regarding the reduction of RSI related complains (Den Held and Cockburn, 2000).

An HSE awareness-raising information campaign, “good health is good business”, started in 1995 and is still running. One of its initial focal areas of concern was musculoskeletal risk, including upper limb disorders, and has subsequently covered other health risks as well. (Den Held and Cockburn, 2000).

2.3.1.2. – Causes of RSI

Several factors in everyday activities affect the soft tissues present in the upper limbs and cause a slow and progressive loss of capacity for performing those activities. The factors responsible can be divided in three main groups:

- physical,
- workplace organisational,
- and external factors.

Physical risk factors include those where a substantial amount of time is spent performing a repetitive task, like typing on a computer keyboard. An uncomfortable workplace that results in poor posture or bad positioning, awkward postures maintained for long periods of time, extended periods of overhead work, repetitive loading or lifting actions are also contributing physical risk factors. These may be aggravated in situations where excessive forces are applied by twisting or gripping motions or where working in extreme hot or cold temperatures or vibrations from power tools is required (Pascarelli and Quilter, 1994, Peddie and Rosenberg, 1997).

Workplace organisation risk factors include prolonged periods of manual work without adequate breaks, work to tight deadlines, excessive workload, monotonous work, low job control, job insecurity or dissatisfaction, poor workplace social support, unclear job roles, lack of information about workplace design, workstation and equipment design, work psychological stress and ignorance of RSI risks (Pascarelli and Quilter, 1994, Peddie and Rosenberg, 1997).

External risks identified in connection with the RSI syndrome are the degree of work difficulty and the working style:

- Weaknesses or resistance to RSI are partly inherited. While gender has been named as a factor with many authors concluding that women are more vulnerable to RSI due to their physiology and hormonal changes. Other studies contest this view and point out that there is no significant difference between genders and that men are statistically losing more work time to RSI than women (Sprout, 1997)
- A person's general health, an underlying physical condition such as diabetes or rheumatoid arthritis, fatigue or an earlier trauma to the body can be also affective.
- With respect to activities outside work, some hobbies may require repetitive activities such as when playing a musical instrument, playing video games, sewing or carpentry.

- Some studies have shown that RSI mainly affects experienced workers, although there are concerns that a new generation of young workers that are using computers and consoles may be increasing their time of exposure in addition to work related stress loads and thus negatively affect their resilience.
- The Body Mass Index (BMI) is also a factor not just because of obesity but body shape can affect workers adopting wrong postures.
- Psychology may be a contributing factor, for example, a shy person may be hesitant to openly show symptomatic signals and thus that aggravate the situation.

A downturn in the economy can contribute to RSI, increasing employee workload as can someone's lifestyle, the use of drugs, smoking and alcohol abuse, diet or even sedentary behaviour (Pascarelli and Quilter, 1994, Peddie and Rosenberg, 1997).

2.3.1.3. – Occupations at risk

Some work activities carry higher risk than others, as a result workers undertaking certain types of activities increase the probability of developing RSI. Occupations with high a risk are:

- assembly-line workers engaging in repetitive movements, reaching overhead or twisting to the side, applying thumb pressure, pinch gripping, producing ulnar deviation and having generally little control over the layout of the place of work;
- manual labourers such as butchers or bricklayers, who regularly have to twist their hands, extend and flex their wrists while applying great force;
- clerical workers such as typists and computer users are at risk due to static posture, repetition and bending wrists;
- professionals like journalists or telephone operators often assume static posture, work to deadlines while putting pressure on elbows.

The list continues with musicians, (repetition, hunching shoulders and forceful wrist motions), graphic designers (gripping with fingers and hunching shoulders), supermarket cashiers (pulling, lifting and twisting wrists repeatedly), construction workers (repetition, awkward postures and use of vibrating tools), postal workers (carrying mailbags), and many more. (Peddie and Rosenberg, 1997).

2.3.1.4. – Symptoms

There are a number of signs that are indicative of RSI, one sign by itself may not be significant for diagnosing the syndrome. A grouping of symptoms, however, is often a good indicator that RSI is present. Accepted signs that could reveal indices of RSI syndrome are:

- pain in the upper limbs, shoulders or neck,
- fatigue or lack of endurance,
- weakness in the hands and forearms,
- tingling or numbness,
- loss of sensation,
- heaviness, clumsiness of movements,
- stiffness,
- lack of control or coordination,
- cold hands,
- heightened awareness, frequent self-massage,

These signs are normally present in health assessment questionnaires for upper limb work related disorders, and according to the two following tables (table 1 and table 2) they can reveal the severity of RSI to some degree. In both tables the grade of injury is quantified according to the severity of the symptoms together with suggested corrective actions (Pascarelli and Quilter, 1994, Peddie and Rosenberg, 1997).

Degree of injury	Characteristics of pain	Remedy
Grade one	Pain is present only when performing the aggravating tasks, outside activities of daily living are not affected.	Modifications to workstation usually eliminate symptoms.
Grade two	Pain continues long after having stopped aggravating tasks, activities of daily living are affected to a small degree.	Modifications to workstation usually eases or eliminates symptoms.
Grade three	Pain continues long after work, activities of daily living are affected. Physical signs, such as tenderness or swelling are present.	Patients at this level need rest. They usually can resume work after allowing themselves time to heal and if their workstations have been modified.
Grade four	Pain is present in the morning and usually at night, but may subside on weekends; activities of daily living are greatly affected.	Patients usually require lengthy time away from work. Recovery is uncertain, though not impossible.
Grade five	Pain is continuous; activities of daily living are substantially restricted.	Patients need lengthy period of time away from work. Recovery is uncertain.

Table 1: Degrees of injury in RSI (Peddie and Rosenberg, 1997).

	Pre- RSI	Early RSI	Danger Zone	Chronic Pain	Complex Chronic Pain (RSD)
Symptom	“Funny” feeling in arms and hands	Intermittent twinges of pain or tingling while typing.	Weakness, clumsiness, pain intermittent but not necessarily relieved by rest, daily activities impaired, depression	Weakness, constant pain, not relieved by rest, made worse by any activity, disability.	Chronic pain, Reflex Sympathetic Dysfunction, dystonia, severe depression
Outcome	Relieved by rest.	Relieved by rest and rehabilitation.	Moderate risk of permanent impairment.	High risk of permanent impairment.	Permanent disability.

Table 2: The continuum of RSI (Helliwell and Taylor, 2004).

2.3.1.5. – Diagnostic methods

The most frequently used methods to assess signs and symptoms indicating RSI are questionnaires and the analysis of medical history. The most common approach is to identify all existing symptoms and the level of discomfort to the patient and then to eliminate symptoms that may suggest alternative causes such as a non-RSI related neurological deficit, joint swelling, vascular changes, young or old age (outside the 15 to 55 years bracket) and systemic symptoms.

The following step is then to consider specific diagnosis for which there may be appropriate investigations or treatment. After this the clinician attempts to identify all physical factors, which are known to be RSI risk factors (section 2.3.1.1 above).

The next step is to identify which of these risk factors are indeed important and applicable in the respective case and to isolate potential obstacles to recovery which can be:

- psychological (maladaptive illness belief and depression or psychological distress),
- workplace issues (monotony, low degree of control, poor personal relationships and high work demands),
- workplace issues,
- financial issues (disability allowance, compensation issues),
- and attitudes of the individual.

After this, the clinician will need to assess if there is evidence of physical damage and that continued activity (moderated according to the “Remedy” column of Table 1) will not lead to damage. It is recommended that the patient should not take time off work, if possible. If symptoms persist advice is taken about activity modification, this must be coordinated with the person’s work supervisor or employer. Some analgesic may be provided if necessary for symptom control, often being prescribed regularly rather than when is required. If symptoms persist the whole process is reviewed after a few days or weeks (Helliwell and Taylor, 2004).

The above procedure is common in many places and countries; it does not contribute a solution to the problem and it does not satisfy the needs of the patient.

In only a few cases the diagnosis is solely based on symptom descriptions collected by questionnaire using tables such as the ones shown above, in most cases clinicians will also perform a dedicated RSI examination after reviewing the medical history of the patient. This is normally achieved using three main avenues of examination: looking for clinical signs, testing muscular functions, and testing for nerve damage (Helliwell and Taylor, 2004).

Appendix 1 provides an overview table of current diagnostic methods in use for RSI. Briefly, there are four main muscle test performed, the wrist flexion test, the grip strength test, the pulp pinch test and Finkelstein’s sign test.

Seven tests are conducted to assess nerve damage; they are: Phalen’s manoeuvre, detection of Tinel’s sign, nerve conduction studies (or electromyography, EMG), the Semmes-Weinstein monofilament test, the Weber two-point discrimination test, the use of Magnetic Resonance Imaging (MRI) and the use of X-Rays. On rare occasion’s video analysis has also been used in

order to isolate the problem. (Pascarelli and Quilter, 1994).

To date only three pilot projects have been conducted that were aimed at introducing a standard test for the assessment of the syndrome:

- The first project used computer assisted thermography and was undertaken in Cambridge in 1997. Using thermography the project attempted to quantify temperature changes in the forearm of keyboard users suffering from chronic forearm pain. A specific typing speed and an acclimatised room were used, but the results reported were found not to be significant, probably due to the poor protocol guiding the use of the technique (Sharma et al., 1997).
- In the same year another study was performed at Middlesex Hospital School of Physiotherapy using a vibration meter to obtain threshold vibration measurements in patients with RSI and in computer keyboard users. These tests were performed under a more rigorous protocol in a controlled temperature room with a patient acclimatisation period of 20 minutes. Office workers presenting early signs of RSI were identified from a quantitative measurement of vibration perception. This approach may prove useful in patient assessment and for detection of the early onset of RSI in the work environment (Greening and Lynn, 1998).
- The latest of the three studies was a pilot conducted in Vienna (Austria) with the goal of demonstrating a relationship between cold fingertips developing while type writing and the duration of keyboard operation. 15 healthy females participated in acclimatised room at 24°C and after 15 minutes of acclimatisation. From this study it was concluded that in healthy subjects after 5 minutes of typing the temperature initially increased in the forearm and fingers, but after 15 minutes typing a high percentage showed cold fingertips and further increased temperature in the forearm. The pilot suggested that continuous typing eventually results in a vasoconstriction (narrowing of blood vessels) in the fingertips – causing them to cool, while muscular activity in the forearm produced the heat excess observed there (Ammer et al., 2001).

In conclusion, currently there is:

1. no standardised test for the diagnosis of RSI,
2. a total lack of methods for a preventive screening test and
3. no objective and repeatable means for quantifying existing lesions.

These are the three problems that will be addressed in this work.

2.3.2. – Hand-Arm Vibration Syndrome (HAVS)

HAVS is the second main proponent of Hand Arm Syndrome. Workers exposed to hand-transmitted vibrations may experience various vascular and neurological related disorders of the hand, although not all frequencies, magnitudes or durations of vibration cause the same effects. In order to enable reporting and comparison of exposures, there is a need for the exposure to be measured and evaluated using defined standardised protocols. Furthermore it is necessary to identify what should be measured and how measurements should be expressed, taking in account the components of vibration (magnitude, frequency, direction, waveform and duration) and assessing their impact according to criteria such as the probability of a specific severity for a specific form of the disease. With current assessment protocols it is also difficult to gauge the importance or weight of different frequencies, the axes of vibration, vibration magnitude and daily exposure durations for HAVS (Griffin, 2006).

It is understood that Hand-Arm Vibration Syndrome affects the circulatory, nervous and musculoskeletal systems and is provoked by a progressive and excessive exposure to vibration over a prolonged period of time. The term HAVS is used to describe a range of injuries that can be incurred after excessive exposure to vibration when using vibrating tools with Vibration White Finger (VWF) syndrome having the highest prevalence, clustered around certain industries (Claim, 2007).

VWF is composed of three main components:

- circulatory disturbances i.e. vasospasm and finger blanching,
- sensory and motor nerve damage resulting in tingling, numbness and/or loss of dexterity,
- musculoskeletal disorders with changes in the structure of the joint, bone or muscle

(Coughlin et al., 2001).

It is of importance to this work that VWF, like RSI is one of the conditions producing so called secondary Raynaud's phenomenon, where exposure to a mild cold stress (water at 20°C for 1 minute) provokes intense and often painful narrowing of peripheral blood vessels and thus a reduction of the blood supply (hence the white finger) followed by unusually long recovery times where dilatation of blood vessels and re-perfusion only eventually cause the affected limb to warm up again (Claim, 2007). These changes can be monitored and quantified with digital thermography given the right methodology is followed.

2.3.2.1. – Prevalence of HAVS

One of the largest personal injury schemes in British legal history, is the scheme to compensate coal miners and their families for occupational respiratory diseases and HAVS. A Medical Research Council (MRC) survey in 1997-8 gave an estimate of 288,000 sufferers of VWF in Great Britain - 255,000 males and 33,000 females (HSE, 2007). To illustrate the cost to society it is worthwhile to consider that in the same year the High Court awarded £127,000 each in compensation to 7 coal miners for VWF.

In 2000 a survey by Southampton University concluded that the exposure to hand-transmitted vibration is surprisingly prevalent and although Raynaud's phenomenon is common in the general population, many cases can be attributed to hand-transmitted vibration, especially in men. This emphasises the public health importance of this common occupational hazard in Great Britain (Palmer et al., 2000a, Palmer et al., 2000b). The number of annual new cases of VWF assessed for disablement benefit under the Industrial Injuries Scheme (IIS) was 865 in 2004/05. An estimated provisional of 549 cases of HAVS was seen by rheumatologists and occupational physicians in 2005 (HSE, 2007). The government is at the moment paying around £2 million every working day in compensation for vibration related injuries. Until November 2006 around 120,000 VWF claims were made, more than 21,000 in Wales alone, excluding many others that have not yet been registered with HSE (Claim, 2007).

HAVS is very difficult to prove in court, the process is slow, the evidences should be strong, and courts are facing the task of striking a balance between suspicious false claims and awarding legitimate compensation. A claimant's detailed, clear and accurate but subjective description of

symptoms is not enough. Support, for example by objective photographic evidence of vascular symptoms corroborated by expert medical opinion has shown to be helpful (Platt, 2006).

An Italian physician (Acciari, 1977) has performed the first study on occupational lesions from vibrating tools with infrared thermography. In that study he defined a vibrating tool as a device operating at high speed with low amplitude oscillating movements. He stated that the most dangerous vibrations to the human extremities were in the range from 30Hz to 80Hz. The vibration amplitude was described as the distance travelled through one oscillation and vibration acceleration as the parameter perceived by the person exposed and reported in meters per square second. The methodology followed by this study was to take a thermal image of the hands before a cold vascular provocation, then using an exposure to water at 5°C for 5 minutes, followed by thermographic recordings in 5 minute intervals. This test was not considered 'fair' in law due to the difficulty in turning the fingers white without previous exposure to vibration. The infrared thermal imaging technique was compared with the photoplethysmography modality.

The outcomes from this study were:

- Control healthy subjects had recovered from thermal stress within 15 minutes.
- Vibration injured affected subjects had recovered from thermal stress in an average of 40 minutes.
- After the provocation:
 - Thermography was extremely useful in objectifying the subjective symptoms.
 - Thermography was very demonstrative under standard conditions.
 - Infrared thermography had identified 84% of the pathological cases and photoplethysmography had identified only 24% of the clinical confirmed cases.

This study concluded that thermography is a suitable choice for a diagnostic method in liability and insurance cases, and also in occupational and forensic medicine (Acciari, 1977).

The same Italian researcher, Acciari, conducted a subsequent study assessing vibration tool angiopathy with thermal imaging. His findings in mean temperature differences from the fingertips to the metacarpals per each finger after vibration exposure were -1.2°C for the thumb and -1.9°C, -1°C, -0.9°C and 0.2°C for the index, middle, ring and little finger correspondingly. The dorsal hand

presented to be warmer at the radial region and cooler at the ulnar region. The author suggested the usage of thermography for the assessment of vascular, nervous and osteoarthritis diseases. He strongly proposed to use thermal imaging as a diagnostic tool for pathologies involving vibration and prognostic data for vascular or neuronal traumatic lesions or in sudden atrophy (Acciari, 1978).

2.3.2.2. – Causes

As already indicated above HAVS can be caused by the progressive and excessive exposure to vibration that is transferred from a tool to a worker's hands and arms and workplace exposed to cold temperatures.

This disorder is characterised by a complete episodic closure of digital blood vessels. Although either central and/or local pathogenic mechanisms may be involved, this pathogenesis is not fully understood yet because the pathophysiological mechanisms underlying muscular disorders in workers operating vibration tool are often unclear. Disorders of organs, nerve fibre dysfunction resembling entrapment neuropathy and diffuse or multi-focal neuropathy are thought to be related to working with vibrating machines causing neuropathy to peripheral nerves, mainly sensory ones but also those of the motor and nervous system. Any of the nerves of the upper limbs may also be affected as this disorder is not confined to the digits. It can also extend to the palm and the arms (Griffin and Bovenzi, 2002).

The consumption of alcohol, tobacco or drugs as well as the individual lifestyle also influence the risk of contracting HAVS. Age is another important factor that is thought to be linearly correlated with vibration exposure history. People that work a long time exposed to hand-transmitted vibration tend to be more susceptible to acquiring the syndrome. According to a 2004 study from Sweden that examined working women exposed to hand-transmitted vibration, there is no difference between genders with respect to power absorption during vibration exposure (Bylund, 2004).

2.3.2.3. – Symptoms

The main symptoms of HAVS are apparent in the fingers. Patients report that these can become numb and turn white, and spasm may occur due a lack of blood supply. The main symptoms of HAVS are thus two fold: vascular effects are expressed as coldness and blanching of one or more fingers and neurological effects manifest themselves as tingling sensations, “pins and

needles” and numbness. The neurological symptoms can arise independently and pre-date vascular symptoms.

In most individuals the condition is not severe and attacks only cause minor discomfort. In more extreme cases, however, repeated or constant ischaemic episodes can result in skin ulcers and even gangrene requiring surgery or amputation. Picking up small objects such as pins or nails will become more difficult as the sensory capacity of the fingers decreases, along with a loss of strength and grip of the hands. Pain, tingling and numbness in the arms, wrists and hands can make sleeping difficult (Griffin and Bovenzi, 2002).

2.3.2.4. – Vibration and vibration quantification

The term vibration can be defined as mechanical movement that oscillates in the form of a wave about a fixed point. Each wave produced by vibration is characterised by four components, as can be observed in fig. 23: frequency (number of cycles per second, measured in Hertz [Hz]), acceleration (change in velocity over time, measured in meters per square second [m/s^2]), velocity (the rate of change of position, measured in metres per second [m/s] and displacement (vector that specifies the change in position of a point to a previous position, quantified in metres [m]) (Mansfield, 2005).

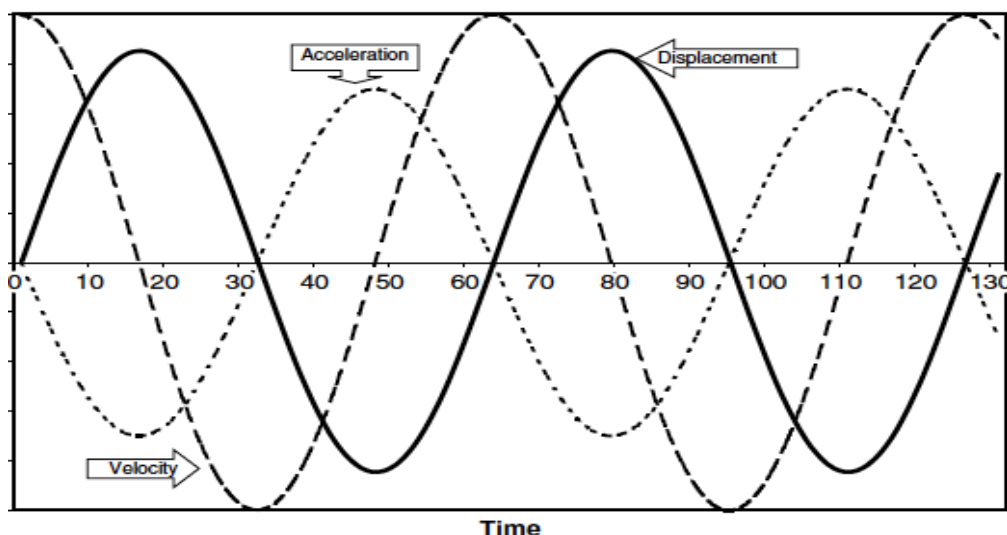


Fig. 23: Components of a vibration wave, (South, 2004).

These quantities can be used to assess the magnitude of a body's exposure to vibration. The frequency (f) is normally known and the acceleration (a) is the value usually measured, knowing these two values the other two can be obtained:

$$v = a / (2 \pi f)$$

$$d = v / (\pi f) \text{ or } d = (2 v^2) / a$$

where v is velocity, d is displacement and a is acceleration.

Calculating the averaging vibration levels over time is difficult because these levels are rarely constant. In order to simplify this calculation the 2001 edition of ISO 5349 therefore recommends the following formula to obtain a daily average vibration level:

$$a_{hv(eq, 8h)} = \sqrt{\frac{a_{hv1}^2 x t_1 + a_{hv2}^2 x t_2}{T}}$$

where a_{hv} is the acceleration averaged over the entire period T, a_{hv1} is the acceleration for the first sub-period t_1 and a_{hv2} the acceleration for the second sub-period t_2 . T is the sum of sub-periods t_1 and t_2 . In order to calculate an 8h or daily equivalent level, known as A(8) the above formula can be simplified into the one presented below (South, 2004).

$$A(8) = \sqrt{\frac{a_{hv1}^2 x t_1 + a_{hv2}^2 x t_2}{8}}$$

The current exposure limit value to vibration is defined in the 2002 version of ISO 5349 and is addressed by an European Directive recommended for all member states to incorporate into their national legislation. The UK government agreed with this and accepted to accommodate it in its domestic legislation. The directive established as exposure limit a value for A(8) of 2.5 ms^{-2} and an exposure maximum limit value of 5.0 ms^{-2} . The HSE, in order to simplify the exposure calculation from a single period of exposure, has implemented the chart presented in fig. 23 where by knowing the time of exposure and the weighted acceleration the draw of a line “calculates” the partial vibration exposure without the need for calculations (South, 2004).

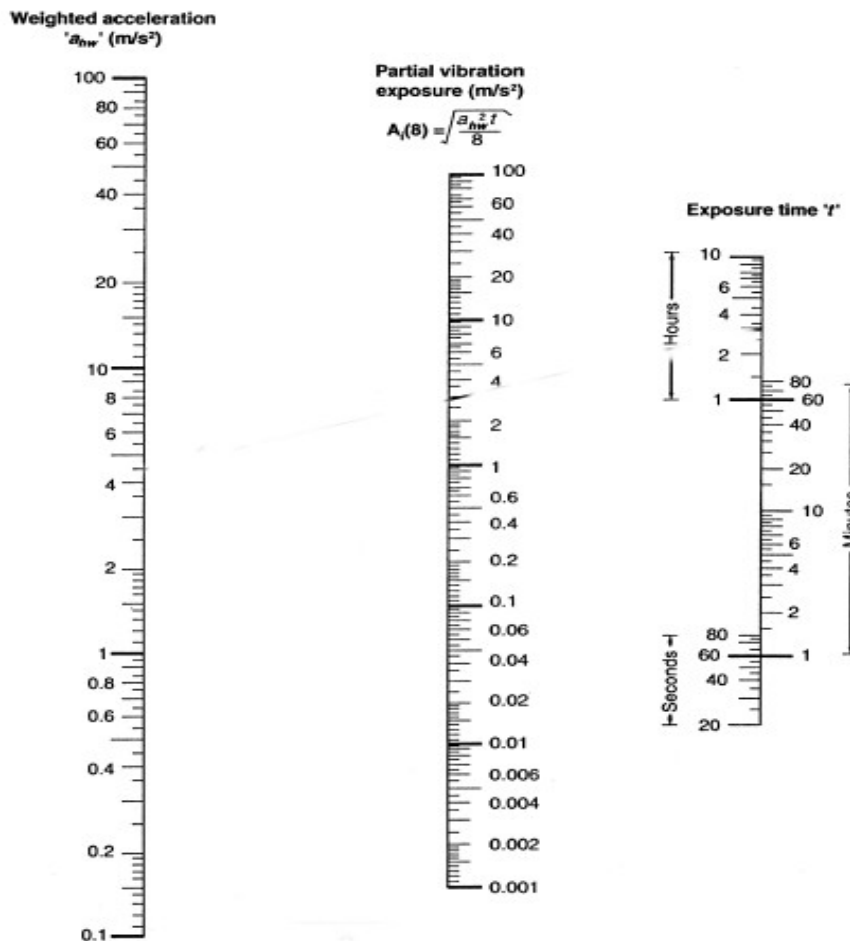


Fig. 24: HAVS partial exposure calculation chart (South, 2004).

2.3.2.5. – Occupations at risk

According to the Industrial Injuries Advisory Council document ‘Prescribed Disease A11’ (PD A11), HAVS is defined as:

“[...] cold-induced, clearly delineated, episodic blanching occurring through the year, affecting the distal with the middle phalanges or proximal phalanges, or in the case of the thumb the proximal phalange [...] persistent numbness or persistent tingling of the digits and a significant and demonstrable reduction in both sensory perception and manual dexterity of the digits [...] onset occurs after work involving one or more of the tools or occupational exposures listed [...]” (McGeoch et al., 2005).

The same document defines the type of jobs at risk of developing HAVS as those where vibrating or rotation tools such as chainsaws, hand-held rotary tools for grinding, sanding or polishing metal are used. Activities involving the holding of material being ground, working with

percussive tools, riveting, chipping, hammering, fettling or swagging are also increasing risk. Heightened risk can also be attributed to the use of hand-held powered percussive drills or hand-held percussive hammers in mining, quarrying demolition, roads or footpaths construction or pounding machines in shoe manufacture (McGeoch et al., 2005).

2.3.2.6. – Diagnostic methods

Vibration injury to the hands was first reported in 1911 in Italy by Loriga in workers using compressed air tools (Pelmear, 2003). In 1975 the Taylor-Palmear scale shown in table 3 for assessing vibration effect injuries was published. Only ten years later it was listed in the UK by the Industrial Injuries Advisory Council (IIAC) as PD A11.

Stage	Grade	Description
0	--	No attacks
1	Mild Occasional	attacks affecting the tips of one or more fingers
2	Moderate Occasional	attacks affecting the tips and middle sections of the fingers (rarely the base of the fingers) on one or more fingers
3	Severe Frequent	affecting the entire length of most fingers attacks
4	Very Severe	As in stage 3, with damaged skin and possible gangrene in the finger tips

Table 3: Taylor-Palmear scale (Gemne et al., 1987).

Two alternatives to the Taylor-Palmear scale were introduced in Stockholm in 1987. The vascular scale shown in table 4 and table 5, however, was subsequently exposed as deficient in that the frequency of blanching attacks is supposed to be used to determine severity. This turned out not to be the case and severity can instead be determined from the results of properly conducted objective vascular tests, such as using a mild cold stress test (water at 20°C for 1 minute) together with thermal imaging (Pelmear, 2003). Both scales, like the Taylor-Palmear scale, are entirely subjective.

Stage	Signs and symptoms
0V	No attacks
1V	attacks affecting only the tips of the distal phalanges of one or more fingers
2V	Occasional attacks of whiteness affecting the distal and middle (rarely also the proximal)
3V	Frequent attacks of whiteness affecting all of the phalanges of most of the fingers
4V	As 3V and with tropic changes

Table 4: Vascular stages of the Stockholm Workshop scale for HAVS.

Stage	Signs and symptoms
0SN	Exposed to vibration but no symptoms
1SN	Intermittent numbness, with or without tingling
2SN	Intermittent or persistent numbness, reduced sensory perception
3SN	Intermittent or persistent numbness, reduced tactile discrimination and/or manipulative dexterity

Table 5: Sensory-neural stages of the Stockholm Workshop scale for HAVS.

In 2002 Griffin developed a method of scoring (fig. 25), that can be used to map where blanching symptoms occur. It can be applied to any other type of symptoms that occur in relation with HAVS. The shaded areas correspond to the zones where blanching typically occurs. The author of this map has assigned a score value to each anatomical region of the fingers to record the severity of the condition (Mansfield, 2005).

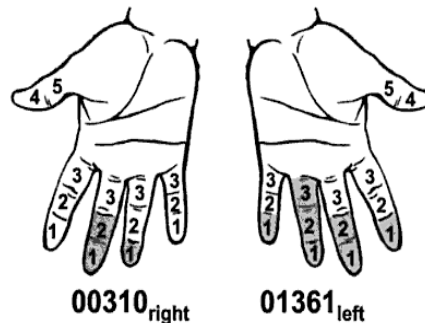


Fig. 25: Griffin's method of scoring areas of the fingers affected by blanching, (Mansfield, 2005).

Several clinical and laboratory tests have evolved and became available over the years to assist physicians in evaluating the three components of HAVS. A recent paper, however, concluded that diagnosis and medical tests for HAVS are notoriously crude and can be inaccurate due to clinicians using unsophisticated methods to assess patients (Platt, 2006).

In the UK the current “gold standard” method to diagnose HAVS is based on the five stages in table 3. Every year workers at risk complete a questionnaire, followed by a routine health surveillance performed by a “responsible person”. If symptoms or signs of HAVS are shown, a long series of examinations commences. In order to demonstrate the complexity (and inadequacy) of this process the various stages are briefly outlined below. (Appendix 2 presents an overview table of the diagnostic methods mentioned).

1. Inclusion tests:

These tests establish if HAVS could be present.

- Musculoskeletal tests are prescribed to assess the injury severity. These tests should be performed by a “qualified person” (McGeoch et al., 2005). An examination of the fingers, hands and the upper body is carried out by a clinician to assess trophic changes and/or the presence of musculoskeletal abnormalities. Four tests are performed: the Allen, the Phalen, the Tinel and the Adson test.
- In addition muscular tests are used to verify if weakened muscle and losses of dexterity are present. These tests are the grip force measurement test, the pinch force test, the Moberg pick up test and the Purdue pegboard test. (Sampson, 2006).

2. Exclusion tests:

If the muscular and musculoskeletal tests are positive, the clinician will continue to exclude certain conditions which may cause HAVS-like symptoms.

- Vascular tests. A check on the peripheral pulses, for example, is used to exclude peripheral vascular disease, a check on the blood pressure in both arms is used to assess if unequal blood pressure indicative of proximal vascular occlusion is the problem.
- This is followed by tests for connective tissue disease, which can also produce HAVS like symptoms. If no symptoms such as hair loss, alteration of skin texture, a deposit of calcium in soft tissues or focal red lesions due to visible dilation of small blood vessels under the skin are suggesting connective tissue disease "*we can be in presence of HAVS, although some more tests need to be conducted also to act as a recorded proof of the injury, and also to assess its state of severity*" (McGeoch et al., 2005).

3. Confirming tests:

If doubts about the state of the disease persist the following confirming tests will be performed.

- In order to assess the normal blood flow pattern, some additional vascular tests will be performed e.g.: cold provocation test, finger systolic blood pressure test (Lawson and Navell, 1997), the use of colour charts and the nail compressions test (Lewis Prusik test).
- In order to detect if there is a loss of nerve function the sensorial and neurological tests

available are: light touch test, pain sense test, two-point discrimination test, deep sense perception test, monofilaments, vibration sense test, vibration threshold test (VTT) and thermal aesthesiometry (TA). (Lawson and Navell, 1997, Sampson, 2006).

Only now, when a patient is finally found to develop or is already suffering from the disorder provoked by hand-transmitted vibration in a work situation, it is recommended that he/she should not be returned to the same work vibration exposure situation or that changes should be made to their work situation (Griffin and Bovenzi, 2002).

In contrast to this elaborate procedure the already mentioned Italian study that used thermography as a diagnostic technique for assessing vibration injury (Acciarri, 1977) in conjunction with a study by Bovenzi et al. (2000) may offer a faster and more accurate means of diagnosis. Bovenzi concluded that acute exposures to vibration (with equally weighted magnitude) reduces the finger blood flow for all frequencies between 31.5 and 250Hz. While duration of digital vasoconstriction after vibration increases with frequency the constriction severity diminishes: results the study showed that for an exposure time of 2 minutes the frequency with highest reduction of finger blood flow and simultaneously with the shortest recovery time was 31.5Hz.

In conclusion:

1. HAVS is a particular manifestation of RSI.
2. As an RSI sub-group it suffers from the same the problems as RSI (no single standardised test, lack of simple and effective methods for a preventive screening test and no objective and repeatable means for quantifying existing lesions).
3. In addition, as shown above, HAVS is difficult to diagnose.
4. Thermography of hands exposed to low frequency vibration at 31.5 Hz for 2 minutes may be a more suitable alternative.

2.4. RSI related questionnaires

A Canadian questionnaire was run on an adult working population to assess the predictors of work-related RSI. From the 2806 respondents, 10% reported RSI related conditions and it could be concluded that women of ages between 30-50 years old with a high demand of repetitive tasks and working more than 30 hours were more associated with RSI. The same study revealed that subjects having smoking habits demonstrated to be more affected than non-smokers, however the difference is very small (Cole et. al., 2005).

In order to characterise hand injury incidence and severity in a sample population, a group of scientists (Levine et al., 1993) developed a self-administrated questionnaire. The questionnaire is assessed according to the sum values of the answers per respondent using a grading into 5 different symptomatic stages (no symptoms, mild symptoms, moderate symptoms, severe symptoms and very severe symptoms) and 5 different functional stages (no difficulties, mild difficulties, moderate difficulties, severe difficulties and very severe difficulties). This questionnaire has demonstrated to be reproducible (Pearson coefficient of $r=0.91$), internally consistent (Cronbach alpha of 0.89), responsive to clinical change ($p<0.01$) and able to measure dimensions of outcomes not captured by traditional measurements of impairment of the median nerve (Levine et al., 1993). This questionnaire will be used to characterise the incidence and severity of hands injuries in the academic population at the University of Glamorgan as one of the scopes of this work.

2.5. Thermography

This sub-section describes the basic concepts of thermography, introduces the thermal imaging parameters and quality assurance techniques, emphasises the importance of standardisation in thermal imaging, presents the software available for capture and analysis of thermal images, resumes the use of thermal imaging in medicine and its relevance, states the suggested medical IR imaging capture protocols and enumerates the non-invasive alternatives to thermography comparatively.

2.5.1. Physical principles

The National Physics Laboratory (NPL) defines “*temperature (T) as the measurement of the average energy of the microscopic components (usually atoms or molecules) of which an object is made. If the measurement is made based on the temperature of a black-body (an object that absorbs all radiation that approaches it at any wavelength and emits it again in a continuous spectrum) then the microscopic components are the photons which make up the electromagnetic field within the blackbody cavity*” (NPL, 2009). The temperature difference between two points, hotter and cooler, can be expressed by the rate of heat transfer.

Over the ages different methods have been used to measure that function and different scales have been developed, the current international standard is the Kelvin (K), which is based on the triple point of the water (absolute zero corresponds to $-273.15\text{ }^{\circ}\text{C}$). The common scale derived from this used in occidental Europe is the Celsius ($^{\circ}\text{C}$), a centigrade scale between the ice and boiling points of the water. The conversion of these two scales can be obtained by the formula $T(\text{K}) = T(^{\circ}\text{C}) + 273.15$. In this study and thesis all temperature values will be given in Celsius.

The quantity of electromagnetic energy radiated from an object is related to its temperature. An object can be characterised by emitting or absorbing electromagnetic radiation, such radiation distribution forms the electromagnetic spectrum, which is characterised by frequency and wavelength and it influences physiological responses such as vision. The visible light is a small portion of that radiation distribution but the only one that the human eye can discriminate. On the higher frequency side of the electromagnetic spectrum, as can be observed in the fig. 26, are the ultraviolet, the x-rays and the Gamma rays , in the opposite direction with longer wavelengths and frequencies, as indicated by fig. 26, are the infrared, microwaves and radio waves.

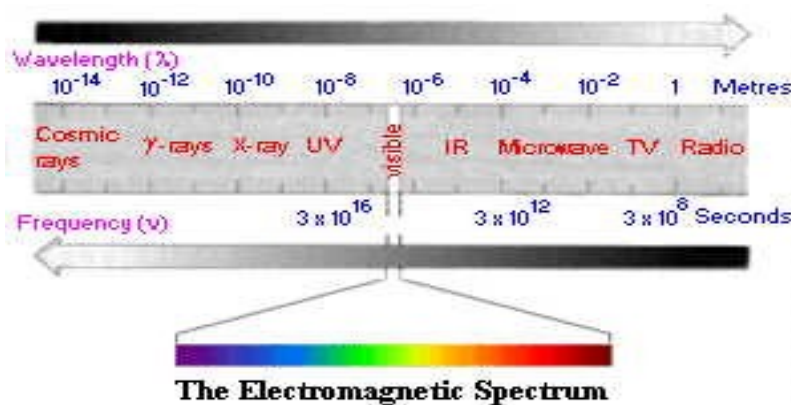


Fig. 26: The electromagnetic spectrum, Webliography[15].

Infrared radiation was discovered in 1800 by Sir William Herschel in an experiment where he demonstrated (measuring with mercury thermometers) the heat of colours produced by sun light passing through a glass prism, as can be seen in fig. 27.

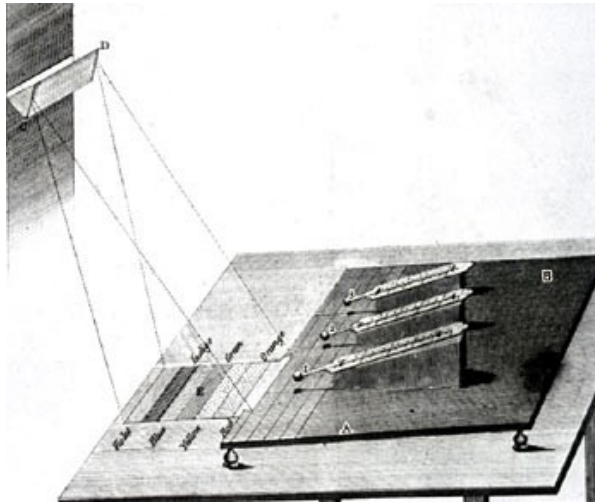


Fig. 27: Herschel's apparatus on discovering infrared radiation, Webliography[16].

The black-body is taken as a standard of comparison for radiation sources. The radiation emitted from a black-body can be described by three expressions: Plank's radiation law, Wien' displacement law and the of Stefan-Boltzmann equation (Thomas, 1999).

The Planckian distribution of temperature, is described in this formula and demonstrates that short wavelengths result from high temperatures and long wavelengths from low ones (fig. 28). Wien's displacement law mathematically illustrates that colour may vary from red to orange or yellow as the temperature of the radiation increases (fig. 29). The Stefan-Boltzmann equation states that the total radiated energy from a black-body, per unit area, per unit time, is proportional to the fourth power of its absolute temperature (fig. 30). Most total radiation thermometers are based on this equation (Thomas, 1999).

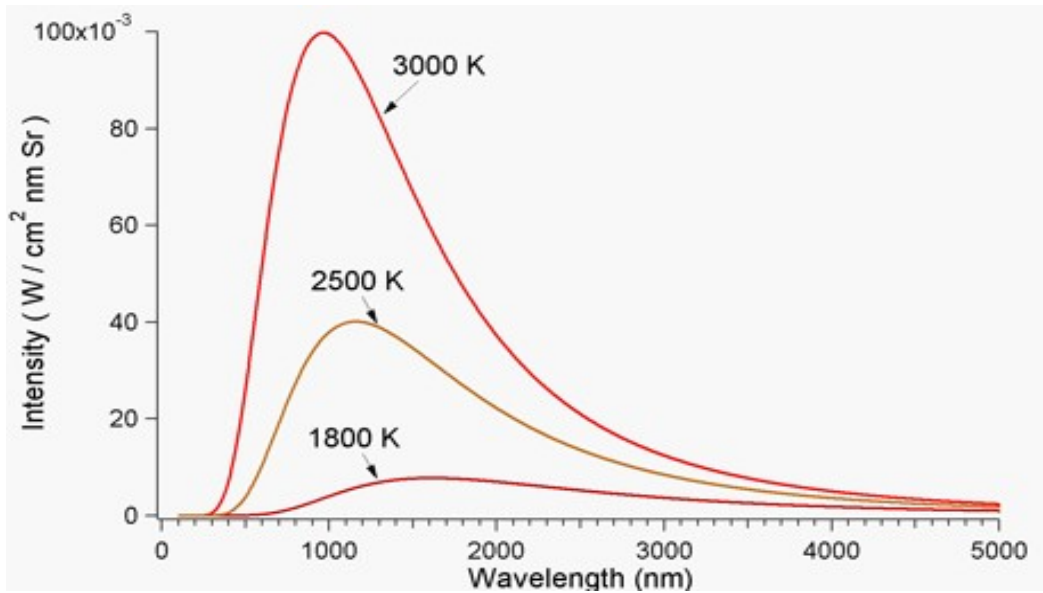


Fig. 28: Planck's radiation law, Webliography[17].

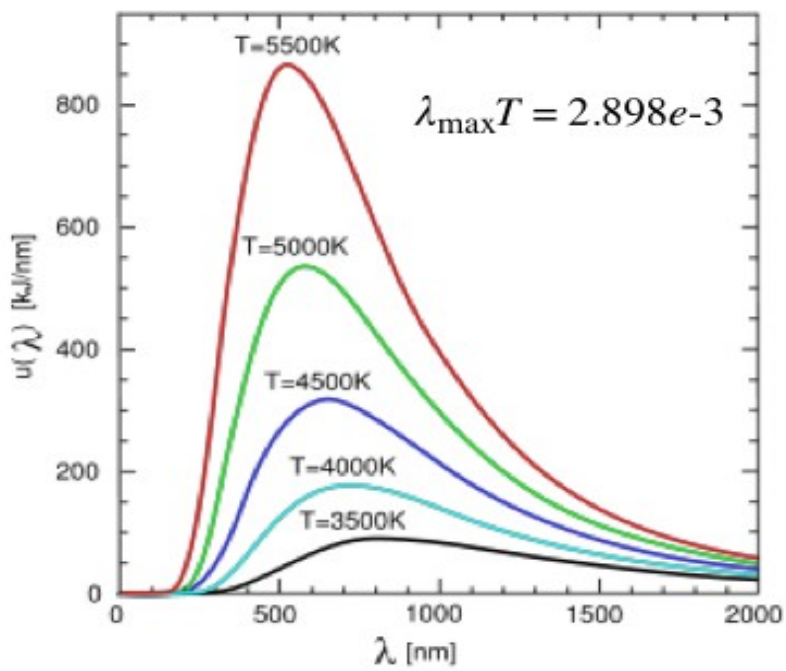


Fig. 29: Wien's displacement law, Webliography [18].

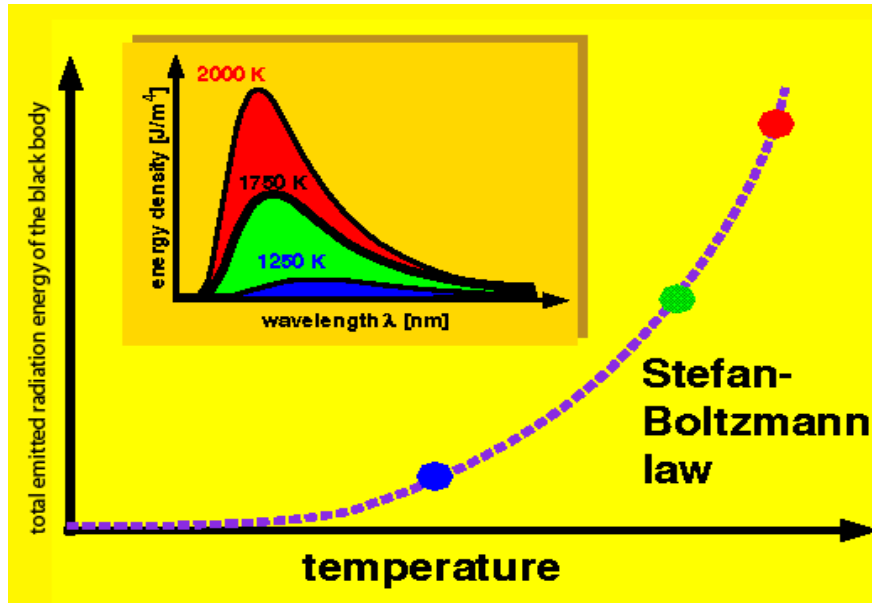


Fig. 30: Stefan-Boltzmann function, Webliography[19].

$$M = \sigma T^4$$

M – total radiance (W/m^2)

σ – Stefan – Boltzman constant (5.6697×10^{-8})

T – absolute temperature of emitted material (K)

Fig. 31: Stefan-Boltzmann equation, Webliography[20].

It is very difficult to obtain an object that complies completely with the Stefan Boltzmann equation (fig. 31) over an extended wavelength region. Several factors may affect the radiation on the object surface such as spectral absorption, spectral reflectance and spectral transmittance. The relationship between these three factors can be explained by Kirchoff's law (Thomas, 1999).

The fraction of the radiant emittance of a black-body produced by an object at a specific temperature is known as emissivity. This factor also affects the accuracy of temperature measurements through infrared radiation. The emissivity value of a material can be obtained by calculating the ratio of the energy emitted at a given wavelength to that of a black body at the same temperature. The emissivity value range is between 0 and 1. A perfect black-body has an emissivity value equal to 1 (Thomas, 1999). Human skin, studied in this project, is almost a perfect radiator, and has an average emissivity of 0.98 irrespective of skin color (Houdas and Ring, 1982).

The use of infrared detectors to monitor temperature changes goes back to 1880 when Langley invented the bolometer which could detect heat from an object 400 meters away. The

temperature detection by infrared detectors relies on the radiated heat reaching its detector cell. These cells can be thermocouples, microbolometers, pyroelectric or ferroelectric elements. The thermistor bolometer is based on the change in resistance of a semiconductor when heated by radiation, which can be a slow response due to a variety of thermal processes involved. However, new developments in detector technology offer increasingly faster responses. Examples of this are radiometric microbolometers which are DC coupled for detecting temperature change and ferroelectric and pyroelectric devices, which detect temperature by changes in capacitor charges. By being AC coupled and chopper dependent, however, it is difficult to make them radiometric (Thomas, 1999).

2.5.2. Infrared cameras

Infrared cameras are the instruments used in thermography to record and monitor object temperatures through surface irradiated heat. Manufacturers often hide important aspects of equipment technical specifications or over-simplify them, which can make it difficult to fully understand and characterise the equipment in use. The relevant camera characteristics, however, have to be known when the aim is to accurately monitor temperature changes. A brief summary of the relevant factors is presented in this section, which is just an introduction to the technology. For a better understanding (a full review is beyond the scope of this work) refer to Thomas (1999).

Wavelength

There are generally two types of cameras available, grouped by the spectral wavelengths they are susceptible to. So called 'long wavelength systems' (2-5 μm) are more sensitive to lower temperatures and are less affected by radiation attenuation over long distances, 'short wavelength systems' (9-12 μm) in contrast are more sensitive to higher temperatures but normally this type of camera is restricted in terms of distance from the target (maximum about 200m). These 2 camera types usually also differ in the type of detector they use. Commonly, the long wavelength systems are characterised by using Platinum Silicide (PtSi) or Indium Antimonide (InSb) detectors, cooled by liquid nitrogen, Peltier elements or other refrigeration devices. They are more expensive but offer a better thermal sensitivity. The short-wavelength systems are usually uncooled cameras that use Mercury Cadmium Telluride (MCT), Microbolometer and Quantum Well Infrared Photodetectors (QWIP) as detectors (Thomas, 1999).

Lenses

As important as detectors are the lenses. They are made of Silicon (Si) or Germanium (Ge), which are materials that have good mechanical properties, are mechanically resistant, non-hygroscopic and can be formed into lenses with advanced turning methods. Germanium lenses are used for long-wavelength cameras and Silicon ones for short-wavelength cameras. IR camera lenses have antireflective coatings and block visible light and other non-desired wavelengths from reaching the detector. There are two main types of lens: normal angle lenses (ca. 24° opening angle), which are used for closer distances, and wide angle lenses (ca. 45°) for circumstances where the target is further away. The internal design of the lens system is also very important; if adequate the system should transmit close to 100% of incident radiation (FLIR, 2009).

Mode of operation

IR cameras can be also characterised by the image construction system employed by the detector. Two types are commonly used: scanning systems and Focal Plane Arrays (FPA). FPAs are more common nowadays due to a significant decrease in the price of technology in recent years. They also perform faster and now tend to provide higher image quality (Thomas, 1999).

Sensor range

One of the major issues in medical thermography is that camera manufacturers generally have not produced devices exclusively for clinical use (although some are starting to come onto the market at the time of writing). The temperature range advertised by the manufacturers varies from -40 to +1000 or +2000°C, mainly to suit industrial applications. The temperature range is the ability of a thermal sensor to detect heat radiation over a given range and over such a large range the accuracy of detectors tends to be in the region of +/- 2°C (e.g. for a typical microbolometer). For medical use, however, the recommended range is usually only from 25°C to 42°C, but in situations involving cold provocation stress this may be between 17°C and 42°C (Ring and Ammer, 2000). The accuracy should be higher by at least a factor of 10 (i.e. +/- 0.2°C). This could not be achieved by the camera itself, an external calibration source is required to ensure the required accuracy.

When capturing images using a thermal camera a range of parameters have to be taken into consideration. These are: thermal resolution, spatial resolution, accuracy, repeatability, responsivity, dwell, portability, focus, temperature range, operating distance, emissivity, ambient radiant reflectance and the presence of varying objects shapes and surroundings (Thomas, 1999). All these parameters may affect the measurements and lead to errors. A brief description of these parameters is presented in the next paragraphs.

Thermal Resolution

Thermal resolution is the smallest difference in temperature that an instrument can discriminate. Camera manufacturers describe this parameter usually provided in the form of Noise Equivalent Temperature Difference (NETD). In practice this measure is not particularly useful or even meaningful because NETD degrades over time, its measurement requires specialised equipment (e.g. oscilloscope) and its measurement procedure is not standardised (Plassmann et al., 2006). Thermal resolution is characterised by two main factors: noise and digitisation step width (Plassmann et al., 2006). Inappropriate thermal resolution results in measurement errors. This parameter can also be quantified by the Minimum Resolvable Temperature Difference (MRTD), a curve that indicates the relationship between the temperature difference needed and a particular size of object to be perceptible. The latter is described by the Slit Response Function (SRF). This variable is determined by imaging a blackbody source through a slit which is initially opened wide and then reduced gradually in width producing a graph of apparent temperature over slit width. The common SRF width of the slit value quoted is the milliradian angle at 50% of the radiance received by the imager and obtained from the traced graph (Thomas, 1999).

Spatial Resolution

The minimum size that can be resolved by a thermographic system is given by the spatial resolution measure, which defines the clarity or fineness of object detail reproducible in an image. This parameter is often referred as the total number of pixels (picture elements) displayed in an image. It is calculated by multiplying of the number of pixel displayed horizontally by the number of pixels displayed vertically. The smallest area that can be resolved by a detector is defined by the

Instantaneous Field of View (IFOV). This is the projection of one detector element in the image, or part of it. A system with high spatial resolution has small detector elements and a correspondingly smaller IFOV. It is calculated from the ratio between the detector dimension by the focal length and its values is presented in milliradians (Thomas, 1999).

Accuracy

Accuracy in thermographic terms is a measure that represents how much a measured temperature is deviating from the true value. It can be presented as an absolute uncertainty (e.g. $\pm 2^{\circ}\text{C}$) or a proportion of the indicated temperature (e.g. $\pm 2\%$). Another word for accuracy is 'bias' or 'offset'.

Precision

In the context of this work precision is defined as repeatability. It is the degree to which repeated measurements under unchanged conditions show the same results.

Responsivity

The time response of an infrared detector to incoming radiation is its responsivity. The type of detector (e.g. thermal, photon) and the efficiency of the detector cooling system determine this specification (Thomas, 1999).

Dwell

Dwell describes the period of time over which the detector is exposed to radiation before the signal is taken from it. For small detectors a longer integration time is needed due to smaller amount of radiation that it can receive. A typical integration time for a FPA is about 16ms in which one complete image frame is produced. The amount of energy that a detector captures at any given

temperature may be reduced by shortening the dwell time. In FPAs it is simpler to measure higher temperatures by changing the detector dwell electronically rather than to install an attenuation filter (Thomas, 1999).

Object emissivity

Emissivity is the ratio of radiated emissive power of an observed object to that of a blackbody at the same temperature. Its value varies in the interval between 0 and 1 (where 1 corresponds to the blackbody value). Infrared cameras therefore have the ability to change their emissivity settings so that it matches that of the observed object. This has to be done manually which is a potential source of error. The recommended emissivity value of 0.98 to analyse human skin temperature is well known and documented (Houdas and Ring, 1982). Temperature measurements rely on the correct setting of emissivity values. Both emissivity and environment temperature combined affect the temperature readings, it can be corrected retrospectively by image processing. When the emissivity value is set to 1, the environment temperature setting of the camera does not affect the measured temperature of the observed object. The environment can have a significant impact in the emissivity particularly when sweating or shivering.

Camera to object distance

Accurate temperature measurements are influenced by the distance from the target to the camera lens. A greater distance from a target results in a lower temperature reading due to the absorption of radiation by air, especially air moisture.

A second factor is the diminishing apparent size of an object at increasing distance. Here an important indicator to help the camera operator in placing the instrument at a correct distance from the target is given by the spot size ratio of the lens. This provides the minimum target size for valid measurement, although it varies according on the lens and camera. The maximum distance from the target is given by multiplying the minimum target size by the spot size ratio (Thomas, 1999). The recommended operating distance for monitoring temperature changes in the upper limbs of the human body with an IR camera is between 1m and 1.5m (Ring, 1988).

Stray Radiation

Another factor that affects accuracy and precision of temperature measurements is the reflection of ambient radiation on observed objects. This is radiation that is transmitted and/or reflected by the surroundings from a number of sources straight into the lens or reflected off the surface of the object of interest. Since human medical infrared examinations are not normally conducted outdoors (veterinary ones may, however) there is no need to consider sun light in this work although concern must be given to artificial room lighting which should be carefully chosen in order to prevent ambient radiant reflection (i.e avoiding incandescent spot light sources in favour of colder ones such as strip lighting).

A second source of stray radiation is the inside of the camera itself and caused by internal radiation produced by the materials that the camera is made from. In order to minimise these internal effects a re-imaging lens system is recommended by Thomas (1999).

Object characteristics

An object's physical characteristics such as shape and surface condition can influence temperature measurements by IR imaging. Object shape influences the angle between the infrared camera and sections of the object. If the incident angle is less than 60° the energy emitted into the camera by human skin starts to decrease significantly thus altering the measured temperature. This phenomenon can be observed at the edges of limbs which always appearing cooler than the centre part of the limb. For thermographic examinations an incidence angle between camera and object of interest which is close to 90° is therefore recommended.

All aspects and parameters mentioned above are relevant to this work and have to be taken into consideration in order to obtain correct temperature measurements and to develop a valid standard technique of temperature recording with thermography. This standardisation aspect is explored further in the following section.

2.5.3. Thermography in medicine

The technique of infrared imaging has been developed and was used primarily for military purposes. The first known usage of this technique in medicine was in 1957 by Ray Lawson, a Canadian physician, when he was investigating surface temperature changes in female subjects suffering from breast cancer with an Evaporagraph (a device where heat induced evaporation of a volatile substance is used to record temperature). In Europe, in the early 1960s, Lloyd Williams, at the Royal National Hospital for Rheumatic Diseases in Bath (England), has been a pioneer of the usage of the technique in medicine, with a particular emphasis on limb disorders (Ring, 2003). The application of this technique in medicine had in the beginning several limitations such as poor quality of the image, and the large size of the capture devices. With the evolution of the electronic components on which this imaging modality depends and improved image capture procedures the number of applications increased as did their quality and results (Ring and Ammer, 2000).

From these beginnings the conditions where the applications of infrared thermography is nowadays indicated were: vascular diseases, myeloma, spinal disorders, rheumatic disorders, nerve pathology, neurological disorders, deep venous thrombosis, reflex sympathetic dystrophies, referred pain syndromes, diabetic microangiopathies, open heart surgery, early detection of skin cancer and breast disease and general cancer (Head, 2002). With the evolution and miniaturisation of the electronics in the infrared imaging systems in tandem with the development of appropriate image capture protocols the application of this imaging technique is growing in medicine (Jones and Plassmann, 2002). However, attention to underlying physical principles is required to avoid malpractice.

As already mentioned this medical procedure is based on a process of recording the radiant emitted energy in the form of heat from the body surface and transforming the obtained signals into visible digital images through an imaging system (Jiang et al., 2005). Apart from the before mentioned parameters that affect the IR camera itself there are series of factors that influence the proper use of this modality in a clinical context: the most prominent ones are the parameters of the investigation room, the ambient temperature control, the imaging system, the temperature control reference and patient positioning. These aspects will be addressed in the following sections.

2.5.4. Importance of standardisation

The existing literature lacks information on reference values of temperature distribution on the human body surface. Infrared thermography, unlike any other medical imaging modality such as radiology, does not have a generally accepted range of standardised positions to improve the quality of temperature recordings. Although it is obvious that the standardisation of the technique would reduce substantially the errors. Literature describe the reproducibility of the technique only vaguely (Ammer, 2003).

It is known that environmental conditions such as temperature, humidity and air circulation affect the measurements as well as laboratory conditions (e.g. false ceilings where air may be filtered and no direct air flow is affecting the subject, double glazed windows and illumination). Patient preparation and clothing have an influence in the measurements; likewise the pre-examination acclimatisation period. The imaging system has to comply to quality assurance requirements (section 2.5.6) to avoid affecting the process of acquiring the image. The usage of standardised area of interest (AOI) masks (discussed later in this document), for example, will enforce the quality of the recording by facilitating correct subject positioning and distance from the camera as well as the size and position of the AOI itself. All these variables have to be taken into consideration in order to homogenise the capture and analysis process and to allow comparisons and the generation of reference data (Ring et al., 2004).

In the specifications of the University of Glamorgan project aimed at building a reference database of the distribution of the temperature of human body surface (Ring et al., 2005), 24 views of the human body were defined and the following aspects of medical thermal imaging were standardised:

- Subject preparation, before and during examination;
- Imaging system, including calibration and quality assurance requirements;
- Capture protocol;
- Image analysis;
- Image storage;
- Examination reporting;
- Education and training of clinical users of thermal imaging.

According to Ring et al. (2004) the usage of standard procedures allows repeatability, facilitates understanding and knowledge exchange and reduces the amount and influence of variables. In medical thermography this is a relevant aspect as some past errors were made due to the lack of using a standard image capturing methodology (Ammer, 2003). This in turn lead to a decreased application in medicine and considerable loss of credibility. The aspects that influence this technique are described in the section 2.5.2 of this document can only be addressed properly if a standard protocol is followed.

2.5.5. Proposed standard medical thermographic protocols

In 2006 the American Academy of Thermology (AAT) suggested a document which specifies the purpose, common indications, contraindications and limitations of using Infrared Thermography in medicine (Schwartz, 2006). This document describes how this technique should be conducted in terms of:

- Patient communication and preparation;
- Patient assessment;
- Examination guidelines;
- Reviewing the examination;
- Presentation of the examination findings;
- Examination time recommendations;
- Continuing professional education.

The objective of this document is to standardise the technique, offering the opportunity for multi-centre data exchange and modality improvement.

Ammer (2008) suggested what is called the 'Glamorgan Protocol'. It establishes the guidelines for a standard medical thermographic examination specification based on:

- using standard views;
- the indication of the reliability of each view;

- cold challenge tests;
- patient preparation pre and during examination;
- examination room conditions;
- imaging system operation;

This protocol is now being followed worldwide as it is based on the experience of several years of usage of the modality and it accommodates and integrates the AAT proposal. An important factor of this protocol is that it is generic. It therefore has to be adapted to the actual area and object of interest to be investigated.

2.5.6. Quality assurance in a thermal imaging system

In order to ensure that the infrared camera system is giving optimal performance and consistent reliability, Plassmann has developed a set of practical tests (Plassmann et al., 2006) to determine the most critical parameters that affect thermal image recording. These are:

- Start-up drift. The amount of time needed after powering-up of the system for its stabilisation. This time can differ considerably from the value advertised by the manufacturer, which is a severe concern. This parameter should be checked every three months.
- Long-term drift. A temperature drift may be introduced into the measurements by the ageing of the camera's electronics components. This aspect is important, because it can indicate when the camera needs to be recalibrated by the manufacturer. This aspect is considered to be of medium severity. This parameter should be checked every three months.
- Offset variation over a temperature range is an error in the measurement that can be introduced by the camera sensor array readout having a different amplification for different temperatures. This aspect is medium severe. This parameter should be checked every couple months.
- The thermal flooding effect is caused by the introduction of a warm (or cold) object into

the observed scene. In the case of a warm object this causes flooding by stray radiance. All imager types have this problem and it is important to know its expected value. An increased value is indicative of sensors malfunction but overall this is an effect of low severity. This parameter should be checked every couple of months.

- Image non-uniformity occurs when the sensor cannot detect the correct radiation of the objects in the corner edges of the imager as a result of deficiencies in the optical path. It results in a degradation of the captured image and is an aspect of medium severity. This parameter should be checked every couple of months.

2.5.7. Software for medical thermography

The vast majority of infrared imaging software available in the market was not developed for medical use, Camera manufacturers produce software to operate in a much wider range of temperatures than those used in medicine. The applications are dedicated mainly to industrial applications and consequently offer only basic statistical analysis of the images but highly specialised, industry specific reporting features. The Medical Imaging Research Unit at the University of Glamorgan has, in cooperation with Polish collaborators, developed the C THERM software package and specifically designed it for medical thermography (Plassmann and Murawski, 2003). The package runs on the Microsoft Windows[®] operating systems and is independent of the camera hardware provided that the camera manufacturer provides the correct device drivers. It aids the investigator by providing pre-defined AOI masks that help to position the patient at the correct distance and position.

After providing image capture features, the C THERM software stores the infrared images in a local database which provides support for image handling operations such as searching, deleting, importing/exporting to and from Bitmap format and the definition of colour palettes. The stored images can be statistically analysed either by user-defined AOIs or cross-sections. Importantly for this work a particular tool allows cold stress test assessments and provides detailed reporting features.

The C THERM software, however does not have any tools for image enhancement, edge detection, interpolation and warping of images all of which are thought to be required in the context of this work in order to allow an automatic or semi-automatic solution for analysing AOIs of

thermograms of upper limb disorders.

2.5.8. Non-invasive alternatives for medical thermography

In this subsection some non-invasive imaging alternatives to infrared imaging used in medicine to record human body peripheral temperature are presented along with a brief characterisation and comparative information with respect to the advantages and disadvantages when compared with infrared thermography. From a group of temperature monitoring techniques the selected representatives are: Liquid Crystals Thermography, Laser Doppler Flowmetry, Full-field Large Perfusion Imaging and Photoplethysmography.

Liquid Crystal Thermography is a system that uses thermally sensitive liquid crystals embedded between two sheets of flexible plastic material. This system reacts to heat flow by producing different colours as a function of temperature when illuminated by white light (Meyers et al., 1989). This response remains present for a short period of time only, which implicates that for a permanent record a digital photography of the liquid crystal sheet has to be taken. While the liquid crystals themselves have a temporal resolution of up to 10 milliseconds the fact that they are embedded in thermally slowly adapting plastic sheets means that the overall response time is in the range of several seconds. The technique is nevertheless widely used in medicine when screening of a large group of subjects is required. Its major applications in medicine are the diagnosis of inflammations, evaluation of skin tests, traumatology and forensic medicine (Stasiek et al., 2006). The advantages of this technique are that it is inexpensive, easy to use, virtually unbreakable, has an accuracy of 0.1°C, is very simple to calibrate, suitable for curved surfaces, has very high spatial resolution (< 1 micron) and is reusable after a short period of time. It has as disadvantages the necessity of an additional method for producing a permanent record, the difficulty of reading temperatures under low light conditions, having a limited temperature range, the fact of being a slow technique and not being suitable for large surfaces or surfaces with non-uniform deepness (Meyers et al., 1989).

Laser Doppler Flowmetry is a modality for measuring blood flow in the peripheral blood vessels. When a laser beam is pointed towards tissue and the flowmetry system scans the movement

of the red blood cells by analysing the Doppler scattered signal reflected back into a photocurrent sensor. The result is a dimension-less blood flow measurement value (called 'flux') expressed in a quantity proportional to the product of the average speed of the blood cells and their concentration. These systems screen tissue samples to about 1 millimetre depth and resolve blood flow speeds from 0.01 to 10 mm/s. This method is able to register flow in various types of blood vessels such as arterioles, capillaries and venules. It maps the blood flow speed to a colour map according to the defined colour scales. It is an easy to use technique with an output directly proportional to blood flow speed (not volume) that allows instantaneous measurements of dynamic processes. Scanning a larger skin is, however, a slow process (although faster, all real-time systems are coming onto the market at the time of writing), and only moderately eye safe which requires the use of safety goggles. This technique is used in medicine for analysing vascular areas, burns, looking for inflammations and abnormalities such as tumours (Terada et al., 2007, Stikbakke and Mercer, 2008). A strong correlation was found when examining healthy controls and primary Raynaud's patients after cold provocation stress (section 2.7). From this study Schlager (2010) concluded that thermography can substitute Laser Doppler perfusion imaging for skin surface temperature assessment, the main reason being that it is more time effective and there is no laser required.

Full-field Laser Perfusion Imaging (FLPI) is a non-invasive instantaneous technique of monitoring 2D microvascular flow maps. It is based on Laser Doppler Perfusion Imaging but behaves differently due to the diverging laser beam illumination of the skin and contrast assessment in the resulting speckle pattern (Buick et al., 2009). This technique performs up to 4 times faster than conventional scanning laser Doppler imaging methods (Serov et al., 2005). The advantages of this modality are that it is a very fast recording method, allows dynamic processing, is easy to use and is safe. On the other hand are the disadvantages of being expensive and the maximum skin areas that can be record being limited in size to an area of 8cm x 12cm. FLPI is a very recent screening technique and consequently more studies are required to correlate the proportionality of its outcome to blood flow values. Preliminary studies demonstrated that assessing cold stress challenges with this method follows a similar trend but to a different time-scale (Buick et al., 2009).

Photoplethysmography is an optical technique of measuring blood volume changes in peripheral tissues based on the optical properties of the selected skin area. With a naked eye it is possible to perceive that regions with less blood are apparently more white in colour and regions with more blood are darker. This method uses the same principle (Allen, 2007). The underlying

mode of operation is to emit a non-visible (near-)infrared light into the skin and according to the amount of light absorbed by the skin the blood volume is calculated. The advantages of this technique are the low cost, facility of use, instantaneous results, applicability for dynamic monitoring and can be used to measure bilateral symmetry. The major disadvantage of the method is that it measures across a small skin area only. Medical applications of this method are clinical physiological measurements, including monitoring, vascular and autonomic function assessment (Allen, 2007). At the time of writing an emerging photoplethysmography (PPG) imaging technique is being proposed by scientists at Loughborough University for non-contact measurement of skin blood perfusion over a wide tissue area. They claim that with such technique it is possible to measure both pulse rate and blood perfusion (Zheng et al., 2009).

None of the alternative techniques summarised above satisfy all the requirements for this work of being easy to use, fast and providing measurements across a large area of skin from a single measurement. On the positive side they are able to provide a direct measure of blood flow while in thermography (being an indirect method) the relationship between thermographic image and blood flow is inconclusive (Buick et al., 2009).

2.6. Thermal physiology reference data

When conducting temperature studies in areas of interest (AOIs), two of the values taken in consideration are the mean temperature of the AOI and its standard deviation. In order to identify pathological manifestations or abnormal temperature patterns, these values alone do not provide sufficient information. Based on the fact that the human body is bilateral and practically fully symmetric with respect to its extremities the indication is that the human body could have a bilateral temperature symmetry between two AOIs in co-lateral locations. This had been suggested by Freeman in 1936 when he and his team conducted a study demonstrating a different bilateral temperature distribution between healthy controls and schizophrenic patients (Freeman et al., 1939). Based on this measure Lloyd Williams (1964) in England stated that significant differences in bilateral temperature symmetry could be related to pathological states such as structural abnormalities of blood vessels, abnormalities of vascular control, local effects on blood vessels, changes in thermal conductivity of the tissues and increased heat production in the tissues.

- The first attempt to characterise reference values of bilateral thermal symmetry using thermal imaging was made by Uematsu (1986). He used an Agema thermal camera with an image resolution of 140x140 pixels and equipped with a computer interface. He did not specify any acclimatisation period for the study volunteers or any examination room conditions. The skin surface area was divided into 32 segments (AOIs) with hair covered areas of the body being avoided. His findings in bilateral temperature differences are summarised in table 6. He used 32 healthy controls and 24 patients with peripheral nerve impairment. In the symptomatic patients the presented average difference between the normal side and the side with the nerve damaged was 1.55°C; six times the difference found in normals that was 0.3°C. The difference between temperature symmetry in healthy controls and patients was statistically significant ($P < 0.001$).
- In the same year Goodman and his team (Goodman et al., 1986) performed a study on temperature symmetry in the back and extremities using computer assisted infrared imaging. The infrared camera they used was the same model as Uematsu's. They used a sample of 31 healthy volunteers that had been physiologically assessed by physical examination and clinical records. A pre-recording protocol enforced 2 days avoidance of prolonged sun exposure and 2 hours without eating, drinking, smoking or drugs before examination. In the examination room the volunteers disrobed and underwent an acclimatisation period of 20-25 minutes at 20.5°C ($\pm 0.5^\circ\text{C}$), with a low relative humidity. As a calibration device a pair of (near-)infrared light-emitting diodes spaced at 10 cm situated alongside of the subject were used (which have a relatively constant far infrared, i.e. heat output to be used as calibration reference). Each thermogram was performed in such a way that a spatial resolution of about 1mm and a temperature resolution of 0.5K at 1m was achieved. Repetitive temperature calibration was performed with standard blackbody sources. A total of 9 different body views were used. Each image AOI was divided into slices and compared with those obtained from the other side. The results are shown in table 6. It was concluded from this study that mean temperature bilateral differences in the same AOI higher than 1°C should be considered as abnormal.
- In 1988, Uematsu and his colleagues performed a second, larger study aimed at the quantification of thermal symmetry with consideration given to normal values and reproducibility (Uematsu et al., 1988). A total of 90 healthy subjects collaborated in this study. Two infrared systems (JTG-500 M thermometry and Eye 160 thermometry) both

controlled by computers were used. An acclimatised examination room with temperature ranging from 23° to 26°C and humidity between 45% and 60% was used. The thermography guidelines of Pochaczewsky were followed (Pochaczewsky et al., 1986). All subjects disrobed and acclimatised in the room for 20 minutes. The body surface was scanned using 90,000 data points per scan, one every mm, and the distance between the body and the recording equipment was of 50cm. The system used was able to discriminate differences of 0.03°C and able to quantify mean temperature and standard deviation values for each defined AOI. In this study some sympathetic bilateral symmetry responses were recorded in the context of a cold stress to the feet. The results are shown in table 6. The AOIs studied in this investigation demonstrated to be reproducible with a coefficient of variation of 0.1%. On healthy controls the recovery from cold challenge to the feet presented to be bilateral symmetrical, for pathological states a discrimination value of 0.1°C was suggested. No significant difference was noted from using two different capture systems.

- The latest large study into study bilateral temperature symmetry was conducted in Taiwan on 57 healthy subjects (35 males and 22 females with ages ranging from 24 to 80 years old) investigating 25 different AOIs with thermography (Niu et al., 2001). An acclimatised room at 21 ± 1 °C and 50-60% relative humidity was used. The thermal camera used was an Avionics TVS-2000, a Japanese cooled camera with thermal detectors of indium antimonide (InSb) with a 10 element array detecting wavelengths from 3 to 5.4µm, distinguishing a difference as small as 0.1°C and with the ability to scan an image in about 0.033 second. After 20 minutes of thermal equilibrium a set of three full-body thermal images were taken at 15 minute intervals. From each image 25 AOIs were analysed. An analysis was conducted where the researchers obtained overall values and verified differences between genders and age groups (where subjects with age less or equal to 60 were compared to older than 60). The results are shown in table 6. This study concluded that the human thermoregulatory system is substantially symmetrical, the maximum difference value obtained for an upper limb AOI in healthy subjects was of 0.5 ± 0.4 °C. From the age group comparison no difference was found between hands, digits and anterior forearms ($p < 0.05$). Elderly people presented a lower average skin temperature than younger ones. From gender comparisons it is clear that only the palm of the hands, digits and arm AOIs did not present statistical evidence of difference ($p < 0.05$). The average skin temperature was higher in the distal extremities.

Study		Uematsu, 1986	Goodman,1987	Uematsu, 1988	Niu, 2001
AOI	dorsal arm	0.22 ± 0.15°C	NO DATA	0.39 ± 0.26°C	0.50 ± 0.40°C
	anterior arm	0.13 ± 0.15°C	NO DATA	0.27 ± 0.23°C	0.50 ± 0.40°C
	dorsal forearm	0.32 ± 0.16°C	0.95 ± 0.10°C	0.31 ± 0.22°C	0.50 ± 0.30°C
	anterior forearm	0.23 ± 0.20°C	0.42 ± 0.06°C	0.31 ± 0.25°C	0.30 ± 0.20°C
	dorsal hand	0.38 ± 0.06°C	0.62 ± 0.10°C	0.31 ± 0.25°C	0.40 ± 0.30°C
	palmar hand	NO DATA	0.59 ± 0.10°C	0.31 ± 0.23°C	0.40 ± 0.30°C
Abnormality value		> 1.55°C	> 1°C	> 1°C	>0.5°C

Table 6: Reference values of bilateral thermal symmetry of AOI using thermal imaging (from previous studies).

From the above 4 studies it can be concluded that bilateral temperature symmetry can be a relevant indicator for identifying pathological states, however, the concept of thermal symmetry requires further specification since different methodologies appear to provide different results. An updated set of data produced under the control of a standard capture and analysis protocol for medical thermal images and generated with the current generation of high resolution thermal cameras and analysis software is therefore required.

2.7. Hand vascular test

Episodes of constriction of small arteries and/or arterioles of hands and feet, with sequential changes in colour of the skin, pallor, cyanosis and usually following exposure to cold is a condition known as Raynaud's phenomenon (Chucker et al., 1971). This frequent medical problem was firstly described by Maurice Raynaud, a French physician who in 1862 stated that it is related to a large number of conditions such as neurological and/or vascular diseases that can affect the extremities (Ring, 1988, Ammer, 1996). Thermography is a well known method to document this reaction of hands to a moderate cold challenge, e.g. diagnosis of Raynaud's phenomenon and Complex Regional Pain Syndromes.

Ring proposed, designed and implemented an objective and quantitative vascular provocation test to assess the presence of Raynaud's phenomenon in the hands (Ring, 1995). The test protocol prescribes that after a period of acclimatisation in a room of 22°C for 10 to 15 minutes

a thermal image of the hand should be taken as a baseline. After this first record the subject is asked to wear a thin plastic glove and to immerse the whole gloved hands avoiding any contact for a period of 60 seconds in a bucket filled with water at 20° C. After withdrawing the hands from the bucket and removing the gloves the hands are positioned in a resting position facing the thermal camera at a 90° angle (perpendicularly) and an infrared image is taken 10 and 20 minutes after the cold challenge. (The 20 minute image is only needed if the subject experiences difficulties in recovering to normal temperature within 10 minutes). Other authors suggested different water temperatures for the cold provocation and different times for exposure recovery, but the method described above has proved to be effective and provides a statistically significant difference between healthy controls and Raynaud's affected subjects. Other reasons for these time and temperature values are that the subjects remain comfortable (water at 10 degrees, can, for example, be very painful for Raynaud's sufferers) and that the recovery will be achievable within the limited time available for a routine clinical test (Ring, 1995).

To present the results of the cold stress test to clinicians Ring defined a simple index that expresses the temperature gradient difference between the fingers and metacarpal areas of the hand (fig. 32). It can be calculated automatically by a computer program application from the two IR images taken before and after the cold challenge. The index value is calculated by first determining the temperature change in each area shown in fig. 32. For each hand the two area figures are then added to arrive at the final index value. This is graphically shown in fig. 33. The thermal gradient in both hands is given by the formula: $F1-M1+(F2-M2)$, where F1 is the average mean temperature of the fingers area of the right hand, M1 is the average mean temperature of the metacarpals area of the right hand, the F2 is the average mean temperature of the fingers area of the left hand and M2 the average mean temperature of the metacarpals area of the left hand.



Fig. 32: Mean Thermal Areas (MTA) method to assess hands cold stress test recovery.

To interpret the obtained index values a scale was proposed, fig. 33, where indices in the range between 0.0 to -5.0 are regarded as normal recoveries while indices from -5.0 to -15.0 are said to be vasoplastic, with increasing severity in the presence of higher hypothermia (Ring, 1995). Ammer later suggested to use -4.0 as threshold value between normal recovery and presence of hypothermia (Ammer et al., 2007). In non-affected subjects the area temperature of the fingers should be less than the area temperature of the metacarpal before the cold provocation test and the opposite (fingers warmer than metacarpals) after the challenge. In Raynaud's affected people the expected pattern after provocation is that the fingers are still cooler than the metacarpals, fig. 34 (Ring, 1995).

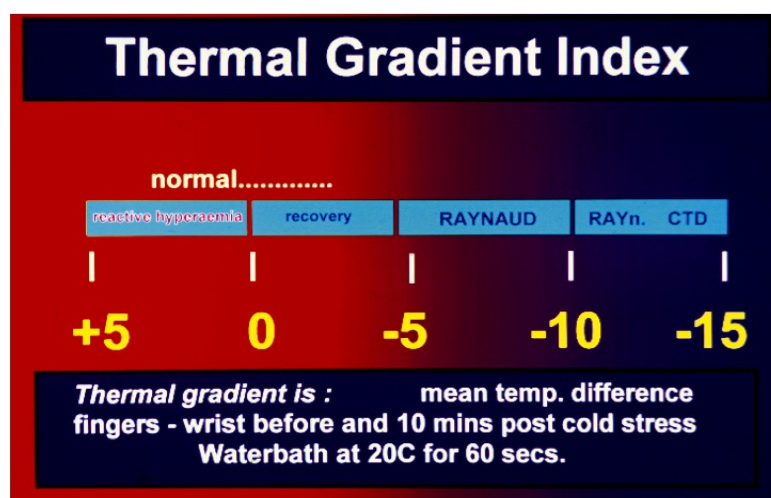


Fig. 33: The thermal gradient index scale for grading the severity of Raynaud's phenomenon (Ring, 1995).

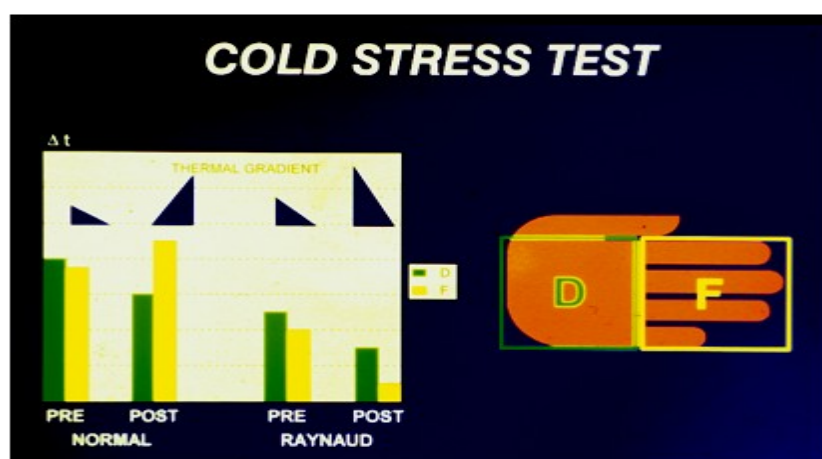


Fig. 34: One approach to quantification - estimating mean temperature difference between fingers to dorsal hand F-D (Ring, 1995).

Ammer proposed two similar approaches for obtaining the thermal gradient index when recuperating from a cold stress challenge of the hands. In the first method the mean temperature of a region of at least 25 pixels at the centre of each distal finger (intra phalanx) is subtracted from the values measured at exactly the same size region but at the proximal area of the correspondent metacarpal, fig. 35. The final index per hand is then obtained from the average of four fingers index differences. Ammer's second method is based on the temperature profile of each finger, which corresponds to a line from the centre of each finger (distal, intra phalanx) to the intraphalangeal-metacarpal joint and a second line with same thickness (5 pixels) and length from there to the proximal edge of the correspondent metacarpal. The index per finger is calculated by subtracting the mean temperature of each line, finger side - metacarpal side, fig. 36. As before the final index per hand is obtained from the average of four index fingers differences (Ammer et al., 2007).

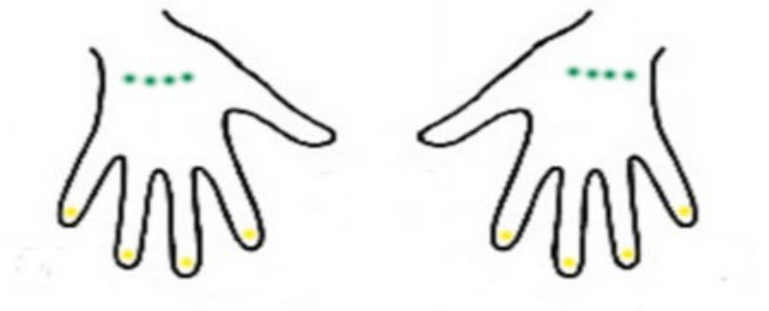


Fig. 35: Mean Thermal Gradient (MTG) method to assess hands cold stress test recovery.

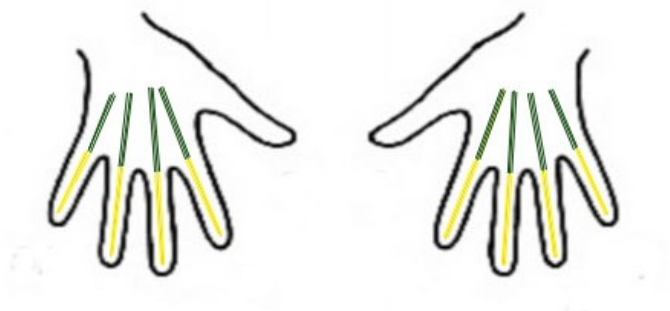


Fig. 36: Mean Thermal Profile (MTP) method to assess hands cold stress test recovery.

This vascular test with a comparison of the three assessment approaches will be used in this

project to document the severity of injury of Raynaud's affected subjects with the intention to discriminate between different stages of injury.

2.8. Image processing

This section outlines the different techniques involved in infrared image processing. It forms the underlying foundation for the computational aspects of this research work.

2.8.1. Introduction

Digital images are formed of pixels, which correspond to signals captured by digital detectors sensitive to specific wavelengths of the electromagnetic spectrum. The multiplication of the number of vertical and horizontal pixels characterises the image in terms of resolution, the pixel depth (in bits) indicates the amount of different signals that can be stored in a pixel (normally $2^{\text{pixel depth}}$).

Once images are captured three stages typically describe the subsequent operations: processing, analysis and understanding (fig. 37). While these three operations are linked, processing is related to the task of signal detection, storage and preparation for analysis; in the analysis part information is extracted and selected; and in the final phase this information leads to knowledge and subsequently understanding.

The evolution of the techniques for digital image processing is driven by military, astronomical, industrial and medical needs. It was in the 1960's that major underlying parts of modern techniques for image processing and manipulation were developed at the Bell Laboratories, Maryland, USA, for applications ranging from satellite reconnaissance to medical imaging (Rosenfeld, 1969).

The use of digital imaging in medicine brought several improvements such as: the ability to post-process images, the development of permanent record systems, the possibility send images to third parties over networks, environmental improvements (e.g. avoiding paper and chemicals) and in the case of radiology images a substantial reduction of radiation levels due to technological improvements. Some resistance still exists to the use of digital imaging in medicine mainly due to the initial costs and technology dependency. On the other hand digital technology allows users to post-process images in order to improve results, for example by correcting image brightness and

contrast, which can result in an improved diagnosis while the number of repeated examinations is reduced in parallel with the examination costs. Maintaining a permanent record of patient images leads to better pathological understanding and improved treatments and clinician knowledge. Image exchange through networks increases the spread of knowledge and understanding. It allows advice from remote specialists and the establishment of reference information based on image comparison. The correct implementation of digital image processing technologies reduce human error.

In the context of this research 5 different digital image processing modalities are studied. They are: image enhancement(section 2.8.2), feature extraction (2.8.3), template matching (2.8.4), interpolation techniques (2.8.5) and registration (2.8.6). These techniques will all be used on the thermal images processed in this work.

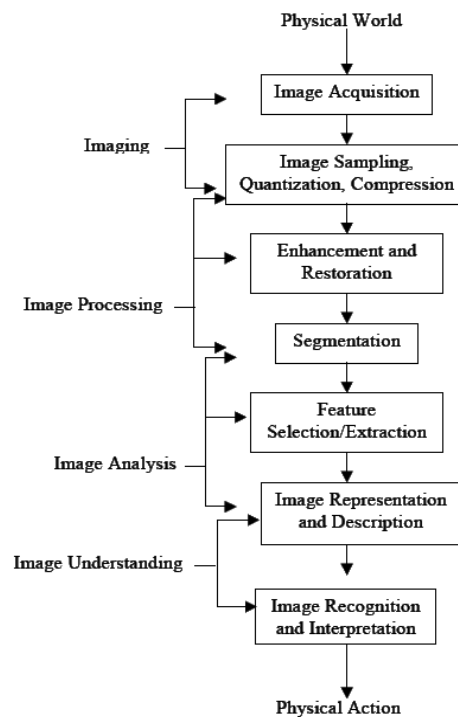


Fig. 37: Steps involved in digital imaging processing, *Webliography*[21].

In infrared cameras the focal plane array (FPA) typically captures a frame (image) every 16ms. Pixels are usually digitalised with 12 or 14 bits, providing 4096 or 16384 discernible temperature levels respectively. The temperature range for studying the human body is normally from 25° to 35°C, a 10°C difference. It is interesting to note that in principle only an 8-bit frame grabber is needed for this range as with an 8-bit pixel resolution it is possible to represent 256 levels of temperature. This equates to a thermal resolution of slightly more than 0.1 °C over the said 10 °C range and this happens to be also the thermal resolution limit of most microbolometer based

cameras.

The smallest spatially resolvable distance is the spatial resolution, it refers to the precision in discriminating two object temperatures at a given distance. It is calculated by dividing the double of the distance between the target and the imager by the number of pixels times the tangent of the angle between the target and the camera divided by two. The typical value is between 1 and 4 meters (Jones and Plassmann, 2002).

Thermal imaging processing techniques can be divided into 4 phases: capture, pre-processing, segmentation/registration, and post-processing. During capture the usual processing is an image non-uniformity correction, made by the imager itself. After capture, most cameras perform some degree of simple pre-processing. This can be low pass filtering (for reducing the noise caused by the scene or the equipment), thinning (for simplifying the objects in the scene) and binarisation (for separating objects from the background). More complex functions are then executed by computer based software. In the context of this work segmentation and registration techniques are used for partitioning the image into the objects that it contains, e.g. hands, fingers and background. Examples of this techniques are: edge detectors, gap bridging techniques, fill area operations, histogram equalisation, and Hough transforms (for shape detection). Common post-processing techniques in thermal imaging are high-pass filters (to detect hot or cold spots), temperature averaging and computing spatial, temporal or frequency variations of temperature (Jones and Plassmann, 2002).

Jiang (2005) classifies thermal image processing in two groups: low level processing and high level processing. In the low level processing group he identifies: image enhancing techniques (that improves the clarity of the image), temperature measurement processes (absolute or relative temperature measurements with interpretation of the pixels in the AOI) and other auxiliary imaging processing tools such as: isotherms, line profilings and histograms. The high level processing group is sub-divided into two object detection sections: static and dynamic. The static sub-group uses techniques based on the spatial distribution of temperature using only one image. In the context of this work these techniques can be used for assessing asymmetries and briefly consist of edge detectors (e.g. Canny), features detection (e.g. Hough transform) or segmenting images (e.g. Bezier histogram). The dynamic methods use a sequence of images and in this work could be used for assessing a stress challenge. This sub-group may employ artificial intelligence techniques such as Artificial Neural Networks, Bayesian Belief Networks, Linear Discriminate Analysis and Fuzzy

Logic.

In this work the image enhancing techniques that present the best results when applied to the thermal images of upper limbs will first be used to emphasise those image features. That will then be extracted for the second segmentation phase which identifies those areas of the image which are of interest from the background. This delineation of AOIs could ideally be automated and improve the consistency and thus quality of the analysis. Operations of template matching, interpolation and registration through feature based image morphing together with methods of identifying landmarks used for guiding subsequent algorithms will lead to a standard methodology of IR image analysis of the hands.

2.8.2. Image enhancing techniques

In most cases even in a controlled environment and when making use of standardised procedures images records are acquired with what is called noise. Image noise can be described as the random variation of individual pixel values appearing in the image while being non-existent in the real scene. This type of interference can be caused by the surrounding environment, i.e. thermal reflectance, and/or by the acquisition equipment itself due to the camera sensor or electronics sensitivity to spurious or transient electromagnetic signals. The presence of this destructive effect can seriously affect the main purpose of image acquisition, namely to measure the temperature values of the object in the scene.

There are three types of noise that can be found in digital images:

- Random noise, where fluctuations above and below the actual image intensity occur in intensity and/or colour.
- Fixed pattern noise appears when some pixels' intensity surpasses far beyond that of the ambient random noise fluctuations. This is also known as “Hot Pixels”;
- Banding noise is introduced by the camera when it reads the information from the digital sensor.

Changes in image noise do not only occur with environmental changes or when changing the camera model, there are other characteristics like fluctuations in luminance, “chroma” (colour composition), spatial frequency and magnitude that will affect the noise in the image. Noise affects all image regions equally although darker regions will (percent-wise) be affected more than brighter ones. In brighter areas noise becomes less pronounced (Gonzalez and Woods, 2002).

There are some techniques known to improve images affected by noise, reducing its impact. Linear smoothing filters operate by processing the original image with a moving convolution mask. While reducing noise the trade-off is a blurring effect on the image. Examples of this type of filters are: mean, Gaussian, Gaussian white noise, high-pass, low-pass, Homomorphic, and Unsharp. Non-linear filters do not generate their output as linear function of the respective input; their function locates and removes noise by determining whether the pixel value is valid or noise affected. Examples for this type of filters are: median, Poisson, Wiener, Lucy-Richardson, speckle, salt and pepper and noise compose (Gonzalez and Woods, 2002). While these filters produce less or no image blurring they introduce new and not necessarily correct information into the image as the assumptions on which they are based may not be true.

A study on image quality suggested as a comparing measure for signal to noise ratio (SNR), the calculation of the root mean square error (RMSE) and the cross-correlation coefficient (CCC). The SNR is a ratio of the mean pixel value to the standard deviation of pixel values; the higher this ratio the less obstructive the noise is. The RMSE measure is used to assess how well a method to reconstruct an image performs relative to the original image; the closer to the value of the original image the better. A standard method of estimating the degree to which two images are correlated is the CCC; the closer to the original image the more advantageous it is (Kinape and Amorim, 2003).

The result of such an experiment is expected to be helpful in terms of enhancing the desired image features for further post-processing in an attempt to build a semi-automated solution for the analysis of medical thermal images of the hand.

2.8.3. Features extraction

In order to reduce the amount of resources required to describe a large set of data accurately (i.e. reducing the number of variables which generally require large amounts of memory and computational power) several techniques for features extraction have been developed. Incidentally, these techniques can also be helpful for selecting those areas of the image that are to be analysed.

The temperature range of the examination room, as explained in a previous section of this document (section 2.5) is close to that of peripheral parts of the body, especially hands. This makes them appear very similar to the room background and it is therefore often difficult to identify their outline correctly in the thermal image. Accurate edge definition, however, is vital for a number of statistical image analysis procedures (Zhou et al., 2004) and a precise approach is needed in order to

produce repeatable results.

This study investigates a range of established boundary extraction techniques to determine their practical performance in identifying infrared imaging objects with poor background contrast. A total of 5 classes of edge detection techniques were selected for processing of the images in order to be benchmarked in this research project. These are:

- Class1: template based detectors or gradient operators work by calculating the first derivative of the spatial intensity distribution. They are simple to implement and detect both edges and their orientation. Noisy image data affects their performance. Although this can be minimised by applying a Gaussian filter this also removes much of the high frequency information present in edges. The 4 techniques selected from this class are the Roberts, Sobel, Prewitt and Kirsch detectors. (Gonzales and Woods, 2002, Gonzales et al., 2004) describe these in detail. Briefly, they are:
 1. The Roberts edge detector was amongst the first edge detectors introduced and it is probably the simplest. It is still widely used due to its simplicity and speed (mostly in hardware based implementations). Its disadvantages are that it is asymmetric and that it cannot detect edges orientated at 45, 135, 225 and 315 degrees .
 2. The Sobel edge detector is the most promising of this class of operators as it integrates and implements noise removal and edge detection into a single algorithm. It is, however, also the most complex to implement computationally.
 3. The Prewitt edge detector is simpler to implement than the Sobel one and works well for the images which are corrupted with Poisson type noise but for other types of noises it is deficient.
 4. The Kirsch edge detector has similar properties to that of the Sobel one but tends to perform slightly better on noisy images than the Sobel algorithm. Both Kirsch and Sobel methods are superior to simple derivative operators as they apply rotated versions of masks/templates and thus find edges at different orientations.
- Class 2: second order difference operators have fixed characteristics for all edge orientations. Laplacian, Laplacian of Gauss and Marr-Hildreth were the selected operators in this class. They find the correct place of edges and also test a wider area around the pixel than the above gradient-based detectors. The disadvantages of these operators are their sensitivity to noise, possible multiple detection of the same edges, malfunctioning at corners/curves and problems in places where the gray level function varies. Edge orientation

detection is affected due to the properties of the Laplacian approach, which looks for the alteration of the variation of the gray level value for finding the correct zero-crossing. The Laplacian of Gauss approach uses the Laplacian method combined with a Gaussian smoothing filter. It can be approximated by a discrete mask, which depends on the size of the Gaussian and the size of the kernel. The Marr-Hildreth method is an improvement on the Laplacian of Gauss technique. It locates the original edge from double edges by finding the zero crossings between the double edges but it is highly susceptible to noise (Gonzalez and Woods, 2002, Gonzalez et al., 2004).

- Class 3: the Canny and Shen-Castan algorithms were selected as examples of probabilistic operators. They have good localisation capabilities and response even in the presence of noise. Both compute probability values for determining an error rate. Their major disadvantages are poor detection of zero crossings and the complexity of computations (Gonzalez and Woods, 2002, Gonzalez et al., 2004).
- Class 4: as an example of segmentation based operators the watershed algorithm was the selected. It filters the object's boundaries and effectively removes image noise. This method first finds a gradient based on a threshold value, fills it to obtain edges, then searches for discontinuities in the image and finally tries to connect objects or border. It treats image foreground and background asymmetrically (Karantzalos and Argialas, 2006).
- Class 5: snakes were the selected as examples of active contour operators. Snakes are non-parametric and are based on internal and external energy terms: the internal term holds the curve together and prevents it from collapsing, the external attracts the curve to edges. This method needs an approximate contour outline as a starting input, which it then tries to improve. Snakes are able to reduce a second order problem to just one dimension and optimise it locally. They are, however, relatively slow (Kass et al., 1988). These methods are categorised in two classes: edge-based models and region-based models (Li et al., 2007). In this specific study, with its emphasis on the comparison of different techniques, the edge-based class is used.

Apart from the above 5 classes edge detection solutions using Artificial Intelligence (AI) methods such as Genetic Algorithms or Neural Networks have been suggested (Suzuki et al., 2000, Ghosh and Mitchell, 2006). These methods are computationally expensive and partly depend on

heuristic parameters (empirically found and often subjective “fiddle factors”). If those parameters are not properly defined errors will emerge. Other popular approaches use edge maps, which rely on the correct identification image points both inside and outside the object of interest for adequate performance and their application can be complex (Zhou et al., 2004).

Using (non-thermal) digital images two studies comparing traditional, well documented edge detectors have shown that probabilistic methods (Canny and Shen-Castan) based on Average Risk (AVG) and Signal to Noise Ratio (SNR) measures (Sharifi et al., 2002, Roushdy, 2006) perform better than those mentioned above. For these reasons AI and edge map techniques will not be used here.

An important property of infrared images when compared to normal digital images is the relatively high level of noise. Dependent on the thermal imaging sensor used noise can be up to 5% of the dynamic signal range, e.g. in a thermal image with a measurement range between 16°C and 36°C this could be 1°C. It is therefore important to include noise reduction techniques into any study aimed at improving boundary detection in thermal images, and to evaluate if their inclusion aids subsequent segmentation. In the context of thermal images homomorphic filters are thought to be useful as they allow noise to be modelled as an additive term to the original image data, reducing image luminance and improving reflectance (Arsenault and Levesque, 1984, Gonzalez et al., 2004). Importantly, this is a close approximation of the physical processes inside a thermal camera sensor.

From a comparative experiment using the above methods the expected outcome is the knowledge which of the feature extraction methods perform more accurately and efficiently. In the task of identifying the landmarks that will delineate the thermal image AOI (hands) and how exactly the pre-processing of images enhances or affects this operation.

2.8.4. Template matching

This technique consists of finding features in the image that is being analysed that are common to a template reference image. This method is useful for image comparison or to implement a template based image registration based on the correspondence between image features and reference template features such as landmark, which could be control points or reference lines (Brunelli, 2009). This is a promising approach but lies outside the scope of this work. It may, however, be an avenue for further investigations, especially with a view towards fully automating

the algorithms developed in this work.

2.8.5. Interpolation techniques

Image interpolation is a method of constructing new data points (pixels) in a digital image within the range of a discrete set of known data points (pixels) thus calculating a new point between two existing data points (Lehmann et al., 1999). In a situation where a change in scale of the object may be needed (e.g. when morphing an object into a standard shape), interpolation can play an important role in that operation. Thermal images are quantitative images and not qualitative as normal digital images. Preserving the original pixel value is therefore imperative. The three more common and very well documented interpolation techniques are described by Poth (2004). Briefly, these are:

- **Nearest Neighbour interpolation** is a simple method that consists in a new pixel receiving the value of the nearest pixel. Is a very fast method but can easily generate errors.
- **Bilinear interpolation** methods consists of assigning a pixel value calculated as the median of the four adjacent pixels values on the closest 2x2 neighbourhood of the pixel, the result of this algorithm is smoother than that of the previous one.
- **Bi-cubic interpolation** methods consider a 4x4 neighbourhood with 16 pixels, these pixels are not required to be at same distance to the one in question, therefore the closer a pixels is the higher a weighting is attributed to it in the calculation of the average value of the new pixel. This method produces noticeably sharper images than the previous two. It is widely used as standard in some commercial applications for image editing.

It will be goal of experiments in this study to identify which of these commonly used interpolation methods has the least impact when a change of scale is forced onto an object with thermal information. The result of this experiment will be used in subsequent registration operations.

2.8.6. Feature based registration

Image registration is the process of transforming the different sets of data in a homogeneous

system in order to facilitate operations such as image comparison or averaging, e.g. translating, rotating or zooming an image until it matches a template image as closely as possible. In this work a morphing operation is associated with registration. Morphing consists of the transformation of one image into another image by non-linear interpolation. This is in contrast to linear operations such as translating, rotating or zooming which preserve the original shapes in the image while morphing produces a change of appearance of objects in the image. Similar to morphing is a second registration operation called warping. When the scale of an object is changed or even its appearance, the two operations occur together. Whereas, however, warping only operates on the source image, changing object shape and attributes image topology and geometry, morphing operates on both the source and the target images, producing a continuous change of shape and attribute blending (Gomes et al., 1999).

A good morphing operation should include feature preservation and smoothness preservation and avoid linearities, it should therefore use adaptive methods. Warping is based on three principles: point based, vector based and spline mesh. None of them is perfect, the point based method is predictable and presents consistency problems but it has simple interpolations and can be used on different types of graphical objects. The vector based method has exactly the same disadvantages as the point based method and also requires high computational effort. The spline mesh method has a difficult specification, multiple pass anomalies and can only be used in restricted types of graphical objects (Gomes et al., 1999).

Image warping is a technique in image processing that performs a pixel to pixel mapping from the original image to an output image. It is a domain transformation useful for removing optical distortions induced by a camera or a particular viewing perspective, to perform image registration with a template, or to align images (Glasbey and Mardia, 1998). There are two types of image warping: forward warping, which is based on the destination coordinates being specified as functions of the source coordinates, and reverse warping where the source coordinates are defined as functions of the destination coordinates (Gomes et Al., 1999).

Reverse warping is performed by scanning the destination image pixel by pixel, calculating the corresponding location in the source image by evaluating the mapping function and copying to the destination pixel the value obtained from the function calculation (Gomes et Al., 1999).

In medicine in recent years interest has increased in using the warp technique to register images produced by medical imaging systems with body atlas information. It allows combination of different medical imaging modalities improving understanding of the body structure (X-rays and CT) and physiological events (MRI and Thermography) (Glasbey and Mardia, 1998).

One dimensional signal warping such as sound has alignment related problems, in order to

address this on 2-D images the warp operation can assume a parametric form, through smoothness, or a non-parametric form penalising roughness (Glasbey and Mardia, 1998).

The parametric form of warp (Glasbey and Mardia, 1998) can be based in the following transformations:

- Simple translation, a simple correspondence is performed using a function that maps along rows, columns or both combined with direct conformity. It has problems associated with alignment and template matching.
- Procrustes transformation, is adding a rotation of a given angle value to a simple transformation along with a magnitude value that corresponds to a possibility of enlargement (value > 1) or shrinkage (value < 1) of the selected pixels to warp. It can lead to heavier computations.
- Affine transformation, is a six-parameter generalisation of the Procrustes transformation and allows different stretching along rows and columns of an image and shearing. It is the most common general linear transformation, facilitates the alignment through a regression algorithm, but it can be a problem when the reference points are not labelled or need to be assigned.
- Perspective transformation, is when a fixed point in space views a planar object. It is a non-linear transformation that requires eight parameters and uses the affine transformation to limit the viewpoint, preventing it becoming too distant or foreshortened. This transformation is able to map straight lines at all orientations to straight lines preserving the conic sections. Nevertheless to use more than four landmarks by least squares in the image space requires an iterative approach and consequentially demands high computations.
- Bilinear transformation, is another eight parameter transformation generalisation of the affine transformation, which preserves straight lines in three particular directions, including the lines parallel to the axis. It is a bijective transformation but can lead to collinearities.
- Polynomial transformation, uses polynomials of third and higher order to perform the transformation, treats as special cases the quadratic, biquadratic, cubic and bicubic transformations. It can be computationally heavy but has the advantage of not leaving gaps.

The non-parametric forms of warping such as elastic deformations, Thin-plate splines and Bayesian approach were introduced to provide a solution for the poor performance with local distortions of the parametric transformations. Giving a set of matched reference landmarks in both

images a triangulation can be obtained and an affine transformation defined by the triangles vertices can be used in the triangle inside pixels correspondence. A continuity along the edges of the triangles is ensured producing a smoother transformation. However the non-parametric transformations produce roughness. The use of Thin-plate splines over the whole image and Bayesian techniques can produce heavy computational load (Glasbey and Mardia, 1998).

There are four main warping techniques described in detail by Gomes et al. (1999):

- Triangulation, the object or objects presented in the image have well known delimitation landmarks, and from them it is possible to build a triangular mesh model representing the whole object or objects. The triangle is the minimal and simplest geometrical shape used in image processing and are able to represent any other geometrical form (Besl, 1995). It triangulates the specification mapping of the source and target triangle pair using for example the barycentric coordinates inside those triangles. With triangulation the previously referred parametric and non-parametric can be used. This avoids triangle mesh foldover and maps each triangle independently.
- Field-based point, uses vectors as features. For each feature vector v in the source image an destination v' vector feature is specified under the transformation. The object shape is reconstructed by considering the distance of the points to the segment feature, the distance is inversely proportional to the influences of the points in the pixels interpolation. There is a field of influence per each feature vector. Each of those vectors an orthogonal coordinates (u,v) are defined, where v is the perpendicular distance to the feature vector and u the distance along it. The coordinate u is normalised in accordance with the segment length, the v coordinate is the absolute distance. Stretching a vector in a direction, the neighbourhood of that feature is also stretched along that direction. A new coordinate system is defined per each vector feature, which is used to define a local transformation using inverse distance weighted interpolation. The final warping is obtained as a blending of the local transformation of each feature. In field-based mapping each pair of points, lines or boxes defines one mapping. The final map is a weighted average. It needs a modified weighting function, provokes ghosting and singularities at crossovers. (Gomes et al., 1999).
- Free-form deformation, uses free-form curves such as B-splines and Bézier curves to define coordinate curves. By changing the control points of the free-form curves, a change in coordinates curves defines a change of the coordinates that performs the warping

transformation. The warping process is composed of four steps:

1. A new coordinate system is defined on the space where the object is embedded based in its Cartesian coordinates. A representation of the coordinate system is used to specify it.
2. The coordinates of the object shape on the new coordinate system are computed.
3. The representation curves of the coordinate system are warped, which causes deformation of the space.
4. The new object coordinates are changed back to Cartesian coordinates in order to reconstruct the warped object.

This mapping defines a global deformation of space and, therefore, deforms all the objects embedded in that space. Free-form deformation uses a high degree polynomials and control points in a grid. It can be very complex to implement (Gomes et al., 1999).

- Multi-pass spline, uses a mesh that has control points defining the image objects to be warped, those objects are delimited by lines which intersect the control points present on the mesh. It is composed of a separable transformation reducing the 2D warping problem into two 1D problems. Each transformation per mesh column depends only on the y coordinate. This separability simplifies computationally when the graphical objects uses a matrix representation reducing substantially the problem of warping processing demands. The process of warping using this technique composes the following steps:

1. Decomposes the horizontal displacements generating vertical splines without vertical displacements.
2. Intersects a scan line with the vertical splines.
3. Constructs a scan line map where it generates a spline with the intersections producing the new localisation of the warped objects.

This method is very efficient, has a laborious specification and the splines cannot cross (Gomes et al., 1999).

A South African study (Delpont, 2007) has compared two morphing techniques: mesh warping and field morphing. These two modalities only vary in the way warping is performed.

- Mesh warping requires a finite number of control points in the mesh. This can occasionally cause regions with too many control points and others with too few. Another problem might be that the user does not have enough control points.
- With field morphing unexpected interpolations known as “ghosts” can be generated. This technique also demands very high computational resources.

In the South African study triangulation was used to help and improve morphing along with warping. Delaunay triangulation was used due to its uniqueness and nearest neighbour approach but a problem known as foldovers (triangle overlap) appeared which would cause inconvenient morphing. The study concluded that the user must select appropriate control points to minimise the error, something that can be a tedious task (Delpont, 2007).

Barycentric coordinates were discovered by Möbius in 1827 (Hormann, 2004) and follows the Ceva's theorem, which states that for any point p inside a planar triangle with vertices $[v_1, v_2, v_3]$ there exist three masses λ_1, λ_2 and λ_3 . Placing these masses at the corresponding triangle vertices, their centre of mass will correspond to c , as shown in the following formula.

$$c = \frac{\lambda_1 v_1 + \lambda_2 v_2 + \lambda_3 v_3}{\lambda_1 + \lambda_2 + \lambda_3}$$

Triangular based interpolation has the advantage of preserving the geometry of lines that are combined (Rase, 2001).

A triangle can be divided into three sub-triangles by its centre of mass, each interior point will have a local barycentric coordinate according to the distance to the triangle vertices. Pixels can be represented uniquely by barycentric coordinates within the triangle due to their position. The barycentric coordinates in a triangle are normalised and the sum of three barycentric coordinates from an interior point related to the vertices is 1 (Hormann, 2004).

The normalised triangular barycentric coordinates are homogeneous and satisfy the linearity, positivity and Lagrange properties (interpolates the original pixel in the destination pixel enforcing linearity along the polygon edges), they are used in computer graphic applications such as image warping, texture mapping and correspondence refinement. Triangular barycentric coordinates are easy to implement and fast to compute. The application of barycentric coordinates is particularly useful for interpolating data that is given at the vertices of the polygons (Hormann, 2004).

The triangular barycentric transformation is based in translating the triangle vertices points and inner points from Cartesian into the barycentric coordinates, translate the pixel values according to the transformation function and copy that value to the corresponding point at the destination point after a coordinate translation from barycentric to Cartesian (Phillips, 2008) as illustrated in fig. 38 and using the following algebraic formulas:

$$A = \begin{bmatrix} V1x & V2x & V3x \\ V1y & V2y & V3y \\ 1 & 1 & 1 \end{bmatrix} ; A1 = \begin{bmatrix} Px & V2x & V3x \\ Py & V2y & V3y \\ 1 & 1 & 1 \end{bmatrix} ; A2 = \begin{bmatrix} V1x & Px & V3x \\ V1y & Py & V3y \\ 1 & 1 & 1 \end{bmatrix} ; A3 = \begin{bmatrix} V1x & V2x & Px \\ V1y & V2y & Py \\ 1 & 1 & 1 \end{bmatrix}$$

$$\lambda1 = \frac{\det A1}{\det A} ; \lambda2 = \frac{\det A2}{\det A} ; \lambda3 = \frac{\det A3}{\det A} ; \lambda1 + \lambda2 + \lambda3 = 1 ; Px = \lambda1V1x + \lambda2V2x + \lambda3V3x$$

$$Py = \lambda1V1y + \lambda2V2y + \lambda3V3y$$

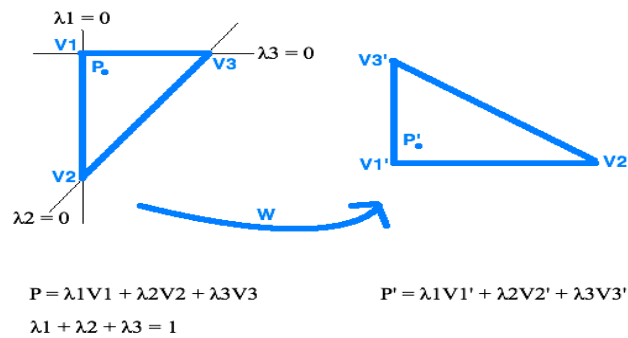


Fig. 38: Point correspondence between source and destination triangles using barycentric coordinates.

Some authors suggested image warping techniques based on meshes and lines (Gomes et al., 1999, Beier and Neely, 1992, Wolberg, 1998, Wolberg, 1996), although these will not be studied here due to their reported implementation complexity and computational cost.

Recent research proposed image warping based on triangulation as a fast, simple and accurate method (Fujimura and Makarov, 1998, Dong-Keun and Yo-Sung, 2004, Hormann, 2004). This approach also uses barycentric coordinates to make the correspondence between pixels of the original and resultant image of the transformation.

In this study a geometrical model of hand will be used and a reverse warp technique using triangles correspondence and barycentric coordinates.

Due to the reported advantages the a goal of experiments in this study will be to contribute to the overall aim of this research project by developing a morphing method based on triangulation with a scope of being accurate, simple and fast.

2.8.7. Conclusion

In this section the background of a wide range of image processing techniques has been presented and those most likely to of use for this work have been selected. In the next chapter the knowledge gained here will be used to design appropriate experiments where the selected approaches will be implemented and tested. The common goal of these tests is find the most useful combination of methods for implementing a semi-automatic solution that addresses the central aim of this research study.

3 – Methodology

This section outlines the methodology used in this research work. It specifies the materials used and how they were selected, and the techniques used to obtain the results.

- Section 3.1 outlines the image capture protocol used throughout this study.
- Section 3.2 describes the process of volunteer recruitment and selection and clarifies ethical considerations.
- Section 3.3 details 2 experiments designed to identify the most suitable method for analysing areas of interest in a thermal image.
- Section 3.4 reports the setup and performance of 2 pilot experiments which informed the design and implementation of 4 objective provocation tests detailed in the following section.
- Section 3.5 explains 4 different objective provocation tests and means to analyse the performance of competing cold stress test methods as well as a comparison of three infrared camera systems.
- The final section 3.6 is devoted to the image processing and analysis steps used in the objective provocation tests above.

3.1. Image capture protocol

The image capture protocol plays an important role in all infrared imaging investigations, it specifies the subject preparation for the imaging appointment and during the data collection, the room conditions and the capture procedure itself. The recording protocol used in this investigation follows the guidelines of the “Glamorgan Protocol”, which recommends the standard procedures for recording and evaluation of thermal images of the human body (Ammer, 2008). It is divided into three sections: the subject, the room and the image recording process.

1. The subject to be investigated has to follow the following instructions:

- Instructions to be sent to the subject together with the appointment outlining:
 - Avoid smoking for two hours (minimum) before the investigation
 - Avoid heavy meals on the day of the examination
 - Avoid cosmetics and ointments on the skin, these substances act as skin thermal insulators.
 - Avoid physiotherapy or sports on day of the examination
 - Report infections and any drugs taken, either prescribed by a general practitioner or acquired from a standard pharmacy.

- On arrival:
 - The investigator explains the procedure.
 - The subject completes the following forms: “Informed Consent” (Appendix 8), “Euro-QoL” (Euro-QoL score HAS to be zero for controls, Appendix 10), “RSI screening questionnaire” (Appendix 11) and “HAVS screening questionnaire” (Appendix 12) (these last two forms are only used in the pilot phase and the final tests of this work).
 - The investigator requests the subject to remove as much clothing as the volunteer is comfortable with (in changing cubicle) leaving the upper limbs exposed. In actual facts all subjects were wearing either a t-shirt or short sleeved shirt ensuring that the forearms were unclothed.
 - The subject must avoid uneven cooling due to jewellery, crossed legs, or hands/arms placed close or on the body.
 - The investigator has to check the room temperature repeatedly and humidity (temperature has to be 22°C and humidity below 50% to prevent subjects from sweating) .

- On scanning:
 - The standard position used is that of both hands in dorsal view as defined in the Glamorgan Standard Capture Protocol (Ammer, 2008).
 - A off-the-shelf MDF board has to be used for enhancing the background to hand contrast. The

MDF board has a high thermal resistance and therefore does not conduct significant amounts of heat to or from the hands during a single investigation. MDF has, however, a high thermal capacitance so that over time it will assume the temperature of the hands and stay at that temperature for several minutes. In extended or consecutively repeated investigations the board must therefore be replaced with an identical one in order to maintain good contrast and to avoid thermal interference from the previous examination.

- Marks from tight clothing or seating have to be avoided.
- No volunteer names/details are stored on any computer system (only a volunteer code is used). This can be cross referenced to the forms which are stored in a locked filing cabinet).

Apart from the member of staff performing the examination, a second member of staff or a person brought in by the volunteer has to be permanently present in the office area (not the laboratory space itself) as a witness/chaperone.

2. The examination room

The examination room has to have a stabilised air conditioning system, that maintains the room temperature at $22^{\circ}\text{C} \pm 1^{\circ}\text{C}$ and the humidity below 50%. The outside laboratory window has to be completely closed with shutters not only to avoid solar radiation but also to maintain privacy during the examination. An acclimatisation cubicle has to be provided close to the examination room and maintained under the same environmental conditions. The subject can disrobe there and rest for 15 minutes before the examination to facilitate thermal equilibrium. All unnecessary equipment should be removed from the laboratory area to ensure adequate space for the examination equipment and to avoid thermal reflections. All equipment and the walls have to be away from the subject as far as possible in order to minimise heat reflections. The laboratory area itself should be equipped with the absolute minimum of furniture only to provide adequate room for manoeuvre of the equipment and sufficient space between the camera and the volunteer. In order to avoid disturbance during the examination process, a door sign “Examination in progress” should be used.

3. The image recording process

For the image recording process the investigator has to make sure that all equipment is set

up correctly (a check list is helpful here). The infrared camera must have been switched on at least 90 minutes before the start of the first capture to avoid start-up drift (Plassmann, 2006). Before starting the capture process on the subject an image from a calibration source must be taken. The same applies to the end of the process. Both calibration images combined allow the investigator to check for recording errors.

For capturing the desired views from the subject, correct placement in terms of distance, angle to the camera, subject position and field of view of the camera has to be achieved. This adjustment process can be significantly simplified by using capture masks (fig. 38) in the computer capture software which are overlaid onto the live image. Additionally a camera stand (fig. 39), facilitates fast positioning and stable fixation onto the target view.

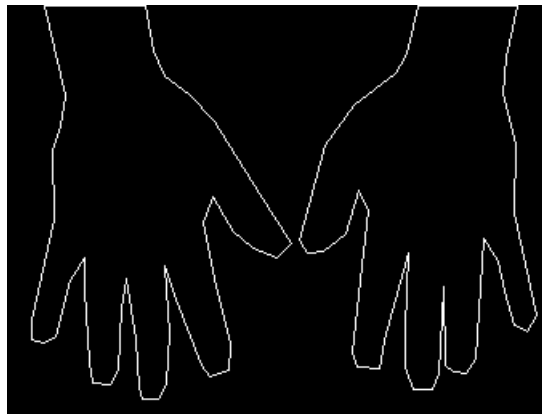


Fig. 39: Example of a live overlay mask.



Fig. 40: FLIR A40 IR camera on laboratory stand.

The above protocol was followed in all investigations in this work. The camera used was the FLIR A40 (thermal) infrared camera with a resolution of 320x240 pixels, a measurement accuracy

(bias, offset) of $\pm 2^{\circ}\text{C}$ and a precision (repeatability) of $\pm 0.1^{\circ}\text{C}$. It was connected to a PC using the CHERM package developed at Glamorgan Medical Imaging Research Unit (Plassmann, 2003). The lenses used in this imaging system were a standard lens (IR-lens 24°) for regional (close-up) views and wide angle lens (IR-lens 45°) for the total (full) body views.

For all tests involving human subjects ethical approval was requested and obtained from the Ethics Committee of the Faculty of Advanced Technology at the University of Glamorgan before starting experiments. All individuals collaborating in this research project were treated identically, their confidentiality was respected and no harm was caused to them. All volunteers collaborating in this work could withdraw at any time from the project without being disadvantaged. The author of this work has acted with integrity and has used the available resources as beneficially as possible.

3.2. Online RSI Questionnaire

In order to characterise the incidence of occupational diseases affecting the hands or upper extremities amongst the 20,000 students and 2,000 members of staff at the University of Glamorgan an online questionnaire based on Levine's (Levine et al., 1993) self-administrated questionnaire for Carpal Tunnel Syndrome assessment was designed and implemented (see Appendix 4).

This questionnaire, coded in HTML and the PHP programming language (Code scripts are provided in Appendix 6), was made available at the author's Research Group website (<http://medimaging.awardspace.co.uk/>) and the data collected was stored in a MySQL database (database schema in Appendix 5). The system was protected by a username and password combination. The architecture of this data collection and analysis setup is shown in fig. 40. The input forms presented online to users had build-in automatic field validation (e.g. check for age between 16 and 80) to improve the quality of the collected data. In order to avoid multiple submissions from a single user, a mechanism that temporarily recorded the user's Internet Protocol address was used. This mechanism did not allow the same machine to perform more than one submission within a 15 minute interval. The questionnaires were anonymous, only an optional text-box existed for entering an email address if the participant was interested to collaborate in future studies. A local copy of the online database was used for analysis using SQL queries and to obtain results. All records with partial or inconsistent data were eliminated from the database prior to analysis.

The questionnaire was advertised using wall posters, email and on the University of Glamorgan intranet pages.

All respondents were graded into four pathological states: severe symptoms, signals, early signals and healthy in order to characterise the state of the respective occupational disease condition. This classification was derived from Levine's score (Levine et al., 1993). Data from the fields for gender, age, BMI (Body Mass Index), occupation, smoking profile, alcohol intake habits, keyboard usage and mouse usage was correlated with the four pathological states in order to study the relationship between these two data sets. Participants were also analysed according to their age group (18-30, 31-40, 41-50, 51-60 and 61-85 years) and four BMI classes (underweight (<18.5), normal weight (18.5-24.9), overweight (25-29.9) and obese - level 1 (30-34.9)). The occupational distribution of participants was divided into four groups: administrative/clerical, lecturers, students with occupation and students without an occupation.



Fig. 41: Architecture of the online questionnaire application for data collection and analysis.

3.3. Image analysis experiments

The thermographic value used as a benchmark for discriminating between healthy and pathological states is that of thermal symmetry. In the context of this work 'thermal symmetry' is defined as the 'degree of similarity' between two Areas of Interest (AOI), mirrored across the human body's longitudinal main axis which are identical in shape and size and as near identical in

position as possible. The degree of similarity is expressed as the difference between the respective corresponding AOIs' mean and standard deviation.

Although the human body is bilateral with two eyes, hands, arms, legs, feet, and ears these are not necessarily 100% identical in shape or size. Image processing techniques developed for this work, however, allowed to compensate for these differences and to achieve near-perfect shape and size symmetry prior to comparison for thermal symmetry.

In this study two experiments were executed in order to establish underlying reference information. Common to both experiments was that all images were recorded using the capture protocol defined in section 3.1 and stored in the laboratory database. The captured images were recorded and retrieved by the CTHERM application.

In the first experiment only the CTHERM software was used for evaluating the temperature values using AOI. For the second experiment all images to be analysed were standardised using a template model following the warping technique described further down in section 3.6.4 which produced the results in a semi-automated manner.

3.3.1 Experiment 1: Suitability of body views

It was aim of this first experiment to establish if with current camera technology it is possible to use only two total body views (front and back) instead of several regional body views, which show more detail but are slower to perform. If this could be demonstrated then the faster and more convenient full body view technique could be used for all subsequent investigations. This first experiment consisted of analysing the images in the CTHERM software package, which has the possibility of graphically defining areas of interest in the thermal images (fig. 42) and then calculating the thermal values of these AOIs for mean temperature and standard deviation.

The seven regional (i.e. close-up) views specified by the standard capture protocol (Ammer, 2008) and used in this investigation were 'Both Hands Dorsal', 'Left Arm Anterior', 'Right Arm Anterior', 'Right Arm Dorsal', 'Left Arm Dorsal', 'Chest Anterior' and 'Upper Back'. 'Total Body Anterior', 'Total Body Dorsal' were used for the total body views. In all the views shown in fig. 43 to fig. 56 the respective AIOs as defined by Ammer (2008) are shown.

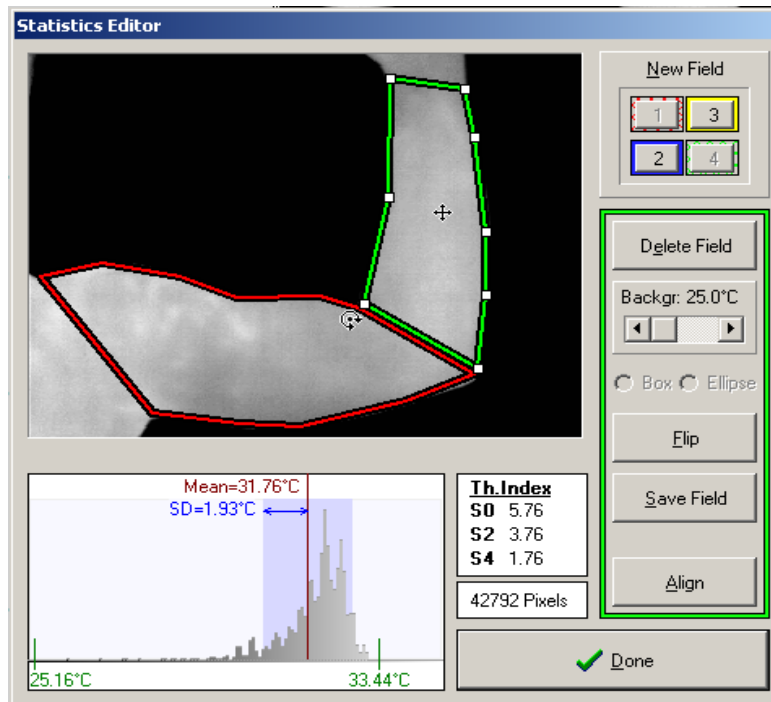


Fig. 42: Statistics editor of CTHERM software package to analyse AOIs.

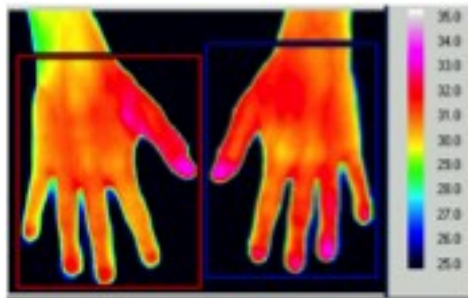


Fig. 43: Both Hands Dorsal regional view, AOI evaluating hand thermal symmetry (a threshold value was used to ignore background temperature).

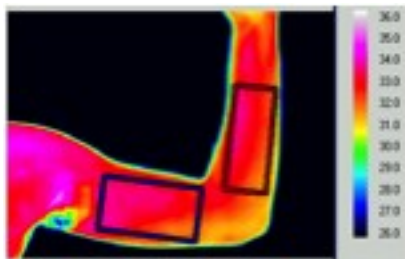


Fig. 44: Left Arm Anterior regional view, AOI evaluating arm and forearm thermal symmetry.

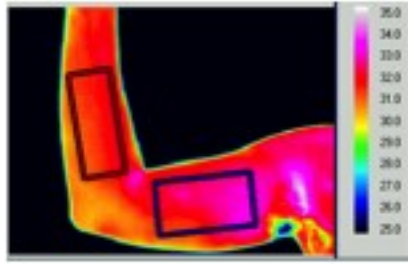


Fig. 45: Right Arm Anterior regional view, AOI evaluating arm and forearm thermal symmetry.

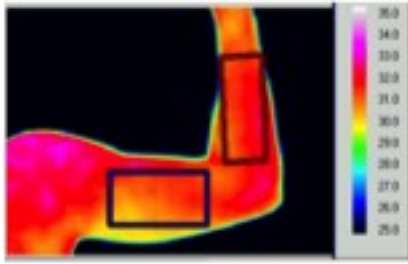


Fig. 46: Right Arm Dorsal regional view, AOI evaluating arm and forearm thermal symmetry.

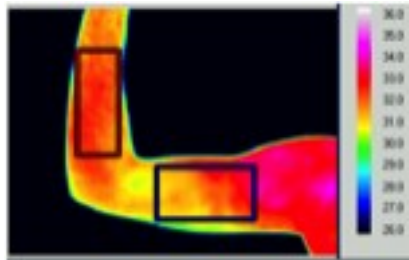


Fig. 47: Left Arm Dorsal regional view, AOI evaluating arm and forearm thermal symmetry.



Fig. 48: Total Body Anterior view, AOI evaluating limbs thermal symmetry, not suitable for hands and feet.



Fig. 49: Total Body Dorsal view, AOI evaluating limbs thermal symmetry, not suitable for hands and feet.



Fig. 50: Both Hands Anterior regional view, AOI evaluating wrist thermal symmetry.

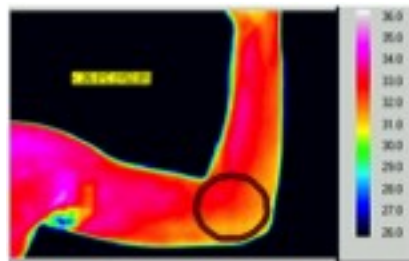


Fig. 51: Left Arm Anterior regional view, AOI evaluating elbow thermal symmetry.

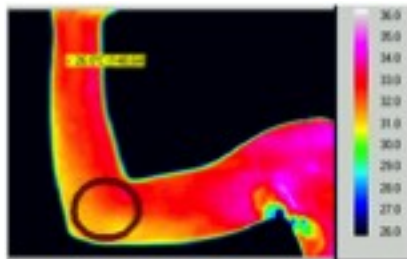


Fig. 52: Right Arm Anterior regional view, AOI evaluating elbow thermal symmetry.

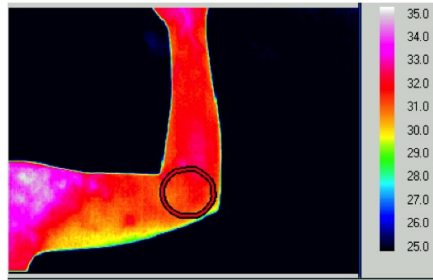


Fig. 53: Right Arm Dorsal regional view, AOI evaluating elbow thermal symmetry.

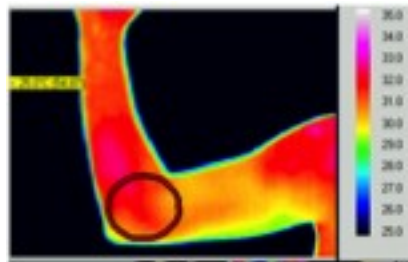


Fig. 54: Left Arm Dorsal regional view, AOI evaluating elbow thermal symmetry.

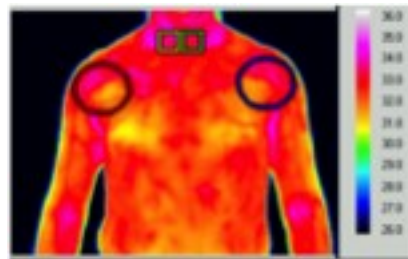


Fig. 55: Chest Anterior regional view, AOI (red and blue) evaluating shoulder thermal symmetry.

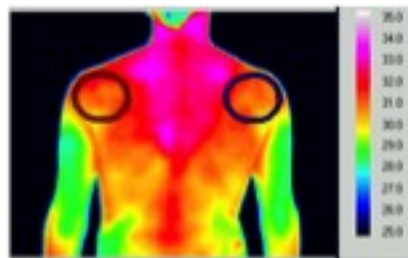


Fig. 56: Upper Back regional view, AOI evaluating shoulder thermal symmetry.

The subjects used in this first experiment were 39 males, with a mean age of 26.9 ± 10.2 . 31 of these were in the age group of 18-30, 5 in the age group of 31-40 and 1 in each in the 41-50, 51-60 and >60 groups. 26 had a BMI classification of 'normal weight' and the remaining 13 one of 'overweight'. The mean BMI value was 23.5 ± 2.4 .

The results of this first experiment are presented in section 4.2 and discussed in section 5.

3.3.2 Experiment 2: Suitability of standardised body views

The second experiment aimed to establish if a more refined method of defining AOIs in a template model could produce better symmetry values than the best method of the previous section 3.3.1 (“Best” in this context means a higher degree of symmetry between corresponding left and right parts of the body) just for the hand, forearm and arm AOIs.

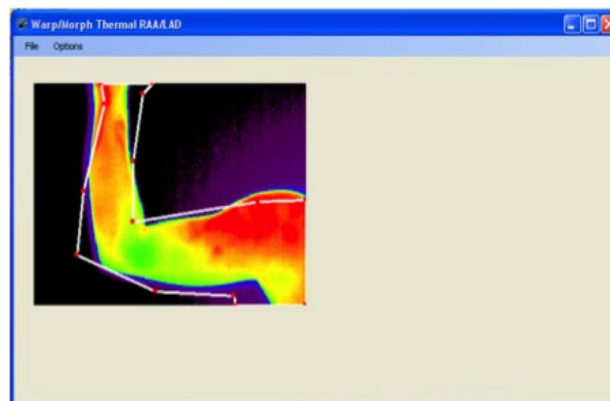


Fig. 57: A standard mask defined by (red) anatomical control points overlaid onto a thermal image on an elbow.

This refined method consisted of loading the image database produced in the previous experiment into a semi automatic software package (which is described in more detail in section 3.6) that would 'warp' the individual shape of a part of the body to a standard shape). It does so by using a standardised 'mask' outline of the respective body part that is composed from well defined and consistently reproducible anatomical control points. Fig. 57 shows such a mask overlaid onto a thermographic image of an elbow. The mask control points are now moved manually by the

operator into their correct position as shown in fig. 58. Fig. 59 shows how the software takes the image from fig. 58 (on the left) and warps it back to the standard mask shape (shown on the right). This way all individual thermal images in the data base can be brought into their respective standard shapes and can then be analysed and compared in a standardised and fully automatic manner.

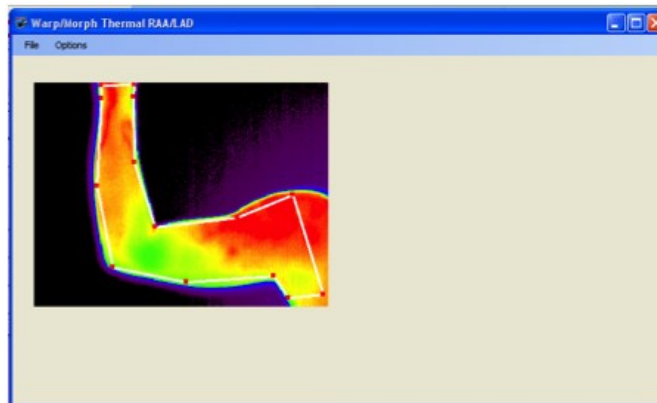


Fig. 58: Mask control points manually adjusted to fit the thermal image outline.

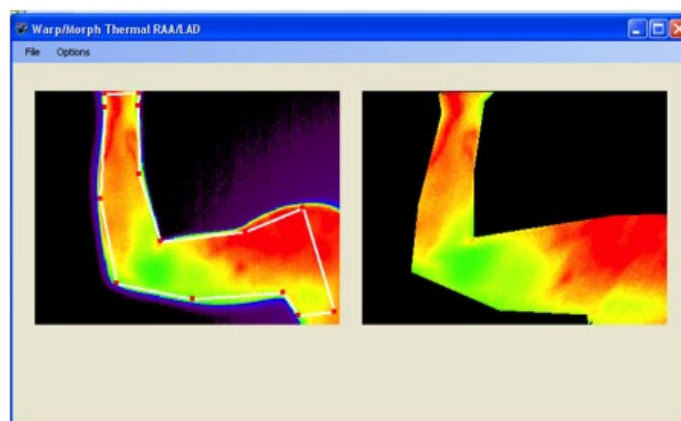


Fig. 59: The captured elbow shape produced in the step shown in fig. 57 (left) is now warped into the standard mask shape.

For this standard analysis method three AOI models, based on anatomical landmarks were defined: one model for both hands (fig. 59) in dorsal view and two further ones for the the left and the right arm (fig. 61 and 62). Due to the body's symmetry the dorsal AOI model for the right arm can be used as the anterior model for the left one and vice versa.

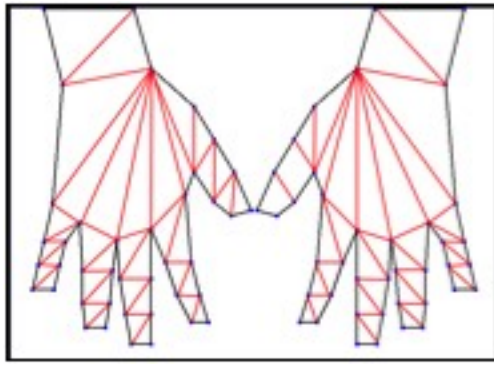


Fig. 60: Reference AOI model defined by anatomical markers and the AOI formed by triangles (17 AOIs for each hand).

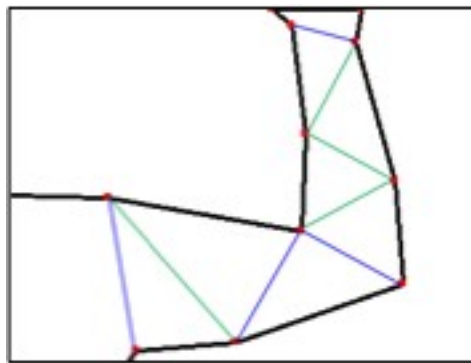


Fig. 61: Reference AOI model for the left arm in anterior view and the right arm in dorsal view (2 AOIs formed by triangles).

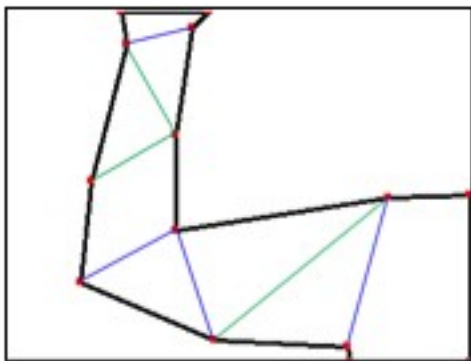


Fig. 62: Reference AOI model for the right arm in anterior view and the left arm in dorsal view (2 AOIs formed by triangles).

The outcome of this experiment together with details on the statistical analysis and a comparison with the results obtained from the first experiment (outlined in 3.3.1) is presented in section 4.2 and discussed in section 5.

3.4. Statistical Methods

The statistical methods used in this research were:

- Alpha Cronbach Coefficient
- Interclass Correlation Coefficient
- Kolmogorov–Smirnov test
- Pearson's Chi Square test
- Z-test
- Student t-test

The Alpha Cronbach Coefficient is a parameter used as a measure of the internal consistency estimate of reliability of test scores, it provides information about the internal consistency of the test, a value closer to 1 would mean a good internal consistency (Cortina, 1993).

For quantitative measures, intra-class correlation coefficient (ICC) is the principal measurement of reliability, it provides a value between 0 and 1, the closest to 1, more reliable the test will be (Lachin, 2004).

The Kolmogorov–Smirnov (K-S) test is a nonparametric test of equality of one-dimensional probability distributions used to compare a sample with a reference probability distribution, based on the empirical distribution function. In the case of this research to verify if the sample follows the normal distribution. The K-S test statistic itself does not depend on the underlying cumulative distribution function being tested and is an exact test. If the p value is higher than 0.05 it means that the sample distribution follows the reference distribution (Chakravart et al., 1967).

The Pearson's Chi Square test is a statistical procedure that test a null hypothesis that the relative frequencies of occurrence of observed events follow a specified frequency distribution. The events are assumed to be independent and have the same distribution, and the outcomes of each event must be mutually exclusive. Pearson's chi-square is used to assess two types of comparison: tests of goodness of fit and tests of independence. A test of goodness of fit establishes whether or

not an observed frequency distribution differs from a theoretical distribution. A test of independence assesses whether paired observations on two variables are independent. A chi-square probability of 0.05 or less is commonly interpreted by applied workers as justification for rejecting the null hypothesis that the row variable is unrelated (that is, only randomly related) to the column variable (Chernoff and Lehmann, 1954).

The Z-test is a statistical procedure where the Null Hypothesis should be an assumption about the difference in the sample means for two samples (note that the same quantitative variable must have been measured in each sample). The data should consist of two samples of quantitative data (one from each sample). The samples must be obtained independently from each other. The samples must have a known variance (standard deviation) and must follow a Normal Distribution. if the distributions of the variables in the samples are non-normal, the two-sample z-test can still be used for approximate results, provided the combined sample size (sum of sample sizes) is sufficiently large, for a minimum of 30 values (Montgomery et al., 2009).

The Z-test used compares two independent means according to the formula:

$$Z = \frac{\pi_1 - \pi_2 - \Delta}{\sqrt{\frac{sd_1^2}{n_1} + \frac{sd_2^2}{n_2}}}$$

Where π_1 and π_2 are the means of groups 1 and 2, sd_1 and sd_2 are the standard deviations of the groups, and n_1 and n_2 the number of samples of each group. The Δ value represents the difference between the groups to be tested. 0 is used to test if they are equal. The obtained Z value is then looked-up in the standard normal table. The number from this table is then subtracted from 1 and the resulting figure is the p-value.

The results of the Z-test in this document will be described as: HS-Highly significant ($p < 0.01$), S-Significant ($p < 0.05$), NS-Non Significant ($p > 0.05$).

A student's t-test is statistical hypothesis test in which the test statistic follows a Student's t distribution if the null hypothesis is supported. It is most common test applied when the test statistic would follow a normal distribution if the value of a scaling term in the test statistic were known and the sample has a significant size (more than 100 values). It is used for testing of the null hypothesis that the means of two normally distributed samples are equal or the null hypothesis that the difference between two responses measured on the same statistical unit has a mean value of zero. A result probability value inferior to 0.05 means that the samples are statistically independent (Zimmerman, 1997).

3.5. Pilot stress tests

The first pilot test involves the application of mechanical stress by using a computer keyboard. The second tests uses a vibration device. The aim of both tests is to investigate the temperature variability of hands and forearms during stress exposure in healthy subjects.

3.5.1. Keyboard provocation test, KPT

The aim of this pilot test is to investigate the amount of temperature increase in the hands and forearms of healthy subjects after 5 and 15 minutes of free typing at constant speed.

This investigation involved:

- A FLIR A40 (calibrated) thermal camera;
- A PC workstation with C THERM, MS Excel and SPSS software packages to process and analyse the thermal images;
- A standard computer keyboard as provocation tool;
- A table with a MDF board on top (to improve thermal contrast between limb and background);
- A chair for seating the volunteer.

12 healthy male volunteers with an average age of 22.4 ± 6.3 and average BMI value of 23.9 ± 1.9 (9 with ages between 18 and 29, being 3 of them left handed and over weighted; and 3 with ages between 30 and 39, 1 being left handed and 2 over weighted) were recruited for this pilot.

All volunteers were students and 100% healthy (defined as having a score of zero in the EURO-QOL questionnaire (Appendix 10) that they completed together with an informed consent form when recruited). On first arrival all volunteers were informed of the procedure which consisted of two visits on two different days. During the first visit the right hand was provoked while the left remained still (fig. 63). During the second visit the stressed hand was the left while the right one remained unchallenged in a still position.

The experiment followed the protocol defined in section 3.1 of this document. The standard views of dorsal hands and forearms as defined in 3.3 were used. The thermal camera was placed on

a stand at 90° angle (perpendicular) to the top surface of the table at a distance of 1m (fig. 64). A 24° lens was used on the camera.

The subjects were seated in a chair in a comfortable position, thermal reflective table surface was covered by a MDF board in order to improve image contrast between hands and background. 'Free style' random typing at constant speed (3 to 4 characters/second) on an unconnected computer keyboard was performed by the volunteers under the investigator's instruction and constant supervision. A thermal image was taken before starting to type and another 15 images in one minute intervals (fig. 65).

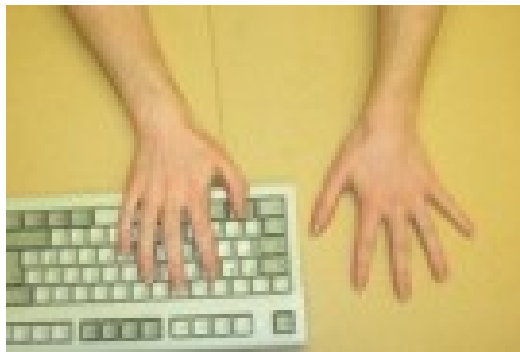


Fig. 63: One hand typing the other one still.



Fig. 64: Perpendicular position of the camera.

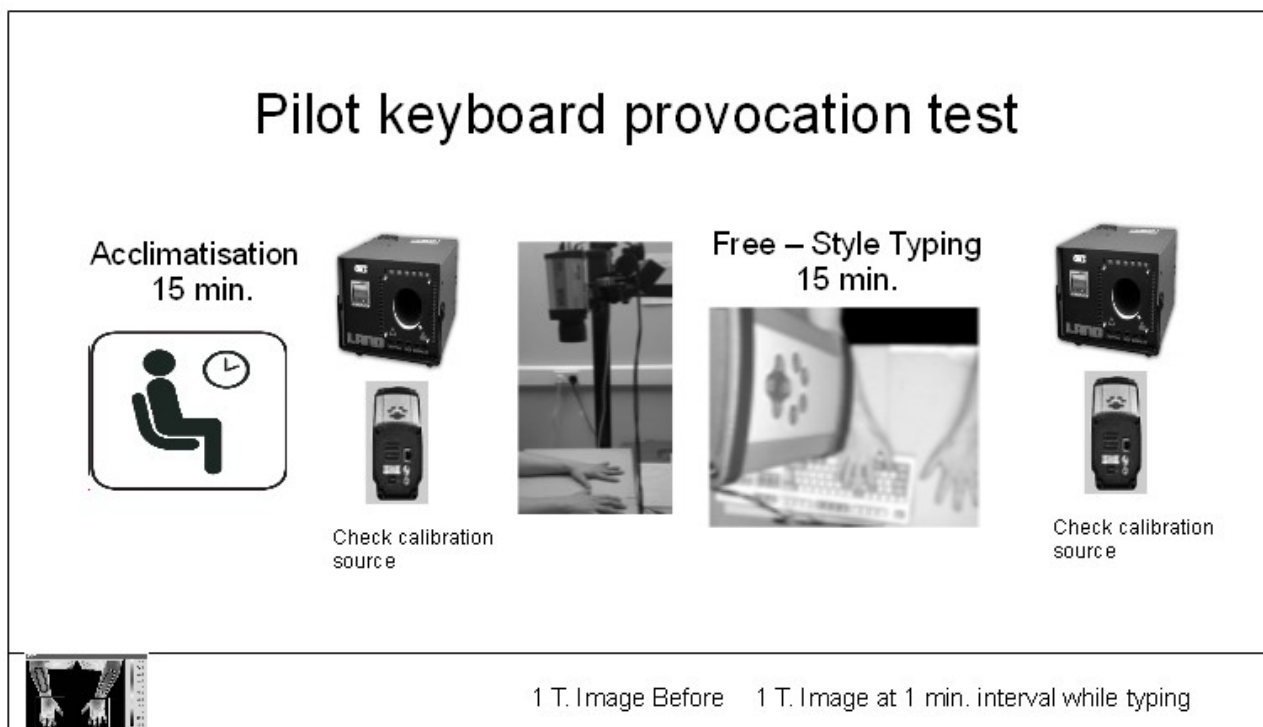


Fig. 65: The pilot Keyboard Provocation Test diagram.

If the images taken from the calibration reference source before and after examination differed in more than 0.1°C the experimental result was not used and the experiment was repeated. This procedure was necessary for quality assurance and was repeated in the other pilot study involving vibration and in the final objective provocative tests.

For the data analysis of this pilot experiment not all AOIs as defined in 3.3.2 were used but only 4 as shown in Fig. 66. These are 2 symmetrical squares covering an area of 5,600 pixels each and also 2 symmetrical rectangles on the inside of the forearms with an area of 2,140 pixels each. Mean temperatures and standard deviations were computed for each AOI and averaged over all volunteers grouped according to handedness, age group and BMI class. All the results were registered in a spreadsheet and statistically analysed using the SPSS® software package. For testing reliability and repeatability of the results the Interclass Correlation Coefficient was calculated for each AOI.

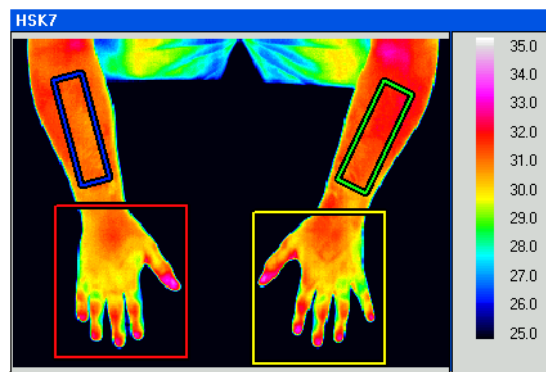


Fig. 66: Areas of Interest for keyboard pilot test.

Fig.67 exemplifies a sample examination of a subject. It demonstrates a typical sequence of captured thermograms during an individual's examination.

Fig. 68 and fig. 69 show the overall results of the keyboard typing pilot experiment on 12 volunteers. Both demonstrate as expected a temperature increase in the stressed extremities.

They also show an initial increase, although smaller, in the non-stressed and passive extremity that , after peaking approximately in the middle of the observation time, somewhat subsided. This effect was expected due to the thermal regulation principles outlined in section 2.1.2.4 that link both sides of the body and is in line with observations made in literature (Sharma et al., 1997, Ammer et al., 2001).

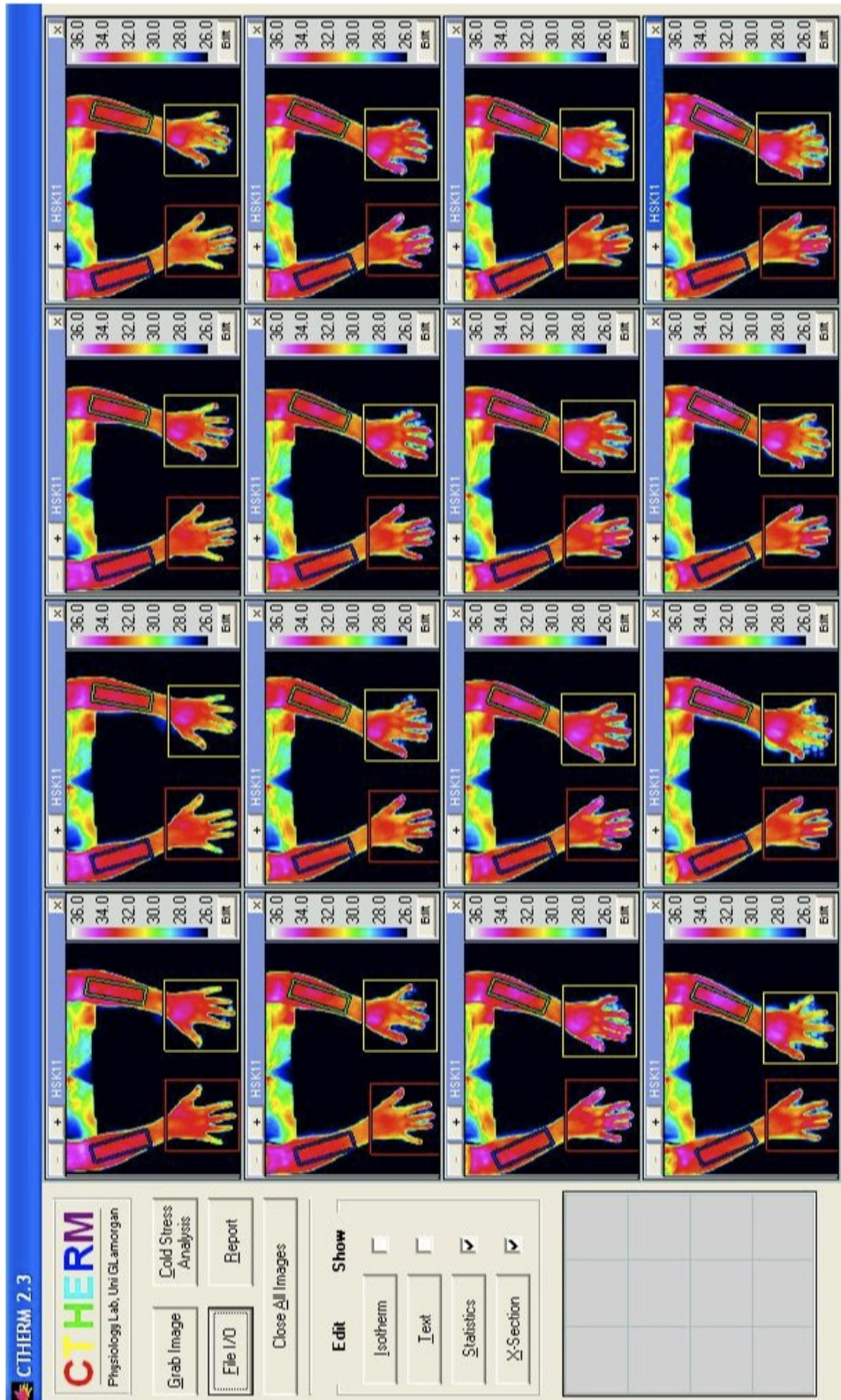


Fig. 67: Thermograms from a capture sequence of a keyboard stress investigation.

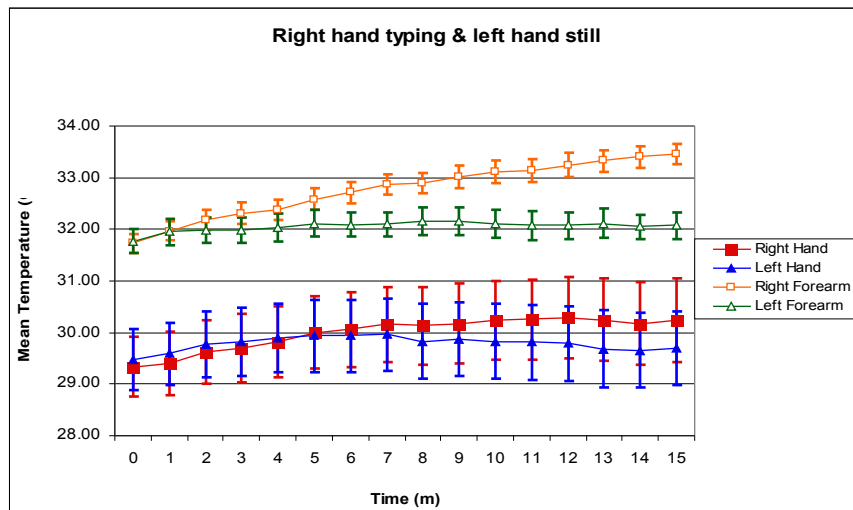


Fig. 68: Average mean temperatures over time on exercising the right hand, keeping the left hand still.

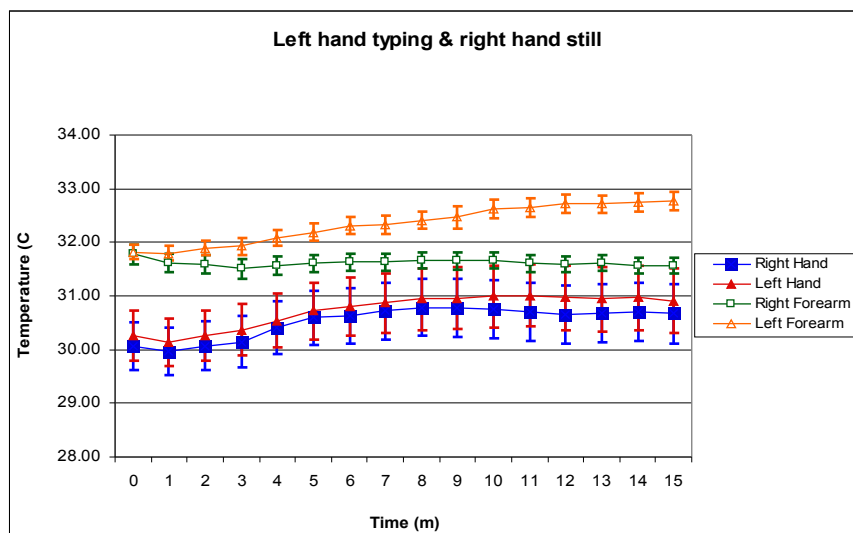


Fig. 69: Average mean temperatures over time on exercising the left hand, keeping the right hand still.

With respect to thermal symmetry (absolute contra-lateral difference between AOIs), it can be seen that independently of the hand stressed, the pattern of temperature changes is very similar in both hands and forearms (fig. 70 and fig. 71). The absolute values, however, are slightly different. In these combined/averaged tables the underlying reason for this remains hidden. It is, however, reasonable to assume that the handedness of individuals, for example, may play a role and that the differences shown are due to the fact that right handed participants outnumbered left handed ones

(and therefore the effect did not cancel out when averaging). This assumption is explored in the following paragraphs.

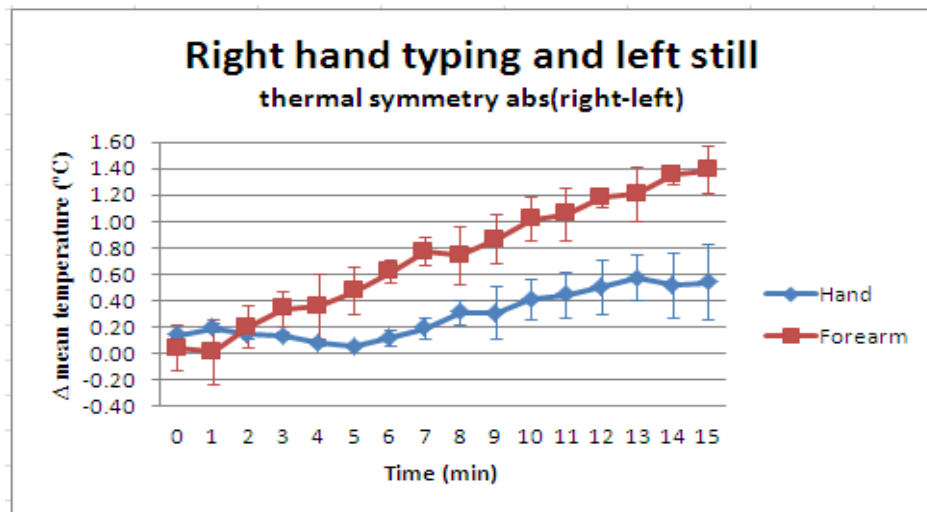


Fig. 70: Hand Thermal Symmetry (Right hand typing and left hand still).

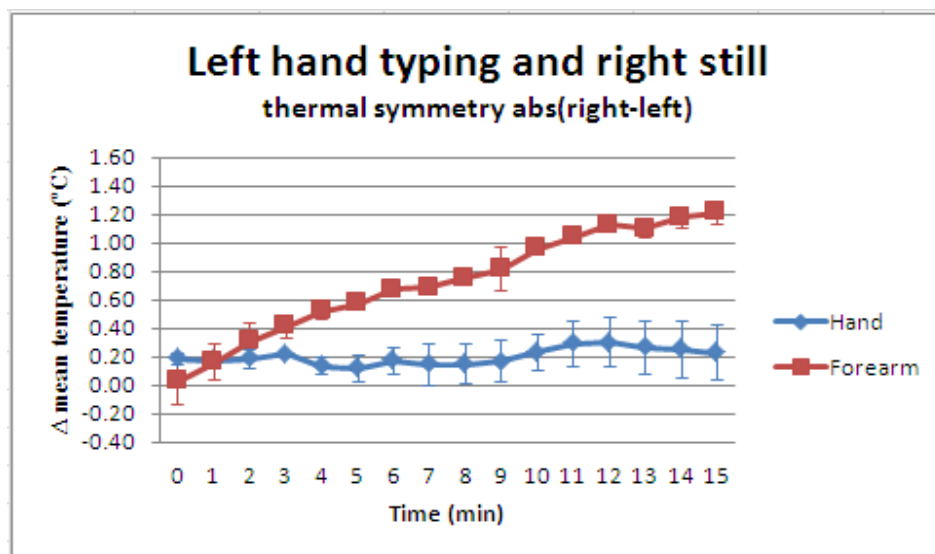


Fig. 71: Hand Thermal Symmetry (Left hand typing and right hand still).

Handedness

The blue and the red bar in fig. 72 and fig. 73 represent the the thermal symmetry of hands in right and left handed participants respectively. Generally, thermal symmetry was higher when the

preferred hand was typing (one exception: 5 minute point in fig. 73). This could be explained by the higher “ability” of the preferred hand that results in more efficient movements and thus heat generating energy consumption.

In figures 74 and 75 this pattern is repeated for the forearm. However, the asymmetry values are significantly more pronounced. This is logical since the heat producing muscles for finger movements (see 2.1.1.3) are located in the forearm and not in the hands.

Age

When separating the experimental group into two age cohorts (18-29 and 30-39) the results are inconclusive. There is no generally coherent pattern. When observing results at the 15 minute point only it appears that the younger participants are less thermally symmetrical than the older ones. It is possible that the older age group is more experienced at typing (Salthouse, 1984), consuming less energy and thus producing less metabolic heat. If this was the underlying reason, however, thermal symmetry differences should be less pronounced when left-hand typing since participants are predominantly right handed and both groups would have to make similar efforts. Since thermal symmetry is higher in these cases this assumption is probably incorrect (fig. 72 and fig. 73).

A alternative explanation is that older participants may already show early signs of some aspects of HAS where topical vasoconstriction (see 2.1.2.4) masks the increase in internal temperature. This assumption is supported by the observation that thermal asymmetry is actually negative when right-hand typing – the right hand tends to be more frequently (ab)used and is thus more susceptible to HAS, hence the negative asymmetry value.

In fig. 74 and fig. 75 this negative asymmetry for the older age group (i.e. apparent cooling of the working limb) can no longer be observed. When analysing lower arms instead of the hands the expected heating effect is present instead as expected (although reduced) indicating that vasoconstriction may still be present but is no longer the overwhelming factor.

BMI

After 15 minutes of typing normal weight participants were more asymmetric in temperature than their overweight counterparts. A possible explanation is that overweight people have both a higher thermal capacity (more body mass) and also better subcutaneous insulation (shielding warm

muscles). This picture is repeated when analysing the lower arm in fig. 74 and fig. 75.

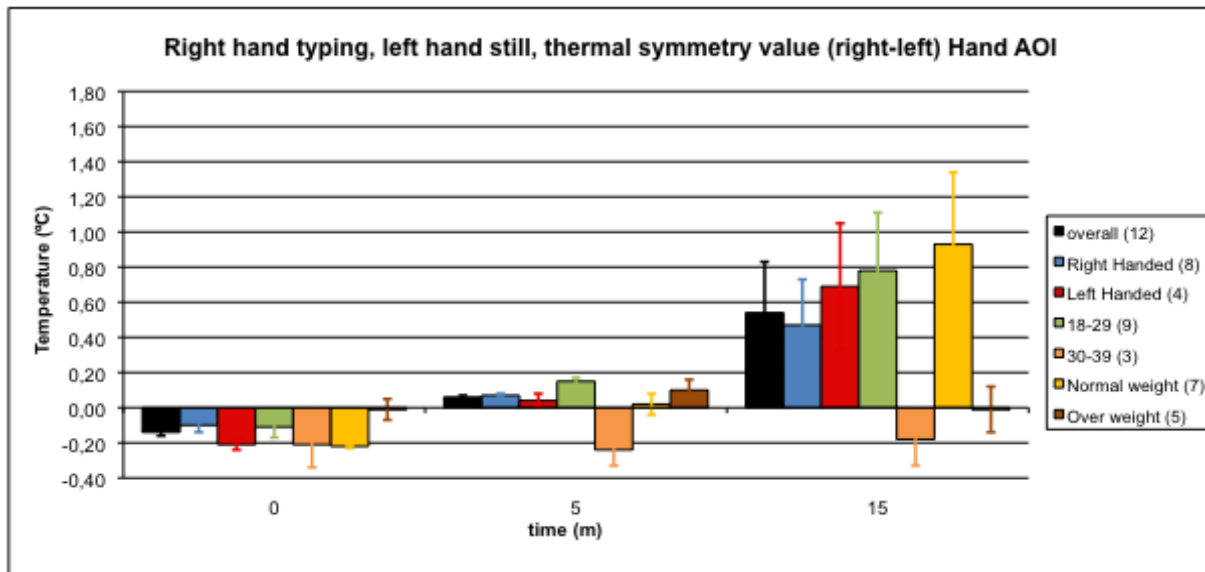


Fig. 72: Hand Thermal Symmetry (Right AOI – Left AOI) characterisation of hand AOI when stressing right hand.

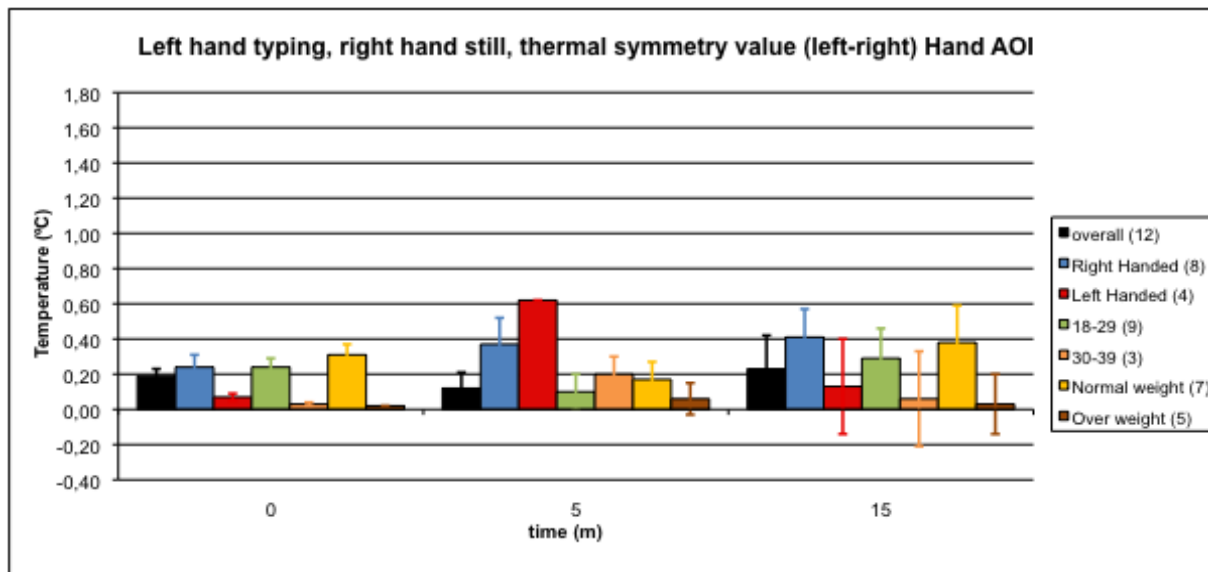


Fig. 73: Hand Thermal Symmetry (Left AOI – Right AOI) characterisation of hand AOI when stressing left hand.

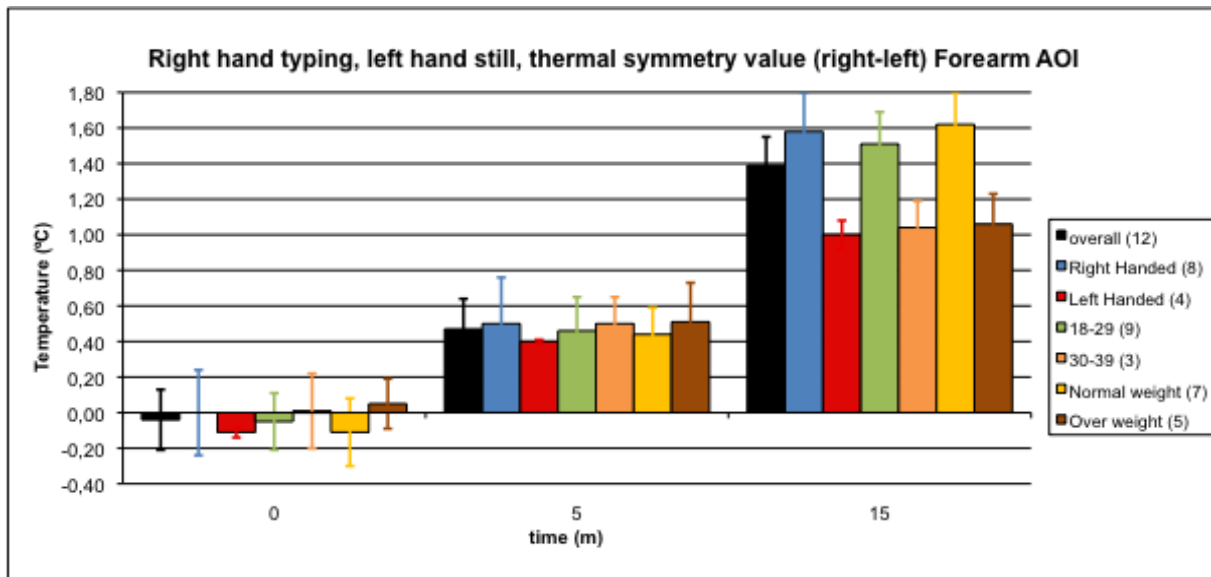


Fig. 74: Forearm Thermal Symmetry (Right AOI – Left AOI) characterisation of forearm AOI when stressing right hand.

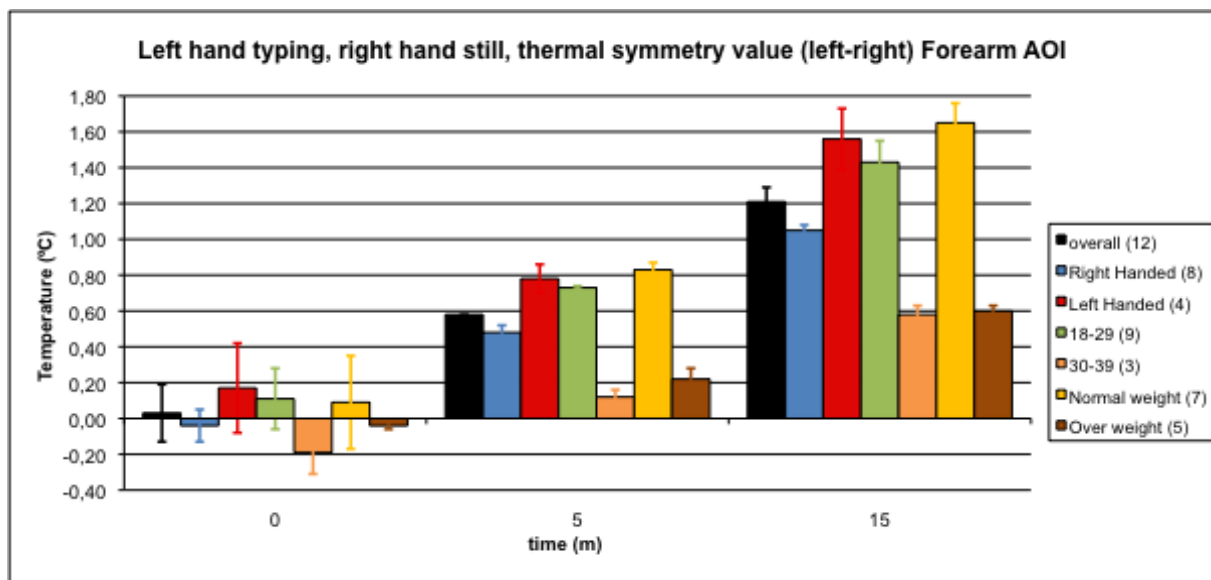


Fig. 75: Forearm Thermal Symmetry (Left AOI – Right AOI) characterisation of forearm AOI when stressing left hand.

Conducting an Inter Class Correlation coefficient test, it can be shown that for the hand AOI the ICC was only 0.67 with a 95% confidence interval of 0.42 to 0.76. These values unfortunately represent **poor repeatability of the hand AOI**. For the forearm AOI in contrast the ICC was 0.92 with a 95% confidence interval of 0.84 to 0.96. To address this outcome new test using a different AOI for the hand in a more controlled manner will be developed (section 3.6.1) and assessed (section 4.3.1).

The participants in this study had complained about the duration of the test (15 acclimatisation + 15 minutes of provocation) and having to come for two visits, questioning if they could not do the test in just one visit. This information was also taken in consideration in the development of the new test (section 3.6.1).

From the results it became clear that the AOIs of the pilot KPT did not produce the expected value of repeatability, and new AOIs for hands need to be specified to improve this situation. The volunteers also complained about the duration of the test and about having to make two visits, a new test was therefore developed (section 3.6.1) to address both issues.

3.5.2. Vibration provocation test, VPT

This second pilot experiment aimed to investigate the temperature changes in the upper limbs of healthy subjects after holding a vertical vibration device for 2 minutes.

This investigation used the same equipment as in the previous experiment and additionally:

- A vibration device (a cinema seat vibration device) as provocation tool, which produces vertical vibration (fig. 76). This type of vibration was suggested by Prof. Griffin in Southampton. This vibration device was isolated with brown paper and plastic (good thermal conductor) to minimise the effect of thermal conductance between the subject and the device.
- A PHILIPS frequency generator set to 31.5 MHz for generating the vibration frequency (fig. 76).
- A PHILIPS frequency counter, to monitor the frequency induced (fig. 76).
- A standard GRUNDIG 400W audio amplifier, to amplify the signal from the frequency generator for the vibration device (fig. 76).
- An oscilloscope, to monitor the waveform produced.

The same 12 healthy male volunteers as in section 3.5.1 participated in this pilot experiment and the same procedure with two visits on two different days was followed. As before on the first visit the provoked hand was the right and the left remained still (fig. 77) while during the second visit this was the other way round. Technical protocol, volunteer preparation, acclimatisation, etc. were identical.

The volunteers were seated in a chair in a comfortable position and a baseline image was taken (fig. 78). The volunteers then stood up, in order to standardise the procedure, and were requested to hold the vibration device with the fingertips of one hand (fig. 77) at an angle of 90° between the hand and chest while the other hand remained still.

The vibration frequency of 31.5Hz frequency was chosen in agreement with literature (Bovenzi et al., 2000). The induced maximum acceleration from the vibrating device was 36 m/s², measured by a calibrated laser vibrometer (fig. 79 and fig. 80) at Swansea Metropolitan University. With the same device the acceleration absorbed by human hands was determined to be 30 m/s² on average. Using the chart shown in fig. 81 and tracing a line from the measured acceleration to the correspondent exposure time of 2 minutes, the partial exposure vibration A(8) was found to be 2.5 m/s². This is half of the maximum allowed by British and EU regulations (5 m/s²) and was thus considered a safe value for this experiment.

After 2 minutes of vibration exposure the subject was asked to assume the same position as in the first image and a second image was recorded under exactly the same conditions as the first one (fig. 82).

All data was analysed using the same methods as section 3.5.1.

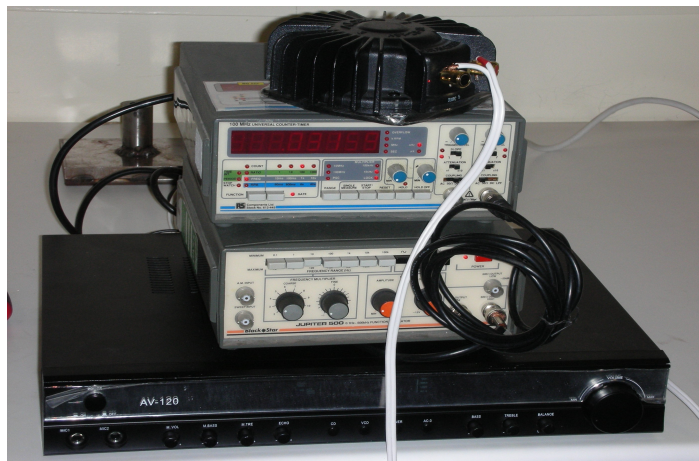


Fig. 76: The vibration test equipment: on top the vertical vibration motor, underneath the frequency counter, frequency generator and at the bottom the audio amplifier.

For data analysis the same 4 AOIs as in the previous pilot experiment in 3.5.1 were used and analysed in the same way.



Fig. 77: A volunteer holding the vibrating device with the fingertips of one hand, position used for the pilot test (holding the device with just one hand) - rejected.



Fig. 78: Hands positioned at 90° angle to the camera.



Fig. 79: The laser vibrometer measuring the vibration magnitude from the vibration device, the posture for the real objective test (holding the device with all fingertips).

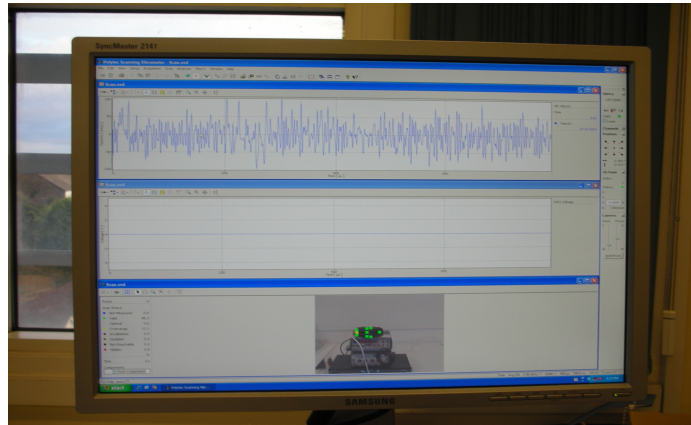


Fig. 80: Laser vibrometer output, the laser measures the acceleration of the vibrating device in several points.

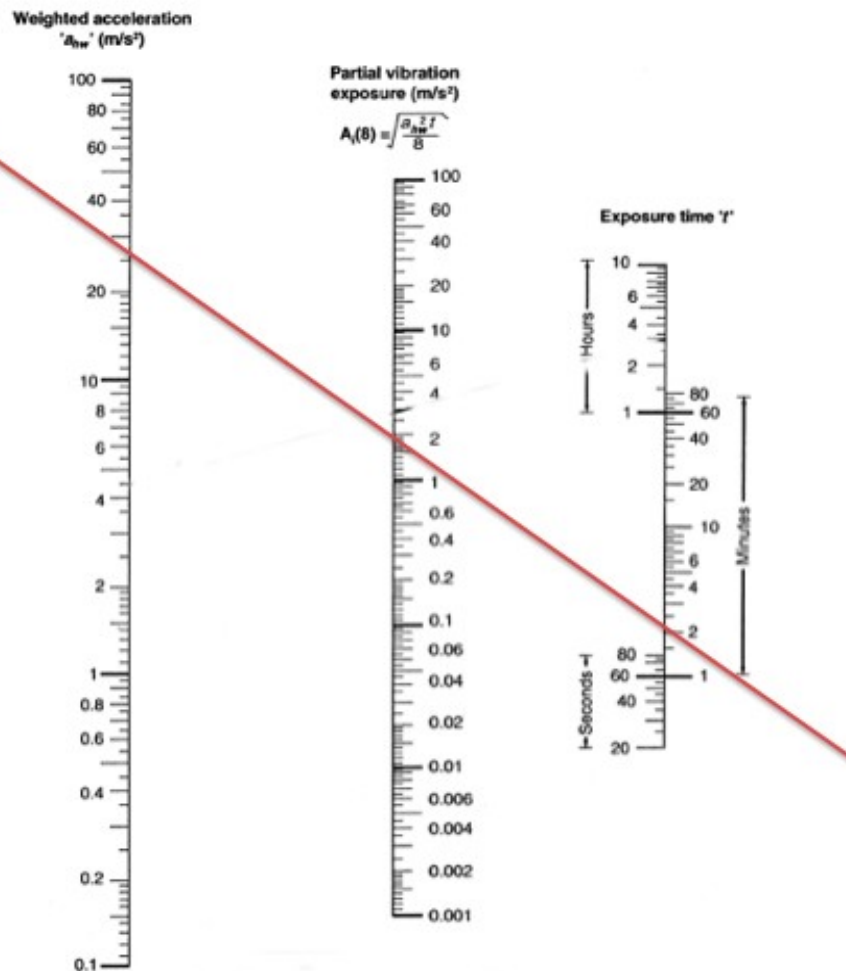


Fig. 81: Vibration magnitude exposure calculation chart, the red line shows the correspondence between weighted acceleration (36 m/s²) and 'daily' partial vibration (2.5 m/s²) exposure and exposure time (2 minutes).

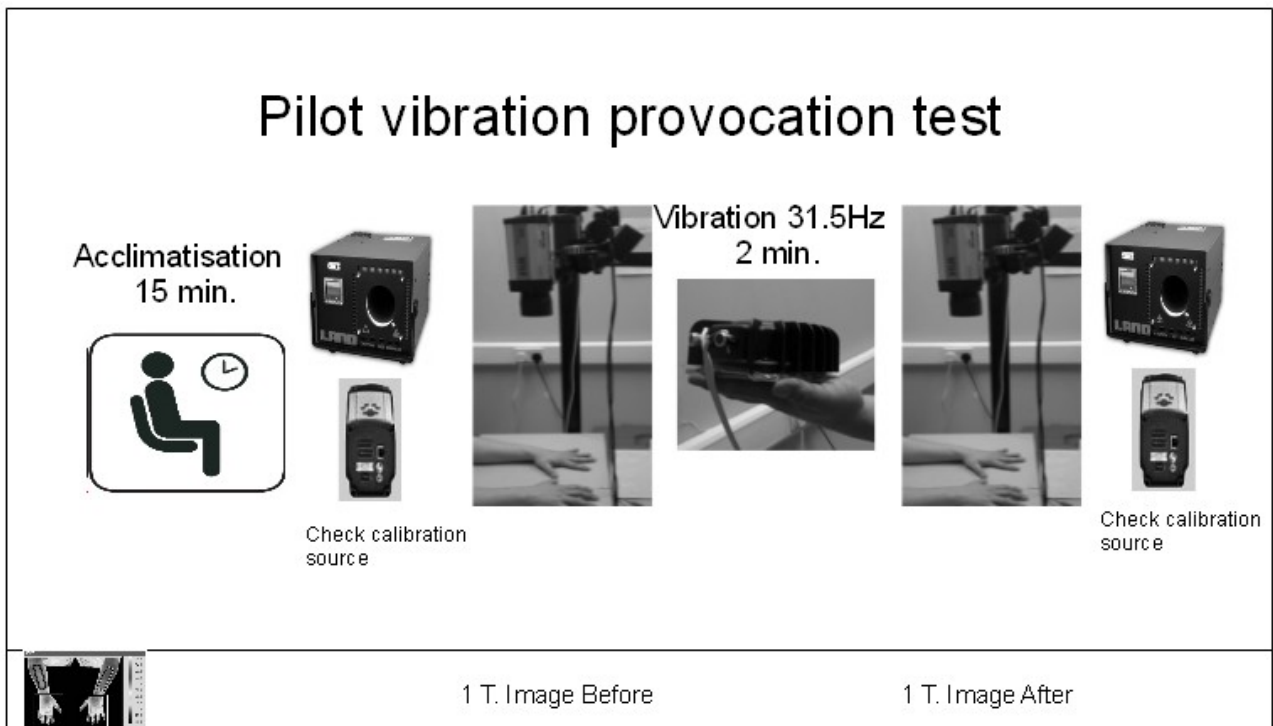


Fig. 82: The pilot Vibration Provocation Test diagram.

The same 12 volunteers as in the previous keyboard provocation test participated in this experiment.

Fig. 83 shows that the mean temperature changes when exposing the right hands of volunteers for 2 minutes to a vibration provocation at a frequency of 31.5Hz and a magnitude of 2.5 mm/s² while keeping the left hand still. Fig. 84 shows the results for the left hand while keeping the right hand still.

Fig. 85 and 86 show the average temperature differences calculated from these data sets. Generally, the stressed hand grows colder as expected from literature (see 2.3.2). Due to the already mentioned link between both body hemispheres the collateral side is also affected but not conclusively so; as shown in fig. 86 where the left hand actually grows slightly warmer as the right hand is stressed.

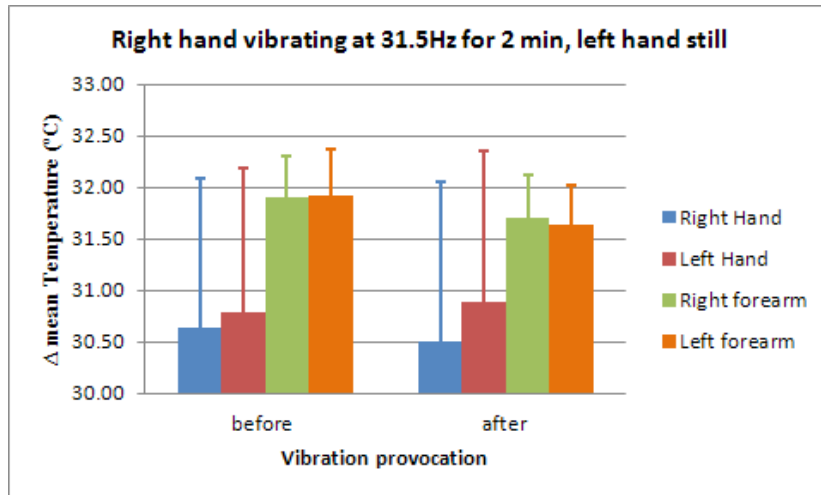


Fig. 83: Average mean temperature on exposing the right hand to vibration keeping left still, just hands were exposed.

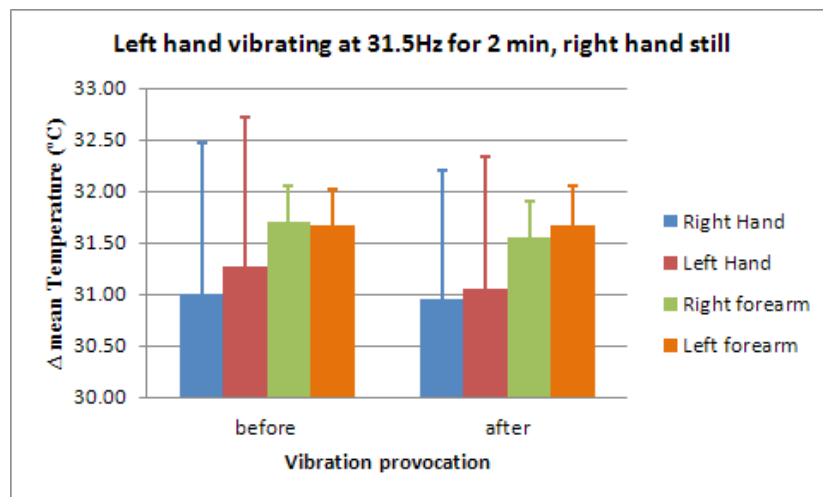


Fig. 84: Average mean temperature on exposing the left hand to vibration keeping right still, just hands were exposed.

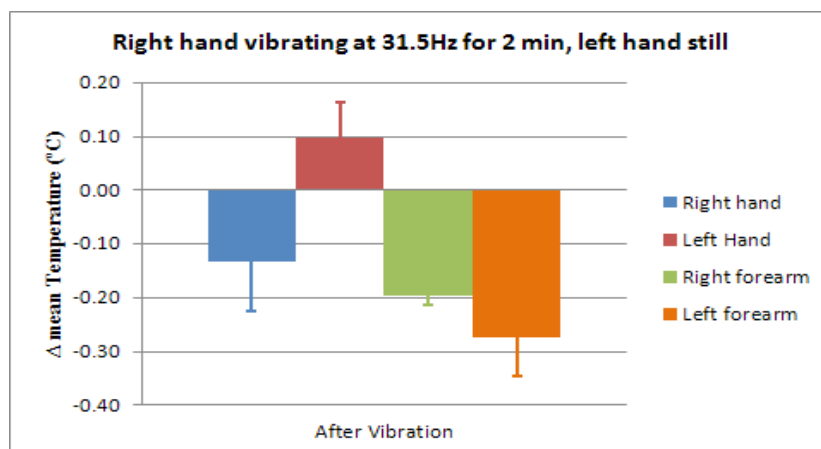


Fig. 85: Mean temperature difference from baseline, right hand vibrating and left hand still, just hands were exposed.

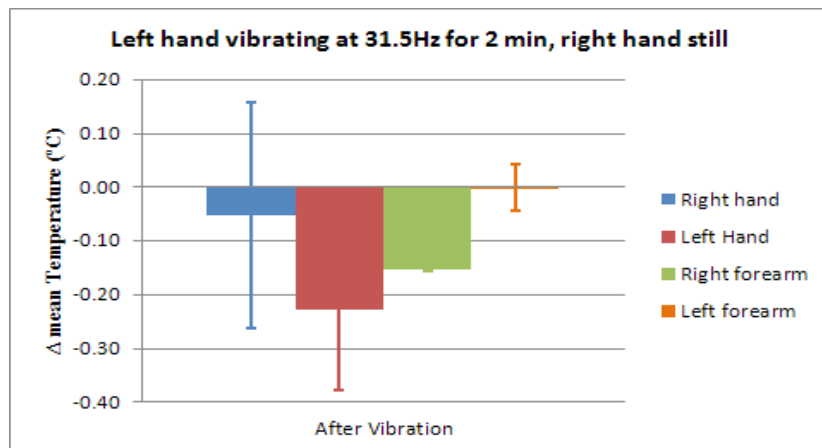


Fig. 86: Mean temperature difference after left hand vibrating and right hand still, just hands were exposed.

Fig. 87 and fig. 88 show the thermal symmetry between left and right hands before and after vibration stress while fig. 89 and fig. 90 do the same for the respective forearms. As in the previous experiment the left extremities are slightly warmer than the right ones at the baseline by about 0.3 degrees C. If now the left hand is stressed (fig. 88) and thus cooling down the lateral asymmetry actually decreases. In the case of the already colder right hand being vibrated the asymmetry increases.

When comparing changes in hands and their respective forearms it is also obvious (and in line with expectations from literature [Acciari, 1978]) that forearms are significantly less influenced by vibration than hands.

There is possibly a difference between groups in terms of handedness, age and BMI class, but due to the low sample number (12 participants) the statistical coefficients this difference cannot be conclusively proven.

Handedness

These result show that right handed subjects are slightly more affected by vibration to the right hand than left handed people are affected to vibration of the left hand.

Age

From the results it could be concluded that with age there is a small loss in the capability of maintaining thermal symmetry after vibration exposure.

BMI

It could be concluded from this experiment that vibration provokes a decrease in thermal symmetry of the hands having a larger impact in the forearms where a small difference can be observed between normal weight and overweight BMI classes.

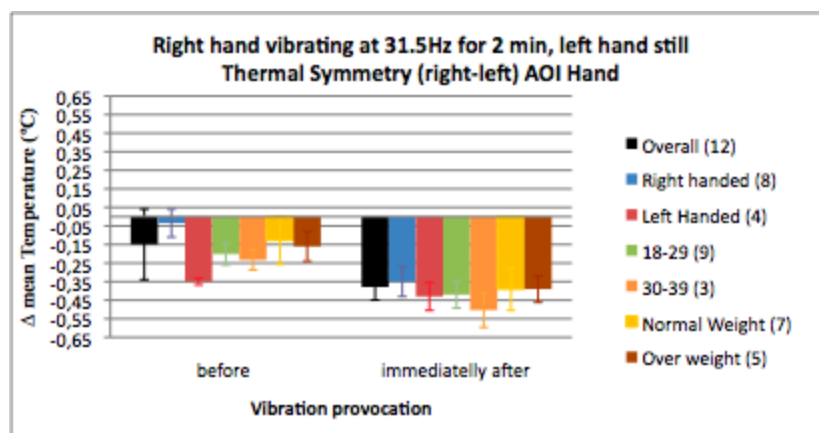


Fig. 87: Hand Thermal Symmetry (Right AOI – Left AOI) characterisation of hand AOI when stressing right hand with vibration.

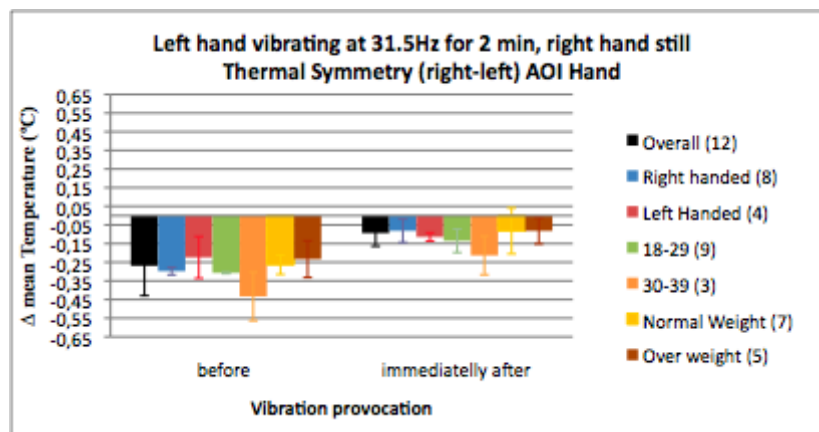


Fig. 88: Hand Thermal Symmetry (Right AOI – left AOI) characterisation of hand AOI when stressing left hand with vibration.

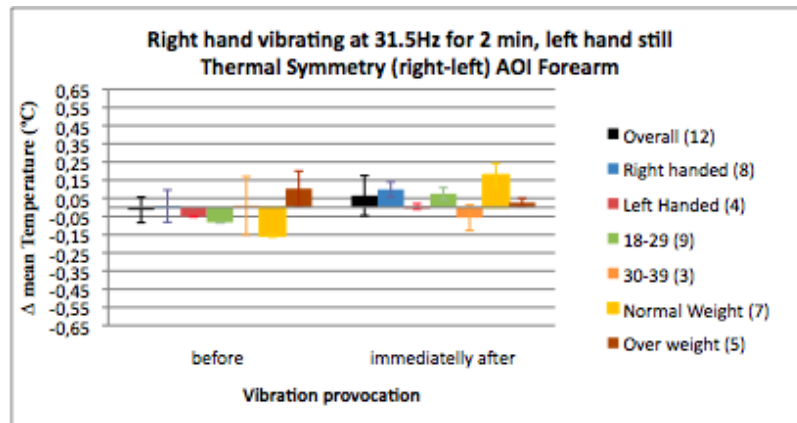


Fig. 89: Forearm Thermal Symmetry (Right AOI – Left AOI) characterisation of forearm AOI when stressing right hand with vibration.

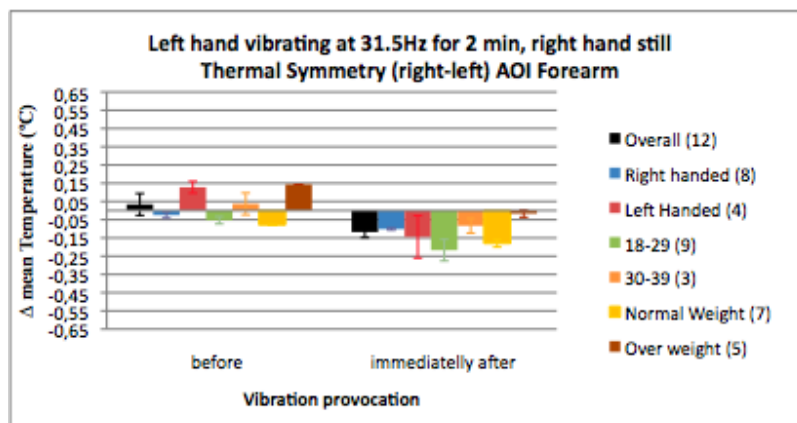


Fig. 90: Thermal Symmetry (Right AOI – left AOI) characterisation of forearm AOI when stressing left hand with vibration.

A Inter Class Correlation coefficient test was conducted, obtaining that for the hand AOI the ICC was 0.81 with a 95% confidence interval of 0.48 to 0.94 and alpha Cronbach coefficient of 0.89, and for the forearm AOI the ICC was 0.89 with a 95% confidence interval of 0.65 to 0.94 and alpha Cronbach coefficient of 0.92. In contrast to the previous keyboard provocation experiment where the hand AOI repeatability was poor, these values represent a good repeatability of the both AOIs.

The participants in this had questioned the reason for two visits and suggested if the test could not be perform in just one test, or combined the provocation of the two hand in one test. A new test had been developed (section 3.6.2) addressing this outcome and posteriorly assessed (section 4.3.2).

Considering the results of the vibration pilot test it can be seen that the AOIs used were reliable and produced repeatable outcomes. However, these could be improved if the hand AOI would be shaped following the outline of the hand rather than being simply a rectangle. This should lead to a better discrimination of data between different groups to be analysed. The possibility of provoking both hands in the same test would also speed up the experiment and remove the need for two visits. The test developed in section 3.6.2 deals with these aspects.

In review the pilot test involving keyboard typing and vibration produced the following outcomes:

1. Hand AOI repeatability low in keyboard provocation test
2. Statistical difference between groups low in vibration provocation test
3. Duration of the keyboard provocation test was acknowledged as uncomfortable from the participants.
4. The participants in both tests had suggested a combination of provocation to both hands in order to avoid a second visit.

3.6. Objective provocation tests

Based on the experience gained from the first two pilot tests four objective tests were designed: three of these involved a mechanical stress followed by a vascular test the fourth included only the vascular test. These tests are described in detail in this section. To support the validity of these 4 tests, two further tests were designed: one to verify the methods for assessing a vascular challenge, the other one for determining any difference in results if other imaging instruments suitable for medical thermal imaging are used.

In order to recruit volunteers, participants from the questionnaire study (section 3.2) who had indicated that they were prepared to be approached again were contacted. Additionally posters advertising this study and asking for volunteers were distributed around the Faculty. Emails were sent to students and staff and an advertisement was posted on the University of Glamorgan intranet website. After volunteers expressed their interest in collaborating in this study, they received information on the experiments and tests (See Appendix 9) and were asked to sign an informed consent form (also in Appendix 8). After that an EURO-QOL form (see Appendix 10) had to be

completed and two screening questionnaires (one for each syndrome, RSI and HAVS) were also given to the volunteers in order to collect information about possible signs or symptoms of these conditions (Appendices 11 and 12). These questionnaires are validated, standard forms for collecting information when screening for the syndromes. The RSI screening questionnaire is the one designed and used by the London Hazards Centre (Tivey, 1997). The HAVS screening questionnaire is the one suggested and utilised by UK HSE and the NHS (HSE, 2008).

Once the volunteers had completed questionnaires and forms, their medical history and information on the syndromes relevant for this work could be analysed. Participants were graded and divided into four groups of injury severity based on HAS syndrome signs, symptoms or medical diagnoses according to the guidelines (Levine et al., 1993, Tivey, 1997, HSE 2008). These four groups are: 'healthy controls', 'signs of syndrome', 'symptoms of syndrome' and 'confirmed with syndrome'. The individuals considered for the control group had an EURO-QOL score of 0 and no complaints in the hands. The distinction made between the 'signs' group individuals and the 'symptoms' group was based on the respective individuals' complaint characteristics and the EURO-QOL score. Those having an EURO-QOL score of less than 2 and absence of numbness, tingling or blanching were considered for the 'signs' group, anyone above that EURO-QOL score and not clinically confirmed as having a condition were considered for the 'symptoms' group. The 'confirmed' group was composed of individuals clinically confirmed of having a HAS condition. Table 7 shows the problems reported by the subjects of the 'symptoms' and the 'confirmed' groups.

Volunteers were then asked to perform the objective provocation test(s). As the protocol stated that they had to wait at least 30 minutes in between individual tests it was suggested to them that they participated in only one test per visit and day.

Confirmed	
Volunteer:	Reported problem:
HAS03	Right index finger and thumb affected with RSI
HAS26	All fingers of both hands affected with RSI
HAS29	Index finger of right hand affected with HAVS
Symptoms	
Volunteer:	Reported problem:
HAS02	Numbness and tingling in the little and ring finger of the left hand.
HAS05	Numbness and tingling in all fingers of both hands.
HAS07	Numbness and tingling in all fingers of right hand.
HAS16	Numbness and tingling in all fingers of both hands.
HAS17	Numbness and tingling in all fingers of both hands.
HAS18	Numbness and tingling in all fingers of both hands.
HAS22	Numbness, tingling and arthritis in all fingers of both hands.

Table 7: Reported problems from the individuals of the symptoms and the confirmed groups.

The order of provocation test was: first the keyboard provocation test, second the vibration provocation test, third a mouse provocation test and finally a standard vascular cold stress test. The mouse provocation test follows a similar rationale to the keyboard test and was included due to the fact that both mouse and keyboard are known to cause repetitive stress. The standard vascular cold stress test was included so that experimental results of the other three tests could be set into the context of this well known, accepted and documented test for comparison and verification.

The volunteers participating in the four tests test are characterised in table 8, according to injury stage group, gender, age, BMI and handedness.

The thermal camera used in all tests was a FLIR A40 (described in section 3.1) and all tests were performed in the Thermal Physiology Lab at the University of Glamorgan. All volunteers while participating in the tests were constantly monitored for the duration of the tests by the author.

Volunteer	Injury grade group	Gender	Age	BMI	Handedness	KPT	VPT	MPT	CST
HAS01	Control	M	20	24,4	Right	x	x	x	x
HAS02	Symptoms	F	32	33,9	Right	x	x	x	x
HAS03	Confirmed	F	38	30,3	Right	x	x	x	x
HAS04	Control	M	51	28,8	Left	x	----	----	----
HAS05	Symptoms	F	35	19,8	Right	x	x	x	x
HAS06	Signs	F	44	21,9	Right	x	x	x	x
HAS07	Symptoms	F	39	20,7	Right	x	x	x	x
HAS08	Control	F	35	24,3	Right	x	x	x	x
HAS09	Signs	F	35	26,2	Right	x	x	x	x
HAS10	Control	F	31	22	Right	x	x	----	----
HAS11	Control	F	61	26,9	Right	x	x	----	----
HAS12	Control	F	34	26,7	Right	x	x	x	x
HAS13	Signs	F	58	19,4	Right	x	x	x	x
HAS14	Signs	M	64	29,6	Right	x	x	x	x
HAS15	Signs	M	31	27,7	Right	x	x	x	x
HAS16	Symptoms	F	30	19,7	Left	x	x	x	x
HAS17	Symptoms	F	34	20,19	Right	x	x	x	x
HAS18	Symptoms	F	54	25,1	Right	x	x	----	----
HAS19	Control	M	20	27,7	Right	x	x	x	x
HAS20	Control	M	21	23,2	Right	x	x	x	x
HAS21	Control	F	30	21,8	Right	x	----	----	----
HAS22	Symptoms	F	32	22,9	Right	x	x		
HAS23	Control	M	22	24	Right	x	x	x	x
HAS24	Control	M	32	26	Left	x	----	----	----
HAS25	Signs	F	23	22,3	Right	x	x	----	----
HAS26	Confirmed	M	22	20	Right	x	x	x	x
HAS27	Control	M	38	27,3	Right	x	x	x	x
HAS28	Signs	M	31	30	Right	x	x	x	x

Table 8: Volunteers participating in the four Provocation Test (KPT=Keyboard, VPT=Vibration, MPT=Mouse, CST=Cold Stress Test), the '----' represent the volunteers that have not performed the test.

After arrival, before the volunteer entered in his first test he was requested to complete all forms (consent form, EURO-QOI and both screening questionnaires for RSI and HAVS). After completing them or coming for a second test, in accordance with the protocol defined in section 3.1

the volunteer was requested to keep the upper limbs unclothed and stay still, avoiding any contact for a period of 15 minutes in the acclimatisation room before undertaking the test.

Before starting any of the tests the examiner takes a reference image from the calibration source (blackbody) in order to verify for the performance of the capture equipment. For recording the hands a MDF board is again used to facilitate better contrast with the background. A capture mask proposed by Ammer (Ammer, 2008, Ring et al., 2005), fig. 38, is shown on a screen visible to the volunteer in order to already at this stage produce a good alignment with the standard view. The camera is positioned at a distance of 1 m perpendicularly to the hands' surface.

The description of the procedures of the objective tests are outlined in sections 3.5.1 to 3.5.4. At the end of each test an image from the thermal reference source was taken to validate the capture quality. All the captured images were securely stored in the laboratory's CTHERM database, and subjected to analysis with the results shown in section 4.3 and discussed in section 5. The statistical analysis of this test includes the mean temperature and standard deviation values of AOI of the hand, its calculated thermal symmetry, a ICC test evaluating consistency and repeatability, a K-S test if the collected data follows the normal distribution, a non-parametric chi-square test evaluating the evidence of statistical independence between groups. All test were run in the statistical software SPSS. A Z-test was used to compare hypotheses and ran manually in Microsoft Excel to verify if it was possible to statistically discriminate between groups.

3.6.1. Keyboard provocation test, KPT

The keyboard provocation test is based on the pilot test in section 3.5.1. using its outcomes. In order to respond to the poor repeatability found in the pilot test (section 3.5.1) and simultaneously to design a more standardised test of mechanical provocation this test was designed as outlined below.

The text to be typed by subjects was not reported in previous studies (Sharma, 1997, Ammer, 2001). To overcome this lack of information and in order to minimise the potential psychological stress related with the task of typing a text, a supporting computer application was developed (in the C# language). This tool consists of a virtual keyboard displayed on the computer screen (after: Peper, 2003) that informs the user which key to press (Fig. 91). The user is then informed if the key pressed was the correct one (outlined in green) or not (contoured in red). The

pseudocode of the program is shown in fig. 92. In addition to checking the key pressed by the user, the application allows to count the number of keystrokes in a defined period of time. For a permanent record of the keys to be pressed and the keys actually pressed the application writes two log files and at the end of the test. A summary with the total number of keystrokes and failed attempts is displayed.

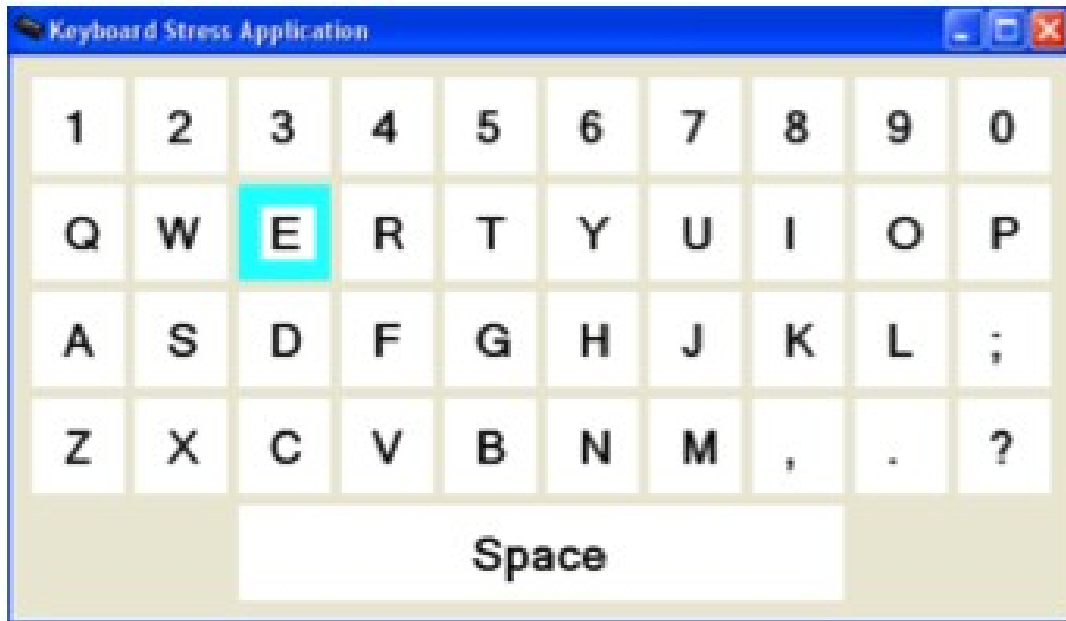


Fig. 91: The virtual keyboard application.

The Keyboard Provocation Test (KPT) begins by recording a baseline image, then the subject begins the task of keyboard typing, aided by the application described before for 5 minutes, sitting in a chair in the correct position and facing the screen at a 90° angle with the arms stretched over to the keyboard. After this the subject is repositioned for recording a new image under the same conditions as the baseline image. This image recording is followed by a vascular provocation test, described in more detail in section 3.6.4, for 1 minute. After this test the subject is again repositioned in the image recording position as before and for 10 minutes an image is taken at 1 minute intervals. This procedure is summarised in the diagram of fig. 93.

```

Pressed keys <- 0

Displays the virtual keyboard on the screen

Reads the duration of the test in minutes

While the duration of the test is not reached

    proposed key = generate a random number (1-41)

    Display the proposed key to be pressed on the screen

    Read a key from the keyboard

    Pressed keys <- Pressed keys + 1

    Records the key proposed in the proposed log file

    Records the key pressed from the keyboard in the pressed log file

    If the pressed key is the same of proposed key

        Outlines the proposed key in the virtual keyboard with the green colour

    Else

        Contours the proposed key in the virtual keyboard with the red colour

```

Fig. 92: Pseudocode of the virtual keyboard application.

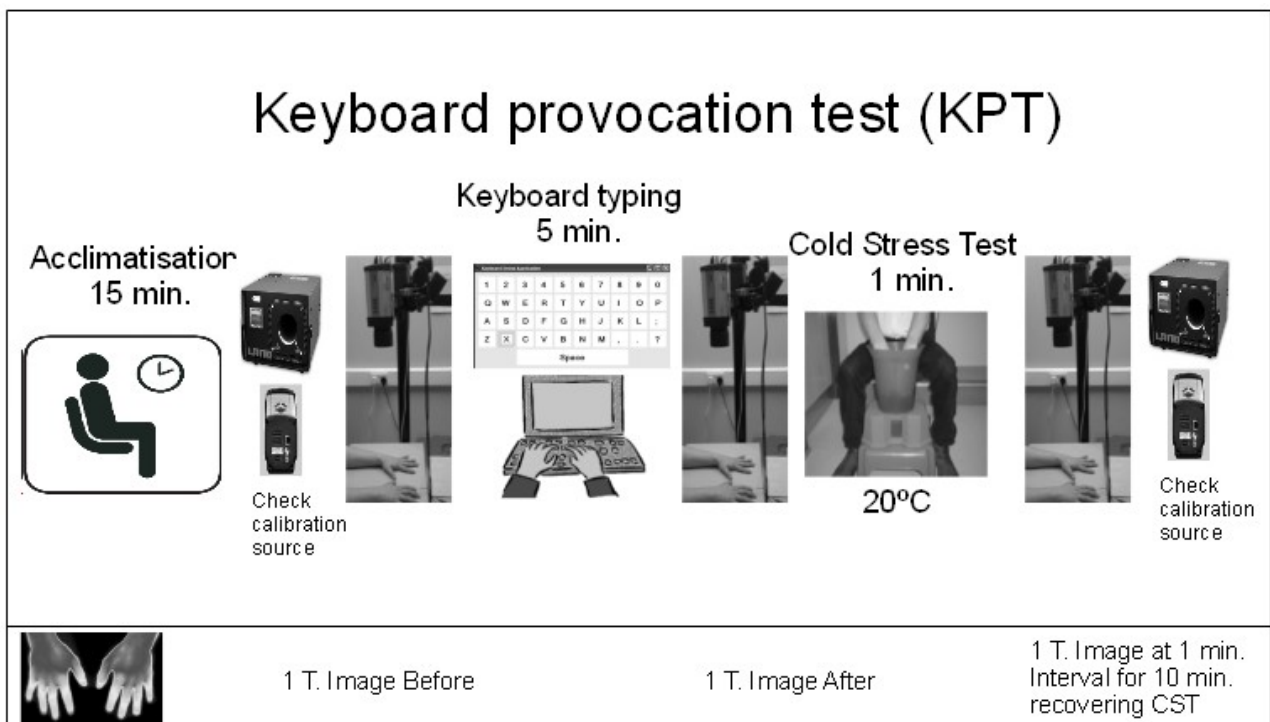


Fig. 93: The Keyboard Provocation Test diagram.

All collected images were analysed in a process outlined later in section 3.7.4.

3.6.2. Vibration provocation test, VPT

The vibration provocation pilot test described in section 3.5.2 has proved to be repeatable. It requires, however, two visits or a longer period of examination on the same day. This test is based on the pilot but reduces the time of examination while maintaining its repeatability and introduces extra information and contextualisation by including a post provocation cold challenge after vibration exposure.

The required equipment is the same as the one in the pilot test and shown on fig. 76. After capturing the baseline image the volunteer is asked to stand up, hold the vibrating device with the fingertips of the hand maintaining an angle of 90° between arms and forearms as shown in fig. 79. The device was then turned on, inducing the before mentioned vibration frequency of 31.5Hz at an acceleration amplitude of 36 m/s² for 2 minutes. After that period the device was turned off and the subject was requested to return to the baseline recording position and a post vibration thermal image was taken as shown in fig. 94. This procedure was immediately followed by a vascular test, described in more detail at section 3.6.4.

All collected images were analysed in a process outlined later in section 3.7.4

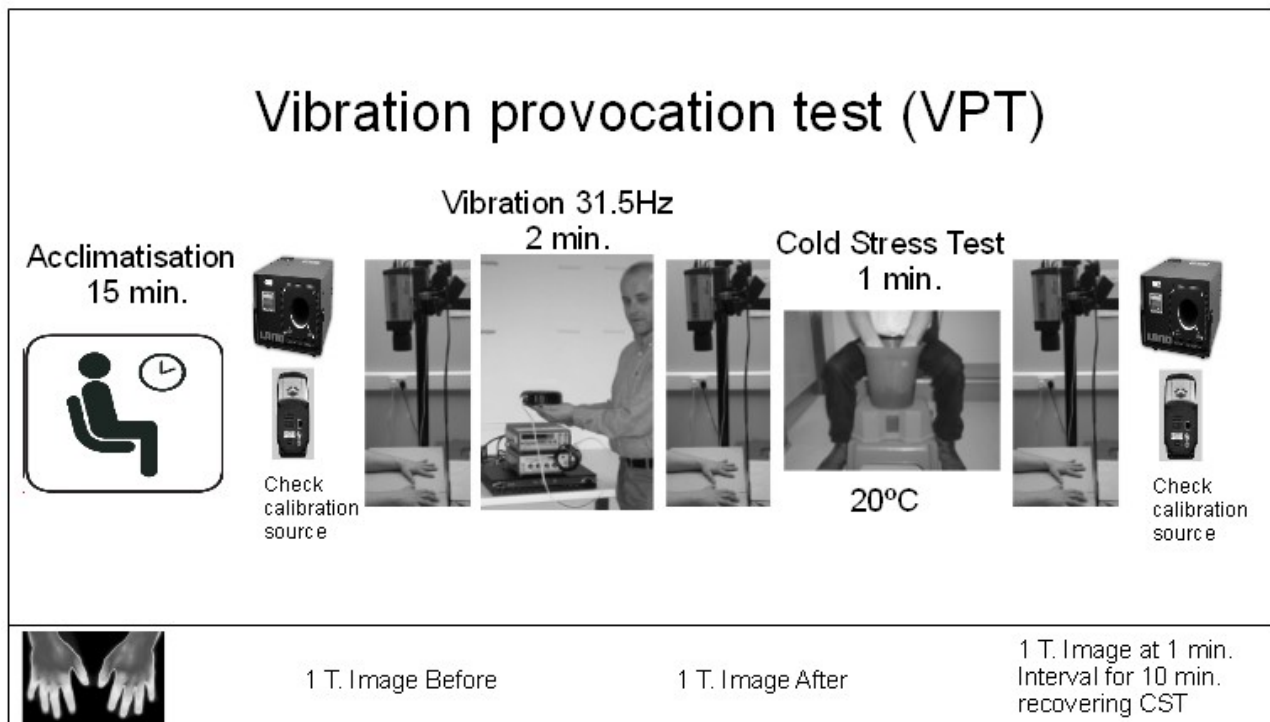


Fig. 94: The Vibration Provocation Test diagram.

3.6.3. Mouse provocation test, MPT

Mouse handling is a very intensive repetitive task, normally performed by just one hand, it involves short and continuous movements of the wrist, metacarpals and index and middle carpals for clicking. These movements are known to provoke RSI, as addressed in chapter 2 , but the effect of these movements towards the development of the condition remain unclear.

It is the aim of this experiment to assess the effect of mouse handling on the temperature of the mouse handling hand compared to the other inactive hand.

As before in the mouse provocation test, a computational application was developed. This tool presents a window on the screen showing a single virtual button (fig. 95). Whenever this button is clicked it will disappear and then reappear at a random position inside the window. This process will run for a specified time. The program has the ability of counting the number of mouse clicks and mouse cursor distances travelled in order to quantify the stress load and to report it at the end of the test. In fig. 96 pseudocode of the tool is shown.

As in the other tests, the Mouse Provocation Test begins with the recording of a baseline image. After this recording the volunteer is requested to sit at a computer desk and to place the left hand still on the desk and the right hand on the mouse. When ready, the provocation program will start and run for a period of 5 minutes. After that and a return to the recording position another image is taken. When this second image is recorded the volunteer is subjected to a vascular test, as described in the next section (3.6.4). The diagram presented in fig. 97 describes the whole procedure of the Mouse Provocation Test.

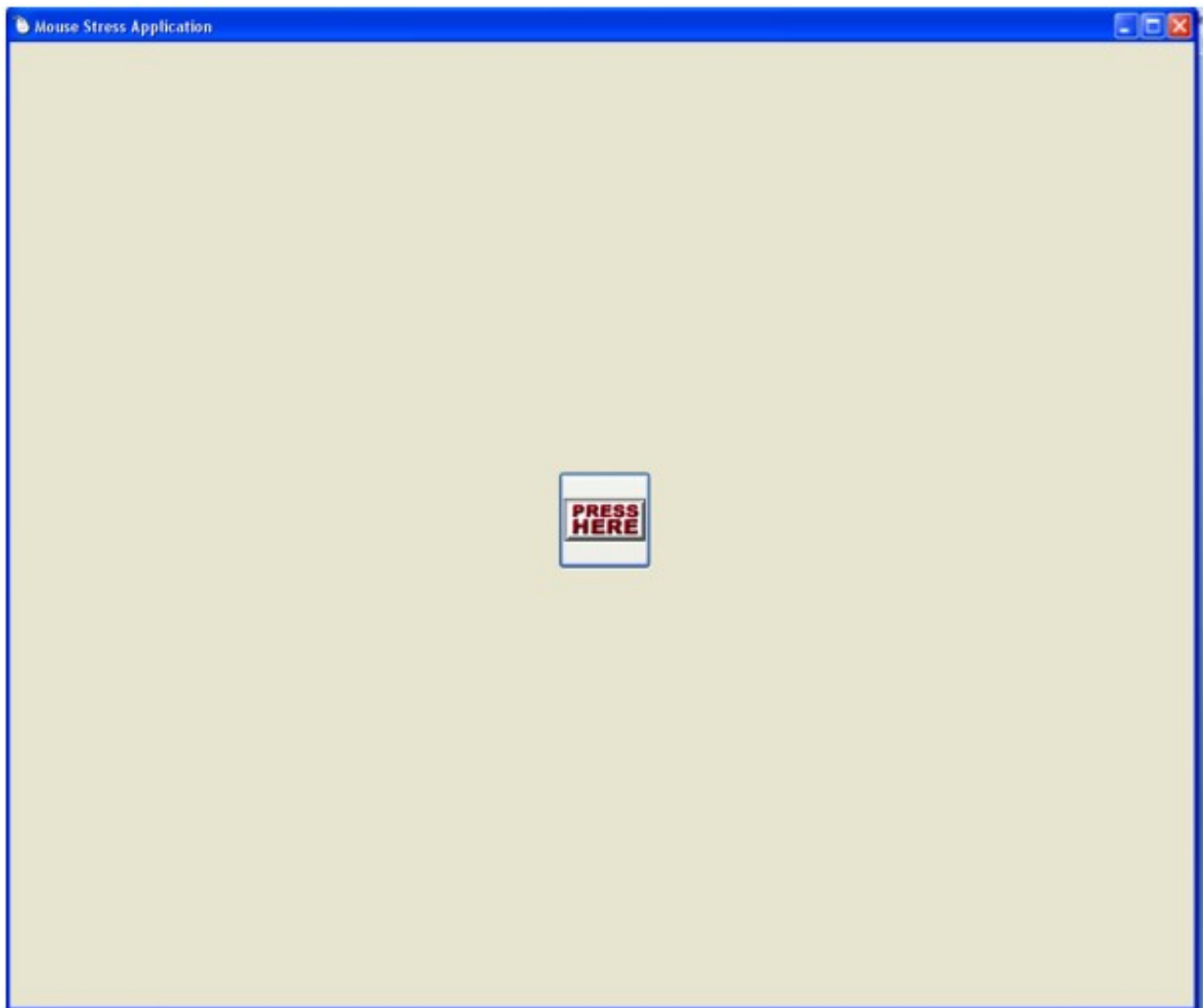


Fig. 95: The Mouse Provocation Test application.

All collected images were analysed in a process outlined later in section 3.7.4.

```

Read Duration

X ← random value (0, 800-button.length)

Y ← random value (0, 600-button.height)

button.center ← (X+button.length/2, Y+button.height/2)

Time ← 0

traversed ← 0

Num_Clicks ← 0

While (Time < Duration)

    if (clicked)

        Num_Clicks ← Num_Clicks + 1

        X ← random value (0, 800-button.length)

        Y ← random value (0, 600-button.height)

        new_button.center ← (X+button.length/2, Y+button.height/2)

        distance ← sqrt (pow2(new_button.X - button.X) + pow2(new_button.y - button.y))

        traversed ← traversed + distance

        button = new_button

```

Fig. 96: The mouse provocation application algorithm pseudocode.

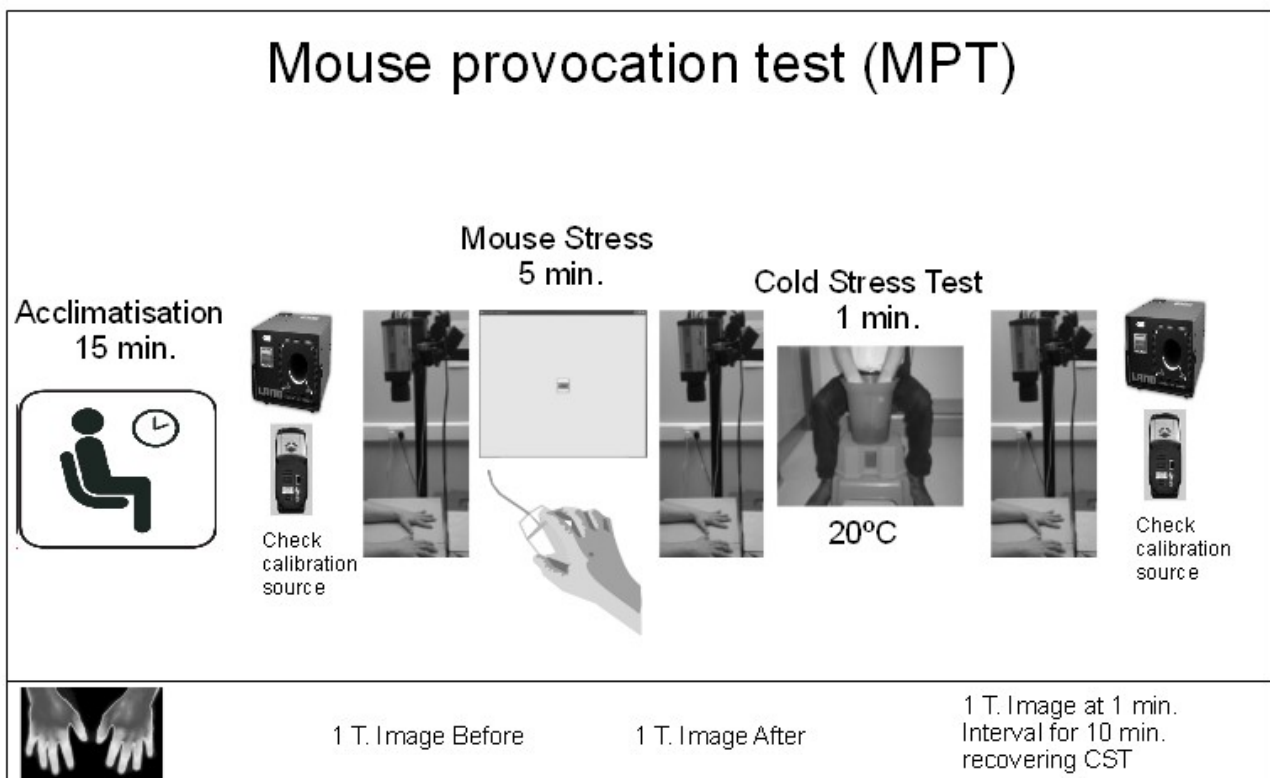


Fig. 97: Diagram of the Mouse Provocation Test.

3.6.4. Cold stress test, CST

The aim of the Cold Stress Test for the hands is to assess the ability of the vascular system to recover from a cold challenge provocation. The recovery pattern provides objective information about the capabilities of the vascular system of the hand. When exposed to cold stress blood vessels constrict in order to avoid hypothermia. This decreases the provision of oxygenated blood and simultaneously the removal of carbon dioxide saturated blood and consequently forces a reduction of hand temperature. Immediately after the challenge blood vessels will start to re-open, increasing blood flow and re-establishing the normal temperature.

After taking the baseline image, the volunteer is asked to wear a pair of thin latex gloves over the hands and immerse them in a bucket filled with water at 20°C (monitored by a mercury thermometer). The volunteer remains seated in front of a desk with the hands in a vertical position inside the bucket avoiding contact with the bucket wall or the other hand for a period of one minute. Immediately after this the investigator helps to take off the gloves and makes sure that no direct contact is made with the water. In order to complete the test, the volunteer now places the hands in the recording position (which is the same as the one for taking the baseline image) and for a recovery period of 10 minutes a thermal image is taken at 1 minute intervals. The whole procedure for the case of applying the vascular test only without any pre-provocation is described by the diagram in fig. 98.

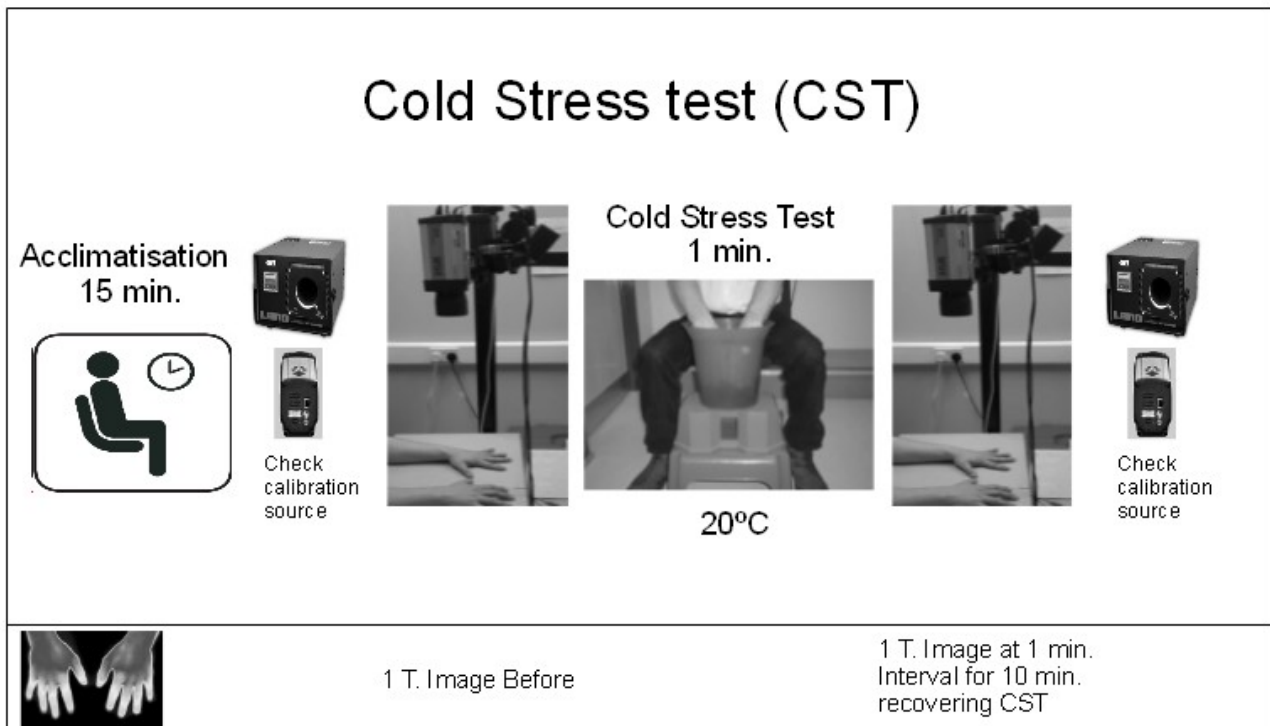


Fig. 98: The Cold Stress Test diagram.

As outlined in section 2.7 of the literature survey there are three methods for assessing the outcome of a cold stress challenge: Ring's Mean Thermal Area (MTA) method and Ammer's Mean Thermal Gradient (MTG) and Mean Thermal Profile (MTP) methods. In order to test and compare the performance of these three assessment methods a computational application was developed in the C# language. The tool loads thermal images of a cold stress test of the hands (i.e. baseline image plus the 10 recovery images) and implements an automated solution for all three methods, generating charts for each hand and statistical tests in addition to the respective index values, the flowchart of this application is shown in fig. 99.

The thermal indexes for each method, each hand and each image are calculated as follows:

- MTA - the difference between the average mean temperature of the area of four finger and the mean temperature of the area of the palm.
- MTG - the difference between the average mean temperature of the fingers from 25 central pixels of DIP and the average mean temperature of the finger's metacarpals from 25 central pixels of the proximal region (at the same distance from the finger metacarpi-phalanger joint of the central finger DIP).
- MTP - the difference between the average mean temperature of the finger's central line 5

pixels large from the central DIP to the metacarpi-phalanger joint and the average mean temperature of the finger's metacarpals central line 5 pixels large from the metacarpi-phalanger joint to the proximal region of the metacarpal with the same length of the finger line.

This analysis is outlined later in section 3.7.4.

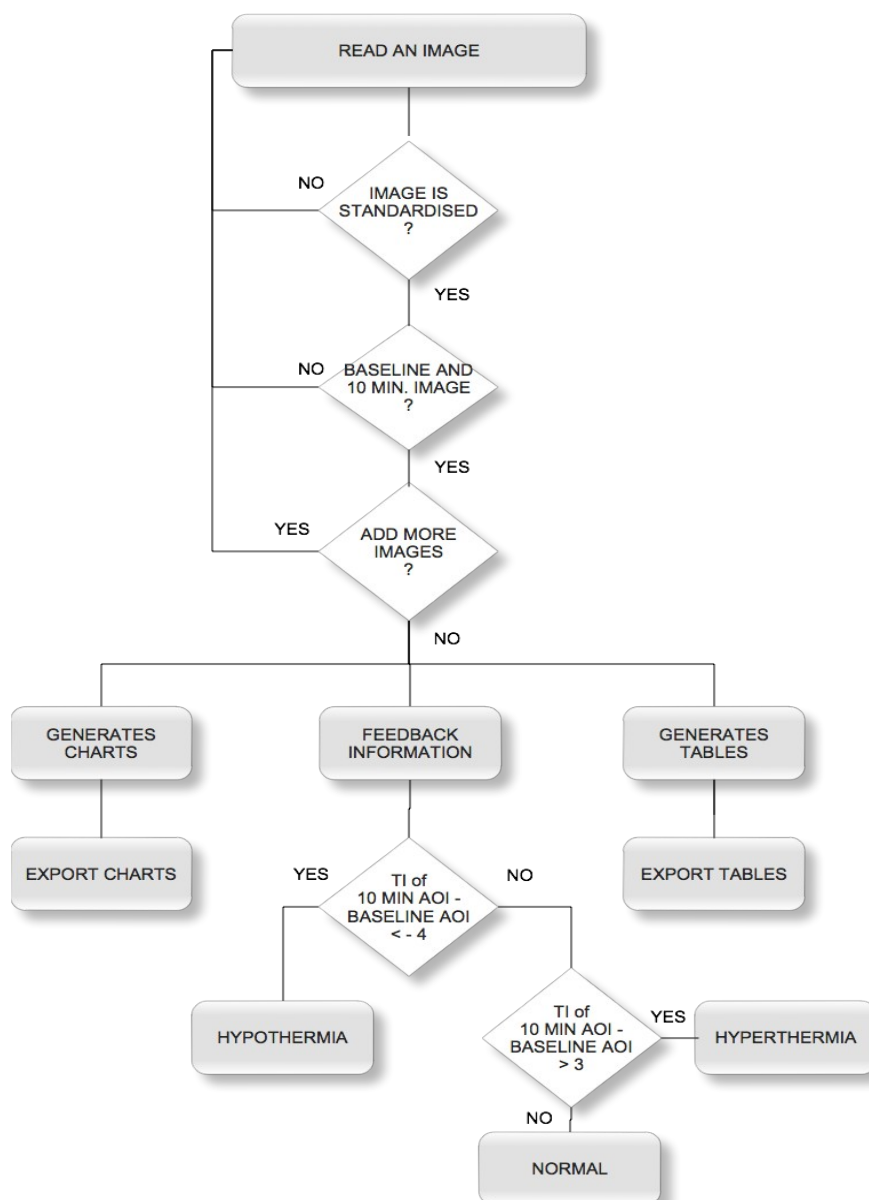


Fig. 99: Flowchart of the application to evaluate the three assessment methods of CST.

3.6.5. Inter-camera assessment test

Different infrared cameras are currently available for medical use and it is important to investigate the impact of different imaging systems. The same methodology (i.e. images captured according to the test defined in section 3.6.4. and each image standardised and analysed by the method described later in section 3.7.4.) could produce different results with different camera systems. In order to assess the impact of camera performance on the described methodology a simple experiment was conducted where 3 cameras were selected, according to the different image resolution produced in the far infrared wavelength, and a volunteer was asked to undergo a CST that was recorded by a different camera every time (For practical reasons it was not possible to monitor the same CST by all three cameras simultaneously). The three cameras' characteristics are shown in table 9.

Characteristic	FLIR B2 Portable	FLIR A40 Thermovision	FLIR SC7000 Titanium
Image resolution	120x120	320x256	640x512
Detector type	Uncooled	uncooled	Cooled
NETD	1K	0.08K at 30°C	<20mK
Thermal Accuracy	±2°C or ±2%	±2°C or ±2%	±1°C or ±1%

Table 9: Operational characteristics of three infrared imager systems

The results of the measurements on the standardised AOIs of the hand were recorded in a spreadsheet and statistically analysed using the SPSS[®] software package. The variances and a student t-test were calculated to verify the degree of equity between the measurements of the three imager systems. The results are shown later in section 4.3.6.

3.7. Image processing developments

Thermal images are, due to the underlying physical principles, different from conventional digital images. Some of the common imaging processing techniques for conventional images can be used without problems others, however, may produce different results from what was expected. In this section a set of four experiments investigates common procedures for conventional digital

imaging processing towards their suitability for thermal image processing.

3.7.1. Image enhancement

As already pointed out in Chapter 2, there are no image capture processes that do not introduce noise. Image enhancement techniques that deal with noise and its suppression and/or removal may be grouped into two categories: linear smoothing filters and non-linear filters.

The linear smoothing filters are: Mean, Gaussian, Gaussian white noise, Low pass, Band pass, High pass, Homomorphic, and Unsharp.

The non-linear filters are: Median, Poisson, Wiener, Lucy-Richardson, Speckle, Salt & Pepper, and Noise compose.

The methodology followed in this experiment consisted of selecting 20 noisy thermal images (with poor contrast between the object in the scene and the background) from the Glamorgan laboratory database. Utilising the CTHERM software 'Export' function the images were converted to Bitmaps and loaded into MATLAB™ analysis software for processing with the various filters implementations. The filtered images were then loaded back into CTHERM and compared against the original noisy images. Within the MATLAB™ software 3 image noise evaluation parameters were calculated: the 'Signal to Noise Ratio', the 'Root Mean Square Error' and the 'Cross Correlation Coefficient'. The diagram in the fig. 100 shows the scenario of the experiment.

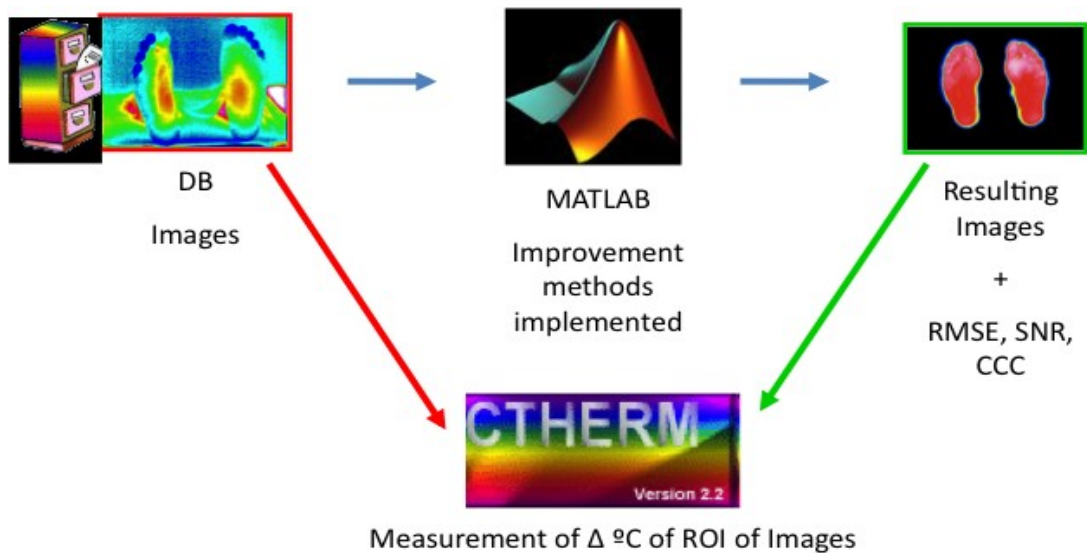


Fig. 100: The scenario of the medical thermal images noise improvement experiment.

The results of this experiment are shown in section 4.4.1.

3.7.2. Edge detection

Hands, like feet, are the body areas where heat transfer with the environment occurs most frequently and effectively.

This in turn influences the boundaries of these extremities in thermal images, making them often difficult to detect as they may assume temperatures close to those of the environment. It is, however, necessary to have an accurate edge definition in each image so that the analysis of the thermal image neither includes any pixels belonging to the background or the environment nor excludes any parts actually belonging to the body. This is of particular interest for this work.

Some authors suggest the use of Artificial Intelligence methods such as neural networks, genetic algorithms or edge maps to solve this problem (Zhou, 2004, Suzuki, 2000, Ghosh, 2006). In practice these techniques are computational intensive, time consuming, complex and often associated with a high probability of error. The approach taken here consists of testing which of the currently existing and well documented traditional edge detection techniques for digital images is best suited for the demands of medical thermal imaging.

The performance of edge detection techniques is closely related to the presence of noise. It

is therefore a second objective of this experiment to verify the hypothesis that noise pre-processing by a conservative noise reduction filter can improve boundary detection. Based on the outcome of the experiment in 3.7.1 it is thought that in this context one of the most appropriate filters should be the Homomorphic filter. It allows noise to be modelled as an additive term to the original image data (Gonzalez and Woods, 2002) which is a close approximation of the physical processes inside the thermal camera sensor and electronics. Eleven classical edge detection techniques were selected and divided into five groups according to their underlying principle. These techniques are: the gradient based (Roberts, Sobel, Prewitt and Kirsch), the second order difference based (Laplacian, Laplacian of Gauss, Marr-Hildreth), the probability based (Canny, Shen-Castan), the segmentation based (Watershed), and the contour following based (Snakes).

The gradient based algorithms are the most simple ones. They detect both edges and their orientations, although they are sensitive to noise and due to their simplicity too inaccurate for certain applications.

Second order difference operators have fixed characteristics for all edge orientations. They find the correct place of edges and also test a wider area around the pixel than gradient based detectors. The disadvantages of these operators are their sensitivity to noise, multiple detection of the same edges, malfunctioning at corners/curves and problems in places where the grey level function varies. Edge orientation detection is affected due to the properties of the Laplacian approach.

Probabilistic methods have good localization capabilities and response even in the presence of noise, they compute probability values for determining an error rate. Their major disadvantages are poor detection of zero crossings and the complexity of computations (Sharifi, 2002).

Segmentation based operators filter the objects boundaries and effectively remove some of the image noise, but they treat the image foreground and background asymmetrically (Karantzalos, 2006).

Contour following methods finally are able to reduce a second order problem to just one dimension and optimise locally. They are, however, relatively slow (Kass, 1988).

A total of 35 thermal images of hands were recorded according to the protocol defined and imaging system specified in section 3.1 above.

The selected Bitmap images were processed in two ways: the first using pre-process noise reduction filtering with a Matlab™ implementation of the Homomorphic filter followed by the edge detections, the second employed edge detection algorithms only without pre-processing. All edge

detection algorithms were implemented as Matlab™ scripts (Gonzalez, 2004).

The parameters used for defining the Homomorphic filter were: ‘low filter’ value equal to 0.1 and ‘high filter’ value equal to 1 in order to decrease the illumination contribution and increase the reflectance contribution. The value used for the ‘delimiter’ was 7.

The gradient based edge detectors had the usual automatic threshold based on the average grey-level of the image to maintain consistency for subsequent comparisons. Line thinning was applied and all detectors (with the exception of the Sobel one where the direction was rotated in multiples of 45°) used both horizontal and vertical directions of edge detection.

In the Laplacian filter the ‘shape value’ was set to 0.2, whereas the Laplacian of Gauss filter used an automatic threshold and a standard deviation value of 2. The Marr-Hildreth algorithm used a Gaussian kernel of size 11, a standard deviation value of 1 and the median of Gaussian was set to 0.

In the probability based operators, the Canny filter used automatic low and high thresholds and 6 as standard deviation preset. The Shen-Castan filter used 1 as the ‘smoothing factor’, 0 for the low and 3 for the high threshold value (chosen empirically).

The watershed segmentation based edge algorithm used an automatic threshold calculated using the average image grey level together with an 8 pixel connected neighbourhood for each individual location.

The parameters used for the Snake algorithm were 0 for the ‘energy’ contributed by the distance between control points, 0.1 as ‘energy’ contributed by the curvature of the snake and 1 pixel for each incremental move of the snake in order to reduce computation time. For the initial seeding outline the output of the Canny filter was used.

Two evaluation methods were used to compare and assess the edge detection algorithms and to verify any improvements as a result of noise filter pre-processing. The diagram in the fig. 101 shows the scenario of the experiment. In the first (subjective) method 5 image processing professionals graded the edge detection algorithms on a 10 point scale. The algorithm with the cumulative smallest score was considered the best. If the images resultant from noise filter pre-processing obtained better scores than the ones without, the conclusion was that in this instance noise filtering enhanced the results of the respective outlining process. On occasions where the subjective judgement resulted in a draw a second review stage was used to arrive at a ranking. The second (quantitative) method is based on a reference outline that was produced in a graphics package under high magnification and aided by contrast enhancement techniques. The performance

measure here is the total length of the outline (in pixels). The same quantitative method was used to assess noise filtering.

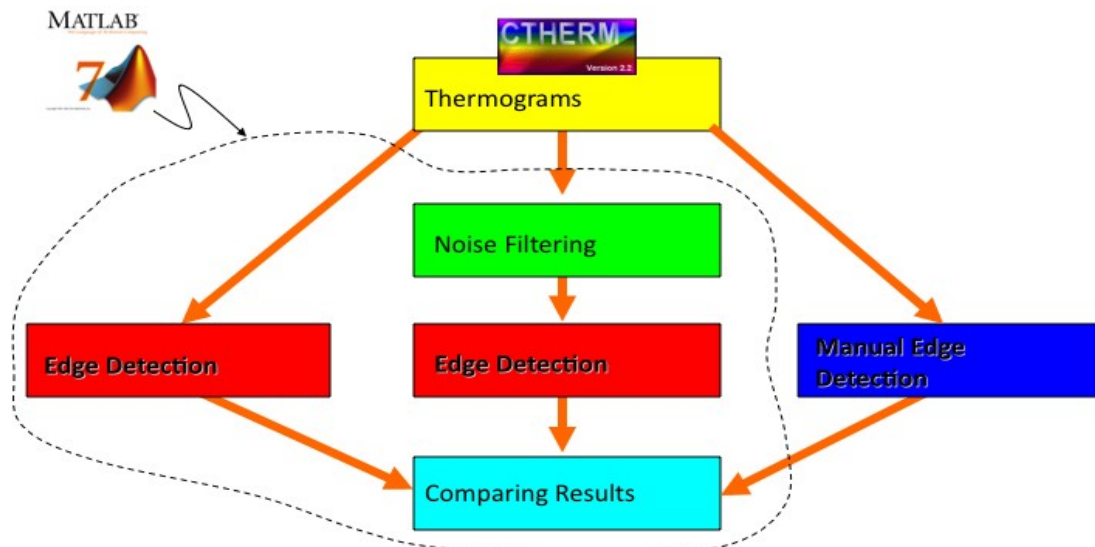


Fig. 101: The scenario of the medical thermal images boundaries detection experiment.

The results of this experiment are shown in section 4.4.2.

3.7.3. Interpolation methods

Image interpolation is a method of constructing new data points (pixels) on a digital image within the range of a discrete set of known data points (pixels) calculating a new point between two existing data points (Lehmann, 1999). In this experiment three more common and very well documented interpolation techniques will be tested. Those methods are: Nearest Neighbourhood, Bilinear and Bicubic.

This experiment follows the previous one in section 3.6.2 on edge detection since image interpolation is usually based on on edge detection or has edge detection as a pre-process.

A selection of 20 thermal images of faces stored in the Glamorgan thermal laboratory database was made. The face anterior view was selected because it is the view with the highest thermal standard deviation values and thus well suited for performing interpolation tests. An application was coded in C# programming language. As shown in fig. 102 an image median noise

removal filter was applied initially and succeeded by a Gaussian blur operation to minimize the remain noise. A Canny edge detection operator was then executed over the noiseless image to discover the object boundaries. In order to improve the edge a thinning transformation was applied to the resulting image to simplify the edges and remove some undesirable artefacts. A one pixel wide continuous shape outline is the result of this operation.



Fig. 102: C# application for Testing image interpolation methods.

The standard mask for a head was then loaded (compare 3.3.2, Experiment 2) and the control points of the mask were automatically aligned with the shape using a process by which the the centres of mass from both, shape and mask are calculated and brought into coincidence first. The control points of the overlaid mask were then moved under consideration of the difference between the 2-D main axes between centres of the regions. Interactions from the user of the application was requested to assist the adjustment of the control points if required. Finally, the automated warping process deformed the original thermal image into the standard form dictated by the mask. This final process used the three interpolation methods under investigation. Fig. 103 illustrates the procedure of the experiment.

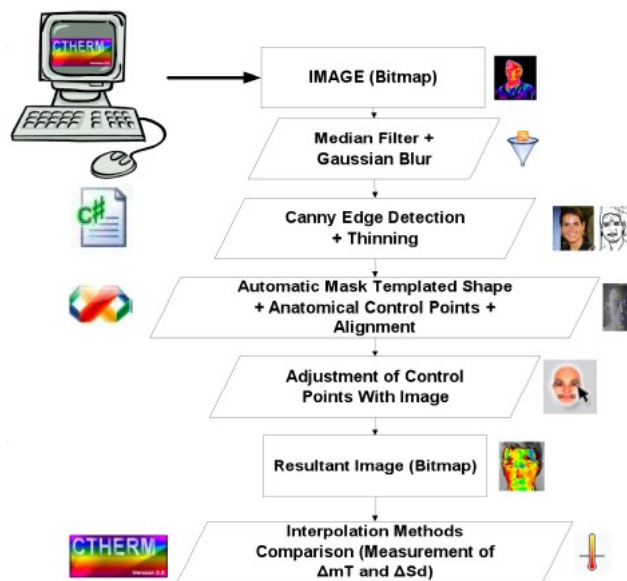


Fig. 103: The interpolation comparison methods in medical thermal images scenario.

To assess the performance of the 3 interpolation methods the mean temperature and standard deviation of a defined AOI was calculated before and after interpolation. The method that produced the smallest difference in both figures was considered 'best'.

The results of this experiment and a detailed analysis are presented in section 4.4.3.

3.7.4. Barycentric warp model

The interpolation method comparison above uses a simple standard warping model. It is one of many possible ones, each with their particular advantages and disadvantages.

In some physiological hand-oriented studies an anatomical anthropometric geometrical shape was developed (Griffin, 1990) that is similar to the mask shown in fig. 39 and suggested thermal imaging usage for analysis of hands (Ammer, 2008).

An identical model has been developed that is based on anatomical control points, that delineate the AOI within the hand. This model is a geometric approximation of the capture mask. Per hand it is composed of 17 AOIs: the wrist, the palm, the thumb metacarpal (due to its substantial anatomical differences from the others metacarpals), the finger phalanges (PIP, MIP and

DIP) and the thumb phalanges (PIP and DIP) as shown in fig. 104. The sizes in pixels of those defined AOI of the hand are presented in table 10.

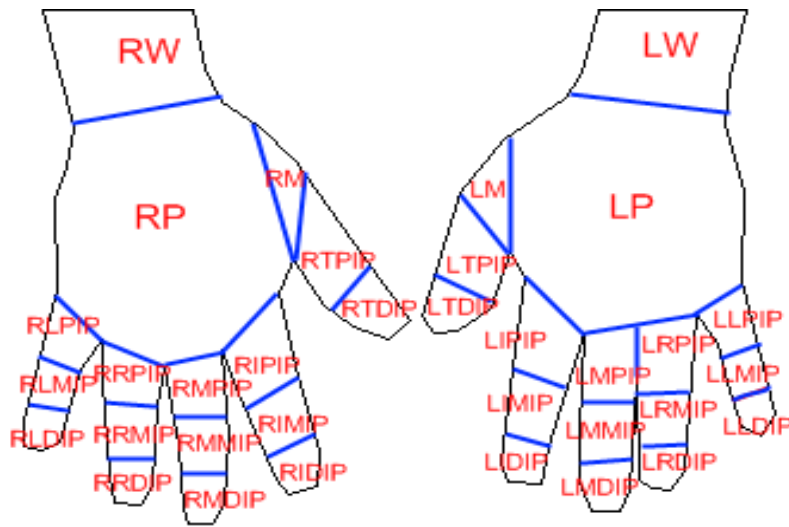


Fig. 104: Geometrical 'anatomical regions' based model of the hand.

The model was developed for images with a resolution 340x256 pixels. (For other camera resolutions it would have to be adjusted.) A warping solution to standardise hand shapes should work without scrambling/deleting/altering relevant data within the different anatomical regions of the hand. This standardised image of the hand should permit to perform comparisons and statistical analysis such as image averaging.

AOI	Number of pixels		
Wrist	3600		
Palm	11400		
Thumb metacarpal	600		
Thumb PIP	800		
Thumb DIP	534		
Fingers	PIP	MIP	DIP
Index	624	546	390
Middle	756	662	474
Ring	730	638	456
Little	428	428	368

Table 10: Size (in pixels) of the AOIs of the hand model.

A fully automatic retrieval of anatomically defined control points can, however, not easily be performed as shown by the experiments described above in section 3.7.2 with results in in section 4.5.2 and discussion in section 5.

For simple shapes some authors therefore suggested image warping techniques based on meshes and lines (Gomes, 1999, Beier, 1992, Wolberg, 1996, Wolberg, 1998), although these are not recommended here due to their implementation complexity and computational cost when dealing with intricate shapes such as hands.

More recent research proposed image warping based on triangulation as a fast, simple and straightforward method (Fujimura, 1998, Dong-Keun and Yo-Sung, 2004, Hormann, 2004). This approach uses barycentric coordinates to create the correspondence between pixels of the original and target image of the transformation. Barycentric coordinates are coordinates based on the weights (distance) from the vertices of a triangle.

The objective of this experiment is to investigate the application of this methodology to medical thermal images and study its impact in terms of thermal accuracy (i.e. the degree by which AOIs in source and target image differ in terms of mean and standard deviation).

Thermal images of the hands used in this experimental work were retrieved from the Glamorgan thermal laboratory database, these images were taken from subjects according to the Glamorgan standard capture protocol (Ammer, 2008).

An object oriented C# coded application was developed to load thermal images and then overlay the anatomical model of the hands with its adjustable control points, fig. 105. These points could be manually moved to the correct positions in the respective thermal images and after the adjustment was completed the warping transformation operation could start (the operator selects that option from the application menu). This creates the regions shown in fig. 104 and the triangles that constitutes them from the control point positions. Although this is a rigid model composed from triangles linked to the control points, which define the AOI within the hand, it can be dynamically adjusted. For each AOI a range of first and second order statistical values (mean, maximum, minimum, standard deviation, skewness and kurtosis) are calculated and saved in a CSV file for subsequent analysis.

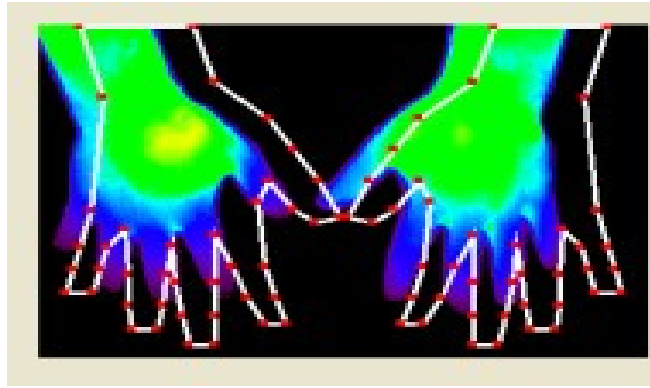


Fig 105: Adjustable control points overlaying the thermal image of the hands.

The creation of the warped image begins with the calculation of a reverse transformation for each pixel of each target triangle. The Barycentric coordinate of that pixel is calculated according to the system shown in fig. 106 and the formulae described in section 2.8.6.

Barycentric Coordinates

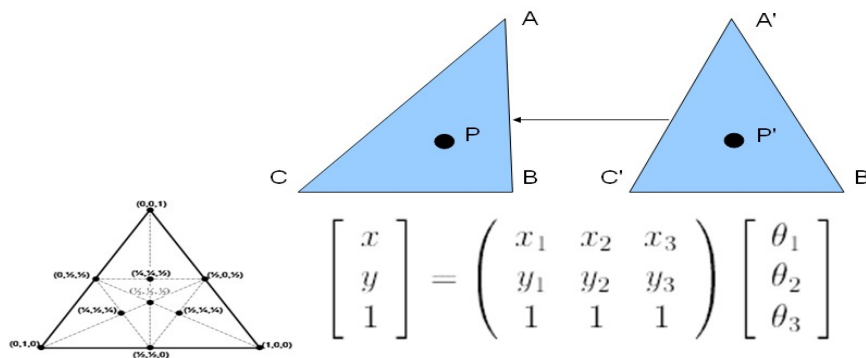


Fig. 106: Barycentric coordinates correspondence system with Cartesian coordinates.

The warping method used in this approach is called 'reverse warping'. From the Cartesian coordinate of the pixel in the target triangle, a Barycentric coordinate is calculated based in the triangle vertices in Cartesian coordinates. The correspondent source triangle of the original image is obtained with the corresponding vertices. Based on the correspondent Barycentric coordinate of the equivalent pixel in the source triangle, using the triangle vertices Cartesian coordinates the original pixel Cartesian coordinate is calculated. Subsequently, this pixel value is copied from the original image to the resultant image using the triangular correspondence. The pseudocode followed by this warping method is represented by fig. 107 and a flowchart representation of the operation is shown

in fig. 108.

```
New Image (img) filled black pixels
For each  $\Delta$ target
  For j= $\Delta$ target_top to  $\Delta$ target_bottom
    For i= $\Delta$ target_left to  $\Delta$ target_right
      if point(i,j) belongs to  $\Delta$ target
        b = barycentric(i,j, $\Delta$ target)
        [x,y] = cartesian (b,  $\Delta$ source)
        img_pixel(i,j) = Image_src_pixel(x,y)
```

Fig. 107: Pseudo-code of the triangular barycentric warping method.

The resultant image is traversed pixel by pixel inside the hand's geometrical outline establishing the hands information translation. Problems can arise if the target and source triangles differ significantly in size. To address this situation when a difference in size of more than 5% appears the values of the translated pixels are multiplied by the ratio between the size (in pixels) of the target triangle by the size (in pixels) of the source triangle, however, an investigation is needed in how it can affect the measurement data. A statistical study was performed to assess the variation between different operators of the developed tool: 10 users were asked to use the application and warp the same image, the obtained results were evaluated in terms of variance and expected standard error.

The result of this experiment and an analysis are given in section 4.4.4 and discussed in section 5.

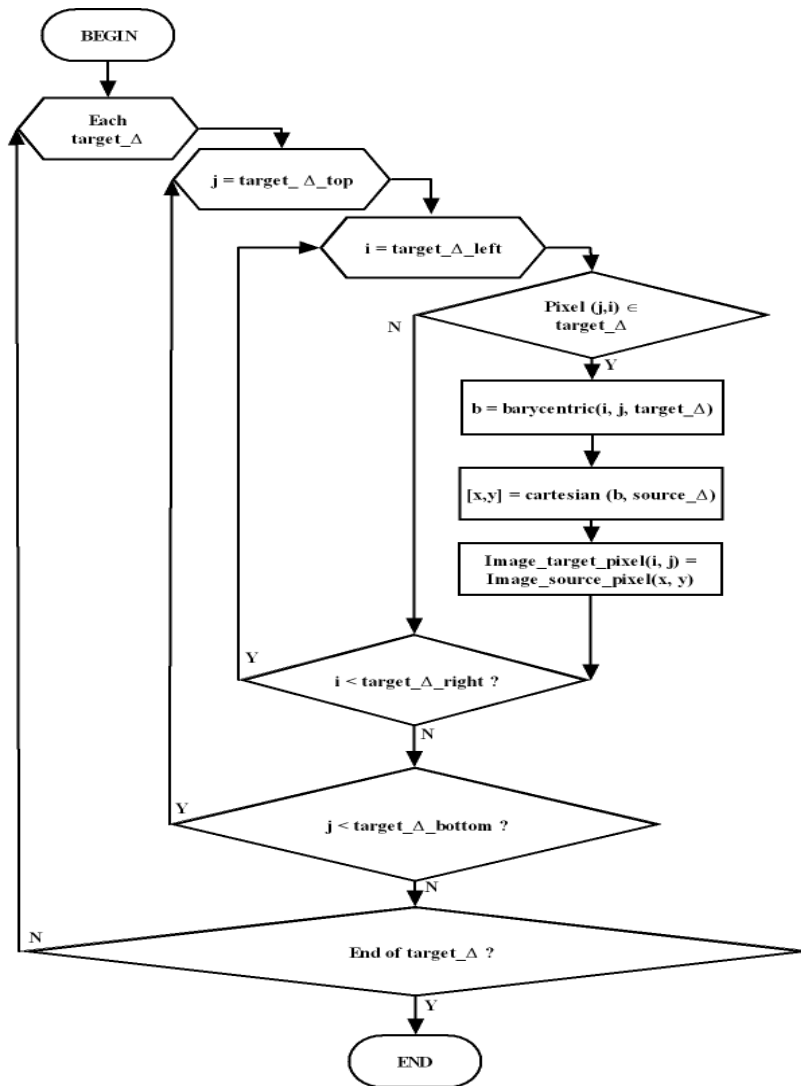


Fig. 108: Triangular barycentric warping method flowchart.

3.8. Summary

In this chapter the design and methodology followed by the outlined experiments to accomplish the objectives were defined and described.

The expected outcomes are:

- A sample characterisation of the incidence of WRULD in a sample population, verifying possible targets of future experiments. It is expected that 10% can be affected and from literature the expected profile of the more affected subjects will be females aged between 30 and 50 years old, having smoking habits, and employed in administrative/clerical settings.

- A thermal symmetry maximum value to be used as a reference discriminative value in distinguishing pathological states from non-pathological states of approximately 0.5°C.
- There were three objective tests involving mechanical provocation stress. In the test using a computer keyboard an increase in the hand mean temperature over a period of 5 minutes is expected. After that period subjects with WRULD problems are expected to present a greater vasoconstriction of the fingers after subsequent vascular cold provocation. A mean temperature decrease is expected from exposure to vibration, affected subjects presumably will take longer to recover from a posterior vascular provocation. There are no reference data about provocation stress using a computer mouse, however, a mean temperature increase is expected in the exercised hand.
- In the cold stress test normal healthy subjects presumably will recover within a period of 10 minutes after vascular provocation presenting a thermal index value above the standard threshold of -4. The subjects affected by Raynaud's phenomenon are expected to not recover within the same period of time (thermal index less than -4). From the proposed methods to evaluate the CST, the Mean Thermal Gradient method (MTG) will presumably be more sensitive than the other two methods, the Mean Thermal Area (MTA) and Mean Thermal Profile (MTP).
- In the usage of thermal cameras in medical thermography for assessment of hand injuries higher resolution cameras are expected to perform better than lower resolution hand-held cameras.
- From using noise reduction techniques images are expected to be improved. The method that presumably will produce a result closer to the originally captured scene is, due to its reported underlying principles, the homomorphic filter.
- The technique of producing outlines that is expected to produce better results are likely to be probabilistic based (Canny and Shen-Castan).
- From literature the interpolation method that presumably will produce better results is the bi-cubic one.
- The image warping technique involving barycentric triangular transformations is expected to produce reasonable results by preserving the AOIs' temperature distribution texture.

In the following chapter 4 the results achieved in reality are presented and then compared with the above expectations in chapter 5.

4 – Experimental Results

In this chapter the results of the following surveys and experiments are presented:

1. incidence of occupational conditions in a sample population (4.1)
2. medical reference data (4.2),
3. final provocation tests (4.3),
4. and the results from imaging processing developments (4.4).

4.1. Online RSI Questionnaire

In order to assess the incidence of the occupational conditions studied here a questionnaire (see Appendix 6) was designed, field-trialled and finally placed online at the University of Glamorgan. The questionnaire had 218 respondents, which is around 1% of the academic population at the University, divided between 103 males and 115 females (fig. 109).

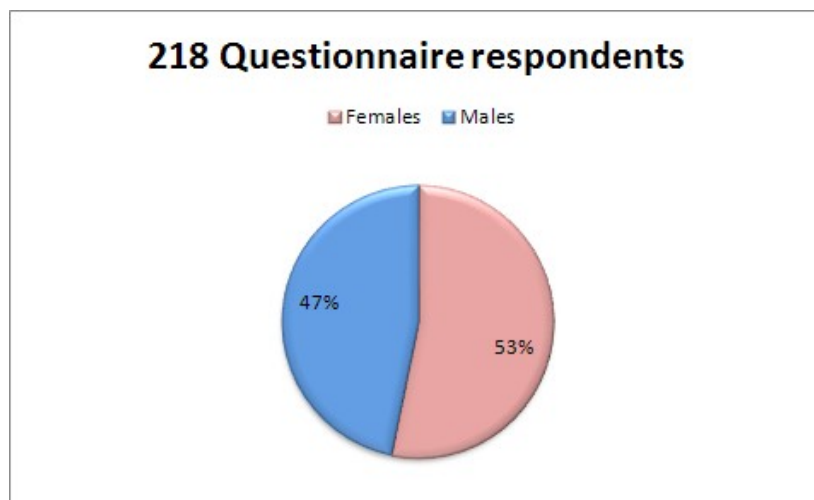


Fig. 109: Gender distribution of the questionnaire respondents.

A full review of the characterisation of the questionnaire respondents can be observed in the Appendix 7. The majority of the respondents were in the age group between 18 and 30 years old (47%). 62% of the women were in the normal weight BMI class, the majority of the men were

divided between the normal weight (45%) and overweight (45%) BMI classes. Observing the respondents occupation, the majority were male students (52%) and female administrators (36%) and lecturers (28%). The majority of respondents of both genders do not have smoking habits.

From the overall results, it can be observed that 13% of the participants of this study indicate having severe symptoms of hand disabilities, other 20% reveal signs, 32% argue to have early signs and only 36% of claim to be free of hand syndromes (fig. 110).

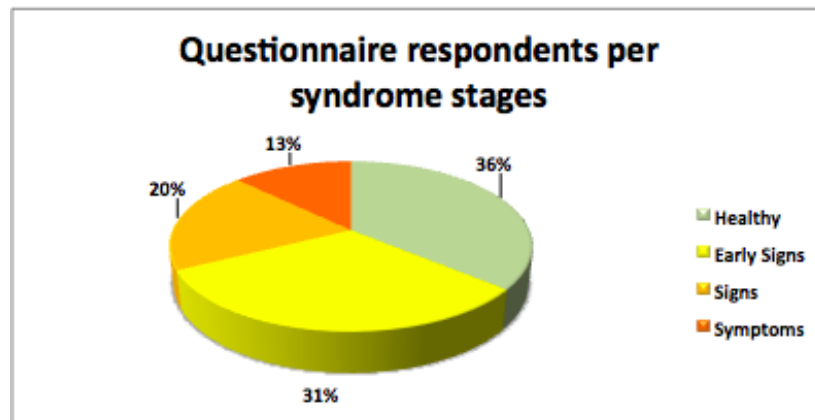


Fig. 110: Overall respondents per hand occupational condition pathological state.

Although this sample is not representative and cannot therefore be used to make statements such as “13% of employees at the University of Glamorgan suffer from severe symptoms of HAS” these results demonstrate clearly that measures for the prevention of hand occupational conditions are required within the University environment in order to avoid further serious injuries and consequently expensive treatments and expenses.

From the chart presented in fig. 111, it can be concluded that women in this sample are more affected by hand occupational conditions than males.

For a better understanding of the factors that influence the 'severe symptoms' stage of the questionnaire among respondents further analysis was performed. From the chart presented in fig. 112 it can be seen that there are over thirteen times more females than males affected by this stage. Given the 47/53 male/female gender distribution in the sample this result can be interpreted as reasonably representative for the UK population as a whole.

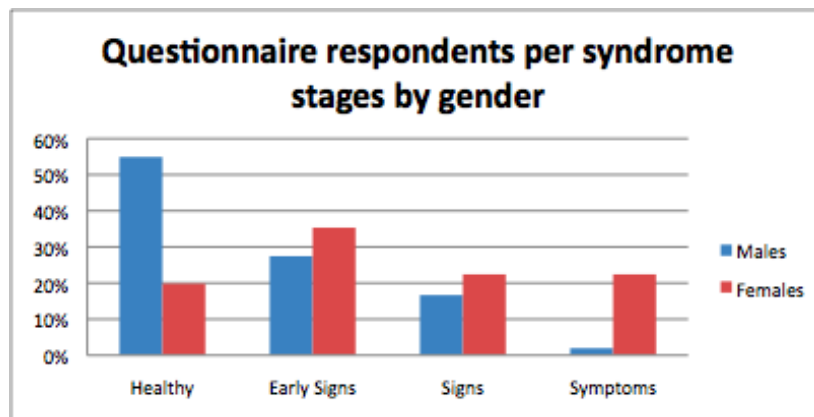


Fig. 111: The gender distribution of the respondents per hand occupational condition pathological state.

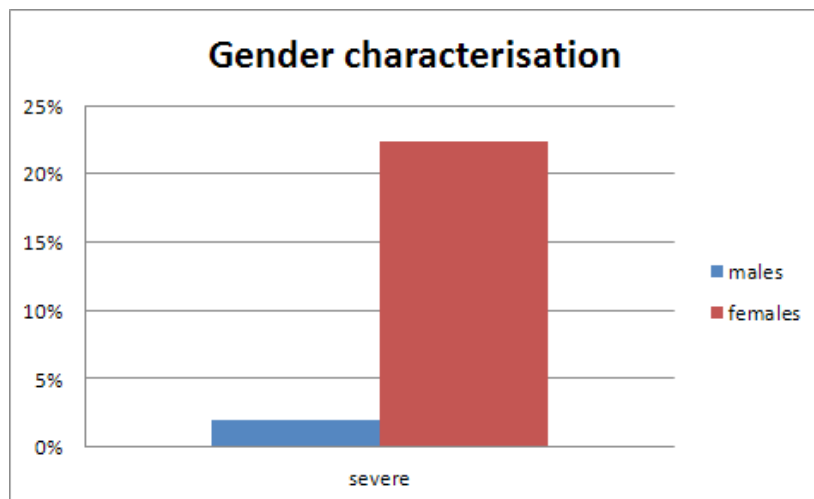


Fig. 112: The gender distribution of the questionnaire respondents that indicated 'severe symptoms' of hand occupational conditions.

According to the obtained answers for the 'severe symptoms' stage, the age group with more incidences was 18-30 and 31-40 for women (age group of 61-65 [1% of the sample] was not taken into consideration and in the men due to the small number of samples), fig. 113.

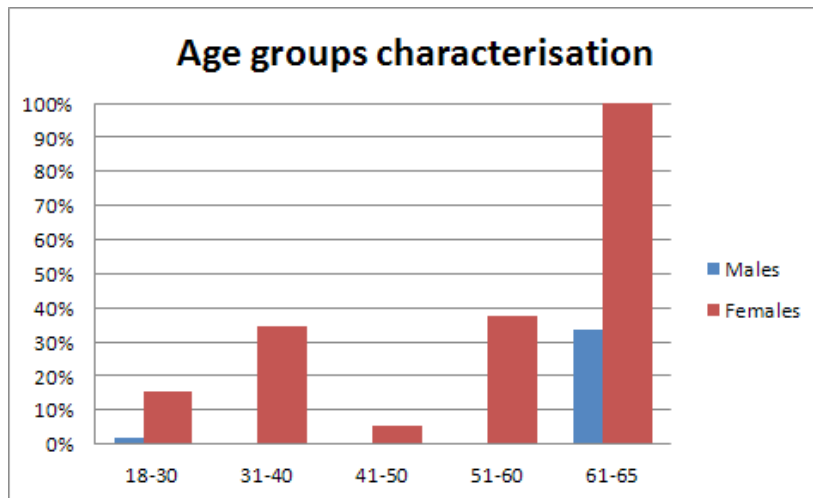


Fig. 113: The age group distribution of the questionnaire respondents per gender that indicated 'severe symptoms' of hand occupational conditions.

Fig. 114 presents the BMI class distribution of the questionnaire respondents graded as having 'severe symptoms' of HAS according to their answer. The BMI class that was shown to be most affected in the sample is the overweight (underweight [2% of the sample] and obese [8% of the sample] was not taken into consideration due to the small number of the samples).

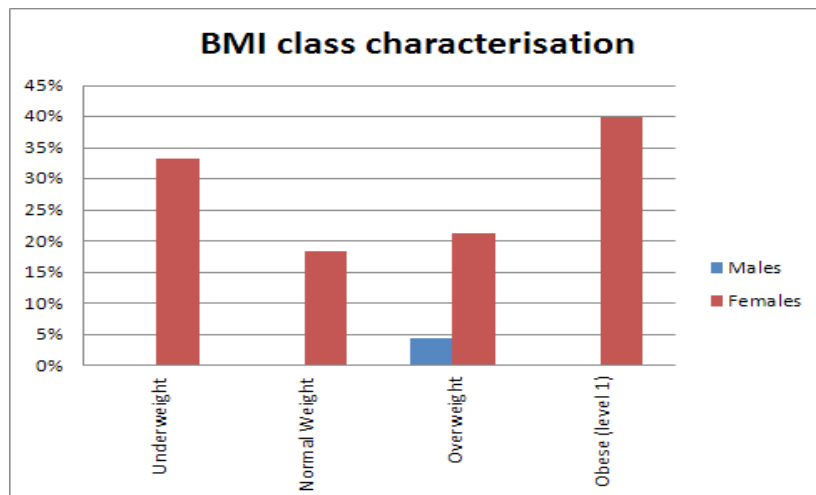


Fig. 114: The BMI distribution of the questionnaire respondents per gender that indicated 'severe symptoms' of hand occupational conditions.

The most affected occupational group in the 'severe symptoms' stage was found in administrators, fig. 115.

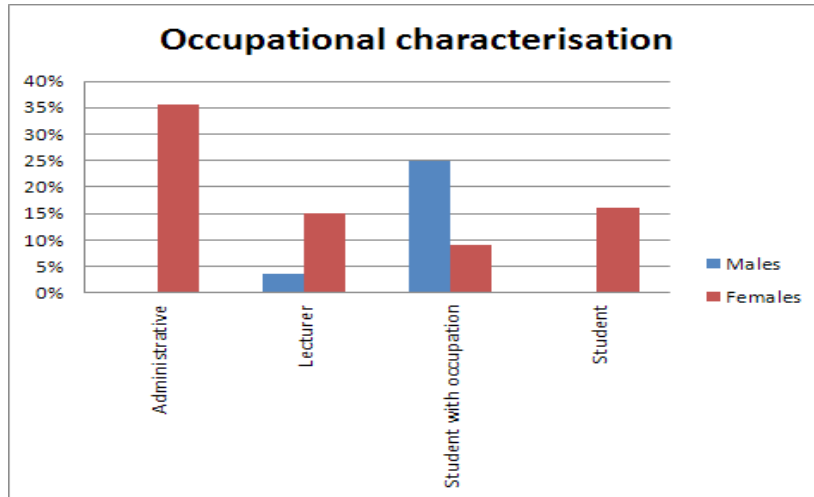


Fig. 115: The characterisation by occupation of the respondents per gender that indicated 'severe symptoms' of hand occupational conditions.

In order to verify the characterisation of the lifestyle habits with respect to smoking, fig. 116 show that about 65% of respondents in the 'severe symptoms' smoke daily.

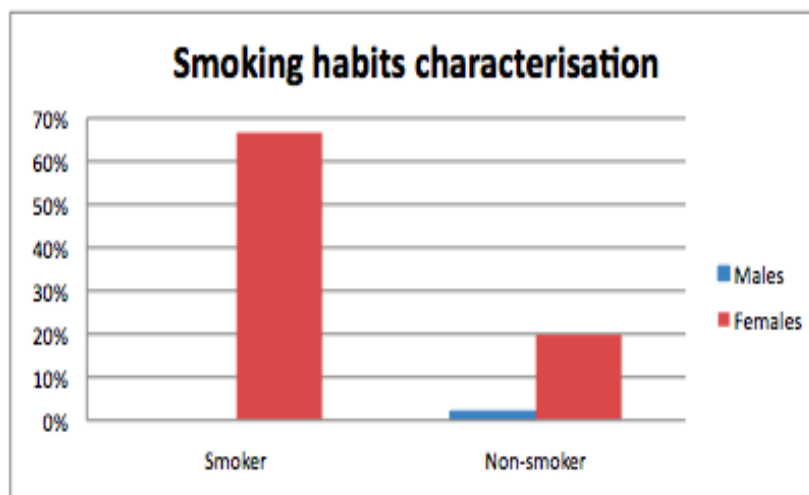


Fig. 116: The characterisation of smoking habits of the respondents per gender that indicated 'severe symptoms' of hand occupational conditions.

In order to relate the stages for hand conditions with exposure to computer keyboard and mouse use, participants were requested to indicate the exposure in hours per week. For the 'severe symptoms', the highest incidence of keyboard and mouse use was an exposure of more than 40 hours per week, fig. 117 and fig. 118.

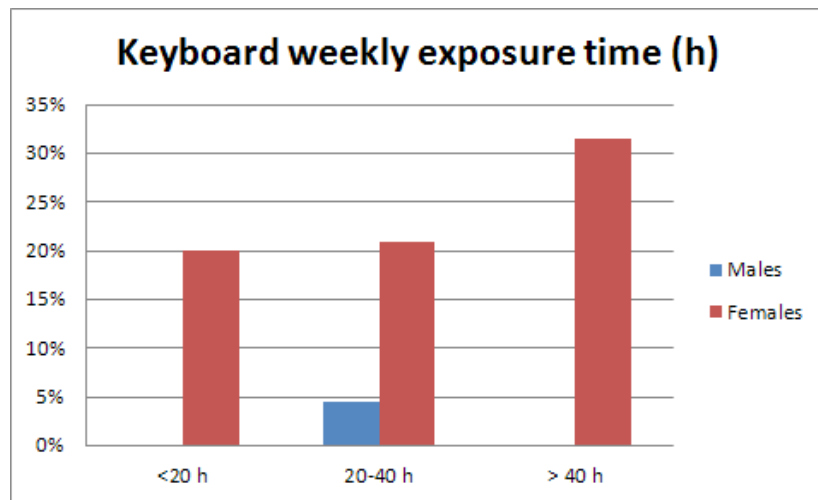


Fig. 117: The computer keyboard weekly exposure time of the respondents per gender that indicated 'severe symptoms' of hand occupational conditions.

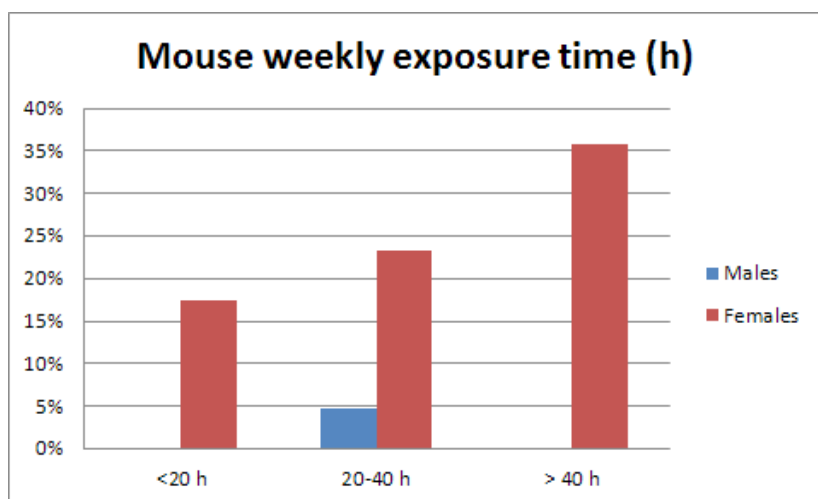


Fig. 118: The computer mouse weekly exposure time of the respondents per gender that indicated 'severe symptoms' of hand occupational conditions.

From the previously outlined results, the following can be concluded: that females on ages from 31 to 40, in BMI class overweight, daily smokers, in administrative work and operating with a computer keyboard and mouse for more than 40 hours a week are more at risk of having symptoms of upper limb occupational conditions. The results of this study are in line with observations made in the literature (Cole et. al., 2005).

4.2. Reference data

This study consisted of two experiments, the first is using measurement with geometrical (rectangles) AOI in the CHERM software package. The second experiment used a geometrical model based in the AOI defined by Ammer (2008) and the barycentric warping method as described in section 3.6.4.

In the first approach for obtaining data on thermal symmetry of the upper limb area (using the experimental setup described in section 3.3.1 on 39 male volunteers) the results are shown in table 11. This indicates that the maximum difference in mean temperatures appears at the dorsal arm in both the regional body view and in the total body view. In terms of standard deviation difference the largest difference found was of $0.47 \pm 0.70^\circ\text{C}$ in the hand AOI for the regional dorsal view of the hands and the anterior arm AOI of the total body view.

AOI	Regional Views				Total Body Views			
	Anterior view		Dorsal view		Anterior view		Dorsal view	
	ΔxT	Δsd	ΔxT	Δsd	ΔxT	Δsd	ΔxT	Δsd
Hand	NO DATA	NO DATA	$0.37 \pm 0.45^\circ\text{C}$	$0.47 \pm 0.70^\circ\text{C}$	$0.28 \pm 0.27^\circ\text{C}$	$0.20 \pm 0.17^\circ\text{C}$	$0.27 \pm 0.20^\circ\text{C}$	$0.20 \pm 0.13^\circ\text{C}$
Forearm	$0.25 \pm 0.19^\circ\text{C}$	$0.14 \pm 0.13^\circ\text{C}$	$0.25 \pm 0.19^\circ\text{C}$	$0.11 \pm 0.09^\circ\text{C}$	$0.32 \pm 0.23^\circ\text{C}$	$0.28 \pm 0.24^\circ\text{C}$	$0.37 \pm 0.25^\circ\text{C}$	$0.25 \pm 0.17^\circ\text{C}$
Arm	$0.37 \pm 0.56^\circ\text{C}$	$0.11 \pm 0.13^\circ\text{C}$	$0.38 \pm 0.38^\circ\text{C}$	$0.11 \pm 0.09^\circ\text{C}$	$0.37 \pm 0.28^\circ\text{C}$	$0.32 \pm 0.24^\circ\text{C}$	$0.32 \pm 0.25^\circ\text{C}$	$0.25 \pm 0.19^\circ\text{C}$
Wrist	NO DATA	NO DATA	$0.34 \pm 0.21^\circ\text{C}$	$0.17 \pm 0.15^\circ\text{C}$	NO DATA	NO DATA	NO DATA	NO DATA
Elbow	$0.29 \pm 0.27^\circ\text{C}$	$0.27 \pm 0.25^\circ\text{C}$	$0.30 \pm 0.21^\circ\text{C}$	$0.16 \pm 0.28^\circ\text{C}$	NO DATA	NO DATA	NO DATA	NO DATA
Shoulder	$0.23 \pm 0.19^\circ\text{C}$	$0.10 \pm 0.09^\circ\text{C}$	$0.18 \pm 0.17^\circ\text{C}$	$0.07 \pm 0.05^\circ\text{C}$	NO DATA	NO DATA	NO DATA	NO DATA

Table 11: Thermal asymmetry values (mean temperature absolute differences and standard deviations) for upper limbs and joints in regional and total body views for dorsal and anterior perspectives using the first analytical approach.

The values signed with 'NO DATA' in the table 11, correspond in the regional views to the palmar and wrist AOIs, which do not constitute a suitable AOI to be examined as referred in section

2.1.1.8. In total body views the size of pixels per AOI did not satisfied the requirements of at least 25 pixels (Ammer, 2008).

In the second approach (using the refined analysis method outlined in section 3.3.2 on the same 39 subject data set as above) the results shown in table 12, demonstrate that the highest asymmetry values are $0.49\pm 0.29^{\circ}\text{C}$ in the forearm AOI in the anterior view and $0.33\pm 0.34^{\circ}\text{C}$ in the hand AOI in the dorsal perspective. Standard deviation differences of $0.33\pm 0.23^{\circ}\text{C}$ indicate the maximum in the forearm AIO in the anterior view and $0.47\pm 0.28^{\circ}\text{C}$ in the forearm AOI in the dorsal perspective.

AOI	Regional Views			
	Anterior view		Dorsal view	
	ΔxT	Δsd	ΔxT	Δsd
Hand	NO DATA	NO DATA	$0.33\pm 0.34^{\circ}\text{C}$	$0.39\pm 0.29^{\circ}\text{C}$
Forearm	$0.44\pm 0.24^{\circ}\text{C}$	$0.33\pm 0.23^{\circ}\text{C}$	$0.34\pm 0.25^{\circ}\text{C}$	$0.47\pm 0.28^{\circ}\text{C}$
Arm	$0.49\pm 0.29^{\circ}\text{C}$	$0.12\pm 0.15^{\circ}\text{C}$	$0.23\pm 0.16^{\circ}\text{C}$	$0.28\pm 0.29^{\circ}\text{C}$

Table 12: Thermal asymmetry values obtained using the second analytical approach.

A statistical analysis to assess the reliability and repetitiveness of the AOIs used in both approaches is shown in the following table 13 and table 14. The analysis demonstrates that apart from the shoulder AOI in the first approach, all AOIs have a Reliability Coefficient alpha above 0.8 and all AIOs (excluding forearm, arm, elbow and shoulder in the first approach and arm in the second approach) have an Interclass Correlation Coefficient greater than 0.8. Both statistical markers indicate that the AOIs used are reliable and ensure repeatability.

	AOI	Reliability Coefficient alpha	Interclass Correlation Coefficient	95% confidence interval of ICC
Regional views	Hand	0.99	0.99	0.98 to 0.99
	Forearm	0.83	0.71	0.59 to 0.87
	Arm	0.86	0.76	0.59 to 0.89
	Wrist	0.99	0.97	0.95 to 0.99
	Elbow	0.89	0.67	0.53 to 0.79
	Shoulder	0.74	0.41	0.26 to 0.57
Total body views	Hand	0.98	0.94	0.90 to 0.96
	Forearm	0.98	0.93	0.89 to 0.96
	Arm	0.94	0.81	0.71 to 0.88

Table 13: Statistical analysis of the AOIs used in the first approach of obtaining thermal symmetry values.

	AOI	Reliability coefficient alpha	Interclass Correlation Coefficient	95% confidence interval of ICC
Regional views	Hand	0.99	0.97	0.97 to 0.98
	Forearm	0.97	0.89	0.83 to 0.93
	Arm	0.94	0.78	0.68 to 0.87

Table 14: Statistical analysis results of the AOIs used in the second thermal symmetry method.

From the first approach to the second it can be observed that in anterior and dorsal forearm and anterior arm AOI the differences in mean temperature have increased, however for all others upper limb AOI this value have diminished. For all AOI excluding the hand the differences in standard deviation have increased. These differences are related to the AOI as it could be observed from section 3.3.1 and 3.3.2 being a little different.

Analysing the values of consistency (reliability coefficient alpha) and repeatability (interclass correlation coefficient) in both approaches it can be observed that in the second approach they have improved. Another outcome of this experiment is that the usage of a standardised AOI enforces the repeatability and also implements a semi-automated image analysis solution. This may form the basis for future work.

4.3. Objective provocation tests

In order to address the weaknesses found in the pilot provocation tests (section 3.5) a set of four new objective provocation tests were developed (section 3.6). The results of these provocation tests are presented in this section along with the data statistical analysis, a comparative study to assess the vascular tests and the different imaging systems. The volunteers participating in this test were divided into four groups, each one corresponding to a different pathological stage of the HAS: controls, signs, symptoms and confirmed.

In the following sections the reader should bear in mind the lower number of volunteers, especially in the 'confirmed' group. This means that some statistical figures (e.g. standard deviation for error bars) that were calculated for reasons of completeness have to be treated with caution.

4.3.1. Keyboard provocation test

The pilot keyboard provocation test demonstrated poor repeatability and required two visits for examination. In order to answer to this challenge a visual aid, computational tool described in section 3.6.1, was developed which involved both hands typing on the keyboard. This application monitors the typing speed and the eventual psychological stress which was measured by the number of miss-typed characters.

Table 15 shows the mean temperatures evaluation during the test (before mechanical provocation, after mechanical provocation, 5 minutes and 10 minutes after vascular test following the mechanical provocation) for both hands and thermal symmetry (H Symm) expressed for all four stage groups.

Keyboard Provocation Test		Before Test		After Test		5 min CST		10 min CST	
		MeanT	sd	MeanT	sd	MeanT	sd	MeanT	sd
Controls (12)	L Hand	30,69	0,95	30,96	0,79	29,15	1,22	29,94	1,02
	R Hand	30,87	0,95	31,24	0,78	29,45	1,28	30,23	1,05
	H Symm	0,18	0	0,28	0,01	0,3	0,06	0,29	0,03
Signs (7)	L Hand	29,64	1,35	29,9	1,3	27,94	1,66	28,63	1,53
	R Hand	29,57	1,47	29,76	1,34	28,03	1,67	28,75	1,41
	H Symm	0,07	0,12	0,14	0,04	0,09	0,01	0,12	0,12
Symptoms (7)	L Hand	27,84	1,34	28,34	1,16	27,03	1,54	27,21	1,32
	R Hand	28,5	1,56	28,88	1,24	27,41	1,45	27,68	1,34
	H Symm	0,66	0,22	0,54	0,08	0,38	0,09	0,47	0,02
Confirmed (2)	L Hand	30,96	0,72	30,81	0,65	29,04	1,49	30,74	0,9
	R Hand	30,71	0,85	30,84	0,62	29,21	1,38	30,97	0,84
	H Symm	0,25	0,13	0,03	0,03	0,17	0,11	0,23	0,06

Table 15: HAS stage groups mean temperatures over the KPT.

Table 16 presents the volunteer results in terms of typing speed and miss-typed char and also characterises the four HAS stage groups considered in this experiment. On average a typing speed of 49.1 characters per minute with a miss-typed value of 5 characters in the whole period of the test (5 minutes). The confirmed group presented a higher mean number of characters typed per minute as well as an higher number of those miss-typed when compared with the other three groups (table 16).

Volunteer	Group	Keyboard typing		
		Chars	cpm	Wrong
HAS01	Control	286	57,2	1
HAS02	Symptoms	258	51,6	4
HAS03	Confirmed	288	57,6	13
HAS04	Control	191	38,2	6
HAS05	Symptoms	227	45,4	0
HAS06	Signs	218	43,6	0
HAS07	Symptoms	315	63	3
HAS08	Control	317	63,4	22
HAS09	Signs	217	43,4	1
HAS10	Control	261	52,2	1
HAS11	Control	151	30,2	1
HAS12	Control	242	48,4	1
HAS13	Signs	260	52	8
HAS14	Signs	216	43,2	2
HAS15	Signs	261	52,2	2
HAS16	Symptoms	263	52,6	1
HAS17	Symptoms	252	50,4	1
HAS18	Symptoms	232	46,4	4
HAS19	Control	292	58,4	18
HAS20	Control	241	48,2	6
HAS21	Control	222	44,4	8
HAS22	Symptoms	215	43	2
HAS23	Control	249	49,8	3
HAS24	Control	200	40	7
HAS25	Signs	212	42,4	2
HAS26	Confirmed	358	71,6	12
HAS27	Control	194	38,8	2
HAS28	Signs	231	46,2	10
Statistics	Overall	245,3	49,1	5,0
	Controls	237,2	47,4	6,3
	Signs	230,7	46,1	3,6
	Symptoms	251,7	50,3	2,1
	Confirmed	323,0	64,6	12,5

Table 16: KPT volunteers characterisation in speed typing and miss-typing.

Observing the results of the KPT per hand, it can be seen that after 5 minutes keyboard typing provocation the mean temperature of right hand AOI higher increase was verified in the controls and the symptoms groups. At 5 minutes after the vascular test all the mean temperatures of the four groups in the right hand AOI had decreased, this decrease being smaller in the symptoms group.

At the end of the test only the confirmed group had shown a total recovery of the right hand AOI mean temperature.

The signs and the symptoms groups presented a mean temperature that was lower than the control group, fig. 119.

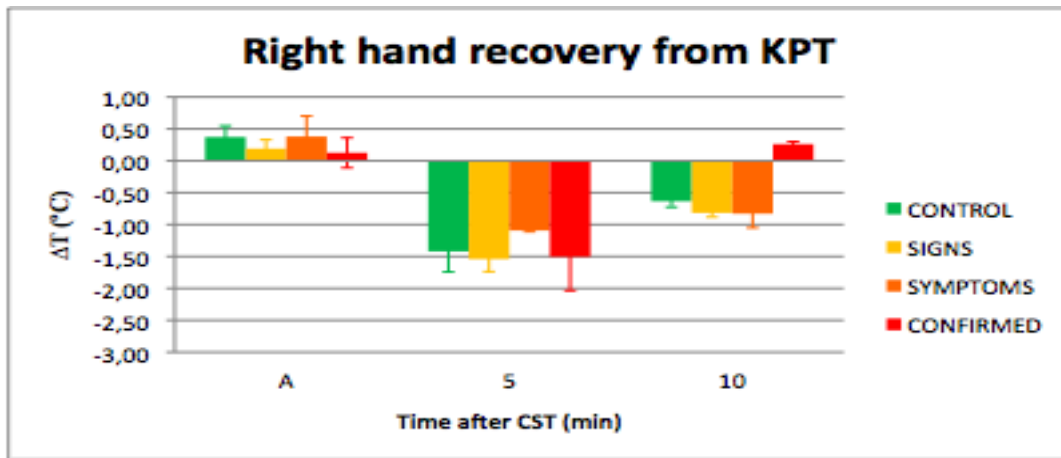


Fig. 119: Right hand mean temperature difference from baseline when recovering from KPT.

In the left hand AOI, after typing for 5 minutes, a higher mean temperature increase was found in the symptoms group. While a decrease in mean temperature was observed in the confirmed group. After five minutes recovery from post vascular test in all groups the mean temperatures had decreased, with the lowest value being shown by the confirmed group. The smallest decrease was in the symptoms group. At the end of the test the recovery close to the baseline value for mean temperature of the left hand AOI was found in the confirmed group followed by the symptoms group. The signs group presented lower mean temperature values, fig. 120.

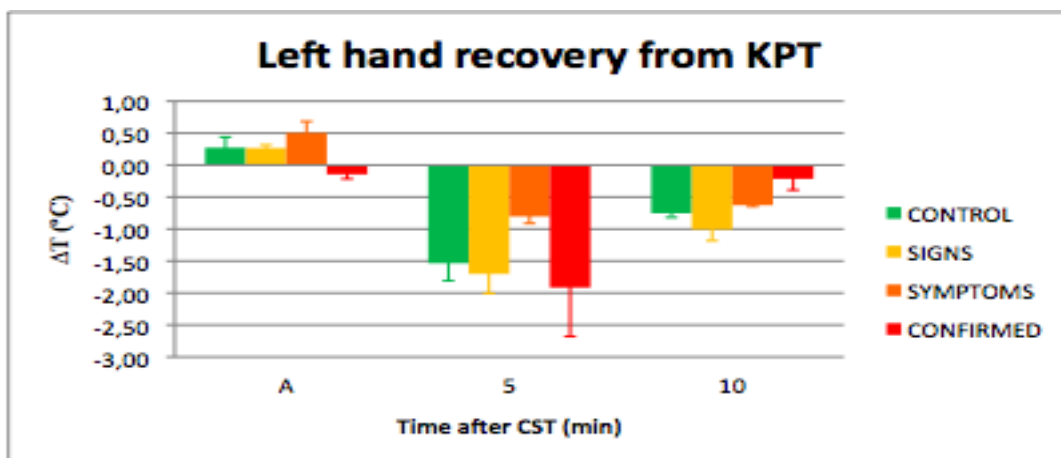


Fig. 120: Left hand mean temperature difference from baseline when recovering from KPT.

When observing the values of mean thermal symmetry (bilateral absolute difference between left hand and right hand AOI's), immediately after the mechanical provocation the confirmed group presented a higher value. At 5 minutes in recovery from post vascular challenge

It was possible to distinguish differences in mean thermal symmetry between the four groups, this value was more accentuated in the confirmed group followed by the symptoms group, the control group had the smaller value. At the end of the test the highest mean thermal symmetry value was observed in the confirmed group, and conversely, the smaller values were in the control group, the two other groups presented a similar value, fig. 121.

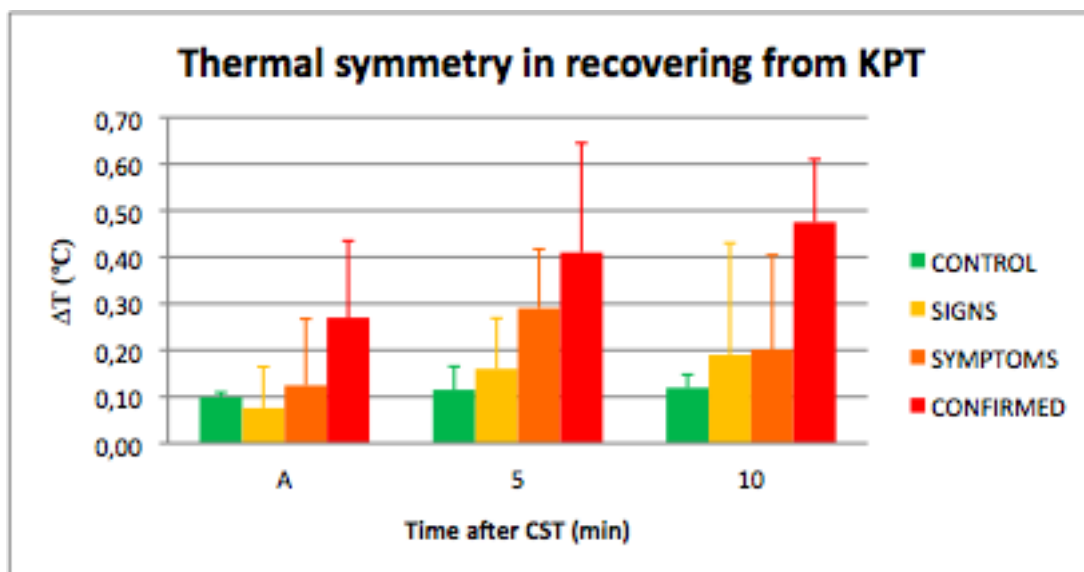


Fig. 121: Hand thermal symmetry difference from baseline when recovering from KPT.

Considering the mean value of thermal symmetry in the distal inter-phalanges of the fingers after the KPT, it was observed that there was no specific involvement in any particular finger in any of the four groups as shown in fig. 122.

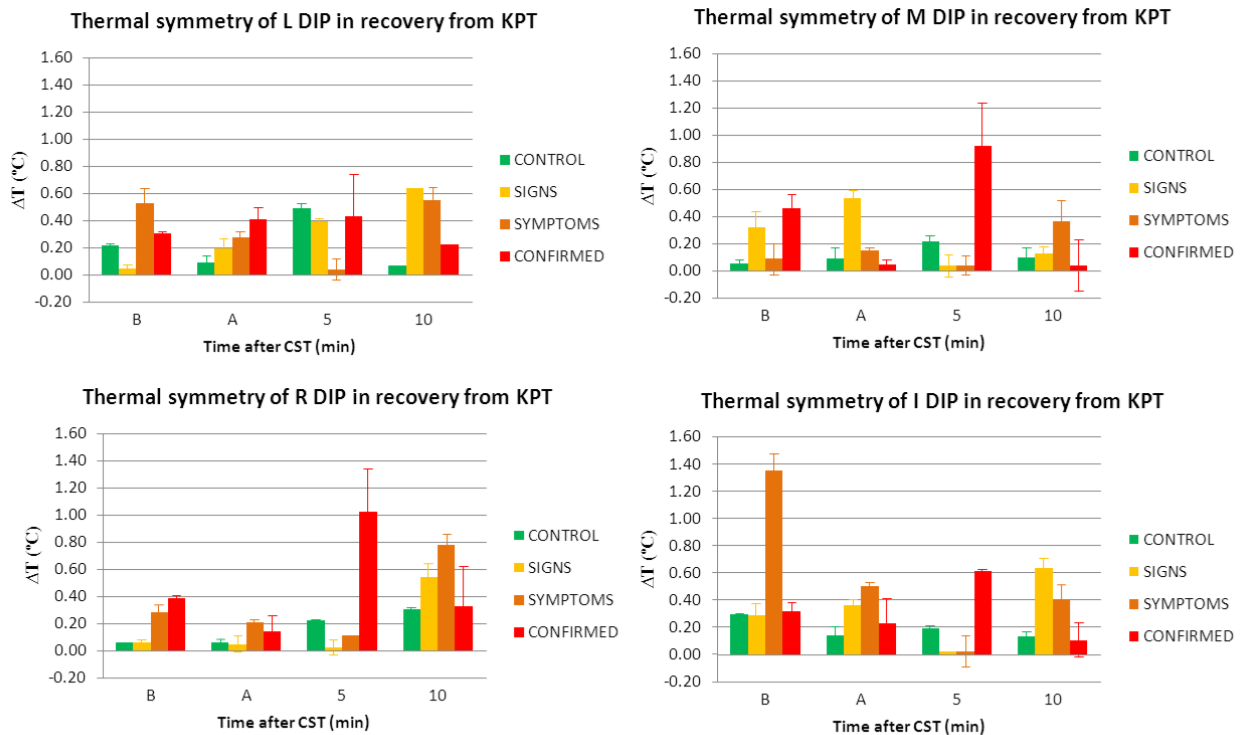


Fig. 122: Hand DIPs thermal symmetry difference when recovering from KPT.

Fig. 123 is an example of the collected thermal images after being standardised (as described in section 3.7.4.). This example shows a set of images from a sample from the control group and from a subject that has been clinically confirmed as having RSI.

From statistical analysis, it was obtained a Cronbach Coefficient Alpha for the hand AOI in the KPT test of 0.976, which represents good data consistency. The Interclass Correlation Coefficient was of 0.954 with a confidence interval varying from 0.905 to 0.978 demonstrating higher reproducibility.

The normal distribution of the data was assessed by the Kolmogorov-Smirnov test (K-S test) and the p values obtained were 0.597 for the right hand AOI and 0.646 for the left hand AOI. As the K-S test p value was greater than 0.05 this means that the collected data was not different from the normal distribution and the statistical methods associated with this distribution can be used.

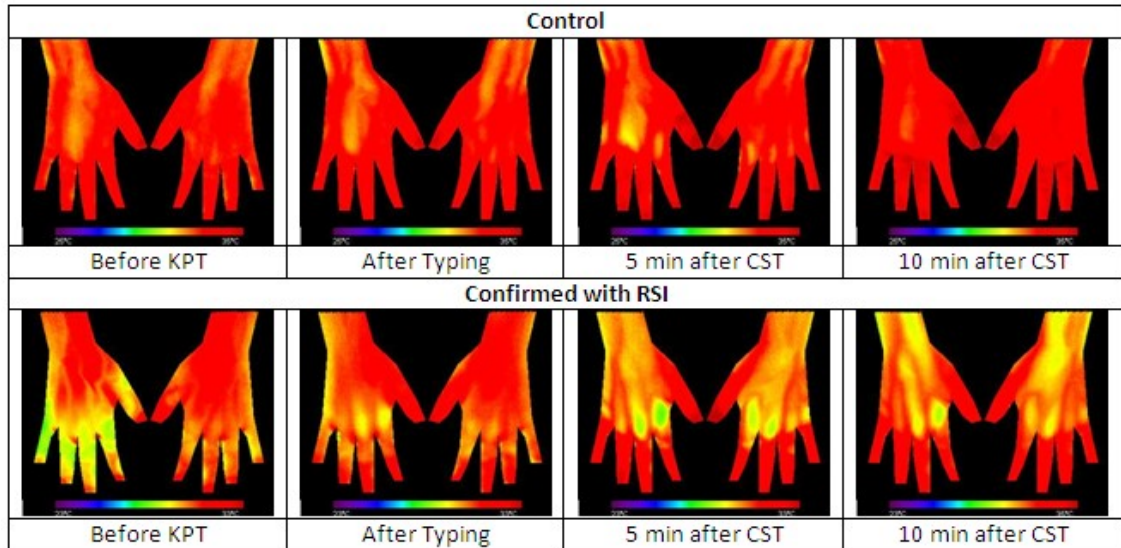


Fig. 123: An example comparative set of standardised images between a control subject and a clinically confirmed subject with RSI.

A non-parametric Pearson chi-square test was applied between the groups and the result was a value of 168.000 for the right hand AOI and of 153.333 for the left hand AOI with a significance level inferior to 0.05 ($p=0.000$ in both AOI). This demonstrates that if the null hypothesis was true it would be expected that an x^2 value of 150.000 or superior less than 5 times in each 150.000 would be found. This result therefore rejects the null hypothesis and indicates that the variables are independent.

It can be concluded that using thermal images and the KPT test it is possible to identify different HAS stage groups.

From the statistical analysis of hypothesis Z-test there is statistical evidence of independence between all groups ($p<0.05$) based in both hands AOI excluding the signs and symptoms based in the right hand AOI ($p>0.05$) as it can be observed from table 17.

KPT	Z-test (p value)	
	Right hand	Left hand
Control vs. Signs	HS	HS
Control vs. Symptoms	S	HS
Control vs. Confirmed	HS	HS
Signs vs. Symptoms	NS	HS
Signs vs. Confirmed	HS	HS
Symptoms vs. Confirmed	HS	HS

Table 17: Z-test values comparing groups results for hand AOI in the KPT (HS-Highly significant, S-Significant, NS-Non Significant).

There is statistical evidence (Z test $p < 0.05$) of discrimination between subjects from the control group and the confirmed group, the signs group and the confirmed group, and also the symptoms group and the confirmed group when using difference from baseline hand AOI mean thermal symmetry, as shown in table 18.

KPT	Z test (p-value)
Control vs. Signs	NS
Control vs. Symptoms	NS
Control vs. Confirmed	HS
Signs vs. Symptoms	NS
Signs vs. Confirmed	S
Symptoms vs. Confirmed	S

Table 18: Z-test values comparing groups results for hand AOI thermal symmetry in the KPT (HS-Highly significant, S-Significant, NS-Non Significant).

4.3.2. Vibration provocation test

The table 19 shows the mean temperature, mean standard deviation and mean thermal symmetry values of the hand (right and left) AOI before vibration provocation, immediately after vibration and 5 and 10 minutes after post vascular challenge.

Vibration Provocation Test		Before Test		After Test		5 min CST		10 min CST	
		MeanT	sd	MeanT	sd	MeanT	sd	MeanT	sd
Controls (9)	L Hand	31,83	0,93	31,02	0,74	29,59	1,22	31,09	0,99
	R Hand	31,69	0,95	30,93	0,76	29,6	1,24	30,89	1,05
	H Symm	0,14	0,02	0,09	0,02	0,01	0,02	0,2	0,06
Signs (7)	L Hand	29,96	1,2	29,71	1,18	28,35	1,6	29,12	1,34
	R Hand	29,94	1,18	29,69	1,16	28,58	1,39	29,43	1,25
	H Symm	0,02	0,02	0,02	0,02	0,23	0,21	0,31	0,09
Symptoms (7)	L Hand	28,43	1,61	28,14	1,48	27,58	1,82	28,42	1,68
	R Hand	28,78	1,57	28,47	1,46	28,05	1,82	28,8	1,64
	H Symm	0,35	0,04	0,33	0,02	0,47	0	0,38	0,04
Confirmed (3)	L Hand	32,03	0,94	31,19	1,04	29,79	1,55	30,37	1,2
	R Hand	31,95	1,07	31,24	1,25	29,98	1,73	30,55	1,43
	H Symm	0,08	0,13	0,05	0,21	0,19	0,18	0,18	0,23

Table 19: HAS stage groups mean temperatures over the VPT.

Observing the right hand AOI, it can be seen that all the four groups had a decrease of mean temperature, specially the control and confirmed groups. Five minutes after the vascular provocation recovery the greatest negative mean temperature difference was in the control and confirmed groups, the least was indicated by the symptoms group. At the end of the VPT test the greatest negative mean temperature difference was observed in the confirmed group followed by the control group, the symptoms group had recovered the mean temperature showing the smallest mean temperature difference from baseline, fig. 124.

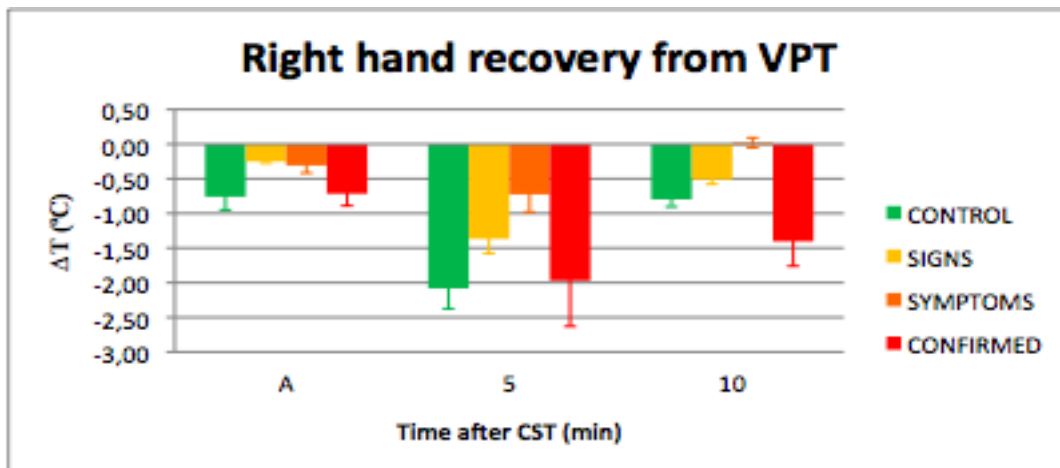


Fig. 124: Right hand mean temperature difference from baseline when recovering from VPT.

The left hand AOI as can be observed by fig. 125 only differed from the right hand AOI in the outcome after the VPT test, in this case the signs group presented a minimal higher difference than control group.

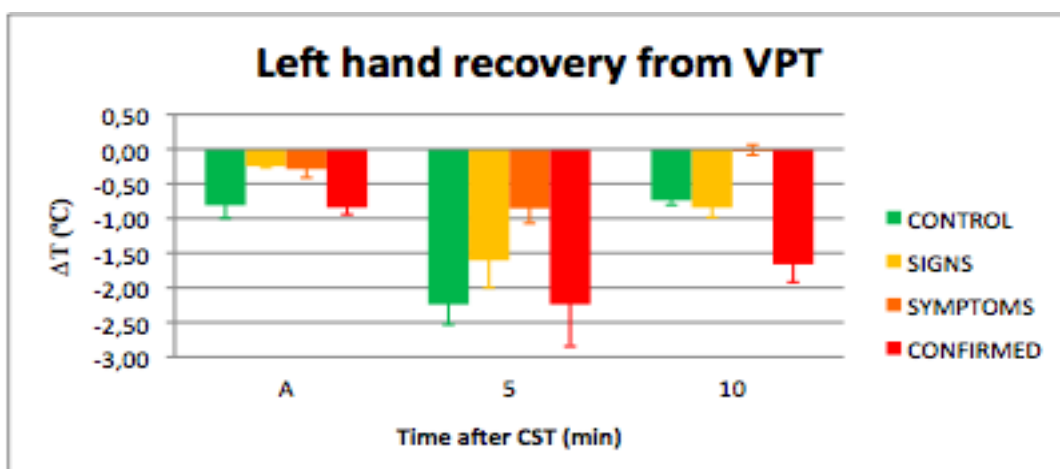


Fig. 125: Left hand mean temperature difference when recovering from VPT.

In the fig. 126 is shown the variation of mean thermal symmetry difference from baseline over the VPT test. After the vibration exposure the value has increased in all groups more significantly in the confirmed group followed by the control group. Five minutes after recovery from vascular challenge the greatest difference was in the confirmed and signs groups. At the end of the VPT test the group presenting the greatest difference was in the signs group closely followed by the confirmed group. The minimal difference was observed in the symptoms group.

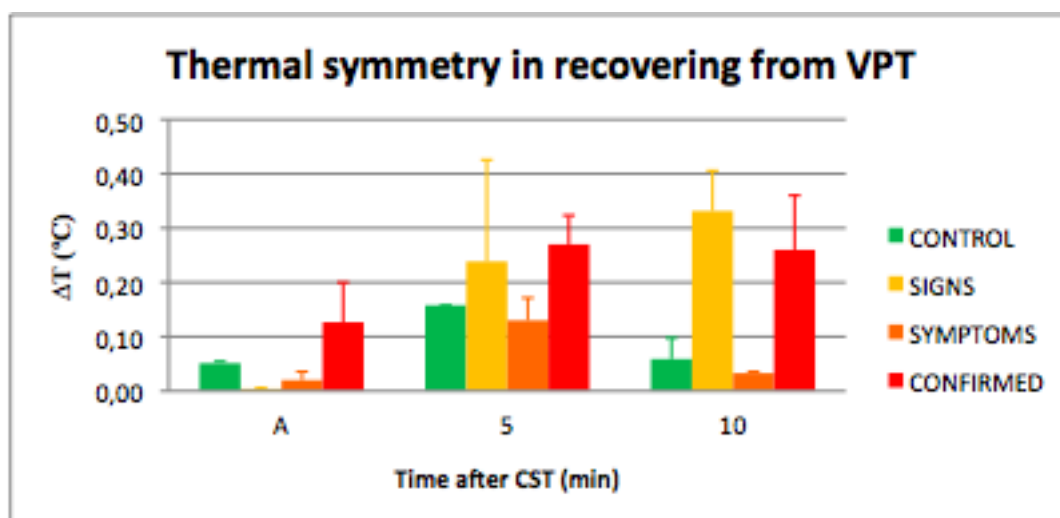


Fig. 126: Hand thermal symmetry difference from baseline when recovering from VPT.

Observing the mean thermal differences in the fingers DIPs AOI after the VPT test, it was observed that there was no specific involvement in any particular finger apart from the index in any of the four groups as shown in fig. 127 In the index finger it can be observed that the confirmed group presented a different pattern than other groups.

These data have shown that classifying people according to signs rather than symptoms is unreliable.

The fig. 128 presents an example of captured images after being standardised (method described in section 3.7.4.), which shows a set of images of a subject from the control group compared with a subject clinically confirmed as having HAVS during a VPT.

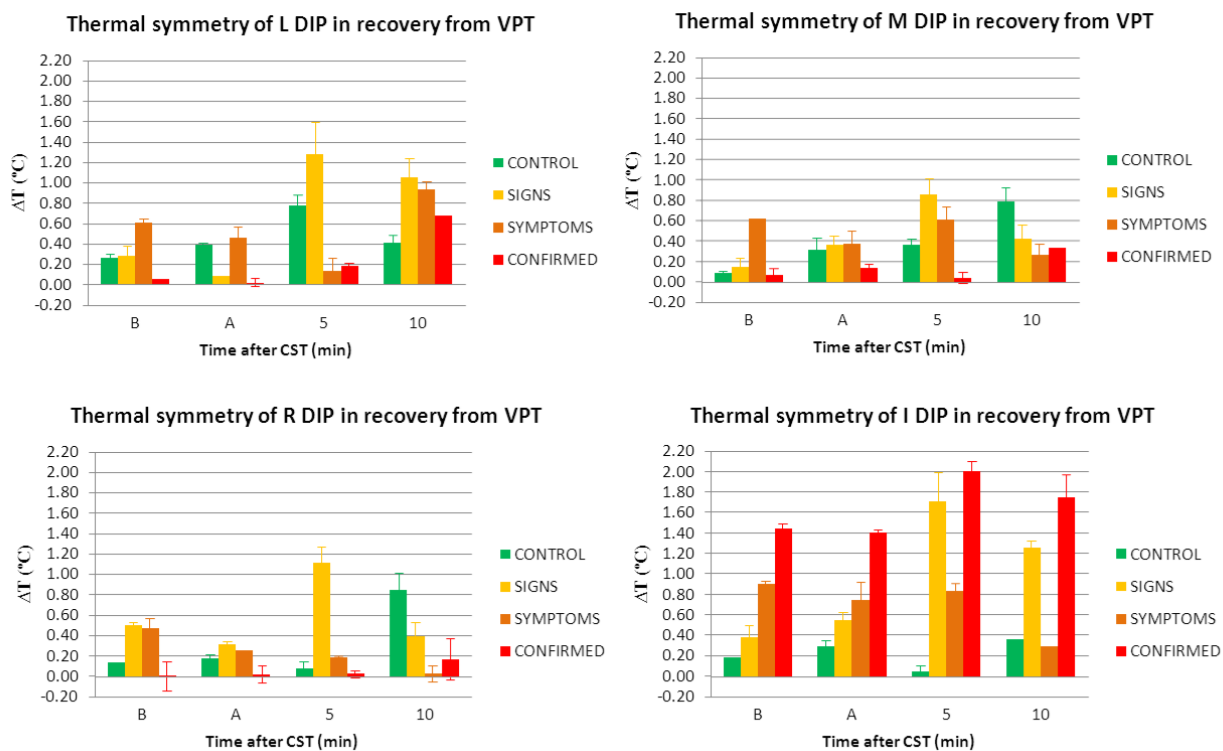


Fig. 127: Hand DIPs thermal symmetry difference when recovering from VPT.

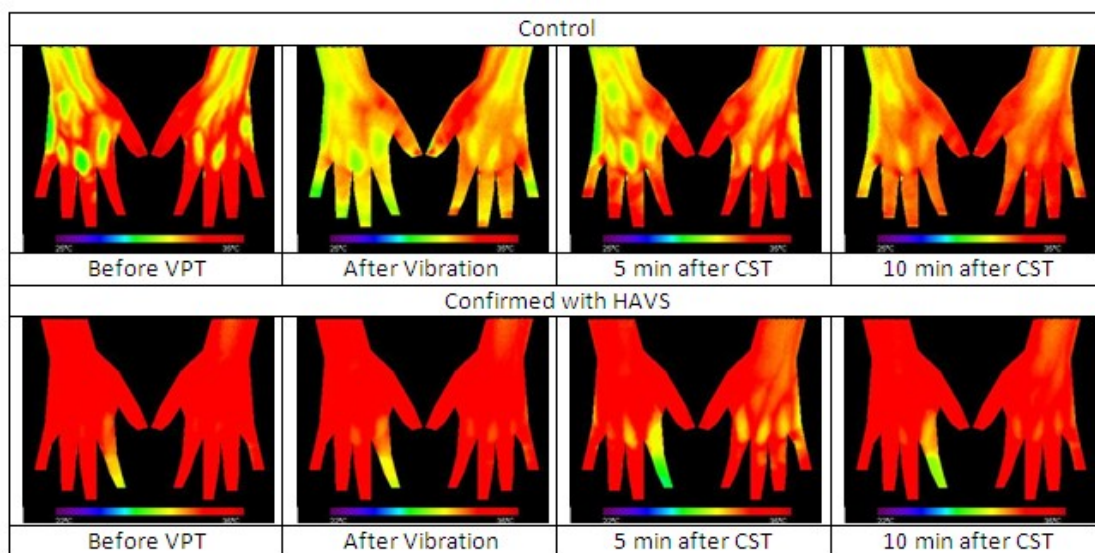


Fig. 128: An example comparative set of standardised images between a control subject and a clinically confirmed subject with HAVS.

Statistical Analysis of the data collected from the VPT test, was obtained a Cronbach Coefficient Alpha for the hand AOI of 0.988, which means good data consistency. The Interclass

Correlation Coefficient was of 0.976 with a confidence interval varying from 0.948 to 0.989 demonstrating high reproducibility.

The normal distribution of the data was assessed by a K-S test, the p values obtained were 0.515 for the right hand AOI and 0.68 for the left hand AOI. As the K-S test p value was greater than 0.05 it means that the collected data is not different from the normal distribution and the statistical methods associated with this distribution can be used.

A non-parametric Pearson chi-square test was applied between the groups. The result gave a value of 168.000 for the right and left hand AOIs with a significance level inferior to 0.05 ($p=0.000$ in both AOI). This demonstrates that if the the null hypothesis was true it would be expected to find a χ^2 value of 168.000 or superior less than 5 times in each 165.000. This rejects the null hypothesis and indicates that the variables are independent. It can therefore be concluded that using thermal images and the VPT test it is possible to identify different HAS stage groups.

From the statistical analysis of hypothesis Z-test shown in table 20. there is statistical evidence of independence between all groups ($p<0.05$) based in both hands AOI.

VPT	Z-test (p value)	
	Right hand	Left hand
Control vs. Signs	HS	S
Control vs. Symptoms	HS	HS
Control vs. Confirmed	HS	HS
Signs vs. Symptoms	HS	HS
Signs vs. Confirmed	HS	HS
Symptoms vs. Confirmed	HS	HS

Table 20: Z-test values comparing groups results for hand AOI in the VPT(HS-Highly significant, S-Significant, NS-Non Significant) .

There is statistical evidence (Z test $p<0.05$) of discrimination between subjects from all the groups excluding between the signs and the confirmed group when using the difference from baseline in terms of hand AOI mean thermal symmetry, as shown in table 21.

VPT	Z test (p-value)
Control vs. Signs	HS
Control vs. Symptoms	S
Control vs. Confirmed	HS
Signs vs. Symptoms	HS
Signs vs. Confirmed	NS
Symptoms vs. Confirmed	HS

Table 21: Z-test values comparing groups results for hand AOI thermal symmetry in the VPT (HS-Highly significant, S-Significant, NS-Non Significant).

4.3.3. Mouse provocation test

The table 22 shows the quantitative data of the mechanical stress exposure by computer mouse operation of the volunteers. It presents in each volunteer the number of mouse clicks and the pixels traversed by the mouse over a period of 5 minutes. The mean overall number of clicks was 71.9 per minute, and the average pixel distance traversed by the mouse was 155.657 within the total duration of the test.

The group that presented the greatest value of these two indicators of stress was the confirmed group.

Volunteer	Group	Mouse		
		Clicks	cpm	Pixels
HAS01	Control	353	70,6	141357
HAS02	Symptoms	402	80,4	164447
HAS03	Confirmed	429	85,8	179144
HAS05	Symptoms	278	55,6	111408
HAS06	Signs	286	57,2	121673
HAS07	Symptoms	432	86,4	181632
HAS08	Control	282	56,4	116611
HAS09	Signs	368	73,6	156483
HAS12	Control	366	73,2	160990
HAS13	Signs	285	57	124962
HAS14	Signs	294	58,8	122301
HAS15	Signs	358	71,6	160445
HAS16	Symptoms	333	66,6	143778
HAS17	Symptoms	357	71,4	162075
HAS19	Control	454	90,8	207160
HAS20	Control	397	79,4	180323
HAS23	Control	414	82,8	185801
HAS26	Confirmed	381	76,2	169963
HAS27	Control	363	72,6	157886
HAS28	Signs	362	72,4	164700
Statistics	Overall	359,7	71,9	155657
	Controls	375,6	75,1	164304
	Signs	325,5	65,1	141761
	Symptoms	360,4	72,1	152668
	Confirmed	405,0	81,0	174554

Table 22: MPT volunteers characterisation in number of mouse clicks and pixels traversed.

The variation of the mean temperature of hand AOI, mean standard deviation and mean

thermal symmetry values across the MPT is presented in the table 23 for all four groups.

Mouse Provocation Test		Before Test		After Test		5 min CST		10 min CST	
		MeanT	sd	MeanT	sd	MeanT	sd	MeanT	sd
Controls (7)	L Hand	30,9	1,1	30,6	0,82	29,24	1,28	30,63	1,05
	R Hand	30,98	1,11	30,71	0,87	29,3	1,34	30,68	1,1
	H Symm	0,08	0,01	0,11	0,05	0,06	0,06	0,05	0,05
Signs (6)	L Hand	30,54	1,23	30,91	0,99	29,72	1,33	30,4	1,1
	R Hand	30,16	1,37	30,67	1,05	29,36	1,34	30,12	1,13
	H Symm	0,38	0,14	0,24	0,06	0,36	0,01	0,28	0,03
Symptoms (5)	L Hand	28,56	1,93	28,39	1,62	27,65	1,72	28,17	1,58
	R Hand	28,77	2,12	28,75	1,78	27,79	1,88	28,56	1,74
	H Symm	0,21	0,19	0,36	0,16	0,14	0,16	0,39	0,16
Confirmed (2)	L Hand	31,06	1,02	30,86	0,75	28,11	1,43	30,38	1,14
	R Hand	30,74	1,3	30,53	1,03	27,77	1,48	30,36	1,06
	H Symm	0,32	0,28	0,33	0,28	0,34	0,05	0,02	0,08

Table 23: HAS stage groups mean temperatures over the MPT.

Fig. 129 shows the right hand AOI mean temperature difference from the baseline (mean temperature after acclimatisation and before mechanical provocation) over the MPT. After the right hand stress exposure, the unique group presenting a mean temperature increase was in the signs group, while the symptoms group showed a very small variation. At five minutes after post vascular challenge all groups presented a decrease in mean temperature, but it was more accentuated in the confirmed group. The group that demonstrated the least decrease was the signs group. At the end of the test only the signs group showed a mean temperature increase compared with baseline, all the remaining 3 groups presented a lower mean temperature difference than baseline.

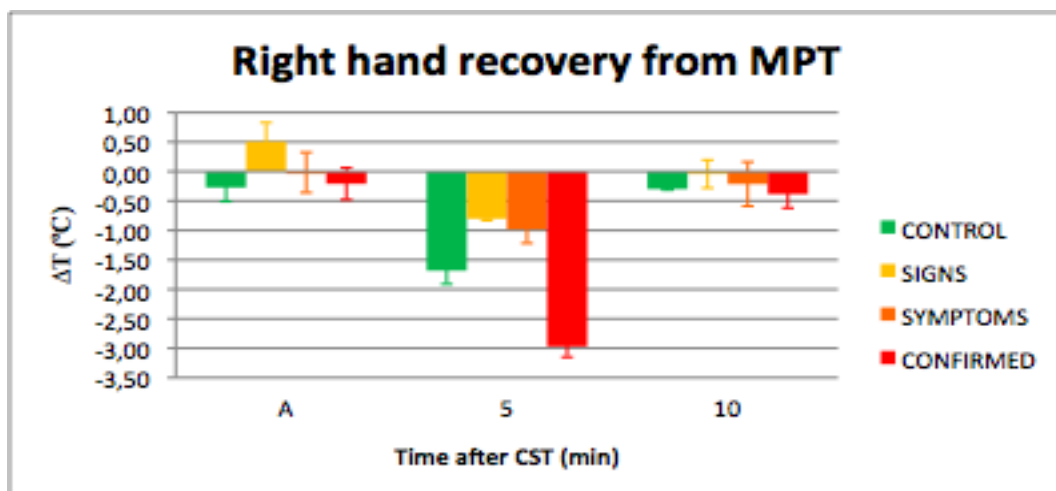


Fig. 129: Right hand mean temperature difference from baseline when recovering from MPT.

The differences in mean temperatures over the MPT in the left hand AOI from the baseline are shown in fig. 130. Here it can be observed that after the mechanical exercise of the right hand with the mouse an increase in mean temperature occurred only in the signs group. The other three groups presented a decrease in mean temperature. At five minutes after cold water immersion challenge the mean temperature has decreased in all groups, At this stage the confirmed group showed the greatest decrease followed by the control group. At the end of the test the mean temperatures of all groups presented a lower value than baseline, with this decrease being greater in the confirmed followed by the symptoms group.

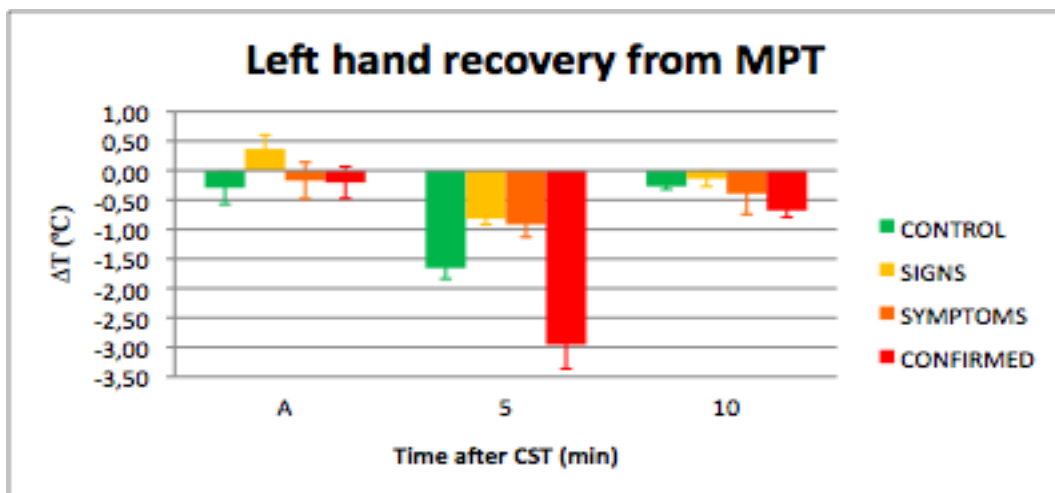


Fig. 130: Left hand mean temperature difference from baseline when recovering from MPT.

Observing the mean thermal symmetry difference from baseline during the MPT test, showed in fig. 131, it can be seen that all groups presented an increase of this value, which was more accentuated in the symptoms and signs groups. At 5 minutes after the post vascular test, the mean thermal symmetry value decreased for both the signs and the symptoms groups. At the end of the test the group that presented the greater mean thermal symmetry difference value when compared with the baseline was the confirmed group, the control group presented the lowest value than the other three groups.

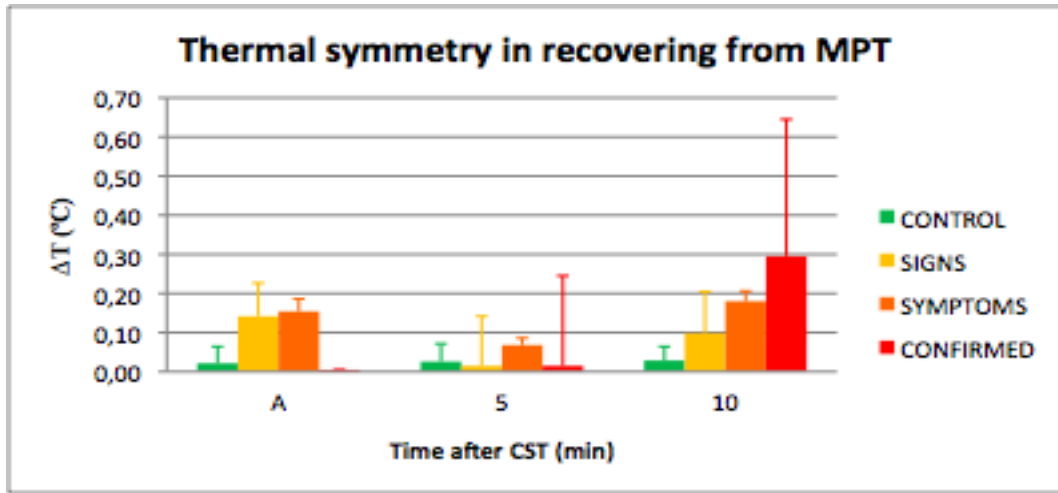


Fig. 131: Hand thermal symmetry difference from baseline when recovering from MPT.

Observing the mean thermal symmetry variations in the fingers DIPs AOI after a MPT, it was observed that there was not specific involvement of little and ring fingers as shown in fig. 132. In the middle finger it can be observed that the confirmed group presented a different pattern than other groups (greater value of mean thermal symmetry), likewise in the index finger the symptoms group.

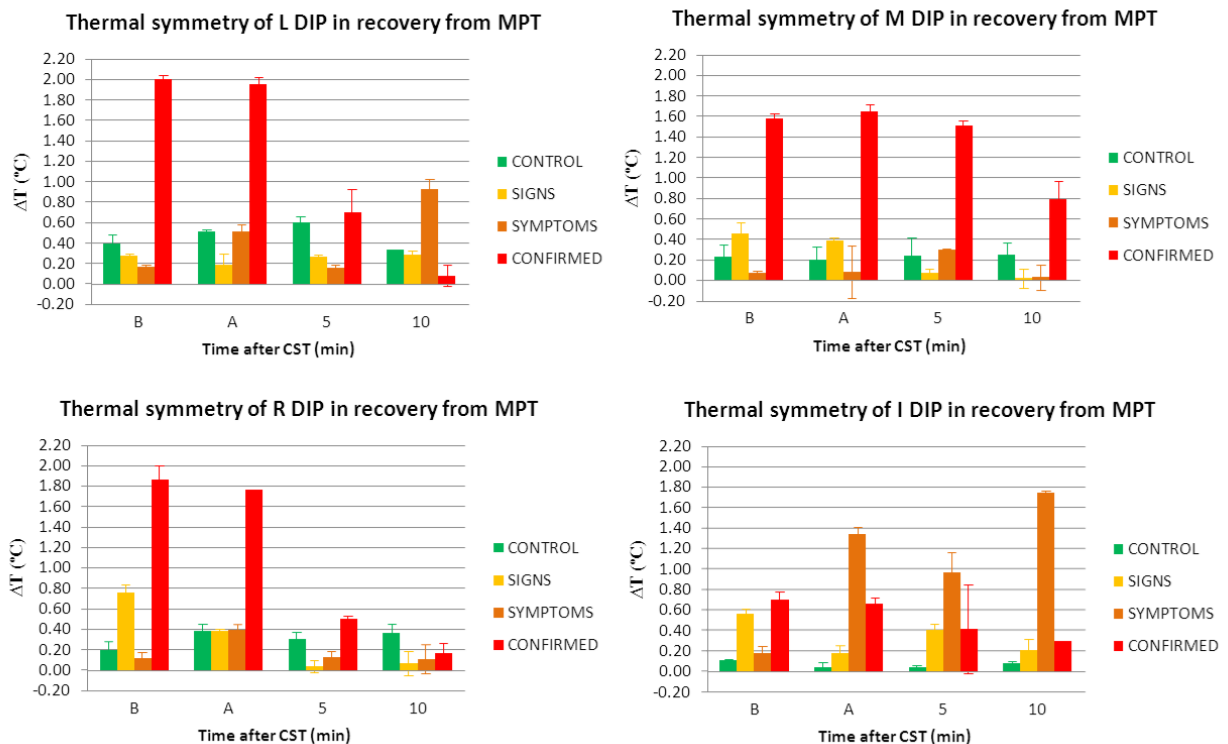


Fig. 132: Hand DIPs thermal symmetry difference when recovering from MPT.

Statistical analysis of the data collected from the MPT test, was obtained using the Cronbach Coefficient Alpha for the hand AOI of 0.977, which means good data consistency. The Interclass Correlation Coefficient was of 0.955 with a confidence interval varying from 0.890 to 0.982 demonstrating higher reproducibility of the AOIs in the test.

The normal distribution of the data was assessed by a K-S test, the p values obtained were 0.829 for the right hand AOI and 0.853 for the left hand AOI. As the K-S test p value was greater than 0.05 it means that the collected data has no difference from the normal distribution and the statistical methods associated with this distribution can be used.

A non-parametric Pearson chi-square test was applied between the groups. The result gave a value of 126.000 for the right and left hand AOIs with a significance level inferior to 0.05 ($p=0.000$ in both AOI). This demonstrates that if the null hypothesis was true it will be expected to find a χ^2 value of 126.000 or superior less than 5 times in each 120.000. Therefore the null hypothesis can be rejected and the result indicates that the variables are independent. It can again be concluded that using thermal images and the MPT test it is possible to identify different HAS stage groups.

From the statistical analysis of hypothesis Z-test shown in table 24. there is statistical evidence of independence between control and signs, and signs and confirmed groups ($p<0.05$) based in both hands AOI. There was no statistical evidence of independence between control and symptoms, control and confirmed, signs and symptoms, and symptoms and confirmed ($p>0.05$) based in both hands AOI.

MPT	Z-test (p value)	
	Right hand	Left hand
Control vs. Signs	HS	S
Control vs. Symptoms	NS	NS
Control vs. Confirmed	NS	HS
Signs vs. Symptoms	HS	NS
Signs vs. Confirmed	HS	HS
Symptoms vs. Confirmed	NS	NS

Table 24: Z-test values comparing groups results for hand AOI in the MPT test (HS-Highly significant, S-Significant, NS-Non Significant).

There is statistical evidence (Z test $p<0.05$) of discrimination between subjects from the control group and the symptoms group, and the signs group and the symptoms group when using the difference from baseline in terms of hand AOI mean thermal symmetry, as shown in table 25.

MPT	Z test (p-value)
Control vs. Signs	NS
Control vs. Symptoms	HS
Control vs. Confirmed	NS
Signs vs. Symptoms	S
Signs vs. Confirmed	NS
Symptoms vs. Confirmed	NS

Table 25: Z-test values comparing groups results for hand AOI thermal symmetry in the MPT (HS-Highly significant, S-Significant, NS-Non Significant).

4.3.4. Cold Stress Test

In the table 26 presents the average mean temperatures, standard deviations and mean thermal symmetry values for a cold stress test (CST) for the hand AOI.

Cold Stress Test		Before Test		5 min CST		10 min CST	
		MeanT	sd	MeanT	sd	MeanT	sd
Controls (7)	L Hand	31,1	0,81	29,6	1,3	30,53	1,1
	R Hand	30,95	0,87	29,52	1,24	30,47	1,06
	H Symm	0,15	0,06	0,08	0,06	0,06	0,04
Signs (6)	L Hand	29,74	1,48	28,39	1,61	28,81	1,3
	R Hand	29,63	1,49	28,32	1,59	28,76	1,32
	H Symm	0,11	0,01	0,07	0,02	0,05	0,02
Symptoms (5)	L Hand	29	1,41	27,41	1,69	27,88	1,49
	R Hand	28,96	1,5	27,2	1,72	27,75	1,52
	H Symm	0,04	0,09	0,21	0,03	0,13	0,03
Confirmed (2)	L Hand	29,7	0,87	27,45	1,44	28,34	1,31
	R Hand	30,07	0,77	27,28	1,35	28,25	1,27
	H Symm	0,37	0,1	0,17	0,09	0,09	0,04

Table 26: HAS stage groups mean temperatures over the CST.

Both the right and left hands AOI had a mean temperature decrease for all groups at 5 minutes after water immersion and after 10 minutes recovery from vascular provocation. At five minutes recovery in both AOI the greater decrease in mean temperature was found in the confirmed group followed by the symptoms group. At the end of the test the sequence in decreased mean

temperature from greatest to lower in relation to baseline for all groups was: the confirmed, the symptoms, the signs and the control, fig. 133 and fig. 134.

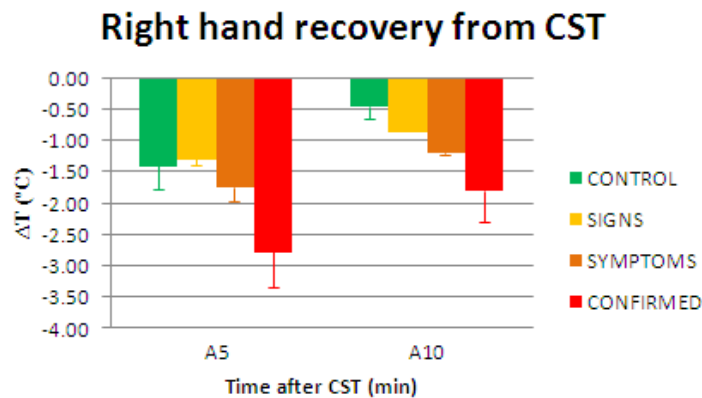


Fig. 133: Right hand mean temperature difference from baseline when recovering from CST.

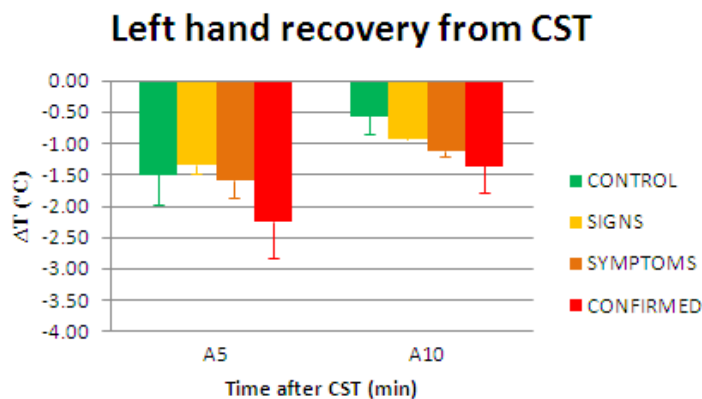


Fig. 134: Left hand mean temperature difference from baseline when recovering from CST.

The differences in mean thermal symmetry from baseline are presented in fig. 135 which shows a higher increase of that value either at 5 and 10 minutes after cold challenge. The symptoms group at 5 minutes recovery presented the second greater increase in mean thermal symmetry, but at the end of the test registered a similar value to both the control and the signs groups. Using this value shows clear discrimination between the confirmed and the control groups, although for discriminating signs from symptoms other indicators are needed.

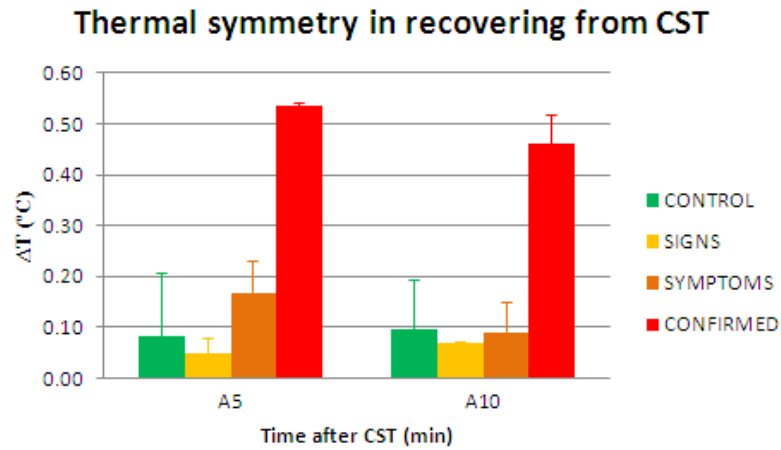


Fig. 135: Hand thermal symmetry difference from baseline when recovering from CST.

Observing the fig. 136, that represents the mean thermal symmetry value in the DIPs AOI, it was observed that there was no specific involvement in any particular finger apart from the index in any of the four groups. In the index finger it can be observed that the confirmed group presented a different pattern than other groups.

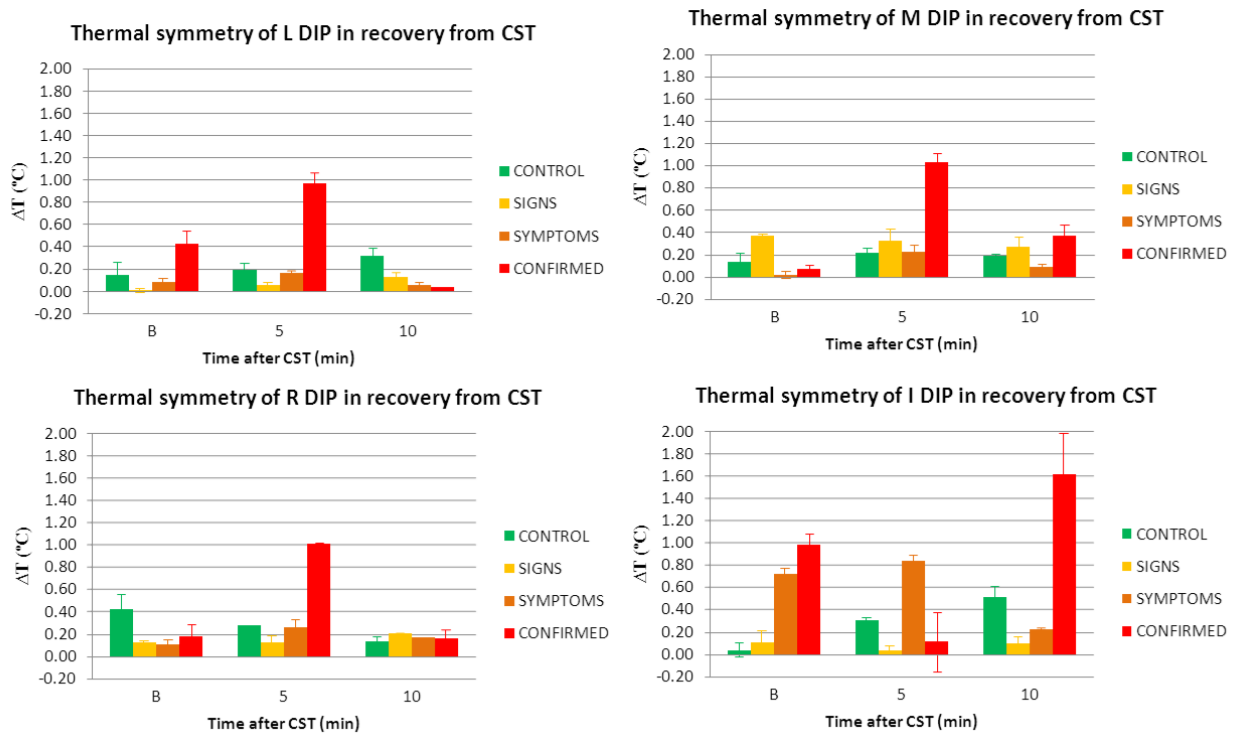


Fig. 136: Hand DIPs thermal symmetry difference when recovering from CST.

Performing a statistical analysis in the data collected from the CST test, with a Cronbach Coefficient Alpha for the hand AOI of 0.979, which showed good data consistency. The Interclass Correlation Coefficient was 0.960 with a confidence interval varying from 0.901 to 0.984 demonstrating higher reproducibility of the test.

The normal distribution of the data was assessed by a K-S test, the p values obtained were 0.743 for the right hand AOI and 0.967 for the left hand AOI. As the K-S test p value was greater than 0.05 which means that the data is not different from the normal distribution and the statistical methods associated with this distribution can be used.

A non-parametric Pearson chi-square test was performed between the groups and the result was a value of 126.000 for the right and left hand AOIs with a significance level inferior to 0.05 ($p=0.000$ in both AOI). This demonstrates that if the null hypothesis was true an expected χ^2 value of 126.000 or superior to less than 5 times in each 120.000. This result therefore rejects the null hypothesis and indicates that the variables are independent. It can be concluded that using thermal images with the MPT test it is possible to identify different HAS stage groups.

From the statistical analysis of hypothesis Z-test shown in table 27. there is statistical evidence of independence between all groups ($p<0.05$) based in both hands AOI excluding between signs and confirmed, and symptoms and confirmed ($p>0.05$) based in both hands AOI.

CST	Z-test (p value)	
	Right hand	Left hand
Control vs. Signs	HS	HS
Control vs. Symptoms	HS	HS
Control vs. Confirmed	HS	HS
Signs vs. Symptoms	HS	HS
Signs vs. Confirmed	HS	NS
Symptoms vs. Confirmed	S	NS

Table 27: Z-test values comparing groups results for hand AOI in the CST (HS-Highly significant, S-Significant, NS-Non Significant).

There is statistical evidence (Z test $p<0.05$) of discrimination between subjects from the control group and the confirmed group, the signs group and the confirmed group, and the symptoms group and the confirmed group when using the difference from baseline in terms of hand AOI mean thermal symmetry, as shown in table 28.

CST	Z test (p-value)
Control vs. Signs	NS
Control vs. Symptoms	NS
Control vs. Confirmed	HS
Signs vs. Symptoms	NS
Signs vs. Confirmed	HS
Symptoms vs. Confirmed	HS

Table 28: Z-test values comparing groups results for hand AOI thermal symmetry in the CST (HS-Highly significant, S-Significant, NS-Non Significant).

4.3.5. Cold stress test evaluation methods comparison

Loading all the performed tests in the developed application gave results for each different method of assessing a cold stress test. Fig. 137 shows a screenshot of the application that assesses the CST. A set of images are loaded in the left, by clicking in the correspondent image to the test time, these images must be standardised as described in section 3.7.4. and in the CTHERM format. For assessment only two images are compulsory: the image after acclimatisation and the 10 minutes after vascular challenge. Clicking over the selected image it is possible to see the demographic details, e.g. patient name, date of examination, etc.

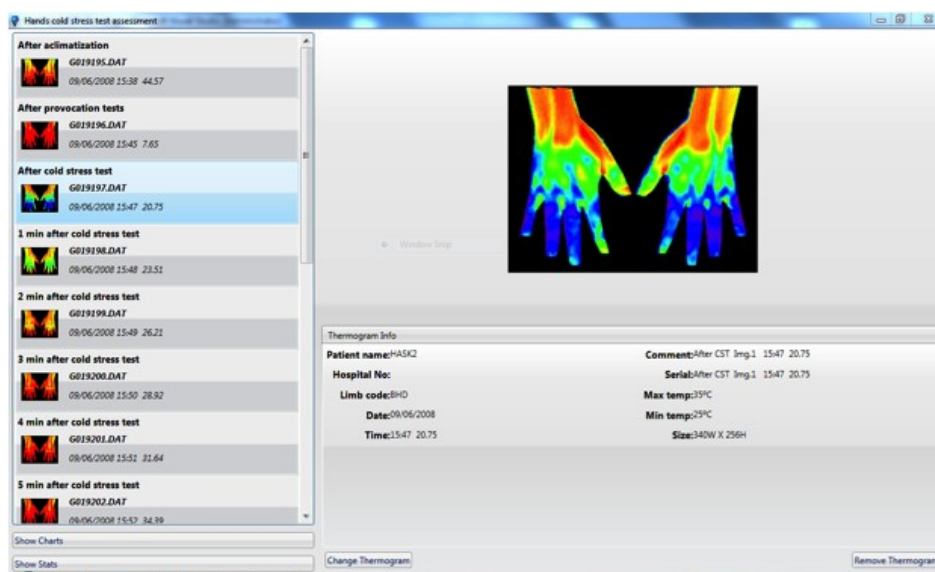


Fig. 137: Screen shot of the application to evaluate the different methods of assessing a CST.

This software has the option of presenting charts, fig. 138, and tables, fig. 139, representing the calculated thermal indexes of the hand AOI for the three assessment methods over the time of the test. These values can also be exported to a CSV file for later statistical treatment.

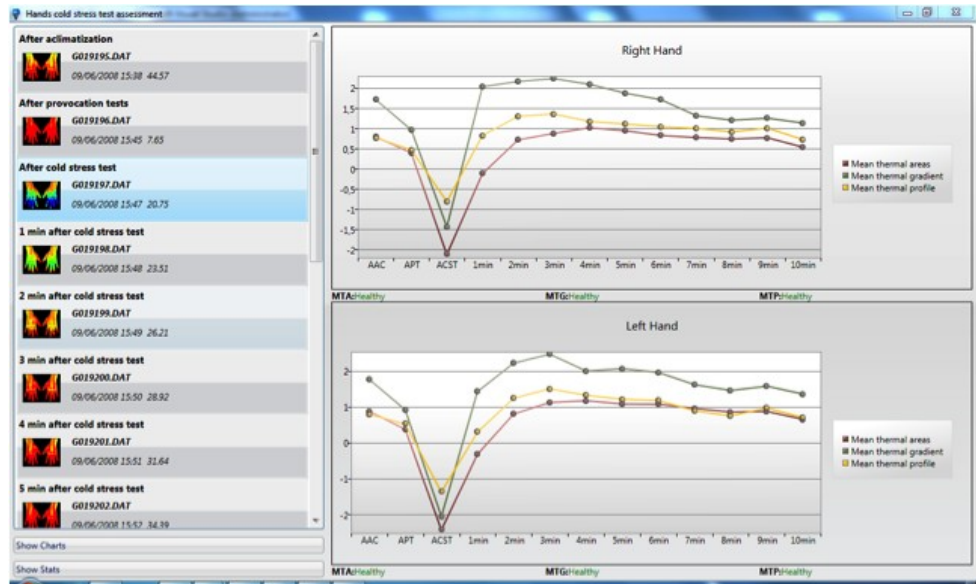


Fig. 138: Chart representation of the calculated thermal indexes of the 3 assessment methods.

Thermogram	Mean thermal area					Mean thermal gradient				
	Fingers-Palm	Little-Palm	Ring-Palm	Middle-Palm	Index-Palm	Fingers-Palm	Little-Palm	Ring-Palm	Middle-Palm	Index-Palm
AAC	0.78	0.21	0.48	0.7	0.86	0.78	0.21	0.48	0.7	0.86
APT	0.38	0	0.5	0.36	0.34	0.38	0	0.5	0.36	0.34
ACST	-2.13	-1.83	-2.56	-2.57	-1.41	-2.13	-1.83	-2.56	-2.57	-1.41
1min	-0.13	-0.83	-0.95	-1.19	-0.5	-0.13	-0.83	-0.95	-1.19	-0.5
2min	0.7	-0.06	0.22	0.13	0.13	0.7	-0.06	0.22	0.13	0.13
3min	0.86	0.35	0.68	0.56	0.38	0.86	0.35	0.68	0.56	0.38
4min	1	0.48	0.98	0.95	0.6	1	0.48	0.98	0.95	0.6
5min	0.93	0.5	0.93	0.93	0.63	0.93	0.5	0.93	0.93	0.63
6min	0.81	0.41	0.88	0.85	0.61	0.81	0.41	0.88	0.85	0.61
7min	0.76	0.3	0.93	0.93	0.64	0.76	0.3	0.93	0.93	0.64
8min	0.72	0.35	0.8	0.94	0.66	0.72	0.35	0.8	0.94	0.66

Thermogram	Mean thermal area					Mean thermal gradient				
	Fingers-Palm	Little-Palm	Ring-Palm	Middle-Palm	Index-Palm	Fingers-Palm	Little-Palm	Ring-Palm	Middle-Palm	Index-Palm
AAC	0.86	0.34	0.84	0.85	0.66	0.86	0.34	0.84	0.85	0.66
APT	0.36	-0.04	0.16	0.48	0.55	0.36	-0.04	0.16	0.48	0.55
ACST	-2.44	-2.17	-2.65	-2.74	-2.27	-2.44	-2.17	-2.65	-2.74	-2.27
1min	-0.33	-1.21	-1.12	-1.54	-0.82	-0.33	-1.21	-1.12	-1.54	-0.82
2min	0.78	-0.12	0.2	-0.1	0.95	0.78	-0.12	0.2	-0.1	0.95
3min	1.11	0.35	0.68	0.49	1.13	1.11	0.35	0.68	0.49	1.13
4min	1.16	0.59	1.01	0.85	1.12	1.16	0.59	1.01	0.85	1.12
5min	1.06	0.56	0.91	0.79	1.09	1.06	0.56	0.91	0.79	1.09
6min	1.06	0.52	0.92	0.86	1.15	1.06	0.52	0.92	0.86	1.15
7min	0.94	0.45	0.95	0.88	1.1	0.94	0.45	0.95	0.88	1.1
8min	0.84	0.38	0.94	0.77	1	0.84	0.38	0.94	0.77	1

Fig. 139: Table with the calculated thermal indexes of the 3 assessment methods.

The results of the analysis of the outcome of each vascular component of the objective provocation tests are now presented.

Thermal indexes after Keyboard Provocation Test, KPT

From the outcome of the vascular component assessment, showed in fig. 140, is noted that the confirmed and signs groups had produced a mean positive thermal index for the three assessment both methods and in both hands, the other two groups (control and symptoms) presented a mean negative value.

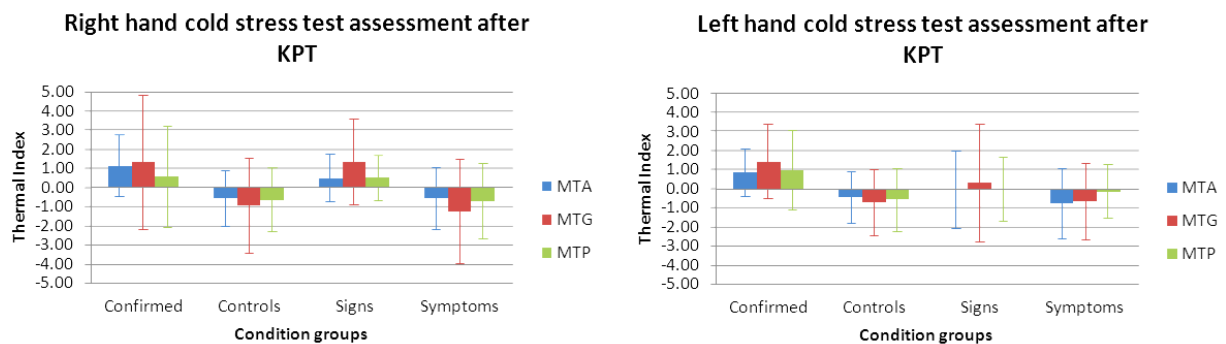


Fig. 140: Thermal indexes per method after KPT.

Testing the hypothesis of discriminating differences between the groups with these results, two sets of Thermal Index mean, from each evaluation method, a Z-test (statistical tests) was conducted. From it (table 29) it can be concluded that is possible to distinguish the control from the signs group for any of the three methods in the right hand AOI, and signs from symptoms using the MTG method in the right hand AOI, because $p < 0.05$. Between all other groups, for all three methods in the left hand AOI there was no statistical evidence ($p > 0.05$) of independence between the groups.

KPT	Right hand Z-test (p value)			Left hand Z-test (p value)		
	MTA	MTG	MTP	MTA	MTG	MTP
Control vs. Signs	S	S	S	NS	NS	NS
Control vs. Symptoms	NS	NS	NS	NS	NS	NS
Control vs. Confirmed	NS	NS	NS	NS	NS	NS
Signs vs. Symptoms	NS	S	NS	NS	NS	NS
Signs vs. Confirmed	NS	NS	NS	NS	NS	NS
Symptoms vs. Confirmed	NS	NS	NS	NS	NS	NS

Table 29: Z-test results from relationship between groups after KPT vascular assessment (HS-Highly significant, S-Significant, NS-Non Significant).

Thermal indexes after Vibration Provocation Test, VPT

Observing the outcome of the vascular assessment after vibration provocation, shown in fig. 141, it is noted that in the right hand only, the signs group presented a mean positive thermal index for the three assessment methods, when all other three groups presented a mean negative. In the symptoms group the data showed that the thermal index was closer to 0.

In the left hand, the controls presented a mean negative thermal index and in the symptoms group a mean negative for all 3 assessment methods. The confirmed group however, had a mean positive thermal index using the MTA and MTG methods, and a mean negative using MTP. The signs group had a mean positive thermal index using the MTG method and a mean negative with the other two assessment methods.

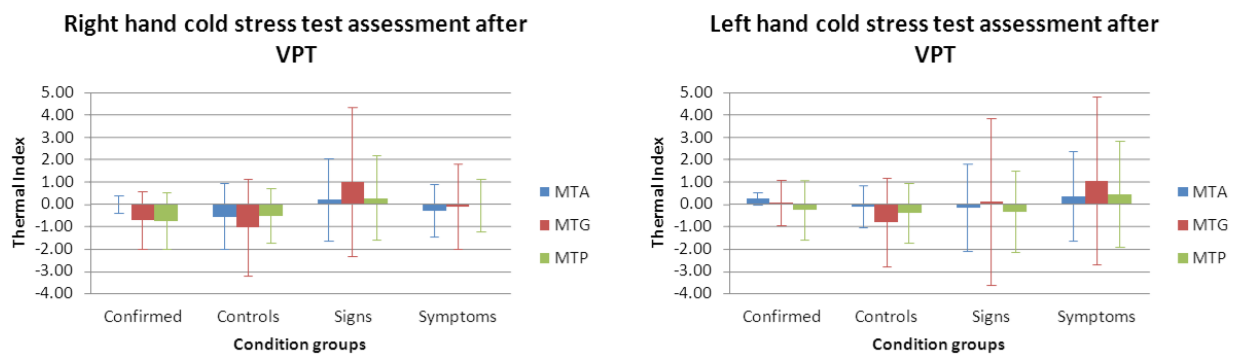


Fig. 141: Thermal indexes per method after VPT.

Testing the hypothesis of discriminating differences between the groups with these results, a two sets of Z-tests (statistical tests) was conducted. From these results (table 30) it can be concluded that is not possible to distinguish between all groups because for all three methods. In both hands

the AOI values there was no statistical evidence ($p>0.05$) of independence between the groups.

VPT	Right hand Z-test (p value)			Left hand Z-test (p value)		
	MTA	MTG	MTP	MTA	MTG	MTP
Control vs. Signs	NS	NS	NS	NS	NS	NS
Control vs. Symptoms	NS	NS	NS	NS	NS	NS
Control vs. Confirmed	NS	NS	NS	NS	NS	NS
Signs vs. Symptoms	NS	NS	NS	NS	NS	NS
Signs vs. Confirmed	NS	NS	NS	NS	NS	NS
Symptoms vs. Confirmed	NS	NS	NS	NS	NS	NS

Table 30: Z-test results from relationship between groups after VPT vascular assessment (HS-Highly significant, S-Significant, NS-Non Significant).

Thermal indexes after Mechanical Provocation Tests, MPT

Considering the outcome of the vascular assessment after the mouse stress test on the right hand, shown in fig. 142, it is observed that for both hands AOI the mean thermal indexes were positive for all groups. The thermal indexes are higher for the confirmed group followed by the symptoms group.

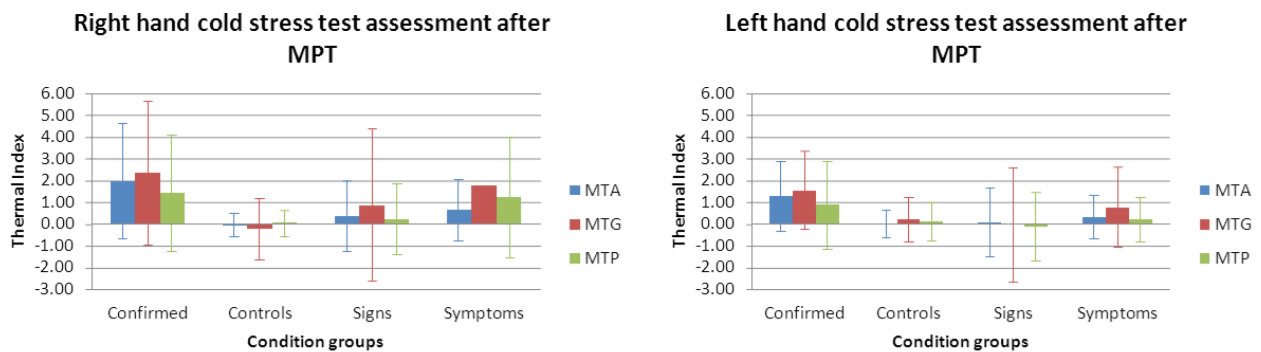


Fig. 142: Thermal indexes per method after MPT.

Testing the hypothesis of discriminating differences between the groups with these results, two sets of means Z-test were conducted. From this result (table 31) it can be concluded that is not possible to distinguish between all groups because for all three methods and in both hands AOI there was no statistical evidence ($p>0.05$) of independence between the groups.

MPT	Right hand Z-test (p value)			Left hand Z-test (p value)		
	MTA	MTG	MTP	MTA	MTG	MTP
Control vs. Signs	NS	NS	NS	NS	NS	NS
Control vs. Symptoms	NS	NS	NS	NS	NS	NS
Control vs. Confirmed	NS	NS	NS	NS	NS	NS
Signs vs. Symptoms	NS	NS	NS	NS	NS	NS
Signs vs. Confirmed	NS	NS	NS	NS	NS	NS
Symptoms vs. Confirmed	NS	NS	NS	NS	NS	NS

Table 31: Z-test results from relationship between groups after VPT vascular assessment, (HS-Highly significant, S-Significant, NS-Non Significant).

Thermal indexes after Cold Stress Test, CST

The outcome of the vascular assessment after thermal provocation, is shown in fig. 143, in the right hand only the signs group presented a mean positive thermal indexes for all 3 assessment methods, while only the symptoms group showed a mean negative thermal index value for all assessment methods. The confirmed group had a positive mean thermal index with the MTG and MTP methods and a negative value with MTA. The control group had a mean positive thermal index with MTA and a negative value with the other two assessment methods. In the left hand for all three methods the confirmed and signs group presented a mean negative thermal index and the control and signs groups a positive value.

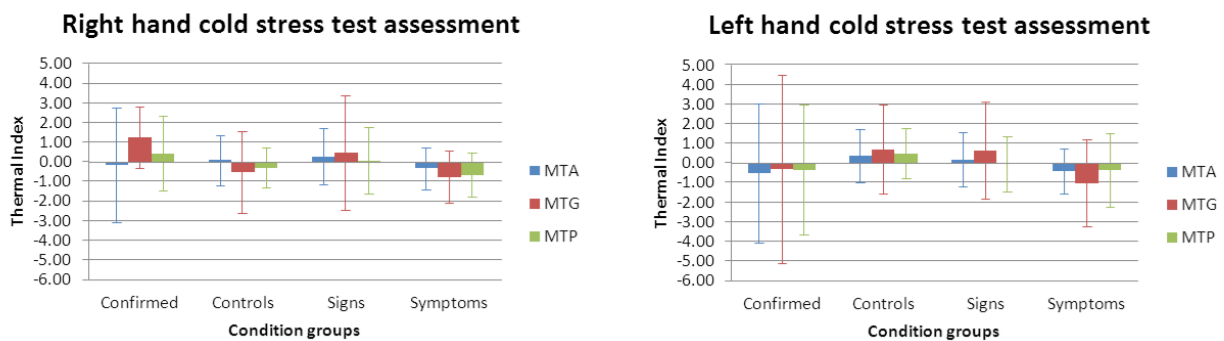


Fig. 143: Thermal indexes per method after CST.

Testing the hypothesis of discriminating differences between the groups with these results, two sets of means, a Z-test was conducted. From this (table 32) it can be concluded that it is possible to distinguish ($p < 0.05$) between symptoms and confirmed in the right hand AOI using the

MTG method. Between all other groups, for all three methods and in the left hand AOI there was no statistical evidence ($p>0.05$) of independence between the groups.

CST	Right hand Z-test (p value)			Left hand Z-test (p value)		
	MTA	MTG	MTP	MTA	MTG	MTP
Control vs. Signs	NS	NS	NS	NS	NS	NS
Control vs. Symptoms	NS	NS	NS	NS	NS	NS
Control vs. Confirmed	NS	NS	NS	NS	NS	NS
Signs vs. Symptoms	NS	NS	NS	NS	NS	NS
Signs vs. Confirmed	NS	NS	NS	NS	NS	NS
Symptoms vs. Confirmed	NS	HS	NS	NS	NS	NS

Table 32: Z-test results from relationship between groups after CST(HS-Highly significant, S-Significant, NS-Non Significant) .

In comparing the three methods to verify and identify a situation of hypothermia in a vascular test, the method that was more sensitive to hypothermia identification (negative thermal index $< -4^{\circ}\text{C}$) was the MTG, which as shown in table 33. that identifies 10 situations, the other two methods MTA and MTP had only identified one situation that coincided. This agrees with the literature studies (Ammer, 2007). However this indicator with the collected data has proven not to be reliable to classify people in degrees of injury.

Test	Method	MTA		MTG		MTP	
	Hand	RH	LH	RH	LH	RH	LH
KPT	Control	0	0	3	1	0	0
	Signs	0	1	1	1	0	0
	Symptoms	0	0	1	0	1	0
	Confirmed	0	0	0	0	0	0
VPT	Control	0	0	0	0	0	0
	Signs	0	0	0	1	0	0
	Symptoms	0	0	0	0	0	0
	Confirmed	0	0	0	0	0	0
MPT	Control	0	0	0	0	0	0
	Signs	0	0	0	1	0	0
	Symptoms	0	0	0	0	0	0
	Confirmed	0	0	0	0	0	0
CST	Control	0	0	0	0	0	0
	Signs	0	0	0	1	0	0
	Symptoms	0	0	0	0	0	0
	Confirmed	0	0	0	0	0	0
Total hypothermic cases:		0	1	5	5	1	0
Total hypothermic cases per Method:		1		10		1	

Table 33: Identified cases of hypothermia per method and provocation test.

4.3.6. Inter-camera assessment test

A cold stress test was recorded from the same subject within the same conditions and monitored with the three different cameras, only the differences from baseline were taken in consideration. The obtained variance between cameras FLIR A40 and FLIR SC7000 was $0.23\pm 0.56^{\circ}\text{C}$ and the value resultant from a t-test was $p=0.89$. The value of variance between cameras FLIR B2 and FLIR A40 was $0.33\pm 0.32^{\circ}\text{C}$ with a $p=0.506$ from a t-test. Based on these experimental results for hand AOI assessments no difference between the cameras was found, however, the higher quality cameras such as FLIR A40 and FLIR SC7000 are recommended.

4.4. Image processing developments

In this section the results of studies in medical thermal image processing will be presented, this studies are a simple image enhancement comparison, scene object outlines discovery comparison, interpolation methods comparison and an advanced warping operation. It is anticipated that an outcome of these results could provide information required to build a new software framework to process medical infrared thermal images to provide more information about specific Areas Of Interest.

4.4.1. Image enhancement

Fig. 144 demonstrates the resultant images from an original noisy image. From the naked eye it can be acknowledge that the filters that have produced high quality results were the Wiener, Lucy-Richardson and the low-pass filter.

The chart present in fig. 145, compares the differences in mean temperatures of the AOI in 20 images produced by each algorithm to the value of the originals. It can be observed that Noise Compose, Homomorphic and Lucy-Richarsson methods presented a higher temperature. On the other hand Median, High pass and Gaussian filters have shown a decreased temperature when compared with the baseline. The only algorithm presenting a similar temperature with the original

was the Low pass filter.

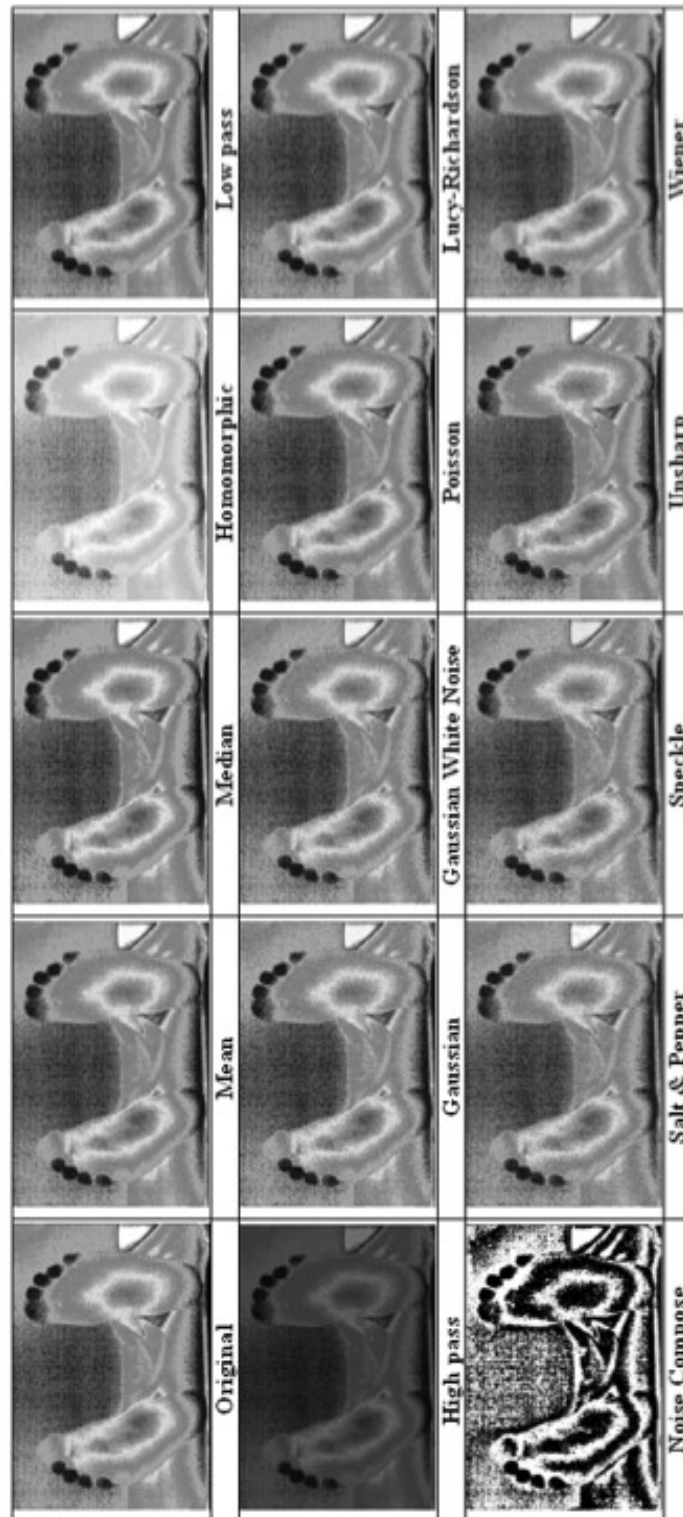


Fig. 144: Example of resulting images from application of the image enhancing filters.

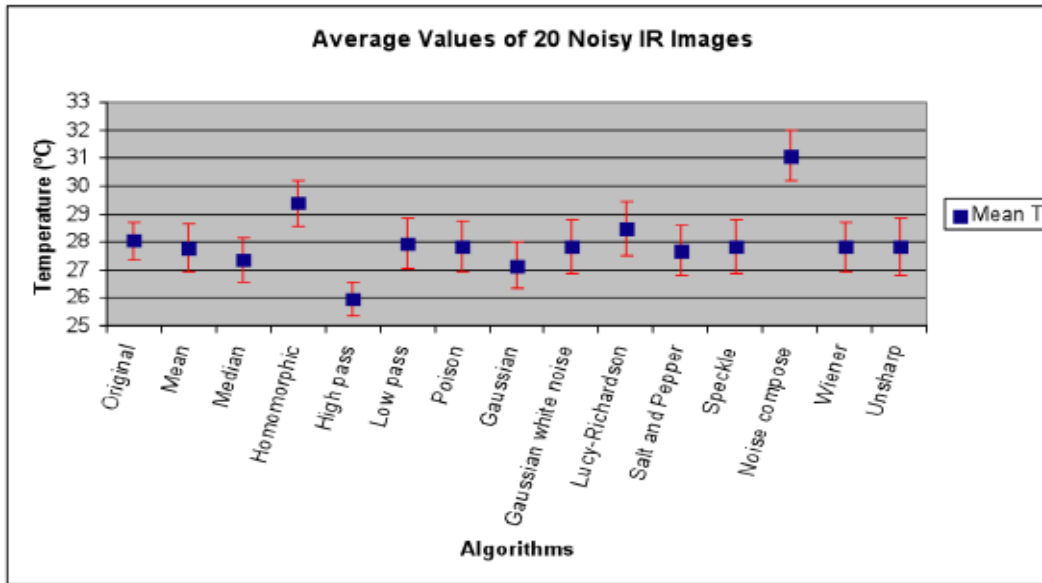


Fig. 145: The average values of mean temperature comparing the results obtained from each algorithm with the original image.

Fig. 146 shows a comparison between the maximum temperature, mean temperature, minimum temperature and standard deviation obtained from each image enhancing method against the original image. It is possible to observe that the algorithm that least affected the maximum temperatures is the Median, and of minimum temperatures is the Median and Wiener. The closest to correct mean temperatures is the Low pass and least sensitive to standard deviation is the High pass filter. The filter with the greatest affect on maximum temperature and of standard deviation is the Unsharp and of minimum temperatures and more variant from mean temperatures is the Noise Compose.

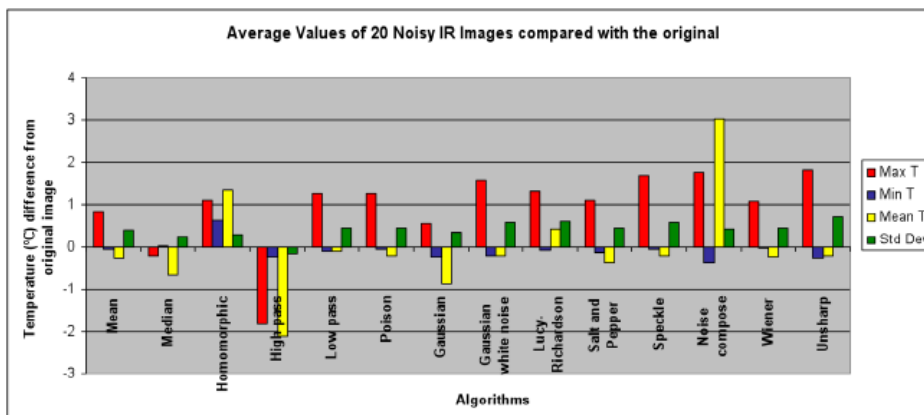


Fig. 146: Temperature differences in average values from the resulting images from filter applications to the original image in terms of maximum, minimum and mean temperatures and standard deviation.

Fig. 147 presents the comparison between the average obtained images from the application of each filter against the calculated average of the original images in terms of Signal to Noise Ratio indicator. The Noise Compose filter presented a higher value than the reference and Homomorphic, Low pass, Band pass and High pass filters presented a substantially inferior value.

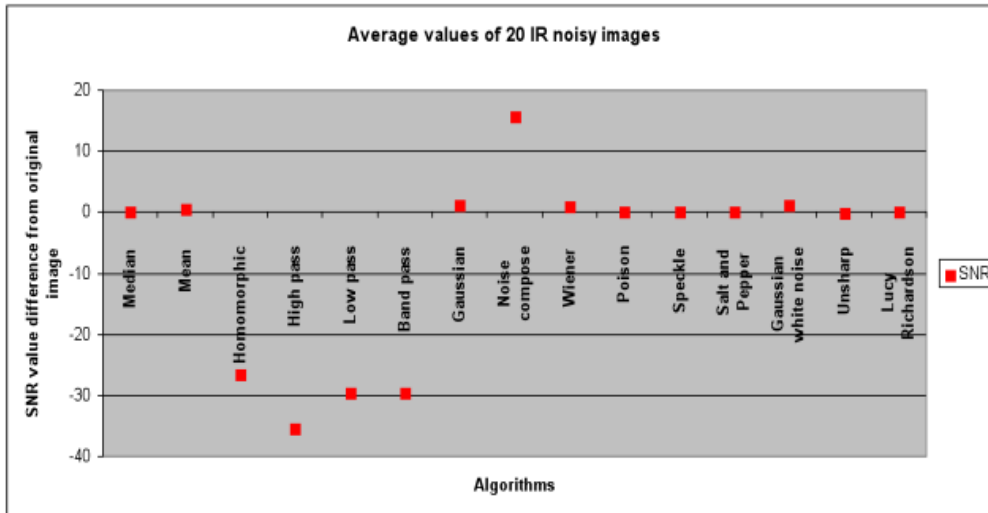


Fig. 147: Signal to Noise Ratio comparison between the noise filtered images and the original.

Fig. 148 shows the comparative relationship in Root Mean Square Error between the original images and images filtered, Salt and Pepper and Unsharp filters presented a value significantly above the reference, a substantially reduced value has been shown by Homomorphic, High pass, Low pass and Band pass filters.

The Cross Correlation Coefficient comparison between resultant images from the application of the image enhancing filters and the original images is presented in the fig. 149. It can be observed that Mean, Homomorphic and Wiener filters have the highest value of this indicator than the reference, on the other hand High pass, Low pass, Band pass, Gaussian and Gaussian white noise filters present a substantially reduced value.

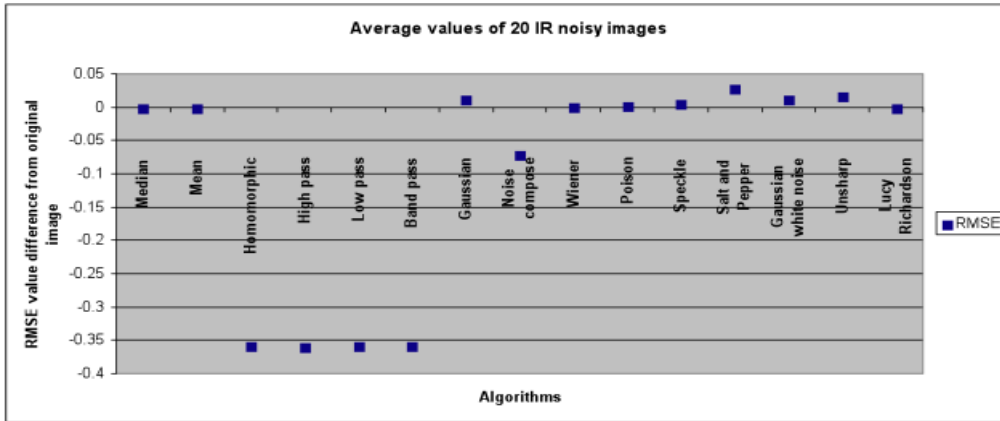


Fig. 148: Root Mean Square Error comparison between the noise filtered images and the original.

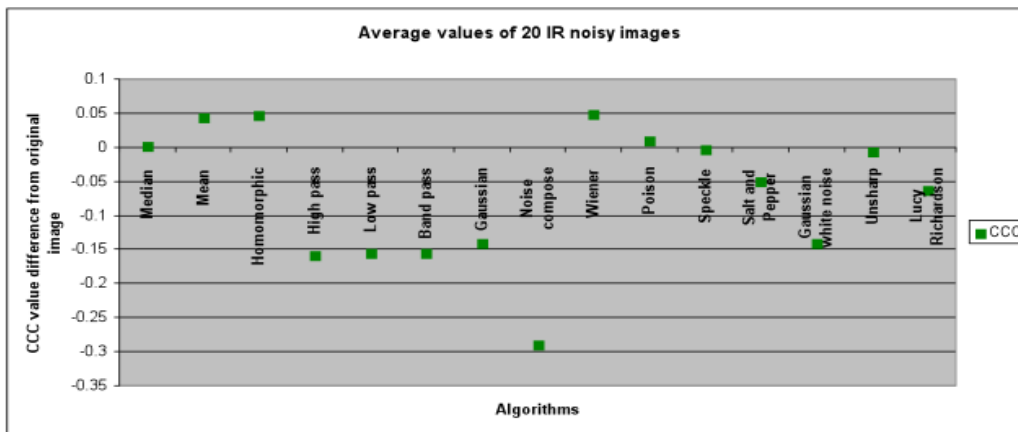


Fig. 149: Cross Correlation Coefficient comparison between the noise filtered images and the original.

Table 34 presents an overall classification of the image enhancing filters in thermal images, all methods are graded by order of performance per parameter. The parameters used were: sensitivity to minimal temperatures, to maximum temperatures, to mean temperatures, to standard deviation, Root Mean Square Error, Signal to Noise Ratio and Cross Correlation Coefficient. From these results the recommended noise removal filters according to this experiment were Median, Mean and Wiener. The methods to be avoided for thermal images are Noise Compose, Unsharp and High pass filters.

Algorithm	Classification according to the difference from original image								Expected value	
	min T	max T	mean T	Std Dev	RMSE	SNR	CCC	Overall	Mean T	SD
Median	1°	1°	10°	2°	2°	8°	1°	1°	-0,67	0,25
Mean	3°	3°	7°	5°	4°	5°	5°	2°	-0,25	0,4
Wiener	2°	4°	6°	8°	1°	4°	7°	2°	-0,23	0,45
Poisson	5°	7°	4°	8°	3°	10°	4°	4°	-0,21	0,45
Gaussian	10°	2°	11°	4°	8°	3°	11°	5°	-0,88	0,36
Speckle	4°	11°	5°	11°	6°	11°	2°	6°	-0,22	0,57
Gaussian White Noise	9°	10°	2°	11°	7°	2°	11°	7°	-0,2	0,57
Salt & Pepper	8°	5°	8°	7°	10°	7°	8°	8°	-0,36	0,44
Lucy-Richardson	6°	9°	9°	13°	4°	6°	9°	9°	0,42	0,6
Low-Pass Filter	7°	7°	1°	10°	13°	13°	13°	10°	-0,1	0,46
Homomorphic	14°	6°	12°	3°	12°	12°	6°	11°	1,33	0,29
Noise Compose	13°	12°	14°	6°	11°	1°	10°	12°	3,04	0,42
Unsharp	12°	13°	2°	14°	9°	9°	3°	13°	-0,2	0,7
High-Pass Filter	10°	14°	13°	1°	13°	14°	14°	14°	-2,1	0,17
Average:									-0,05	0,44

Table 34: Classification of the performance of the image enhancer filters, the recommended methods are in green and the non recommended in red.

4.4.2. Edge detection

The fig. 150 shows a typical input image selected from the database with poor edge to background contrast. The fig. 151 shows the corresponding optimal outline drawn by hand.

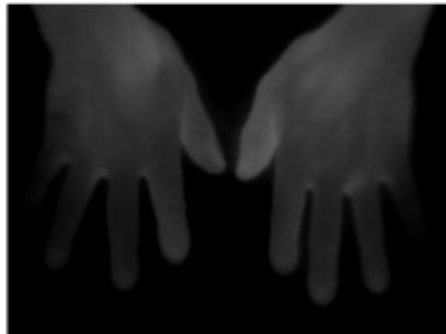


Fig. 150: Original captured image in grayscale.



Fig. 151: Optimal outline drawn by hand.

In the fig. 152 an example is presented of the images resulting from the application of the edge detection algorithms without applying any noise reduction filtering. Subjective grading, selected probabilistic methods and contour following methods as best performers.

Fig. 153 shows algorithm outputs with Homomorphic pre-processing applied. According to the subjective grading scale the best output was produced by second order based methods, followed by gradient based methods (excluding the Kirsch algorithm and probabilistic methods). It can be observed that Homomorphic filtering enhances the results for all algorithms.

Table 35 lists the result of the objective classifying method, (i.e. the number of pixels that form the outline). The best edge detection algorithms when not using noise filtering are the classical gradient based methods (Roberts, Sobel, Prewit, Kirsch). When using pre-process noise filtering the best results are produced by the gradient based, probabilistic based and second order based methods (excluding Marr-Hildreth).

Fig. 154 demonstrates the benefit of the Homomorphic filter by plotting the line length percentage difference between the optimum edge and the output of the respective filters.

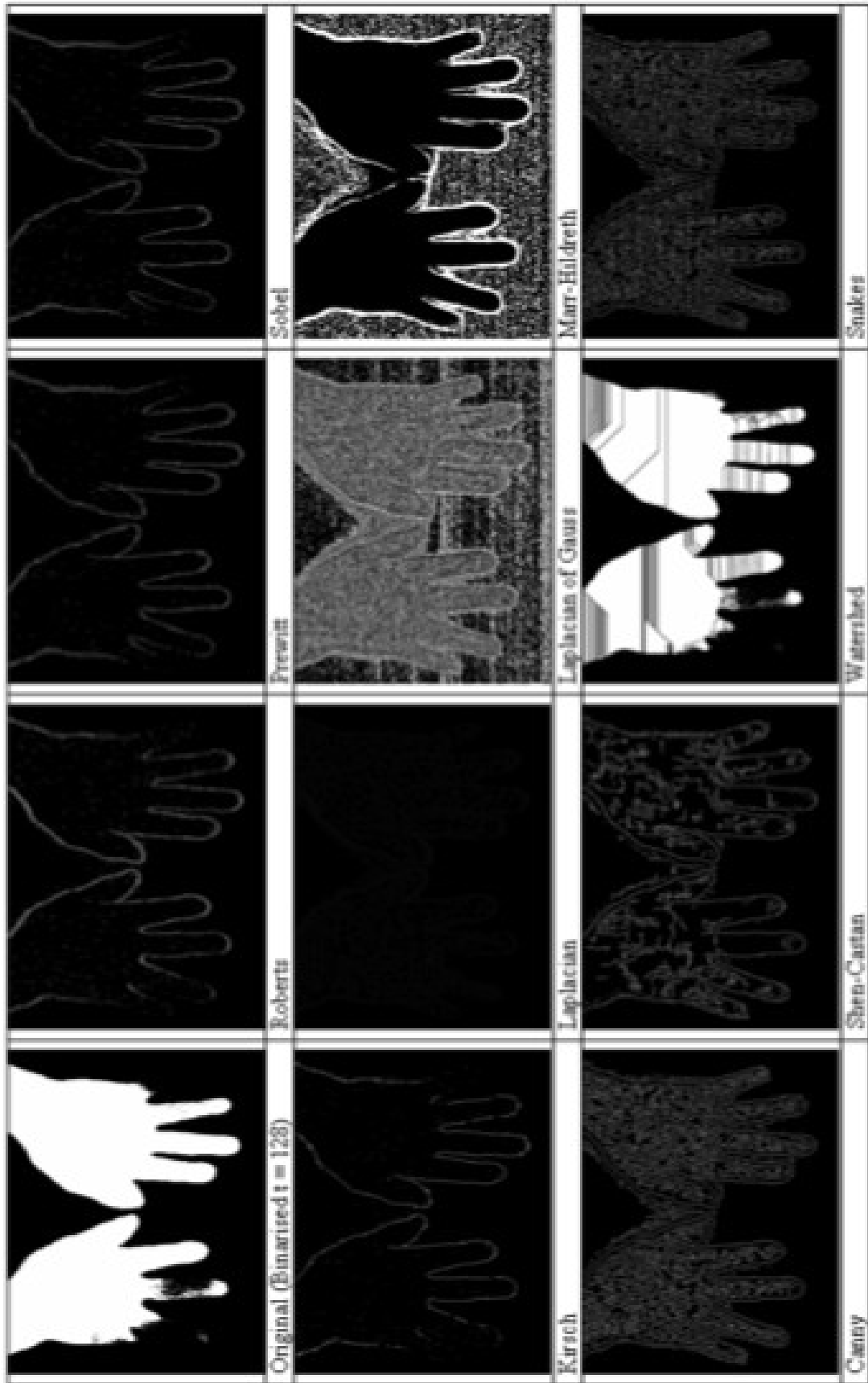


Fig. 152: Edge detection without noise pre-processing.

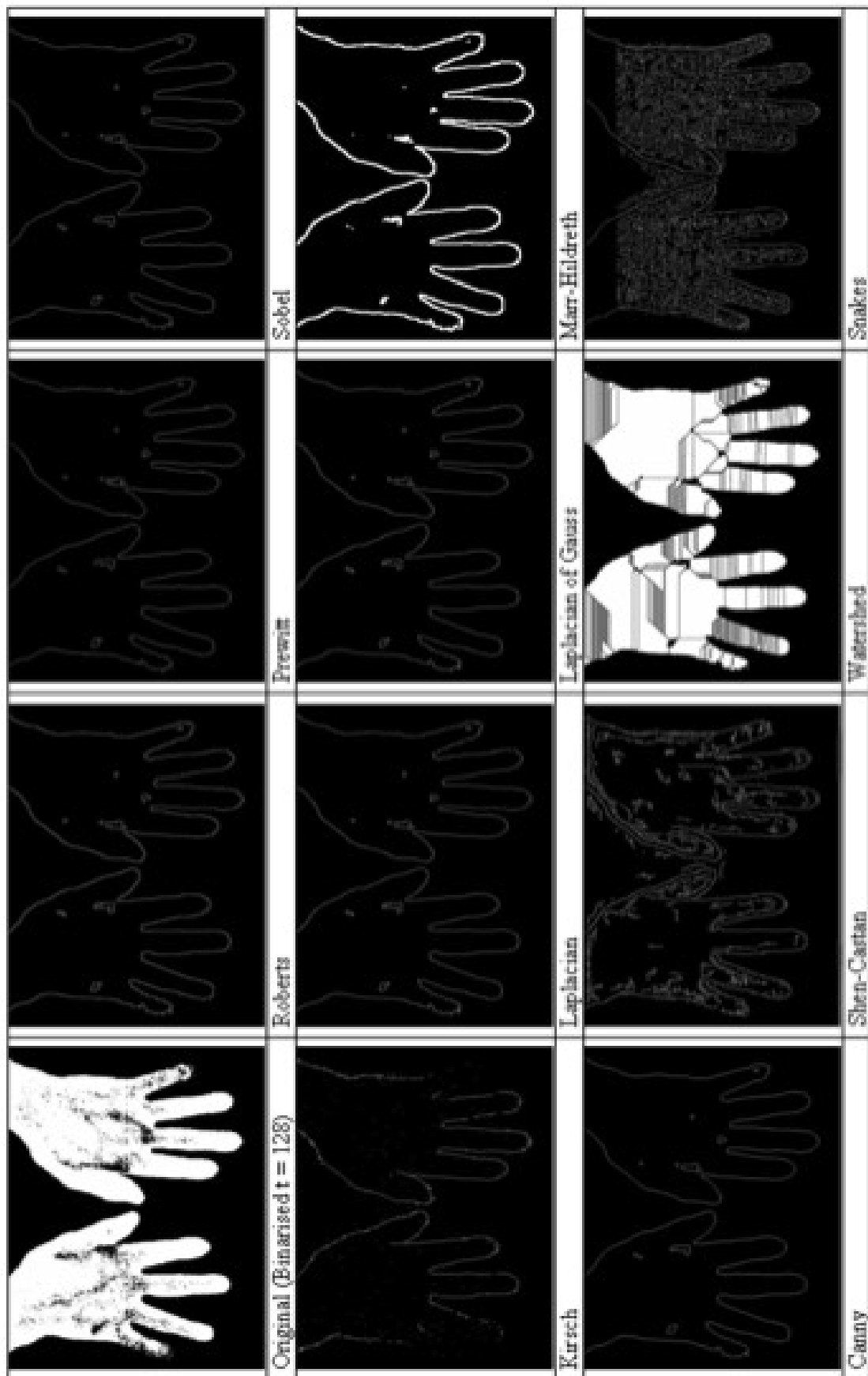


Fig. 153: Edge detection with noise pre-processing.

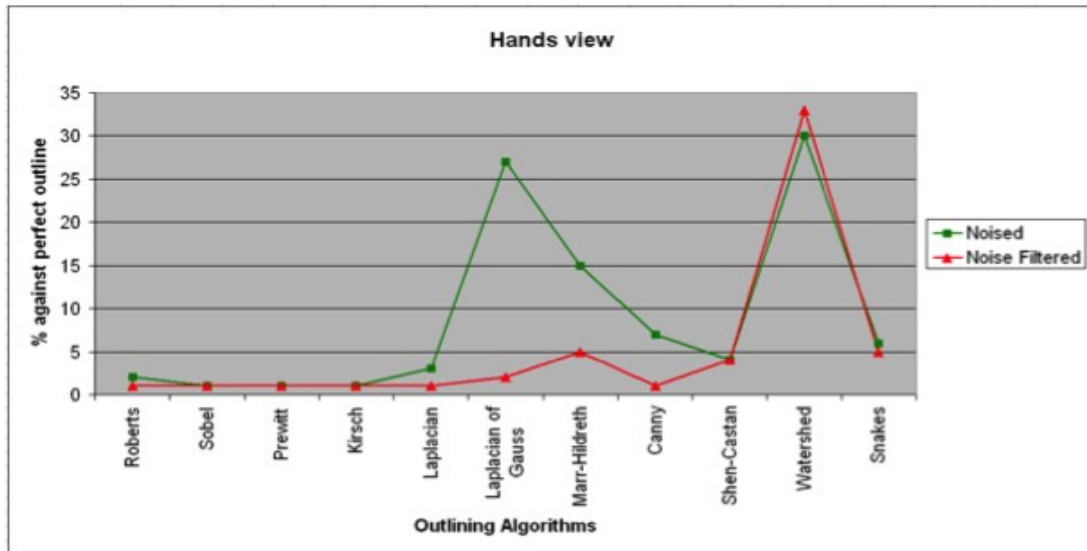


Fig. 154: Difference between optimum edge length and algorithmically produced edges with and without noise pre-processing.

Edge detector	With Noise	Without Noise	Closeness to optimal
Optimal	4562	4562	0
Original	151720	156750	152188
Roberts	7217	5442	880
Sobel	5989	4320	-242
Prewitt	5991	4224	-338
Kirsch	4007	4221	-341
Laplacian	15097	4630	68
Laplacian of Gauss	122374	10838	6276
Marr-Hildreth	70199	24415	19853
Canny	29888	2804	-1758
Shen-Castan	16853	16246	11684
Watershed	138456	150622	146058
Snakes	26428	22806	18244

Table 35: Comparison of the number of outline pixels, in the closeness to optimal only the images pre-processed with noise removal were considered.

4.4.3. Interpolation methods

The computational application developed for this experiment produced resultant CTHERM images per each interpolation method after using the same pre-processing techniques, the fig. 156 to fig. 158 are examples of results produced from the original fig. 155.

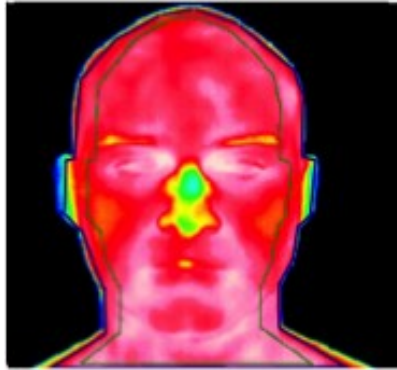


Fig. 155: Original image loaded from database.

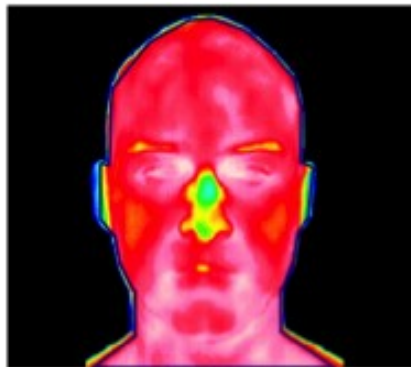


Fig. 156: resultant image from application of Nearest Neighborhood interpolation technique.

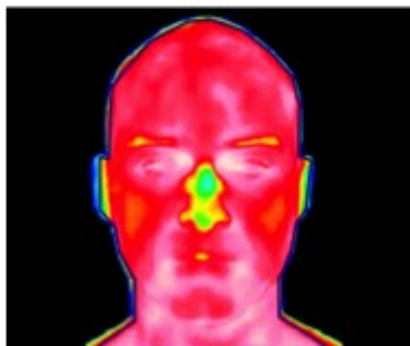


Fig. 157: resultant image from application of the Bilinear interpolation method.

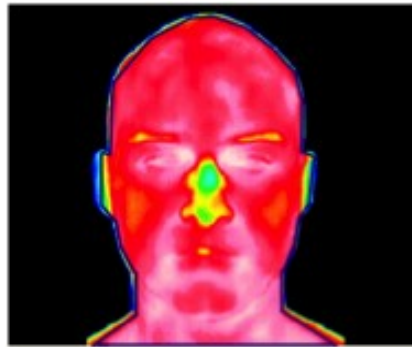


Fig. 158: resultant image from application of the bi-cubic interpolation technique.

The average of the mean temperature value obtained from measuring on the original images was $30.21^{\circ}\text{C} \pm 4.28^{\circ}\text{C}$, in the result of application the nearest neighborhood algorithm was $30^{\circ}\text{C} \pm 3.25^{\circ}\text{C}$, with the bilinear method was $29.95^{\circ}\text{C} \pm 3.28^{\circ}\text{C}$ and with the bi-cubic process was $29.72^{\circ}\text{C} \pm 3.60$. The difference in mean temperature from the application of the three interpolation methods against the original image can be seen on the fig. 159 and the difference in standard deviation on the fig. 160.

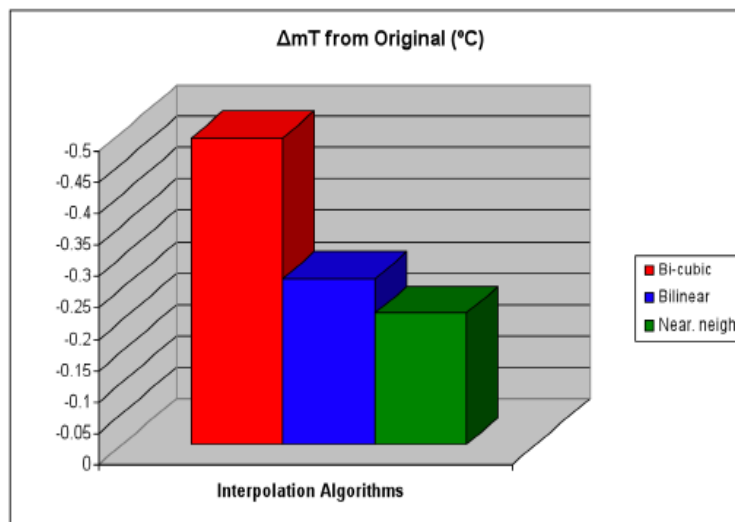


Fig. 159: Difference in mean temperature between the original and the result of interpolation methods, shows that the less affected algorithm is the Nearest Neighbourhood.

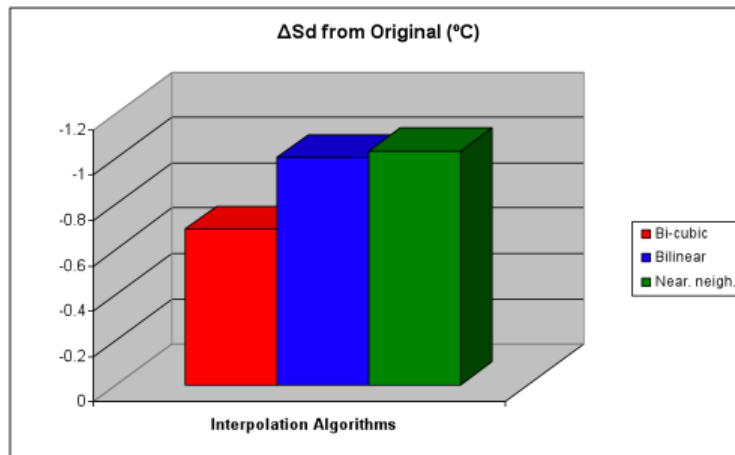


Fig. 160: Difference in standard deviation between the original and the result of interpolation methods, shows that the interpolation algorithm that less affects the standard deviation is the bi-cubic.

The results of the measurements of the four different types of images of the 20 samples were analysed with the SPSS statistical package software. Operating a student t-test with 95% interval confidence in the pairs of the 3 interpolation methods results we can conclude that the pairs Bi-cubic - Bilinear and Bi-cubic Nearest Neighborhood are not correlated, demonstrating a significant difference shown by $p < 0.05$, the same study has been inconclusive with the pair Bilinear – Nearest Neighborhood were $p > 0.05$.

The results of the three methods together were submitted to the Kendal correlation coefficient test that has shown a significant correlation with the data, assuming that the 3 methods results are directly related, interpretation is given by $p < 0.05$.

The Friedman correlation coefficient test has exhibited a statistical evidence of the results of the three applications being significantly different according to $p > 0.05$.

4.4.4. Barycentric warp model

From a total of 120 processed images, when measured back to C THERM a maximum variance of $0.18 \pm 0.09^\circ\text{C}$ was found in the difference of mean temperature and standard deviation compared with the corresponding original recorded and non-standardised image. An example of a

converted image is presented on fig. 161. The statistical significance of the correspondence on the vales obtained when performed a standard t-test for means comparison was $p=0.0000183$ ($p < 0.01$).

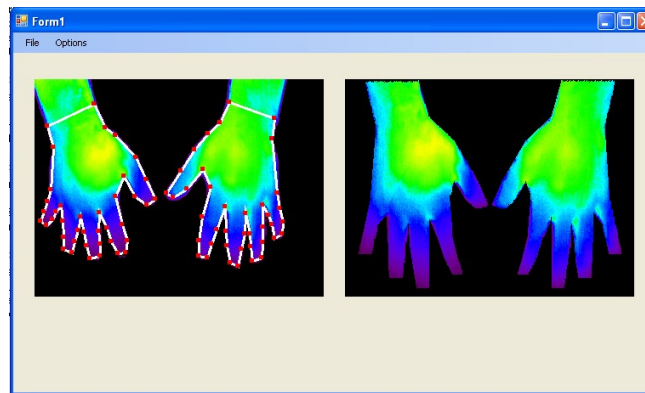


Fig. 161: Resultant image of barycentric triangulation warping.

Standardising the thermal images of hands, as presented in fig. 161, aids in the comparison of AOI and average AOI. Fig. 162 shows a set of thermal images of hand that differ in size, positioning and shape. Even these differences are small, analysing them accurately still a difficult, adjusting them to a standard model will facilitate that task and provide a better understanding.

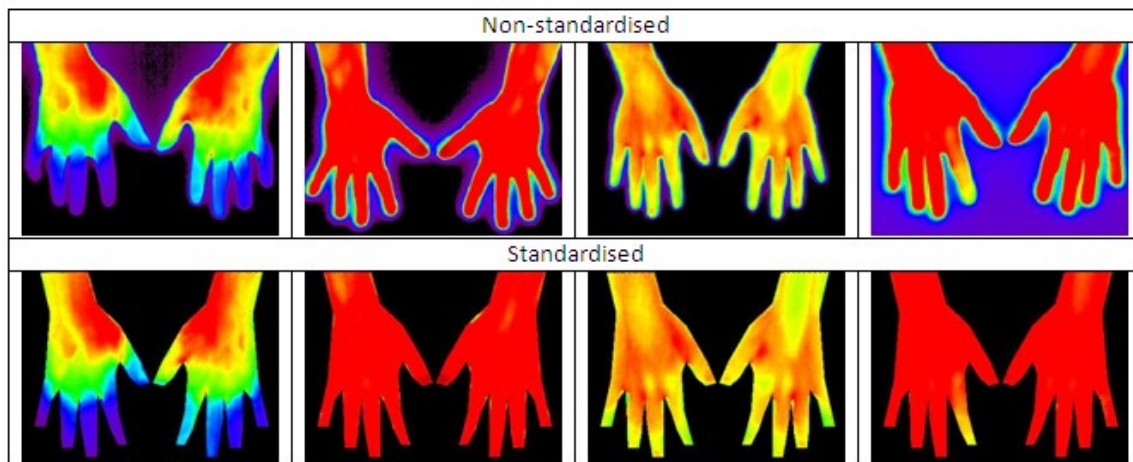


Fig. 162: Comparison between non-standardised and standardised thermal images of the hands.

The time needed for produce a resultant standardised image after adjusting the control points was 1.72 ± 0.5 seconds. In average from 80 control point adjustments the time required for that operation was 1.5 ± 0.3 minutes. The results were more effective (error of about 2%) when the

scaling transformation was less than 10%, higher than that, the error has an exponential growth tendency.

A statistical test of ICC was performed in the two groups of 120 images before and after standardisation. The values are shown in table 36.

AOI Hands	Reliability coefficient alpha	Interclass Correlation Coefficient	95% c.i. of ICC
Before standardisation	0.97	0.94	0.91 to 0.96
After standardisation	0.99	0.98	0.93 to 0.99

Table 36: The Interclass correlation statistics of the hand AOI before and after standardisation.

According to the obtained values from the statistical analysis, it can be concluded that the standardised hand AOI data is more reliable and enhances repeatability.

An experiment was conducted using the same original image, and asking 10 subject to use the developed application to standardise it in a accurate way, the resultant images were compared and the variance found between users was $0.04 \pm 0.03^\circ\text{C}$, the calculated standard error between measurements was 0.016.

4.5. Summary

The outcomes of this experimental work are:

- Females on age group between 31 and 40 years old, with daily smoking habits, in the BMI overweight class, in an administrative occupation, operating with a computer keyboard and mouse for more than 40 hours per week are more at risk of having a occupational condition affecting the upper limbs.
- A mean thermal symmetry value of $0.4 \pm 0.4^\circ\text{C}$ for the dorsal hand AOI is accepted as clinical reference, likewise $0.3 \pm 0.3^\circ\text{C}$ for arm AOI and $0.5 \pm 0.3^\circ\text{C}$ for forearm AOI.
- The pilot test using a keyboard revealed poor reproducibility, however it indicated that after constantly typing for 5 minutes a mean temperature increase value of $0.6 \pm 0.4^\circ\text{C}$ is expected for the dorsal hand AOI and $0.9 \pm 0.1^\circ\text{C}$ for the forearm AOI. After 15 minutes the expected values will be $0.9 \pm 0.8^\circ\text{C}$ for the hand AOI and $1.7 \pm 0.1^\circ\text{C}$ for the forearm AOI. This experiment also revealed the handedness, age and BMI had minimal indication of influencing those values.

- The pilot test involving vibration had shown to be reproducible, after holding a vibration device weighting 1.35kg with a frequency of 31.5Hz and a magnitude of 36 mm/s² for 2 minutes a decrease in mean temperature of 0.2±0.2°C and 0.3±0.1°C was expected for hand and forearm AOI respectively. Aging may influence these values.
- The value of mean thermal symmetry has indicated to be valid to discriminate different degrees of injury when using the proposed objective provocation tests. CST by itself would only identify the confirmed cases from healthy, it is needed some mechanical provocation to an early indication of injury.
- The proposed objective provocation tests had proven to be consistent and reproducible.
- The MTG method for assessing the hand vascular challenge has proven to be more sensitive in identifying hypothermic states, however the thermal indexes are not recommended for identifying HAS degrees of injury.
- High quality and resolution cameras should always be preferred than the low resolution handheld infrared cameras for conducting hand temperature studies.
- The recommended medical thermal image enhancing techniques are median, mean and wiener filters when trying to improve images quality.
- The recommended edge detection techniques for medical thermal images are probabilistic based (Shen-castan and canny) or gradient based (Roberts, Prewitt, Sobel, Kirsh) operators.
- The interpolation method recommended for medical thermal images is the Nearest Neighbor.
- The proposed barycentric warp model has proved to be simple, fast, accurate and reproducible.

5 – Discussion

In this chapter the results of this work are discussed and considered under the following headings; Image capture protocol, survey and laboratory experiments:

1. Image capture protocol (5.1)
2. Incidence of occupational conditions in a sample population (5.2)
3. Medical reference data (5.3)
4. Image processing developments (5.4)
5. Objective provocation tests (5.5)

5.1 - Capture protocol

Infrared thermal imaging had lost interest as medical screening technique in the end of 70's due to the limitation imposed by the technology. Equipment presented lowest sensitivity and specificity in image capture when compared to other techniques such as radiology and ultrasound. Image processing at time has not yet been sufficiently developed to be used in analysis of thermal images. Another factor that most contributed to the discredibilisation of thermography was the absence of standard recording procedures (Kennedy et al., 2009, Cleek, 1988).

Over time the equipment and technology associated with thermography presented a considerable evolution, allowing high resolution images with acceptable values of reproducibility, sensitivity and specificity when compared with other medical imaging modalities. Recent advances in thermal image processing and in parallel an increase in the number of standard recording procedures enforced image analysis and restored the lost credibility of the technique for medical use (Kennedy et al., 2009).

A number of reasons for this have been identified at The University of Glamorgan, some being due to camera performance, but more commonly due to a lack of standardised technique in both image capture and image analysis. The proposed protocol for capturing thermal images of the hands in this work is based on the Glamorgan protocol (Ammer, 2008), which has proven that the defined AOI provides high reproducibility of recorded images and temperature readings. These

procedures when appropriately applied avoid an important source of error and unreliability. The factors related to patient pre-examination preparation, examination room and temperature control when strictly applied contribute to high reliability of thermal images.

The battery of tests purposed by the members of the Medical Imaging Research Unit at University of Glamorgan (Plassmann, 2006) provide methods for easy and inexpensive quality control assessment of infrared imaging equipment, preventing the problems caused by its malfunction.

5.2 - Incidence of occupational conditions in a sample population

The results obtained from the online questionnaire were from females aged from 31 to 40 years, in BMI class overweight, daily smokers, in administrative work and operating a computer keyboard and mouse for more than 40 hours a week. These have been identified to be more at risk of having occupational symptoms that affect the upper limbs. From 1% of the Academic population of the University of Glamorgan, 13% of the respondents indicated that had severe symptoms of affecting the upper limbs. However this sample is not representative and can therefore not be used to make statements such as “13% of employees at the University of Glamorgan suffer from severe symptoms of HAS”. However these results do clearly demonstrate that measures for the prevention of hand occupational conditions are indicated within a University environment, and in the long term could avoid increasing symptoms which might entail the need for treatment or sickness absence.

These results were similar to the results obtained in a Canadian study using a different questionnaire (Cole et. al, 2005). In their study there were 10% of their sample that indicated occupationally related conditions affecting the upper extremities. In women aged between 30 and 50 years old and associated with a high demand for repetitive tasks, and working for more than 30 hours a week, were the most affected.

In this study the major difference is in the relationship between daily smokers and those showing symptoms, that this new experiment work is more related. The questionnaire used had been assessed and validated. It has proved to be reproducible, internally consistent and responsive to clinical change (Levine et al., 1993). Today, most offices use computer technology, and regular daily use is commonplace. It is generally assumed that office workers have transferred their skills from the typewriter to the computer without problems, although the nature of the hand movements

involved has changed considerably. In the absence of any proven health test, operators of keyboard systems are assumed to be unaffected by their manual tasks unless they complain to an occupational health service. Such facilities tend to exist only in manufacturing industries, where there are a large number of manual workers.

5.3 - Medical reference data

The thermogram collection followed the standard capture protocol for medical infrared imaging specified by Ammer (2008). From all views and positions the maximum variation of mean temperature between a left and corresponding right body areas of interest was 0.47°C (hands, dorsal view). The greatest difference in standard variations between the contralateral areas was found to be 0.37°C (hands, dorsal view). These results were obtained using a IR camera with a higher resolution (320x240), than those used in previous similar studies (Uematsu and Goodman have used a resolution of 140x140).

The 1985 study by Uematsu (1986) resulted in a maximum mean temperature symmetrical variance of 0.38°C (hand, dorsal view) and also a greater standard deviation variation value 0.20°C (forearm, anterior view). Another study by Goodman et al. (1986) concluded that the greatest mean temperature variation was 0.95°C (forearm, dorsal view) with Standard Deviation difference 0.10°C (hand and forearm, dorsal view). A second study by Uematsu in 1988 reported a mean temperature difference maximum of 0.39°C (arm, dorsal view) with a greater Standard Deviation value of 0.26 °C (arm, dorsal view).

In 2001 Niu and his team in Taiwan using a camera with similar resolution (320x240) in a controlled environment and subjects preparation, found a maximum mean temperature difference between collateral upper limb sites of 0.5°C (arm, dorsal and anterior view) with a maximum Standard Deviation of 0.4°C (arm, dorsal and anterior view).

This study does not contradict these published studies that were conducted 20 years ago, but the use of a significant different methodology (period of acclimatisation, environment temperature and humidity, imaging system, subject preparation) can explain the differences. The results of this research agree with the published results of 9 years ago in Taiwan (Niu, 2001), where a similar approach to the first methodology was followed but using a different human race as samples. The second approach has improved since the first approach used for assessing thermal symmetry,

standardisation has been used on both image capture and analysis.

It is considered that improved understanding of the results of this study has two main factors:

- a) the application of a rigorous protocol for volunteer selection, preparation and imaging;
- b) the increased performance in terms of stability and resolution of these modern infrared cameras compared to those used in previous studies.

With improved image resolution and the now currently available wide angle lenses, it is possible to image a much larger area, even a whole human body surface in one image. This phenomenon has been examined as part of this study, because in the event that a more automated test might be developed for medical thermography, wide angle lens use might prove to be an advantage. However, imaging regional body views with a standard lens has been shown to achieve slightly higher thermal symmetry than those obtained from full body views, although in a high resolution camera this difference is small. For specific studies on the hands total body views are unnecessary and should be avoided because of small pixel size of the AOI.

Thermal symmetry in healthy subjects between corresponding left and right sides of body extremities in this work has a maximum value of $0.5 \pm 0.3^\circ\text{C}$, which can be used by the majority of clinical practitioners. Having confirmed and improved previous measurements, this benchmark of normal symmetry variance could be of significant value in the assessment of neurological and musculoskeletal disorders that manifest themselves by unilaterally affecting thermal patterns on the human skin.

5.4 - Image processing developments

The imaging processing developments in this research were:

- A comparative experiment in image enhancing techniques in medical thermal images.
- A comparative experiment in edge detection techniques in medical thermal images.
- A comparative experiment in interpolation techniques in medical thermal images.
- A development of a hand geometrical model and a warping algorithm to standardise hand

medical thermal images.

5.4.1 - Image enhancement

The results of this experiment do not agree with suggested methods for digital images (Gonzalez and Woods, 2002) in terms of recommended method. Those methods were focused on the qualitative aspect of the data, the quantitative characteristics of the data was not taken into consideration. On IR images the quantitative feature is more important than the qualitative. The recommended noise filtering methods to be implemented for IR images are Median, Mean and Wiener. Filtering should be avoided on principle, but in some situations it offers unique opportunities to retrieve information.

The results of this experiment provide a benchmark for disagreements between measurements produced by different software packages that implement various improvement techniques.

5.4.2 - Edge detection

The subjective performance evaluation method used human judgement. The number of characteristics that a human eye can reliably distinguish is, however, limited (Roushdy, 2006). For this study a combination of subjective and objective validation was therefore used. The number of pixels forming the outline was used as an objective comparison method as it is simple to compute and provides a single figure for grading results. It could be argued that the difference between the areas enclosed by the outlines would be a more suitable measure since it is these areas that are used for subsequent clinical analysis.

The results of this experiment support previous studies that used other types of digital images (Sharifi, 2002, Roushdy, 2006). It demonstrates that traditional techniques which are usually computationally inexpensive and thus fast and simple to implement can produce adequate if not superior results (Zhou, 2004, Suzuki, 2000, Ghosh, 2006) to more complex recent approaches such as those based on artificial intelligence, edge maps or neural networks.

From this study it can be concluded:

- Probability based and gradient based edge detection techniques are the most suitable methods to outline hands in medical thermal images.
- The Homomorphic filter enhances boundary detection by reducing noise and ‘clearing up’ previously undetectable constructive features that assist edge detection algorithms.
- Some post-processing such as thinning, artifact removal, etc. is needed to improve the results.

It was demonstrated in this experiment that post-processing work should be performed after the image objects boundaries were discovered. It was for this reason that a semi-automated solution was preferred instead of a fully automated solution, that would be difficult to accomplish in the time for this research project.

The outcomes of this experiment had been used in the section 3.6.4 that introduces template outlines in addition to the edge detection process in regions where contrast between background and extremity is low or non-existent and edge detection therefore fails completely. This approach is using anatomical control points (i.e. well defined points such as finger tips) to assist the alignment between the template outline and the outline produced by edge detection. This work will assist hand pathology studies, clinical ‘cold stress’ examinations and the production of an atlas of normal infrared medical images as a reference source for clinicians (Ring et al., 2004).

5.4.3 - Interpolation methods

The choice of median filter composed with the Gaussian blur for noise removing instead of the, section 3.6.1, was just due to simplicity on implantation. This study contradicts some other studies on digital images comparing the application of interpolation algorithms to scale regions of images (Poth, 2004, Park and Sung, 2004), recommending these studies the Bi-cubic algorithm. Medical thermal images are based on temperature measurement on a surface of a body, if a scaling is needed an interpolation method will be needed, a neighbour value assigned instead of average of other pixels will help on maintenance of consistence in temperature values of the AOI when the change of resolution is inferior to 15%.

The medical thermogram proposed protocol (Ammer, 2008) used by major part of European

thermal physiological labs refers for the usage of AOI masks being the distance between the subject and the camera aligned by the guideline, that minimizes the need of resolution change, scaling is more needed in these cases for small positional adjustments caused by involuntary movements of the subjects in the moment of capture. According to the results shown by this experimental study the recommended interpolation method for scaling medical thermal images following the standard capture protocol (Ammer, 2008) is the Nearest Neighborhood.

5.4.4 - Barycentric warp model

The current approach using a hands barycentric warp model when compared with the usage of other warp methods (Gomes et al., 1999) produces equivalent results presenting minimal processing time and complexity. Automatic discovery of the anatomical control points that delimit the model is suggested as further investigation. This method has shown accordingly to its results applicability when the difference in size scaling between the source and target AOI's is inferior to 10%.

As result of this study it can be concluded:

- thermal images standardised with this barycentric based warp method have 98% accuracy.
- accurate analysis of hands regions of interest is possible.
- comparison and/or averaging of images is possible after standardization of images.

5.5 - Objective provocation tests

The objective tests consisted of computer keyboard mechanical provocation, vibration exposure, computer mouse provocation and vascular changes in the hand.

In the keyboard provocation test the main issues are the following:

- After keyboard exposure for 5 minutes all the 4 groups, defined in the context of this research, excluding the confirmed group in the left hand, presented an increase in mean temperature of both hands, this is in line with the literature (Sharma, 1997, Ammer, 2001) that stated that an increase of temperature was expected after keyboard provocation, that

increase being small in people with symptoms of occupational injury.

- Applying a vascular challenge immediately after the mechanical provocation induced by a computer keyboard produced results in hand mean temperature changes with proven statistical evidence (Pearson chi-square and Z-test, $p < 0.05$) of discriminating groups but at the moment not individuals.
- The differences in mean thermal symmetry from baseline proved to be a useful discriminative indicator between the two subjects with confirmed symptoms and the other three groups (Z test $p < 0.05$).
- There was no specific involvement of any finger in any particular group as a result of the application of this test.
- The most significant change in the two subjects with confirmed symptoms was in the change in thermal symmetry from the baseline.

In the vibration provocation test it is interesting that:

- After vertical vibration exposure for 2 minutes at 31.5Hz all the four groups presented a decrease in mean temperature of the hand in conformity with the literature (Acciari, 1978).
- The application of a vascular provocation test after the vibration exposure produced statistical evidence in mean temperature variation of the hand to discriminate controls from subjects with confirmed symptoms. This procedure significantly differs from most of the published studies in cold provocation testing for HAVS where only a thermal challenge is used (Coughlin et al., 2001). This points out the combination of vibration and thermal provocation as objective procedure does provide discrimination between asymptomatic and symptomatic subjects.
- The Stockholm scale as described in section 2.3.2.6 has not been employed in the classification of subjects in this study since all volunteers were not involved with the use of vibration tools except one.
- The variation from baseline of thermal symmetry mean value for the four groups during the VPT constituted a statistical evidence in the discrimination between healthy controls and confirmed affected symptoms.
- There was involvement of the index finger in the subject with confirmed symptoms of HAVS.

In the mouse provocation test the main issues are:

- This study is the first to investigate the possible effects from usage of computer mouse as mechanical provocation for quantifying temperature changes.
- Apart from the individuals of the group classified as 'signs', a mean temperature decrease was presented after the mouse exposure in both hands, however this difference between groups is not statistically significant.
- Even the non-parametric statistical test indicating the possibility of identifying different HAS stage groups, the other statistical method (Z test) has proved to be inconclusive for discrimination when evaluating the hand mean temperature variations at the end of the test.

The cold stress test :

- According to the defined protocol the cold provocation test proved to discriminate the control group from the subjects with confirmed symptoms based in the variation of the hand mean temperature.
- The use of the mean thermal symmetry difference from baseline give statistical evidence ($p < 0.05$ in parametric and non-parametric tests) in the distinction between controls and affected subjects.
- From the three evaluated methods to assess hand cold provocation, the most sensible to identify Raynaud's phenomenon was the Mean Thermal Gradient in agreement with literature (Ammer, 2007), however the thermal index produced by this method and the other two have not produced statistical evidence in the discrimination of the different groups used in this study.

The Areas of interest used in the final provocative tests involving keyboard and vibration stress had statistical evidence of being more reproducible than the AOIs used in the pilot provocation tests.

All the above studies are limited by the sample size available, which limits the weight of conclusions drawn from this study.

6 – Conclusion

In this section, the aim and objectives are assessed and further research is proposed.

6.1. Meeting the aim

The development and assessment of an objective, quantitative and reproducible diagnostic procedure for Work Related Upper Limb Disorders based in the analysis of medical thermal images of the hands was satisfied.

A standard infrared image capture protocol was designed, implemented and assessed and proposed for future work.

A online hand injury incidence questionnaire was designed, implemented and assessed and its results were used as indications to identify the possible volunteers to collaborate in this work.

Hand temperature reference data was designed, implemented, being assessed the results and data suitability. A clinical reference value was proposed for healthy states discrimination.

A set of mechanical stress provocation tests was designed, implemented and the results were objectively assessed. This objective was partially satisfied, results indicate that using these tests monitored by thermal imaging is possible to discriminate groups, however, for individuals discrimination a large sample was required.

Different techniques in image processing such as: image enhancing, edge detection and interpolation were compared and its results assessed, providing important and relevant information for future studies using medical thermal images.

A standard reference method for thermal analysis of the hand was designed, implemented and assessed. It demonstrated to be extremely useful and practical in standardising the thermal analysis of the whole hands and its anatomical regions providing image comparison and averaging.

6.2. Proposed future work

For further work the following research is proposed:

- The application of the developed methodology in a wide study involving a larger affected population. For ethical and bureaucratic reasons it was not possible to establish partnerships with hospitals, companies or trade unions within this research project.
- An investigation using the developed methodology, more particularly the thermal symmetry values and the proposed Campbell's hand injury score system and Griffin's HAVS scoring system to develop an objective and quantitative scale of injury.
- The development of a fully automated solution for the standardisation of anatomical thermal AOIs, with automated discovery of control points.
- Use of the proposed barycentric warp method to overlay different modalities of medical imaging to improve applications in clinical and forensic sciences.
- The enhancement of medical thermography reproducibility integrating state of art equipment and technology with the development of image processing software, standardising image analysis, simultaneously with the development and adoption of standard image recording protocols. In order to continuously increase of the modality credibility for medical use.

References

- ABRAMSON, D.J. (1967) *Circulation in the Extremities*. New York, Academic Press. Vascular responses to temperature, 114-138.
- ACCIARI, L. (1977) Thermography in angiopathy of the hand from vibrating tools. *Acta Thermographica*, 2(3), 182-192.
- ACCIARI, L., CUGOLA, L., MASO, R., NOGARIN, L. (1978) The thermographic hand. *Acta Thermographica*, 3(1), 65-74.
- ALLEN, J. (2007) Photoplethysmography and its application in clinical physiological measurement, *Physiological Measurement*, 28, R1-R39.
- AMMER, K. (1996) Diagnosis of Raynaud's phenomenon by thermography. *Skin Research and Technology*, 2, 182-185.
- AMMER, K., MELNIZKY, P. & KERN, E. (2001) Cold fingers after keyboard operation. Relationship with duration of typing. 12th International Conference of Thermal Engineering and Thermogrammetry (THERMO). Budapest (Hungary).
- AMMER, K. (2003) Need for Standardisation of Measurements in Thermal Imaging. In *Thermography and Lasers in Medicine*, B. Wiecek, Ed., Akademickie Centrum, Lodz, 13-17.
- AMMER, K. (2007) Evaluation of temperature changes in hands after cold stress test, *Clinical temperature measurement & thermography meeting*, IPREM, Cardiff International Arena, 2 May 2007.
- AMMER, K. (2008) Standard Procedures for Recording and Evaluation of Thermal Images of the Human Body: The Glamorgan Protocol, *Thermology International*. 18(4), 125-144.
- ARCHERS SOLICITORS (2004) Archers solicitors website last visited in May 2009, URL: <http://www.archerssolicitors.co.uk/content.asp?id=4&doc=21>
- ARSENAULT, H. & LEVESQUE, M. (1984) Combined homomorphic and local-statistics processing for restoration of images degraded by signal-dependent noise, *Appl. Opt.*, 23, 845-850.
- AUGUSTO, V. G., SAMPAIO, R.F., TIRADO, M. G. A., MANCINI, M. C., PARREIRA, V.F.

- (2008) A look into Repetitive Strain Injury/ Work-Related Musculoskeletal Disorders within physical therapists' clinical context. *Rev. bras. fisioter.*, 12(1), 49-56.
- BBC (1998) BBC news website. last visited on July 2008, URL:
http://news.bbc.co.uk/2/hi/uk_news/98778.stm
- BBC (2000) BBC news website. last visited on July 2008, URL:
http://news.bbc.co.uk/2/hi/uk_news/879922.stm
- BEIER, T. & NEELY, S. (1992) Feature-based image metamorphosis., *Computer Graphics (SIGGRAPH '92)*, 26, 35-42.
- BESL, P. J. (1995) Triangles as a Primary Representation. In *Proceedings of the international NSF-ARPA Workshop on Object Representation in Computer Vision (December 05 - 07, 1994)*. M. Hebert, J. Ponce, T. E. Boult, and A. Gross, Eds. *Lecture Notes In Computer Science*, vol. 994. Springer-Verlag, London, 191-206.
- BIRD, C., NICHOLSON, A. (1994) Lightening Loads. *Health and Safety at Work*, November, 10-14.
- BOVENZI, M., LINDSELL, C. J., GRIFFIN, M. J. (2000) Acute vascular response to the frequency of vibration transmitted to the hand. *Occup. Environ. Med.*, 57, 422-430.
- BRUNELLI, R. (2009) *Template Matching Techniques in Computer Vision: Theory and Practice*, Wiley.
- BUCKLE, P. & DEVEREUX, J. (1999) *Work Related Neck and Upper Limb Musculoskeletal Disorders*, Brussels (Belgium), European Agency for Safety and Health at Work.
- BUICK, T. A., HOWELL, K. J., GUSH, R., DENTON, C.P., SMITH, R.E. (2009) A comparison of infrared thermography (IRT) and full-field laser perfusion imaging (FLPI) for assessment of hand cold challenge and dermal inflammation, *Thermology International*, 19 (2), 43-46.
- BYLUND, S. H. (2004) *Hand-Arm Vibration and Working Woman*. Public Health and Clinical Medicine. Umea, Umea University.
- CAMPBELL, D. A. & KAY, S. P. (1996) The Hand Injury Severity Scoring System, *Journal of Hand Surgery*, 21(3), 295-298.
- CASEY, K. L., ZUMBERG, M., HESLEP, H., MORROW, T. J. (1993). Afferent Modulation of Warmth Sensation and Heat Pain in the Human Hand. *Somatosensory and Motor Research*, 10(3), 327-337. doi:10.3109/08990229309028841

- CHAKRAVARTI, LAHA, ROY, (1967). Handbook of Methods of Applied Statistics, Volume I, John Wiley and Sons, 392-394.
- CHERNOFF, H., LEHMANN, E.L. (1954) The use of maximum likelihood estimates in χ^2 tests for goodness-of-fit. The Annals of Mathematical Statistics, 25, 579-586.
- CHUCKER, F., FOWLEY, R. & MOTUMUJA, T. (1971) Induced temperature transients in Raynaud's disease measured by thermography. Angiology, 22, 580-593.
- CLAIM, Y. (2007) You Claim: Vibration White Finger. Chirchester.
- CLARK, S., DUNN, G., MOORE, T., JAYSON IV, M., KING, T. A., HERRICK, A. L. (2003) Comparison of thermography and laser Doppler imaging in the assessment of Raynaud's phenomenon, Microvascular Research, 66, 73-76.
- CLEEK, G.C. (1988) The Admissibility of Thermography: Objective Evidence or a Mystical Procedure, 65 Denv. U. L. Rev. 295-302.
- COLE, D.C., IBRAHIM, S., SHANNON, H.S. (2005) Predictors of work-related repetitive strain injuries in a population cohort. Am. J. Public. Health, 95, 1233-1237.
- CORTINA, J. M. (1993). What is coefficient alpha? An examination of theory and applications. Journal of Applied Psychology, 78, 98- 104
- COUGHLIN, P. A., CHETTER, I. C., KENT, P. J. & KESTER, R. C. (2001) The analysis of sensitivity, specificity, positive predictive value and negative predictive value of cold provocation thermography in the objective diagnosis of the hand–arm vibration syndrome. Occupational Medicine, 51, 75-80.
- DAVID, G. C. (1999), Preventing Work-Related Musculoskeletal Disorders. The Safety & Health Practitioner Supplement, July, 4-6.
- DELPOR, M. (2007) Morphing in two dimensions: Image morphing. MSc thesis, 2007, University of Stellenbosch, South Africa.
- DEN HELD, M. & COCKBURN, D. (2000) Repetitive Strain Injury. Brussels, European Agency for Safety and Health at Work.
- DONG-KEUN, L. & YO-SUNG, H. (2004) Fast Image Warping Using Adaptive Partial Matching, Optical Engineering , 43(3), 604-614.
- EASHW (1999) Economic Impact of Occupational Safety and Health in the Member States of the European Union European Agency for Safety and Health at Work, 1999. Institutional

- webpage. Last visited on July 2008, URL: <http://osha.europe.eu>
- EASHW (2007) European Agency for the Safety and Health at Work Report, 2007. Institutional webpage. Last visited on July 2008, URL: <http://osha.europe.eu>
- EFLWC (2005) Fourth European Working Conditions Survey, 2005. Institutional webpage. Last visited on July 2008, URL: <http://www.eurofound.europa.eu/ewco/surveys/EWCS2005> .
- EUROSTAT (2004) The Eurostat yearbook 2004 - The statistical guide to Europe, 2004. Institutional webpage. Last visited on July 2008, URL: <http://epp.eurostat.ec.europa.eu>
- FLIR (2009) FLIR R&D Handbook, 2009. Institutional webpage. Last visited on July 2009, URL: <http://www.flir.com/thermography/eurasia/EN/>
- FREEMAN, H. (1939) Skin and body temperatures of schizophrenic and normal subjects under varying environmental conditions. *Arch. Neurol. Psychiat.*, 42, 724-734.
- FRY, H. J. H. , DENNETT, X. (1988) Overuse syndrome. *Lancet*, 905-908.
- FUJIMURA, K., MAKAROV, M. (1998) Foldover-free image warping. *Graphical Models and Image Processing*, 60, 100-111.
- GEMNE, G., PYYKKO, I., TAYLOR, W. & PELMEAR, P. L. (1987) The Stockholm workshop scale for the classification of cold-induced Raynaud's phenomenon in the hand-arm vibration syndrome (revision of the Taylor-Pelmear scale). *Scandinavian journal of work, environment & health*, 13, 275-278.
- GHOSH, P. & MITCHELL, M. (2006) Segmentation of medical images using a genetic algorithm, *Proceedings of the 8th annual conference on Genetic and evolutionary computation*, Seattle(USA), 1, 1171-1178.
- GLASSEY, C. A., MARDIA, K. V. (1998) A review of image warping methods. *Journal of Applied Statistics*, 25, 155-171.
- GOMES, J., DARSA, L., COSTA, B. & VELHO, L. (1999) *Warping and Morphing of Graphical Objects*. Morgan Kaufmann, San Francisco, CA.
- GONZALEZ, R. C., WOODS, R. E. & EDDINS, S. L. (2004) *Digital Image Processing using Matlab*, 2nd Edition, New Jersey, Pearson Education.
- GONZALEZ, R. C. & WOODS, R. E. (2002) *Digital Image Processing*, 2nd Edition, New Jersey, Addison-Wesley Publishing Company.
- GOODMAN, P. H., MURPHY, M.G., SILTANESE, G.L., KELLY, M.P., RUCKER, L. (1986)

- Normal temperature asymmetry of the back and extremities by computer assisted infrared imaging. *Thermology*, 1:195-202.
- GREENING, J. & LYNN, B. (1998) Vibration sense in the upper limb in patients with repetitive strain injury and a group of at-risk office workers. *International Archives of Occupational and Environmental Health*, 71, 29-34.
- GRIFFIN, M. J. (2000) *Handbook of Human Vibration*. London. Academic Press.
- GRIFFIN, M. J. (2006) Health Effects of Vibration – The Known and the Unknown. IN DONG, R. (Ed.) *First American Conference on Human Vibration*. Morgantown (WV-USA), Engineering and Control Technology Branch.
- GRIFFIN, M. J. & BOVENZI, M. (2002) The diagnosis of disorders caused by hand-transmitted vibration: Southampton Workshop 2000. *International archives of occupational and environmental health*, 75, 1-5.
- HARADA, N. (2006) Diagnosis of Vascular injuries caused by hand-transmitted vibration. In GRIFFIN, M. J., BOVENZI, M. & HAGBERG, M. (Eds.) *2nd International Workshop on hand-transmitted vibration injuries*. Gothenburg (Sweden).
- HEAD, J. F., ELLIOT, R.L. (2002) Infrared imaging: making progress in fulfilling its medical promise, *IEEE Engineering in Medicine and Biology Magazine*, 21(6), 41-48.
- HARDY, J.D. (1934) Radiation of heat from the human body. An instrument for measuring the radiation and the surface temperature of the skin. *J. Clin. Invest.*, 13: 593-599.
- HELLIWELL, P. S. & TAYLOR, W. J. (2004) Repetitive strain injury. *Postgraduate Medical Journal*, 80, 438-443.
- HODGSON, J., JONES, J., ELLIOTT, R. & OSMAN, J. (1993) Self-reported work-related illness Research paper 33 HSE Books ISBN 0 7176 0607 4.
- HORMANN, K. (2004) Barycentric coordinates for arbitrary polygons in the plane. Tech. rep., Clausthal University of Technology. Last visited in September 2008. URL: <http://www.in.tuclausthal.de/hormann/papers/barycentric.pdf>.
- HOUDAS, Y., RING, E.F.J. (1982) *Human Body Temperature*. Plenum Press, New York.
- HSE (1995) Health and Safety Commission Annual Report 1994/5 - Statistical Supplement. HSE Books ISBN 0 7176 1019 5.
- HSE (2007) HSE Hand-Arm Vibration Syndrome statistics. London, HSE.

- HSE (2008) Health & Safety Executive HAVS webpage. Last visited in June 2009. URL: <http://www.hse.gov.uk/vibration/hav/advicetoemployers/healthsurveillance.htm> .
- JAMESON, T. (1998) Repetitive Strain Injuries: Alternative treatments & prevention. McGraw-Hill, 1st edition.
- JANKOVIC, S., STANKOVIC, S., BORJANOVIC, S., TENJOVIC, L., BOGDANOVIC, M. (2008) Cold stress dynamic thermography for evaluation of vascular disorders in hand-arm vibration syndrome. *J Occup Health*, 50(5), 423-425.
- JIANG, L. J., NG, E. Y. K., YEO, A. C. B., WU, S., PAN, F., YAU, W. Y., CHEN, J. H., YANG, Y. (2005) A perspective on medical infrared imaging, *Journal of Medical Engineering & Technology*, 29(6), 257-267.
- JONES, L. (2006) Human Hand Function. Oxford University Press, Connecticut (USA), 1st edition.
- JONES, B. F. & PLASSMANN, P. (2002) Digital infrared thermal imaging of human skin. *IEEE Engineering in Medicine and Biology*, 21, 41-48.
- KARANTZALOS, K. & ARGIALAS, D. (2006) Improving edge detection and watershed segmentation with anisotropic diffusion and morphological levellings, *International Journal of Remote Sensing*, 27(24), 5427–5434.
- KASS, M., WITKIN, A. & TERZOPOULOS, D. (1988) Snakes: Active contour models, *International Journal of Computer Vision*, 1(4), 321-331.
- KELSEY, L. (1997) Upper Extremity Disorders: Frequency, Impact, and Cost. Churchill Livingstone, New York (USA), 1st edition.
- KENNEDY, D., LEE, T., SEELY, D. (2009) A Comparative Review of Thermography as a Breast Screening Technique. *Integrative Cancer Therapies*, 8(1), 9-16.
- KINAPE, R. & AMORIM, M. (2003) A study of the most important image quality measures, *Proceedings of the 25th Annual International Conference of IEEE EMBS, Cancun (Mexico)*, September 17-21 2003, 1, 934-936.
- KYRIAKIDES, K. (1988) Survey of exposure to hand-arm vibration in Great Britain Research Paper 26 HSE 1988.
- LACHIN, J.M. (2004). The role of measurement reliability in clinical trials. *Clinical trials*, 1, 553-566.
- LAWSON, I. J. & NAVELL, D. A. (1997) Review of objective tests for the hand—arm vibration

- syndrome. *Occupational Medicine*, 47, 15-20.
- LEHMANN, T. M., GÖNNER, C. & SPITZER, K. (1999) Survey: interpolation methods in medical image processing, *IEEE Trans. Med. Imaging*, 18(11), 1049–1075.
- LEVINE, D.W., SIMMONS, B.P., KORIS, M.J., DALTROY, L.H., HOHL, G.G., FOSSEL, A.H., KATZ, J.N. (1993) A self-administered questionnaire for the assessment of severity of symptoms and functional status in carpal tunnel syndrome. *J Bone Joint Surg* 1993;75A:1585-1592.
- LI, C., KAO, C., GORE, J. C., DING, Z. (2007) Implicit Active Contours Driven by Local Binary Filtering Energy, *IEEE conference on Computer Vision and Pattern Recognition (CVPR) 2007*, Minneapolis (Minnesota, USA), June 18-23 2007.
- LORIGA, G. (1911) Il lavoro con i martelli pneumatici. *Boll.Isp.Lav*, 2-35.
- LUNDSTRÖM, R. (2002) Neurological diagnosis—aspects of quantitative sensory testing methodology in relation to hand-arm vibration syndrome. *Int Arch Occup Environ Health*, 75, 68–77.
- MANSFIELD, N.J. (2005) *Human response to vibration*, CRC Press, London, 1st edition.
- MCGEOCH, K. L., LAWSON, I. J., BURKE, F., PROUD, G. & MILES, J. N. V. (2005) Diagnostic Criteria and Staging of Hand-Arm Vibration Syndrome in the United Kingdom. *Industrial Health*, 43, 527-534.
- MEYERS, S., CROS, D., SHERRY, B., VERMEIRE, P. (1989) Liquid crystal thermography: Quantitative studies of abnormalities in carpal tunnel syndrome, *Neurology*, 39, 1465-1469.
- MONTGOMERY, D.C., RUNGER, G.C., HUBELE, N.F. (2009) *Engineering Statistics*, Student Study Edition. John Wiley and Sons. New York. 488-490.
- NICHOLS, H. M. (1960) *Manual of Hand Injuries*. Second edition, Chicago, The Year Book Medical Publishers.
- NIU, H.H., LUI, P.W., HU, J.S., TING, C.K., YIN, Y.C., LO, Y.L., LIU, L. & LEE, T. Y. (2001) Thermal symmetry of skin temperature: normative data of normal subjects in Taiwan. *Chinese Med J (Taipei)*; 64:459–68.
- NOBLE, R. (2002) Diagnosis of stress. *Metabolism*, Volume 51, Issue 6, Pages 37-39.
- NPL (2009) NPL website: thermal frequent asked questions page. Last visited June 2009. URL: <http://www.npl.co.uk/engineering-measurements/thermal/temperature/faqs/what-is->

temperature-(faq-thermal) .

- PALMER, K. T., GRIFFIN, M. J., BENDALL, H., PANNETT, B. & COGGON, D. (2000a) Prevalence and pattern of occupational exposure to hand transmitted vibration in Great Britain: findings from a national survey. *Occupational and Environmental Medicine*, 57, 218-228.
- PALMER, K. T., GRIFFIN, M. J., SYDDALL, H., PANNETT, B., COOPER, C. & COGGON, D. (2000b) Prevalence of Raynaud's phenomenon in Great Britain and its relation to hand transmitted vibration: a national postal survey. *Occupational and Environmental Medicine*, 57, 448-452.
- PARK, S., SUNG, H.J. (2004) Assessment of image registration interpolation methods for pressure sensitive paint measurements", 11th International Symposium on Flow Visualization, August 9-12, University of Notre Dame, Notre Dame, Indiana, USA.
- PASCARELLI, E. & QUILTER, D. (1994) *Repetitive Strain Injury - A Computer User's Guide*. New York (USA), John Wiley & Sons, Inc., 1st edition.
- PASCARELLI, E. (1997) *Dr. Pascarelli's Complete Guide to Repetitive Strain Injury: What You Need to Know about RSI and Carpal Tunnel Syndrome*. New York (USA), John Wiley & Sons, Inc. 2nd edition.
- PEDDIE, S. & ROSENBERG, C. H. (1997) *The Repetitive Strain Injury Sourcebook*, Los Angeles (USA), Lowell House.
- PELMEAR, P. L. (2003) The clinical assessment of hand–arm vibration syndrome. *Occupational Medicine*, 53, 337-341.
- PELMEAR, P. L. (2003) The clinical assessment of hand-arm vibration syndrome. *Occup. Med.*, 53, 337–341.
- PEPER, E., Wilson, V.S., Gibney, K. H., Huber, K., Harvey, R., Shumay, D. M. (2003) The Integration of electromyography (SEMG) at the workstation: assessment, treatment, and prevention of repetitive strain injury (RSI). *Appl Psychophysiol Biofeedback*, 28, 167-182.
- PHILLIPS, D. (2008) Baricentric coordinates website. Last visited in December 2008 URL: http://crackthecode.us/barycentric/barycentric_coordinates.html .
- PHYSIOTHERAPY, T. C. S. O. (1999) *Employment Relations & Union Services: Health & Safety –. Repetitive Strain Injury (RSI)*. Bedford, The Chartered Society of Physiotherapy.
- PHYSIOTHERAPY, T. C. S. O. (2001) *Employment Relations & Union Services: Health & Safety*

– Work-related Strain Injuries (Musculoskeletal Disorders). Bedford, The Chartered Society of Physiotherapy.

PLASSMANN, P., MURAWSKI, P. (2003) C THERM for standardised thermography”, 9th European Congress of Medical Thermology, May 30th -1st June 2003, Krakow, Poland.

PLASSMANN, P., RING, E. F. J., JONES, C. D. (2006) Quality assurance of thermal imaging systems in medicine, *Thermology International*, 16(1), 10-15.

PLATT, H. (2006) On shaky ground. *New Law Journal*, 7208, 91-93.

POCHACZEWSKY, R., ABERNATHY, M., BORTEN, M. (1986) Technical guidelines, edition 2. *J Am Acad Thermal* 2: 108-112.

POTH, M. (2004) Image Interpolation techniques, 2nd Serbian-Hungarian Joint Symposium (SISY 2004), October 1-2 2004, in Subotica, Serbia and Montenegro.

RASE, W. D. (2001) Volume-preserving interpolation of a smooth surface from polygon-related data. *Journal of Geographical Systems*, 3, 199-213.

RING, E. F. J. (1988) Raynaud's phenomenon: assessment by thermography, *Thermology*, 3, 69-73.

RING, E. F. J. (1995) Cold stress test for the hands. IN AMMER, K. & RING, E. F. J. (Eds.) *The Thermal Image in Medicine and Biology*. Wien (Austria), Uhlen Verlag.

RING, E. F. J., AMMER, K. (2000) The Technique of Infra red imaging in medicine, *Thermology International*. 10(1), 7-14.

RING, E.F.J. (2003) The historical development of thermal imaging in medicine. *Thermology International*. 13(2): 53-57.

RING, E. F. J., AMMER, K., JUNG, A., MURAWSKI, P., WIECEK, B., ZUBER, J., ZWOLENIK, S., PLASSMANN, P., JONES, C. D., JONES, B. F. (2004) Standardization of infrared imaging. In *Conf. Proc. IEEE Eng. Med. Biol. Soc.* , 2, 1183-1185.

RING, E. F. J., AMMER, K., WIECEK, B., PLASSMANN, P. (2005) Technical challenges for the construction of a medical IR digital image database. *Proc. SPIE, Detectors and Associated Signal Processing II* Eds.: JP Chatard, PNJ Dennis, 5964, 191-198.

ROSENFELD, A. (1969) *Picture Processing by Computer*, New York: Academic Press.

ROUSHDY, M. (2006) Comparative Study of Edge Detection Algorithms Applying on the Grayscale Noisy Image Using Morphological Filter, *GVIP Journal*, 6(4), 17–23.

- RSIA (2007) Repetitive Strain Injury Association Facts & Figures website. Last visited in June 2007, URL: <http://www.rsia.org.uk>
- SALTHOUSE, T. A. (1984) Effects of age and skill in typing. *Journal of Experimental Psychology: General*, 13, 345-371.
- SAMPSON, E. (2006) Development and testing of a screening tool for mine workers with possible Hand Arm Vibration Syndrome. Faculty of Engineering, The built environment and information technology. Pretoria (South Africa), University of Pretoria.
- SCHLAGER, O., GSCHWANDTNER, M. E., HERBERG, K., FROHNER, T., SCHILLINGER, M., KOPPENSTEINER, R., MLEKUSCH, W. (2010) Correlation of infrared thermography and skin perfusion in Raynaud patients and in healthy controls. *Microvasc. Res.*, 80(1), 54-57.
- SCHWARTZ, R. G. (2006) Guidelines For Neuromusculoskeletal Thermography. *Thermology international*, 16(1), 5-9.
- SEROV, A., STEINACHER, B., LASSER, T. (2005) Full-field laser Doppler perfusion imaging and monitoring with an intelligent CMOS camera, *Optics Express*, 13(10), 3681-3689.
- SHARIFI, M., FATHY, M. & MAHMOUDI, M. T. (2002) A Classified and Comparative Study of Edge Detection Algorithms, in proc. IEEE Computer Society International Conference on Information Technology: Coding and Computing, 117-120.
- SHARMA, S. D., SMITH, E. M., HAZLEMAN, B. L. & JENNER, J. R. (1997) Thermographic changes in keyboard operators with chronic forearm pain. *BMJ*, 314, 118-119.
- SLEATOR, A., GORE, D., VIDLER, G. (1998) Work Related Upper Limb Disorders. House of Commons Library Research Paper 1998/51. Institutional webpage. Last visited on February 2009, URL: <http://www.parliament.uk/commons/lib/research/rp98/rp98-051.pdf>.
- SMITH, W., BURNS C. (1999) Managing the hair and skin of African American pediatric patients. *Journal of Pediatric Health Care*, 13(2), 72-78.
- SOUTH, T (2004) Managing Noise and Vibration at Work. A practical guide to assessment, measurement and control. Elsevier Butterworth-Heinemann. Burlington (USA).
- SPROUT, J. (1997) The Gender Differences in Upper-Extremity Occupational Repetitive Strain Injuries in Manitoba. Community Health Sciences. Manitoba (Canada), University of Manitoba.

- SZABO, R. M., KING, K. J. (2000) Repetitive stress injury: diagnosis or self-fulfilling prophecy? *J. Bone Joint Surg. Am.*, 82(9), 1314–1322.
- STASIEK, J., STASIEK, A., JEWARTOWSKI, M., COLLINS, M. W. (2006) Liquid crystal thermography and true-colour digital image processing, *Optics & Laser Technology*, 38, 243–256.
- STIKBAKKE, E., MERCER, J. B. (2008) An Infrared Thermographic and Laser Doppler Flowmetric Investigation of Skin Perfusion In The Forearm and Finger Tip Following A Short Period of Vascular Stasis, *Thermology International*, 18(3), 107-111.
- SUPARNA, K., SHARMA, A. K., KHANDEKAR, J. (2005) Occupational health problems and role of ergonomics in information technology professionals in national capital region. *Indian Journal of Occupational and Environmental Medicine*, 9(3), 111-114.
- SUZUKI, K., HORIBA, I. & SUGIE, N. (2000) Edge detection from noisy images using a neural edge detector, *Neural Networks for Signal Processing X, 2000. Proceedings of the 2000 IEEE Signal Processing Society Workshop*, 2, 487-496.
- TERADA, K., MIYAI, N., MAEJIMA, Y., SAKAGUCHI, S., TOMURA, T., YOSHIMASU, K., MORIOKA, I, MIYASHITA, K. (2007) Laser Doppler Imaging of Skin Blood Flow for Assessing Peripheral Vascular Impairment in Hand-Arm Vibration Syndrome, *Industrial Health* 45, 309-317.
- THE INDEPENDENT (1993) - The Independent Newspaper news website. Last visited in October 2008. URL: <http://www.independent.co.uk/news/uk/journalist-wins-compensation-for-rsi-outofcourt-settlement-of-pounds-11371-follows-judges-ruling-that-strain-injury-does-not-exist-1501386.html> .
- TIVEY, H. (1997) - RSI hazards handbook: a workers' guide to Repetitive Strain Injuries and how to prevent them. London Hazards Centre Trust, London.
- THOMAS, R. A. (1999) *Thermography Monitoring Handbook*. Coxmoor Publishing Company, Kingham (UK), Machine & Systems Condition Monitoring Series.
- TORTORA, G.J., GRABOWSKI S.R. (2003) *Principles of Anatomy and Physiology*. John Wiley & Sons, New York (USA), tenth edition.
- UEMATSU, S. (1986) Symmetry of skin surface temperature comparing one side of the body to the other. *Thermology*, 1:4–7.

- UEMATSU, S., EDWIN, D.H., JANKEL, W.R., KOZIKOWSKI, J. & TRATTNER, M. (1988) Quantification of Thermal Asymmetry, Part 1: Normal values and reproducibility. *J. Neurosurg.* 69(4):552–555.
- VAN TULDER, M., MALMIVAARA, A., KOES, B. (2007) Repetitive strain injury. *Lancet*, 369 (9575): 1815–1822
- WERNER, R.A. & ANDARY, M. (2002). Carpal tunnel syndrome: pathophysiology and clinical neurophysiology. *Clin. Neurophysiol.* 113, 1373-1381.
- WIDMAIER, E.P., HERSHEL R., STRANG, K.T. (2004) In: VANDER, SHERMAN & LUCIANO's human physiology: the mechanisms of body function. 9th ed.. Boston: McGraw-Hill, 632–637.
- WOLBERG, G. (1996) Recent Advances in Image Morphing, *Proc. Computer Graphics Intl. '96*, Pohang, Korea.
- WOLBERG, G. (1998) Image Morphing: A Survey, *Visual Computer*, 14, 360-372.
- ZHENG, J., HU, S., ECHIADIS, A.S., AZORIN-PERIS, V., SHI, P., CHOULIARAS, V. (2009) A remote approach to measure blood perfusion from the human face. *Proc. SPIE* 7169, 716917, DOI:10.1117/12.807354
- ZHOU, Q., LI, Z. & AGGARWAL, J. K. (2004) Boundary extraction in thermal images by edge map, *Proceedings of the 2004 ACM symposium on Applied computing*, Nicosia (Cyprus), 254-258.
- ZIMMERMAN, D. W. (1997). A Note on Interpretation of the Paired-Samples t Test. *Journal of Educational and Behavioral Statistics*, 22 (3), 349–360.

Webliography

[1] – Last visited on April 2009, URL: http://www.joint-pain-expert.net/images/hand_anatomy.jpg

[2] - Last visited on April 2009, URL: http://www.joint-pain-expert.net/images/joints_of_hand.jpg

[3] - Last visited on April 2009, URL: http://www.joint-pain-expert.net/images/hand_anatomy_muscles.jpg

[4] - Last visited on April 2009, URL: http://www.joint-pain-expert.net/images/hand_anatomy2.jpg

[5] - Last visited on April 2009, URL: <http://www.prolo.ca/images/hand1.jpg>

[6] - Last visited on April 2009, URL: <http://www.hss.edu/images/corporate/brachial-plexus-1.jpg>

[7] - Retrieved September 2009, from:

http://www.health.com/health/static/hw/media/medical/hw/h9991344_001.jpg

[8] – Composed from the images last visited on April 2009, URLs:

<http://home.comcast.net/~WNOR/superficialpalmararch.jpg>

<http://home.comcast.net/~WNOR/deeppalmararch.jpg>

[9] – Modified from the image last visited on April 2009, URL:

http://www.childbirths.com/cypress/ivtherapy_files/image009.gif

[10] – Modified from the image Last visited on April 2009, URL:

<http://upload.wikimedia.org/wikipedia/commons/2/20/Skinlayers.png>

[11] - Last visited on April 2009, URL:

<http://upload.wikimedia.org/wikipedia/commons/thumb/3/34/Skin.jpg/300px-Skin.jpg>

[12] - Last visited on April 2009, URL:

http://lh5.ggpht.com/_IRGislJejZ0/SRp8QcExTii/AAAAAAAAAB-U/0HJFUbuu8Hs/image_thumb6.png

[13] - Last visited on April 2009, URL:

http://www.bg.ic.ac.uk/Staff/khparker/homepage/BSc_lectures/2002/Capillary_sketch.jpg

[14] – From Dr. James Betts thermoregulation notes of human physiology at school of health at University of Bath Last visited on April 2009, URL:

<http://people.bath.ac.uk/jb335/Y1%20Physiology-Thermoregulation.pdf>

[15] - Last visited on April 2009, URL:

http://ffden-2.phys.uaf.edu/211_fall2002.web.dir/Andrea_Steffke/images/electromagneticspectrum.jpeg

[16] - Last visited on April 2009, URL:

<http://www.cartage.org.lb/en/themes/arts/photography/fieldskinds/scientificph/medscient/pioneers/herschel/fig5.jpg>

[17] - Last visited on April 2009, URL: <http://alfven.princeton.edu/projects/MCVPIimages/PlanckGraph.gif>

[18] - Last visited on April 2009, URL:

http://sites.google.com/site/delseaphysics2/_/rsrc/1215475171011/Home/modern-physics/classical-view-of-light/notes-for-classical-view-of-light/WiensDisplacement.png

[19] - Last visited on April 2009, URL: http://itl.chem.ufl.edu/4412_aa/Gifs/pc0_02.gif

[20] - Last visited on April 2009, URL:

http://ffden-2.phys.uaf.edu/211_fall2002.web.dir/Andrea_Steffke/images/stehan-boltzman.jpg

[20] - Last visited on April 2009, URL: <http://www.scribd.com/doc/7477336/Digital-Image-Processing>

[21] - Last visited on August 2010, adapted from URL:

<http://www.aafp.org/afp/2010/0115/afp20100115p147-f2.jpg>

Appendices

Appendix 1 – Overview table of current diagnostic methods for RSI

Appendix 2 – Overview table of current diagnostic methods for HAVS

Appendix 3 – Hand Injury Scoring System

Appendix 4 – Occupational conditions incidence questionnaire

Appendix 5 – Occupational conditions incidence questionnaire database schema

Appendix 6 – Occupational conditions incidence questionnaire HTML and PHP scripts

Appendix 7 – Occupational conditions incidence questionnaire results

Appendix 8 – Consent form

Appendix 9 – Information for volunteers

Appendix 10 – EURO-QOL ASSESSMENT SHEET

Appendix 11 – Repetitive Strain Injury Screening Questionnaire

Appendix 12 – Repetitive Strain Injury Screening Questionnaire

Appendix 13 – The author scientific work: publications and presentations

Appendix 1 – Overview table of current diagnostic methods for RSI

Type	Procedure (test)	Description	Advantages	Disadvantages
Pre – diagnostic	Questionnaires	Used to identify signs and symptoms of RSI.	The responses are gathered in a standardised way, so questionnaires are more objective, certainly more so than interviews and improve the speed of information collection.	Participants may forget important issues. Due to the standardisation of the questionnaire text it is not possible to explain any points in the questions that participants might misinterpret. Participants may not be willing to answer the questions.
	Medical History	Used to support signs and symptoms of RSI and relate them with genetic inheritance.	Help clinician to understanding patient's medical background.	Delayed procedure. Insufficient on its own.
Muscular	Wrist flexion test	To test muscle shortening, assessing the range of bend and flex movements. Assesses muscle tightness.	Easy to perform.	Can be painful to the patient and inconclusive as a RSI indicator
	Grip strength test	To test the weakness of grip by squeezing a Jamal dynamometer (an instrument that measures the weight that a patient can pull). This test is also used to assess recovery.	Gives quantitative data according to the weight that a patient can pull.	Can be painful to the patient and inconclusive as a RSI indicator.
	Pulp pinch test	Measures the strength in the fingers by squeezing the meter as hard as possible in different positions.	Gives quantitative data. Is a reasonably good RSI indicator.	Can be painful for the patient.
	Finkelstein's sign test	Where the patient makes a fist with the thumb curled inside, and then the doctor will bend the hand down and ask if it hurts.	Easy to perform.	Can be painful to the patient and inconclusive as a RSI indicator
Nerve	Phalen's maneuver	To see whether fingers go numb or tingle when holding the back of the hands together with the fingers facing the floor for a minute.	Easy to perform, a positive result will indicate diagnosis of Carpal Tunnel Syndrome, one of the cases of RSI.	Can be painful for the patient.

	Tinel's sign	To assess possible nerve irritation or compression by the doctor tapping with his finger on various anatomical sites, like elbow, palm side or wrist.	Easy to perform.	A positive result indicates the possibility of nerve irritation or compression although it is not conclusive of RSI.
	EMG	Used when previous tests are positive, the nerve conduction studies will test what happens in the body when a low voltage of electricity passes through specific areas.	Good quantitative indicator and gold standard for verifying Carpal Tunnel Syndrome.	Expensive and specific equipment. Oils and ointments can interfere with the test, cold hands also impede the test. The amount of pain sensation depends individual's sensitivity to pain.
	Semmes-Weinstein monofilament test	Assess the ability to feel light touches in hands, if nothing is felt nerve damage is indicated.	Cheap, easy and painless.	Inconclusive by itself as an RSI test, needs an EMG to verify this.
	Weber two-point discrimination test	Tests light touch sensitivity in the fingertips between two points with the eyes shut.	Easy and painless.	The instrument used looks like a pizza wheel with irregularly placed spokes, as the space between these decreases it becomes harder to discriminate between one or two points.
	MRI	Assesses inflammation of soft in affected limbs.	Non-invasive and painless procedure. Good imaging system for soft tissues.	Expensive and sometimes claustrophobia producing procedure. Problems when imaging shoulder regions because of low contrast due to the presence of muscles, tendons, ligaments and lubricant sacs with similar (MRI) characteristics.
	X-Ray	Detects bone or joint problems or arthritis.	Good method to assess bone or joint problems or arthritis.	Radiation exposure. Damage to the soft tissue doesn't usually show up on X-Rays.
Other	Video	Videotaping patients at a simulated workstation to see what they are doing to provoke injury.	It gives to the clinicians the idea of the situation and its relationship with the symptoms as well as the correspondent corrective answer.	Time consuming. Good video recording system plus technician is also expensive. Often inconclusive.

Based on: (Helliwell and Taylor, 2004), (Pascarelli and Quilter, 1994).

Appendix 2 – Overview table of current diagnostic methods for HAVS

Type	Procedure (test)	Description	Advantages	Disadvantages
Pre – diagnostic	Questionnaires	Used to identify signs and symptoms of HAVS and exposure to vibration.	The responses are gathered in a standardised way, therefore questionnaires are more objective, certainly more so than interviews. Relatively fast to collect information.	Participants may forget important issues. Due to the standardisation of the questionnaire text it is not possible to explain any points in the questions that participants might misinterpret. Participants may not be willing to answer the questions.
	Medical History	Used to support signs and symptoms of HAVS and relate them with genetic inheritance.	Help the understanding of patient’s medical background	Delayed procedure. Insufficient on its own.
	Annual Surveillance	Routine annual health surveillance performed by a “esponsible person” assessing workers in risk.	Good prevention procedure that helps to mitigate symptoms of the syndrome.	Delayed procedure. Useless if not properly performed.
Musculoskeletal	Allen test	The hand is elevated and the patient is asked to make a fist for about half a minute. Then pressure is applied over the ulnar and the radial arteries so as to occlude both of them. When still elevated, the hand is then opened. It should appear blanched (pallor can be observed at the finger nails). After that the ulnar pressure is released and colour should return within 5 seconds. If colour does not return or returns after 7 seconds there is no integrity of the radial and ulnar artery supply to the arm.	Easy to perform test and clear result can also be observed easily.	Can be painful to the patient and inconclusive as a HAVS indicator.
	Phalen’s test	The patient is asked to hold their wrist in complete and forced flexion, pushing the dorsal surfaces of both hands together for 1 minute, symptoms will show if both hands are held tightly, can also produce a tingling sensation.	Easy to perform, a positive result will indicate diagnosis of Carpal Tunnel Syndrome.	Can be painful to the patient and inconclusive as a HAVS indicator.

	Tinel's test	Detects irritated nerves. Appraising the median nerve compression in the wrist if there is an indicator of a response of tingling in the first three fingers. It is performed by lightly tapping over the nerve to elicit a sensation of tingling in the distribution path of the nerve	Easy to perform test and clear result can be observed also easily.	Can be painful to the patient and inconclusive as a HAVS indicator. Is often "positive" in healthy patients, causing tingling in the thumb, index, and middle finger.
	Adson test	Used to detect any obstruction of the arterial flow to the arm at the level of the neck checking if the radial pulse is present.	Easy to perform test.	Can be painful to the patient and inconclusive as a HAVS indicator.
Muscular	Grip force test	To test the gripping force in both hands with a dynamometer.	Gives a quantitative data, being helpful to be used as an injury indicator.	Can be painful to the patient and inconclusive as a HAVS indicator.
	Pinch force test	To assess finger strength the arm of a pinch meter is pressed between the thumb and index finger.	Gives quantitative data, and can also be helpful as an injury indicator.	Can be painful to the patient and inconclusive as a HAVS indicator.
	Finger tapping test	To assess fine motor speed and dexterity by tapping the fingers.	Easy to perform test.	Can be painful to the patient and inconclusive as a HAVS indicator.
	Moberg pick up test	Picking up small objects from a table surface and place those in a small container, time and performance are recorded.	Gives quantitative data, can also be helpful as an injury indicator.	Can be painful to the patient and inconclusive as a HAVS indicator.
	Purdue pegboard test	In order to assess dexterity and loss of movement in either hand. Measures two types of activities: one involving gross movement of hands, fingers and arms; and the other involving fingertip dexterity.	Gives quantitative data, can also be helpful as an injury indicator.	Can be painful to the patient and inconclusive as a HAVS indicator.
Vascular	Cold provocation test	Room temperature maintained at between 20 and 22°C. A thermocouple is attached to each of the 8 fingers. 2 minutes of stabilisation period is used and after it plastic gloves are wearied and hands immersed up to the wrist in water at 15° C for 5 minutes. Finger skin temperature is measured 10 minutes after exiting the bath.	Gives a good quantitative data of vascular assessment.	Can be painful to the patient. Reduced time of exposure, higher temperature water and a recording procedure without contact could improve this method.

	Finger systolic blood pressure	Finger systolic blood pressures were measured using strain-gauge plethysmography following local cooling in accord with International Standard 14835-2 (2005). The FSBPs were measured simultaneously in the thumb and the index, middle, ring, and little fingers of the dominant hand using a multi-channel plethysmograph.	Gives a good quantitative data of vascular assessment.	Can be painful to the patient.
	Colour charts	An epidemiological study consisting in a series of photographs illustrating various degrees of blanching and cyanosis of the hands.	Easy to use.	Subjective test.
	Nail compression test	Tests the digital flow when occlusion of blood to the fingertip has taken place. Finger skin temperature is taken with a thermistor to check for damaged arterial blood flow that results in lower temperatures than normal, (i.e. 30 °C).	Easy to use and gives a reasonable quantitative data of vascular assessment.	Can be painful to the patient.
Nerve	Light touch test	To test the sensitivity of fingertips by using cotton wool stroked lightly over them.	Easy to perform.	This test shows some unreliability.
	Pain sense test	A disposable needle is pressed sharply against the fingertip and the patient is expected to report when a sharp or dull sensation is felt, the stimulus varies with the pressure applied to the needle.	Easy to perform.	This test is painful to the patient.
	Weber two-point discriminator test	To evaluate large nerve function in the fingertips by differentiating between two single point of pressure on the skin at variable distances.	Easy and painless.	The instrument used looks like a pizza wheel with irregularly placed spokes, as the space between these decreases it becomes harder to discriminate between one or two points.

Deep sense perception	To determine digital sensibility dysfunction. Uses monofilaments. Determines whether patients have the ability to sense a point of pressure on the finger	Easy to perform.	Can be painful to the patient.
Monofilaments	To determine whether patients have the ability to sense a point of pressure on the finger.	Easy to perform.	Can be painful to the patient.
Vibration sense	Has been used as a non-invasive diagnostic technique for nerve compression and dysfunction detection and it allows an early detection of loss of vibration sensation. This technique uses instruments such as the traditional tuning fork, the graduated tuning fork and the vibration sensimeter. Tests <i>joint position sense</i> by moving one of the patient's fingers or toes up and down and asking the patient to report which way it moves. Hold the digit lightly by the sides while doing this so that tactile inputs don't provide significant clues to the direction of movement.	Easy to use and gives a reasonable quantitative data of nerve assessment.	The digit should be moved very slightly because normal individuals can detect movements that are barely perceptible by eye.
Vibration threshold test	To check at mechanoreceptors (the sensation sensitive nerve endings). These respond to stretch and texture at different frequencies and measurements are taken from each hand, from the median nerve (index finger) and the ulnar nerve (little finger) area.	Easy to use and gives reasonable quantitative data of nerve assessment.	The digit should be moved very slightly because normal individuals can detect movements that are barely perceptible by eye. Repetitions should also be avoided because of attempts learning.

	<p>Thermal Aesthesiometry</p>	<p>Measures the degree of tactile sensitivity. Used to determine the sensitivity of thermal stimuli. The simplest is a manual tool with adjustable points similar to a calliper. It can determine how short a distance between two impressions on the skin can be distinguished. A scale on the instrument gives readings in millimetre gradients.</p>	<p>Easy to use and gives a reasonable quantitative data of nerve assessment.</p>	<p>Repetitions should also be avoided because of learning effects.</p>
--	--------------------------------------	--	--	--

Based on: (Lawson and Navell, 1997, Sampson, 2006).

Appendix 3 - Hand Injury Scoring System

Finger	Integument	Skeleton	Motor	Neurological	Total
Thumb					x 6 =
Index					x 2 =
Middle					x 3 =
Ring					x 3 =
Little					x 2 =
Final Severity Score					

Table 1 – Campbell's hand injury severity scoring chart

INTEGUMENT				
Skin loss	Absolut Values (hand)	Dorsum	< 1cm ²	5
			> 1cm ²	10
			> 5cm ²	20
		Palm	Dorsum x 2	
	Weighted Values (digit)	Dorsum	< 1cm ²	2
			> 1cm ²	3
		Pulp	< 25%	
			> 25%	
Skin laceration			< 1cm	1
			> 1 cm	2
Nail damage				1
SKELETAL				
Fractures	Simple shaft			1
	Comminuted shaft			2
	Inter-articular DIP J			3
	Inter-articular PIP/MIP J			5
	Inter-articular MCP J			4
Dislocations	Open			4
	closed			2
Ligament Injury	sprain			2
	rupture			3
MOTOR				
Extensor tendon	Proximal to PIP J			1
	Distal to PIP J			3
Flexor profundus	Zone 1			6
	Zone 2			6
	Zone 3			5
Flexor superficialis				5
Intrinsic				2
NEURAL				
Absolut values	Recurrent branch median nerve			30
	Deep branch ulnar nerve			30
Weighted Values	Digital nerve x 1			3
	Digital nerve x 2			4

Table 2 – The injury scoring system.

Digit	Weighting factor
Thumb	x6
Index	x2
Middle	x3
Ring	x3
Little	x2

Table 3 – The individual digit weighting factors.

Grade	Total points
I - Minor	<20
II - Moderate	21-50
III - Severe	51-100
IV - Major	>100

Table 4 – The grade according to the obtained score points.



ALL THE INFORMATION COLLECTED BY THIS QUESTIONNAIRE IS ANONYMOUS AND STRICTLY CONFIDENTIAL AND WILL JUST BE USED FOR RESEARCH PURPOSES ONLY, AFTER COMPLETION ALL DATA WILL BE DELETED

Gender: Male Female
Age: years
Height: cm (1ft = 30.5 cm)
Weight: kg (1 stone = 6.35 kg)
Occupation: for years

1. Do you use a keyboard?
 Yes, How many hours per week: (average) No
2. Do you use a computer mouse?
 Yes, How many hours per week: (average) No
3. When seated in a workstation do you adopt a correct posture and position?
 Yes No
4. When you type, do you use all fingers in a correct way (i.e. Using all fingers)?
 Yes No
5. Are you experiencing any swelling of the muscles and joints of your hands or arms?
 Yes No
6. Are you experiencing any stiffness with the muscles and joints of your hands or arms?
 Yes No
7. Have you ever had any serious neck, arm or hand injury or operation?
 Yes No
8. Have you ever had any serious diseases of joints, skin, nerves, heart or blood vessels?
 Yes No
9. Do you have any difficulty with muscles or joints in your hands?
 Yes No
10. Do you have any medical history that may affect your hands or arms?
 Yes No
11. Are you on any long-term medication?
 Yes No
12. Are you a smoker?

- Yes, How many cigarettes per day: No

13. Do you drink alcohol?

- Yes, How many units (1/2 pint of beer) per day: No

The following questions refer to your symptoms for a typical twenty-four-hour period during the past two weeks (fill one circle to answer each question).

14. How severe is the hand or wrist pain that you have at night?

- I do not have hand or wrist pain at night
 Mild pain
 Moderate pain
 Severe pain
 Very severe pain

15. How often did hand or wrist pain wake you up during a typical night in the past two weeks?

- Never
 Once
 Two or three times
 Four or five times
 More than five times

16. Do you typically have pain in your hand or wrist during the daytime?

- I never have pain during the day
 I have mild pain during the day
 I have moderate pain during the day
 I have severe pain during the day
 I have very severe pain during the day

17. How often do you have hand or wrist pain during the daytime?

- Never
 Once or twice a day
 Three to five times a day
 More than five times a day
 The pain is constant

18. How long, on average, does an episode of pain last during the daytime?

- I never get pain during the day
 Less than 10 minutes
 10 to 60 minutes
 Greater than 60 minutes
 The pain is constant throughout the day

19. Do you have numbness (loss of sensation) in your hand?

- No
- I have mild numbness
- I have moderate numbness
- I have severe numbness
- I have very severe numbness

20. Do you have weakness in your hand or wrist?

- No weakness
- Mild weakness
- Moderate weakness
- Severe weakness
- Very severe weakness

21. Do you have tingling sensations in your hand?

- No tingling
- Mild tingling
- Moderate tingling
- Severe tingling
- Very severe tingling

22. How severe is numbness (loss of sensation) or tingling at night?

- I have no numbness or tingling at night
- Mild
- Moderate
- Severe
- Very severe

23. How often did hand numbness or tingling wake you up during a typical night during the past two weeks?

- Never
- Once
- Two or three times
- Four or five times
- More than five times

24. Do you have difficulty with the grasping and use of small objects such as keys or pens?

- No difficulty
 - Mild difficulty
 - Moderate difficulty
 - Severe difficulty
 - Very severe difficulty
-

Please grade the pain symptoms on the parts of the upper body where you feel pain when performing your usual tasks.

	No pain	Mild Pain	Moderate Pain	Severe Pain	Very Severe Pain
Neck	<input checked="" type="radio"/>	<input type="radio"/>	<input type="radio"/>	<input type="radio"/>	<input type="radio"/>
Upper back	<input checked="" type="radio"/>	<input type="radio"/>	<input type="radio"/>	<input type="radio"/>	<input type="radio"/>
Lower back	<input checked="" type="radio"/>	<input type="radio"/>	<input type="radio"/>	<input type="radio"/>	<input type="radio"/>
Right shoulder	<input checked="" type="radio"/>	<input type="radio"/>	<input type="radio"/>	<input type="radio"/>	<input type="radio"/>
Left shoulder	<input checked="" type="radio"/>	<input type="radio"/>	<input type="radio"/>	<input type="radio"/>	<input type="radio"/>
Right upper arm	<input checked="" type="radio"/>	<input type="radio"/>	<input type="radio"/>	<input type="radio"/>	<input type="radio"/>
Left upper arm	<input checked="" type="radio"/>	<input type="radio"/>	<input type="radio"/>	<input type="radio"/>	<input type="radio"/>
Right elbow	<input checked="" type="radio"/>	<input type="radio"/>	<input type="radio"/>	<input type="radio"/>	<input type="radio"/>
Left elbow	<input checked="" type="radio"/>	<input type="radio"/>	<input type="radio"/>	<input type="radio"/>	<input type="radio"/>
Right forearm	<input checked="" type="radio"/>	<input type="radio"/>	<input type="radio"/>	<input type="radio"/>	<input type="radio"/>
Left forearm	<input checked="" type="radio"/>	<input type="radio"/>	<input type="radio"/>	<input type="radio"/>	<input type="radio"/>
Right wrist	<input checked="" type="radio"/>	<input type="radio"/>	<input type="radio"/>	<input type="radio"/>	<input type="radio"/>
Left wrist	<input checked="" type="radio"/>	<input type="radio"/>	<input type="radio"/>	<input type="radio"/>	<input type="radio"/>
Right hand	<input checked="" type="radio"/>	<input type="radio"/>	<input type="radio"/>	<input type="radio"/>	<input type="radio"/>
Left hand	<input checked="" type="radio"/>	<input type="radio"/>	<input type="radio"/>	<input type="radio"/>	<input type="radio"/>

On a typical day during the past two weeks have hand and wrist symptoms caused you to have any difficulty doing the activities listed below? Please select the option that best describes your ability to do the activity.

Activity	No difficulty	Mild difficulty	Moderate difficulty	Severe difficulty	Cannot do at all
Writing	<input checked="" type="radio"/>	<input type="radio"/>	<input type="radio"/>	<input type="radio"/>	<input type="radio"/>
Buttoning the clothes	<input checked="" type="radio"/>	<input type="radio"/>	<input type="radio"/>	<input type="radio"/>	<input type="radio"/>
Holding a book while reading	<input checked="" type="radio"/>	<input type="radio"/>	<input type="radio"/>	<input type="radio"/>	<input type="radio"/>
Gripping of a telephone handle	<input checked="" type="radio"/>	<input type="radio"/>	<input type="radio"/>	<input type="radio"/>	<input type="radio"/>
Opening of jars	<input checked="" type="radio"/>	<input type="radio"/>	<input type="radio"/>	<input type="radio"/>	<input type="radio"/>
Household chores	<input checked="" type="radio"/>	<input type="radio"/>	<input type="radio"/>	<input type="radio"/>	<input type="radio"/>
Carrying of grocery bags	<input checked="" type="radio"/>	<input type="radio"/>	<input type="radio"/>	<input type="radio"/>	<input type="radio"/>
Bathing and dressing	<input checked="" type="radio"/>	<input type="radio"/>	<input type="radio"/>	<input type="radio"/>	<input type="radio"/>

If you would like to discuss this questionnaire or collaborate in future studies with us please feel free to leave here your email:

SUBMIT THE QUESTIONNAIRE

© 2007 - enquires: rvardasc@glam.ac.uk

Appendix 5 - Upper limb occupational conditions online questionnaire - Database Schema

The database used to storing the questionnaire data has one table, which has the following format:

```
CREATE TABLE IF NOT EXISTS `trsi` (  
  `dat` datetime NOT NULL default '0000-00-00 00:00:00',  
  `gen` char(1) NOT NULL default '',  
  `age` int(2) NOT NULL default '0',  
  `hgt` int(3) NOT NULL default '0',  
  `wgt` int(3) NOT NULL default '0',  
  `occ` varchar(20) NOT NULL default '',  
  `ocy` int(2) NOT NULL default '0',  
  `keyb` int(2) default NULL,  
  `mou` int(2) default NULL,  
  `cig` int(2) default NULL,  
  `unt` int(2) default NULL,  
  `eml` varchar(35) default NULL,  
  `Q1` char(1) NOT NULL default '',  
  `Q2` char(1) NOT NULL default '',  
  `Q3` char(1) NOT NULL default '',  
  `Q4` char(1) NOT NULL default '',  
  `Q5` char(1) NOT NULL default '',  
  `Q6` char(1) NOT NULL default '',  
  `Q7` char(1) NOT NULL default '',  
  `Q8` char(1) NOT NULL default '',  
  `Q9` char(1) NOT NULL default '',  
  `Q10` char(1) NOT NULL default '',  
  `Q11` char(1) NOT NULL default '',  
  `Q12` char(1) NOT NULL default '',  
  `Q13` char(1) NOT NULL default '',  
  `Q14` char(1) NOT NULL default '',  
  `Q15` char(1) NOT NULL default '',  
  `Q16` char(1) NOT NULL default '',  
  `Q17` char(1) NOT NULL default '',  
  `Q18` char(1) NOT NULL default '',  
  `Q19` char(1) NOT NULL default '',  
  `Q20` char(1) NOT NULL default '',  
  `Q21` char(1) NOT NULL default '',  
  `Q22` char(1) NOT NULL default '',  
  `Q23` char(1) NOT NULL default '',  
  `Q24` char(1) NOT NULL default '',  
  `P1` char(1) NOT NULL default '',  
  `P2` char(1) NOT NULL default '',  
  `P3` char(1) NOT NULL default '',  
  `P4` char(1) NOT NULL default '',  
  `P5` char(1) NOT NULL default ''
```

```
`P6` char(1) NOT NULL default '',
`P7` char(1) NOT NULL default '',
`P8` char(1) NOT NULL default '',
`P9` char(1) NOT NULL default '',
`P10` char(1) NOT NULL default '',
`P11` char(1) NOT NULL default '',
`P12` char(1) NOT NULL default '',
`P13` char(1) NOT NULL default '',
`P14` char(1) NOT NULL default '',
`P15` char(1) NOT NULL default '',
`D1` char(1) NOT NULL default '',
`D2` char(1) NOT NULL default '',
`D3` char(1) NOT NULL default '',
`D4` char(1) NOT NULL default '',
`D5` char(1) NOT NULL default '',
`D6` char(1) NOT NULL default '',
`D7` char(1) NOT NULL default '',
`D8` char(1) NOT NULL default '',
`ip` varchar(15) NOT NULL default '',
`uid` bigint(20) unsigned NOT NULL auto_increment,
PRIMARY KEY (`uid`)
)
```

Database schema

Appendix 6 - Upper limb occupational conditions online questionnaire - Script Code

The online questionnaire consists in two scripting pages, one using simple HTML code to present the questionnaire form, and a PHP for validating it and insert the data on the database.

The HTML code for the implementation of the questionnaire was the following:

```
<!DOCTYPE HTML PUBLIC "-//W3C//DTD HTML 4.01 Transitional//EN"
"http://www.w3.org/TR/html4/loose.dtd">
<HTML>
<HEAD>
<TITLE>RSI Screening Questionnaire</TITLE>
</HEAD>
</BODY>
<FORM name="frm" action="quest.php" method="post">
<TABLE width="70%" align="center" border="0" name="tbp">
<TR><TD align="center">
<IMG src="banner.jpg">
</TD></TR>
<TR><TD align="center">
<B> ALL THE INFORMATION COLLECTED BY THIS QUESTIONNAIRE IS ANONYMOUS AND STRICTLY CONFIDENTIAL AND
WILL JUST BE USED FOR RESEARCH PURPOSES ONLY, AFTER COMPLETION ALL DATA WILL BE DELETED</B>
</TD></TR>
<TR><TD align="center">
<TABLE align="center" border="0" name="tbl">
<TR>
<TD>Gender:</TD>
<TD><input type="radio" name="gender" value="M"> Male<input type="radio" name="gender" value="F">
Female</TD>
</TR>
<TR>
<TD>Age:</TD>
<TD><input type="text" name="age" size="4" maxlength="2"> years</TD>
</TR>
<TR>
<TD>Height:</TD>
<TD><input type="text" name="height" size="4" maxlength="3"> cm (1ft = 30.5 cm)</TD>
</TR>
<TR>
<TD>Weight:</TD>
<TD><input type="text" name="weight" size="4" maxlength="3"> kg (1 stone = 6.35 kg)</TD>
</TR>
<TR>
<TD>Occupation:</TD>
<TD><input type="text" name="occupation" maxlength="20"> for <input type="text" name="otime"
size="4" maxlength="2"> years</TD>
</TR>
<TR>
<TD colspan="2"><HR></TD>
</TR>
<TR>
<TD colspan="2">1. Do you use a keyboard?</TD>
</TR>
<TR>
<TD colspan="2"><input type="radio" name="keyb" value="Y"> Yes, How many hours per week: <input
type="text" name="keybh" size="2" maxlength="2">(average)<input type="radio" name="keyb" value="N">
No</TD>
</TR>
<TR>
<TD colspan="2">&nbsp;</TD>
</TR>
<TR>
<TD colspan="2">2. Do you use a computer mouse?</TD>
</TR>
<TR>
<TD colspan="2"><input type="radio" name="mouse" value="Y"> Yes, How many hours per week: <input
type="text" name="mouseh" size="2" maxlength="2">(average)<input type="radio" name="mouse"
value="N"> No</TD>
</TR>
```

```
<TR>
<TD colspan="2">&nbsp;&nbsp;&nbsp;</TD>
</TR>
<TR>
<TD colspan="2">3. When seated in a workstation do you adopt a correct posture and position?</TD>
</TR>
<TR>
<TD colspan="2"><input type="radio" name="Q3" value="Y"> Yes <input type="radio" name="Q3"
value="N"> No</TD>
</TR>
<TR>
<TD colspan="2">&nbsp;&nbsp;&nbsp;</TD>
</TR>
<TR>
<TD colspan="2">4. When you type, do you use all fingers in a correct way (i.e. Using all fingers)?
</TD>
</TR>
<TR>
<TD colspan="2"><input type="radio" name="Q4" value="Y"> Yes <input type="radio" name="Q4"
value="N"> No</TD>
</TR>
<TR>
<TD colspan="2">&nbsp;&nbsp;&nbsp;</TD>
</TR>
<TR>
<TD colspan="2">5. Are you experiencing any swelling of the muscles and joints of your hands or
arms?</TD>
</TR>
<TR>
<TD colspan="2"><input type="radio" name="Q5" value="Y"> Yes <input type="radio" name="Q5"
value="N"> No</TD>
</TR>
<TR>
<TD colspan="2">&nbsp;&nbsp;&nbsp;</TD>
</TR>
<TR>
<TD colspan="2">6. Are you experiencing any stiffness with the muscles and joints of your hands or
arms?</TD>
</TR>
<TR>
<TD colspan="2"><input type="radio" name="Q6" value="Y"> Yes <input type="radio" name="Q6"
value="N"> No</TD>
</TR>
<TR>
<TD colspan="2">&nbsp;&nbsp;&nbsp;</TD>
</TR>
<TR>
<TD colspan="2">7. Have you ever had any serious neck, arm or hand injury or operation?</TD>
</TR>
<TR>
<TD colspan="2"><input type="radio" name="Q7" value="Y"> Yes <input type="radio" name="Q7"
value="N"> No</TD>
</TR>
<TR>
<TD colspan="2">&nbsp;&nbsp;&nbsp;</TD>
</TR>
<TR>
<TD colspan="2">8. Have you ever had any serious diseases of joints, skin, nerves, heart or blood
vessels?</TD>
</TR>
<TR>
<TD colspan="2"><input type="radio" name="Q8" value="Y"> Yes <input type="radio" name="Q8"
value="N"> No</TD>
</TR>
<TR>
<TD colspan="2">&nbsp;&nbsp;&nbsp;</TD>
</TR>
<TR>
<TD colspan="2">9. Do you have any difficulty with muscles or joints in your hands?</TD>
</TR>
<TR>
<TD colspan="2"><input type="radio" name="Q9" value="Y"> Yes <input type="radio" name="Q9"
value="N"> No</TD>
</TR>
<TR>
<TD colspan="2">&nbsp;&nbsp;&nbsp;</TD>
</TR>
<TR>
<TD colspan="2">10. Do you have any medical history that may affect your hands or arms?</TD>
</TR>
```

```

<TR>
<TD colspan="2"><input type="radio" name="Q10" value="Y"> Yes <input type="radio" name="Q10"
value="N"> No</TD>
</TR>
<TR>
<TD colspan="2">&nbsp;</TD>
</TR>
<TR>
<TD colspan="2">11. Are you on any long-term medication?</TD>
</TR>
<TR>
<TD colspan="2"><input type="radio" name="Q11" value="Y"> Yes <input type="radio" name="Q11"
value="N"> No</TD>
</TR>
<TR>
<TD colspan="2">&nbsp;</TD>
</TR>
<TR>
<TD colspan="2">12. Are you a smoker?</TD>
</TR>
<TR>
<TD colspan="2"><input type="radio" name="Q12" value="Y"> Yes, How many cigarettes per day: <input
type="text" name="cigar" size="2" maxlength="2"><input type="radio" name="Q12" value="N"> No</TD>
</TR>
<TR>
<TD colspan="2">&nbsp;</TD>
</TR>
<TR>
<TD colspan="2">13. Do you drink alcohol?</TD>
</TR>
<TR>
<TD colspan="2"><input type="radio" name="Q13" value="Y"> Yes, How many units (1/2 pint of beer)
per day: <input type="text" name="alc" size="2" maxlength="2"><input type="radio" name="Q13"
value="N"> No</TD>
</TR>
<TR>
<TD colspan="2"><HR></TD>
</TR>
<TR>
<TD colspan="2"><B>The following questions refer to your symptoms for a typical twenty-four-hour
period during the past two weeks (fill one circle to answer each question).</B></TD>
</TR>
<TR>
<TD colspan="2">&nbsp;</TD>
</TR>
<TR>
<TD colspan="2">14. How severe is the hand or wrist pain that you have at night?</TD>
</TR>
<TR>
<TD colspan="2"><input type="radio" name="Q14" value="1">I do not have hand or wrist pain at
night</TD>
</TR>
<TR>
<TD colspan="2"><input type="radio" name="Q14" value="2">Mild pain</TD>
</TR>
<TR>
<TD colspan="2"><input type="radio" name="Q14" value="3">Moderate pain</TD>
</TR>
<TR>
<TD colspan="2"><input type="radio" name="Q14" value="4">Severe pain</TD>
</TR>
<TR>
<TD colspan="2"><input type="radio" name="Q14" value="5">Very severe pain</TD>
</TR>
<TR>
<TD colspan="2">&nbsp;</TD>
</TR>
<TR>
<TD colspan="2">15. How often did hand or wrist pain wake you up during a typical night in the past
two weeks?</TD>
</TR>
<TR>
<TD colspan="2"><input type="radio" name="Q15" value="1">Never</TD>
</TR>
<TR>
<TD colspan="2"><input type="radio" name="Q15" value="2">Once</TD>
</TR>
<TR>
<TD colspan="2"><input type="radio" name="Q15" value="3">Two ot three times</TD>
</TR>

```

```
<TR>
<TD colspan="2"><input type="radio" name="Q15" value="4">Four or five times</TD>
</TR>
<TR>
<TD colspan="2"><input type="radio" name="Q15" value="5">More than five times</TD>
</TR>
<TR>
<TD colspan="2">&nbsp;</TD>
</TR>
<TR>
<TD colspan="2">16. Do you typically have pain in your hand or wrist during the daytime?</TD>
</TR>
<TR>
<TD colspan="2"><input type="radio" name="Q16" value="1">I never have pain during the day</TD>
</TR>
<TR>
<TD colspan="2"><input type="radio" name="Q16" value="2">I have mild pain during the day</TD>
</TR>
<TR>
<TD colspan="2"><input type="radio" name="Q16" value="3">I have moderate pain during the day</TD>
</TR>
<TR>
<TD colspan="2"><input type="radio" name="Q16" value="4">I have severe pain during the day</TD>
</TR>
<TR>
<TD colspan="2"><input type="radio" name="Q16" value="5">I have very severe pain during the
day</TD>
</TR>
<TR>
<TD colspan="2">&nbsp;</TD>
</TR>
<TR>
<TD colspan="2">17. How often do you have hand or wrist pain during the daytime?</TD>
</TR>
<TR>
<TD colspan="2"><input type="radio" name="Q17" value="1">Never</TD>
</TR>
<TR>
<TD colspan="2"><input type="radio" name="Q17" value="2">Once or twice a day</TD>
</TR>
<TR>
<TD colspan="2"><input type="radio" name="Q17" value="3">Three to five times a day</TD>
</TR>
<TR>
<TD colspan="2"><input type="radio" name="Q17" value="4">More than five times a day</TD>
</TR>
<TR>
<TD colspan="2"><input type="radio" name="Q17" value="5">The pain is constant</TD>
</TR>
<TR>
<TD colspan="2">&nbsp;</TD>
</TR>
<TR>
<TD colspan="2">18. How long, on average, does an episode of pain last during the daytime?</TD>
</TR>
<TR>
<TD colspan="2"><input type="radio" name="Q18" value="1">I never get pain during the day</TD>
</TR>
<TR>
<TD colspan="2"><input type="radio" name="Q18" value="2">Less than 10 minutes</TD>
</TR>
<TR>
<TD colspan="2"><input type="radio" name="Q18" value="3">10 to 60 minutes</TD>
</TR>
<TR>
<TD colspan="2"><input type="radio" name="Q18" value="4">Greater than 60 minutes</TD>
</TR>
<TR>
<TD colspan="2"><input type="radio" name="Q18" value="5">The pain is constant throughout the
day</TD>
</TR>
<TR>
<TD colspan="2">&nbsp;</TD>
</TR>
<TR>
<TD colspan="2">19. Do you have numbness (loss of sensation) in your hand?</TD>
</TR>
<TR>
<TD colspan="2"><input type="radio" name="Q19" value="1">No</TD>
</TR>
<TR>
```



```
<TD colspan="2"><input type="radio" name="Q19" value="2">I have mild numbness</TD>
</TR>
<TR>
<TD colspan="2"><input type="radio" name="Q19" value="3">I have moderate numbness</TD>
</TR>
<TR>
<TD colspan="2"><input type="radio" name="Q19" value="4">I have severe numbness</TD>
</TR>
<TR>
<TD colspan="2"><input type="radio" name="Q19" value="5">I have very severe numbness</TD>
</TR>
<TR>
<TD colspan="2">&nbsp;</TD>
</TR>
<TR>
<TD colspan="2">20. Do you have weakness in your hand or wrist?</TD>
</TR>
<TR>
<TD colspan="2"><input type="radio" name="Q20" value="1">No weakness</TD>
</TR>
<TR>
<TD colspan="2"><input type="radio" name="Q20" value="2">Mild weakness</TD>
</TR>
<TR>
<TD colspan="2"><input type="radio" name="Q20" value="3">Moderate weakness</TD>
</TR>
<TR>
<TD colspan="2"><input type="radio" name="Q20" value="4">Severe weakness</TD>
</TR>
<TR>
<TD colspan="2"><input type="radio" name="Q20" value="5">Very severe weakness</TD>
</TR>
<TR>
<TD colspan="2">&nbsp;</TD>
</TR>
<TR>
<TD colspan="2">21. Do you have tingling sensations in your hand?</TD>
</TR>
<TR>
<TD colspan="2"><input type="radio" name="Q21" value="1">No tingling</TD>
</TR>
<TR>
<TD colspan="2"><input type="radio" name="Q21" value="2">Mild tingling</TD>
</TR>
<TR>
<TD colspan="2"><input type="radio" name="Q21" value="3">Moderate tingling</TD>
</TR>
<TR>
<TD colspan="2"><input type="radio" name="Q21" value="4">Severe tingling</TD>
</TR>
<TR>
<TD colspan="2"><input type="radio" name="Q21" value="5">Very severe tingling</TD>
</TR>
<TR>
<TD colspan="2">&nbsp;</TD>
</TR>
<TR>
<TD colspan="2">22. How severe is numbness (loss of sensation) or tingling at night?</TD>
</TR>
<TR>
<TD colspan="2"><input type="radio" name="Q22" value="1">I have no numbness or tingling at
night</TD>
</TR>
<TR>
<TD colspan="2"><input type="radio" name="Q22" value="2">Mild</TD>
</TR>
<TR>
<TD colspan="2"><input type="radio" name="Q22" value="3">Moderate</TD>
</TR>
<TR>
<TD colspan="2"><input type="radio" name="Q22" value="4">Severe</TD>
</TR>
<TR>
<TD colspan="2"><input type="radio" name="Q22" value="5">Very severe</TD>
</TR>
<TR>
<TD colspan="2">&nbsp;</TD>
</TR>
<TR>
<TD colspan="2">23. How often did hand numbness or tingling wake you up during a typical night
```

```

during the past two weeks?</TD>
</TR>
<TR>
<TD colspan="2"><input type="radio" name="Q23" value="1">Never</TD>
</TR>
<TR>
<TD colspan="2"><input type="radio" name="Q23" value="2">Once</TD>
</TR>
<TR>
<TD colspan="2"><input type="radio" name="Q23" value="3">Two ot three times</TD>
</TR>
<TR>
<TD colspan="2"><input type="radio" name="Q23" value="4">Four or five times</TD>
</TR>
<TR>
<TD colspan="2"><input type="radio" name="Q23" value="5">More than five times</TD>
</TR>
<TR>
<TD colspan="2">&nbsp;</TD>
</TR>
<TR>
<TD colspan="2">24. Do you have difficulty with the grasping and use of small objects such as keys
or pens?</TD>
</TR>
<TR>
<TD colspan="2"><input type="radio" name="Q24" value="1">No difficulty</TD>
</TR>
<TR>
<TD colspan="2"><input type="radio" name="Q24" value="2">Mild difficulty</TD>
</TR>
<TR>
<TD colspan="2"><input type="radio" name="Q24" value="3">Moderate difficulty</TD>
</TR>
<TR>
<TD colspan="2"><input type="radio" name="Q24" value="4">Severe difficulty</TD>
</TR>
<TR>
<TD colspan="2"><input type="radio" name="Q24" value="5">Very severe difficulty</TD>
</TR>
<TR>
<TD colspan="2"><HR></TD>
</TR>
<TR>
<TD colspan="2"><B>Please grade the pain symptoms on the parts of the upper body where you feel
pain when performing your usual tasks.</B></TD>
</TR>
<TR>
<TD colspan="2">&nbsp;</TD>
</TR>
<TR>
<TD colspan="2">
<TABLE align="center" border="1" name="tblub">
<TR>
<TH>&nbsp;</TH>
<TH align="center">No pain</TH>
<TH align="center">Mild Pain</TH>
<TH align="center">Moderate Pain</TH>
<TH align="center">Severe Pain</TH>
<TH align="center">Very Severe Pain</TH>
</TR>
<TR>
<TD align="center">Neck</TD>
<TD align="center"><input type="radio" name="P1" value="1" CHECKED></TD>
<TD align="center"><input type="radio" name="P1" value="2"></TD>
<TD align="center"><input type="radio" name="P1" value="3"></TD>
<TD align="center"><input type="radio" name="P1" value="4"></TD>
<TD align="center"><input type="radio" name="P1" value="5"></TD>
</TR>
<TR>
<TD align="center">Upper back</TD>
<TD align="center"><input type="radio" name="P2" value="1" CHECKED></TD>
<TD align="center"><input type="radio" name="P2" value="2"></TD>
<TD align="center"><input type="radio" name="P2" value="3"></TD>
<TD align="center"><input type="radio" name="P2" value="4"></TD>
<TD align="center"><input type="radio" name="P2" value="5"></TD>
</TR>
<TR>
<TD align="center">Lower back</TD>
<TD align="center"><input type="radio" name="P3" value="1" CHECKED></TD>
<TD align="center"><input type="radio" name="P3" value="2"></TD>

```

<input name="P3" type="radio" value="3"/>	<input name="P3" type="radio" value="4"/>	<input name="P3" type="radio" value="5"/>
Right shoulder		
<input checked="" name="P4" type="radio" value="1"/>	<input name="P4" type="radio" value="2"/>	<input name="P4" type="radio" value="3"/>
<input name="P4" type="radio" value="4"/>	<input name="P4" type="radio" value="5"/>	
Left shoulder		
<input checked="" name="P5" type="radio" value="1"/>	<input name="P5" type="radio" value="2"/>	<input name="P5" type="radio" value="3"/>
<input name="P5" type="radio" value="4"/>	<input name="P5" type="radio" value="5"/>	
Right upper arm		
<input checked="" name="P6" type="radio" value="1"/>	<input name="P6" type="radio" value="2"/>	<input name="P6" type="radio" value="3"/>
<input name="P6" type="radio" value="4"/>	<input name="P6" type="radio" value="5"/>	
Left upper arm		
<input checked="" name="P7" type="radio" value="1"/>	<input name="P7" type="radio" value="2"/>	<input name="P7" type="radio" value="3"/>
<input name="P7" type="radio" value="4"/>	<input name="P7" type="radio" value="5"/>	
Right elbow		
<input checked="" name="P8" type="radio" value="1"/>	<input name="P8" type="radio" value="2"/>	<input name="P8" type="radio" value="3"/>
<input name="P8" type="radio" value="4"/>	<input name="P8" type="radio" value="5"/>	
Left elbow		
<input checked="" name="P9" type="radio" value="1"/>	<input name="P9" type="radio" value="2"/>	<input name="P9" type="radio" value="3"/>
<input name="P9" type="radio" value="4"/>	<input name="P9" type="radio" value="5"/>	
Right forearm		
<input checked="" name="P10" type="radio" value="1"/>	<input name="P10" type="radio" value="2"/>	<input name="P10" type="radio" value="3"/>
<input name="P10" type="radio" value="4"/>	<input name="P10" type="radio" value="5"/>	
Left forearm		
<input checked="" name="P11" type="radio" value="1"/>	<input name="P11" type="radio" value="2"/>	<input name="P11" type="radio" value="3"/>
<input name="P11" type="radio" value="4"/>	<input name="P11" type="radio" value="5"/>	
Right wrist		
<input checked="" name="P12" type="radio" value="1"/>	<input name="P12" type="radio" value="2"/>	<input name="P12" type="radio" value="3"/>
<input name="P12" type="radio" value="4"/>	<input name="P12" type="radio" value="5"/>	
Left wrist		
<input checked="" name="P13" type="radio" value="1"/>	<input name="P13" type="radio" value="2"/>	

```

<TD align="center"><input type="radio" name="P13" value="3"></TD>
<TD align="center"><input type="radio" name="P13" value="4"></TD>
<TD align="center"><input type="radio" name="P13" value="5"></TD>
</TR>
<TR>
<TD align="center">Right hand</TD>
<TD align="center"><input type="radio" name="P14" value="1" CHECKED></TD>
<TD align="center"><input type="radio" name="P14" value="2"></TD>
<TD align="center"><input type="radio" name="P14" value="3"></TD>
<TD align="center"><input type="radio" name="P14" value="4"></TD>
<TD align="center"><input type="radio" name="P14" value="5"></TD>
</TR>
<TR>
<TD align="center">Left hand</TD>
<TD align="center"><input type="radio" name="P15" value="1" CHECKED></TD>
<TD align="center"><input type="radio" name="P15" value="2"></TD>
<TD align="center"><input type="radio" name="P15" value="3"></TD>
<TD align="center"><input type="radio" name="P15" value="4"></TD>
<TD align="center"><input type="radio" name="P15" value="5"></TD>
</TR>
</TABLE>
</TD>
</TR>
<TR>
<TD colspan="2"><HR></TD>
</TR>
<TR>
<TD colspan="2"><B>On a typical day during the past two weeks have hand and wrist symptoms caused you to have any difficulty doing the activities listed below? Please select the option that best describes your ability to do the activity.</B></TD>
</TR>
<TR>
<TD colspan="2">&nbsp;</TD>
</TR>
<TR>
<TD colspan="2">
<TABLE align="center" border="1" name="tblub">
<TR>
<TH align="center">Activity</TH>
<TH align="center">No difficulty</TH>
<TH align="center">Mild difficulty</TH>
<TH align="center">Moderate difficulty</TH>
<TH align="center">Severe difficulty</TH>
<TH align="center">Cannot do at all</TH>
</TR>
<TR>
<TD align="center">Writing</TD>
<TD align="center"><input type="radio" name="D1" value="1" CHECKED></TD>
<TD align="center"><input type="radio" name="D1" value="2"></TD>
<TD align="center"><input type="radio" name="D1" value="3"></TD>
<TD align="center"><input type="radio" name="D1" value="4"></TD>
<TD align="center"><input type="radio" name="D1" value="5"></TD>
</TR>
<TR>
<TD align="center">Buttoning the clothes</TD>
<TD align="center"><input type="radio" name="D2" value="1" CHECKED></TD>
<TD align="center"><input type="radio" name="D2" value="2"></TD>
<TD align="center"><input type="radio" name="D2" value="3"></TD>
<TD align="center"><input type="radio" name="D2" value="4"></TD>
<TD align="center"><input type="radio" name="D2" value="5"></TD>
</TR>
<TR>
<TD align="center">Holding a book while reading</TD>
<TD align="center"><input type="radio" name="D3" value="1" CHECKED></TD>
<TD align="center"><input type="radio" name="D3" value="2"></TD>
<TD align="center"><input type="radio" name="D3" value="3"></TD>
<TD align="center"><input type="radio" name="D3" value="4"></TD>
<TD align="center"><input type="radio" name="D3" value="5"></TD>
</TR>
<TR>
<TD align="center">Gripping of a telephone handle</TD>
<TD align="center"><input type="radio" name="D4" value="1" CHECKED></TD>
<TD align="center"><input type="radio" name="D4" value="2"></TD>
<TD align="center"><input type="radio" name="D4" value="3"></TD>
<TD align="center"><input type="radio" name="D4" value="4"></TD>
<TD align="center"><input type="radio" name="D4" value="5"></TD>
</TR>
<TR>
<TD align="center">Oppening of jars</TD>
<TD align="center"><input type="radio" name="D5" value="1" CHECKED></TD>

```

```

<TD align="center"><input type="radio" name="D5" value="2"></TD>
<TD align="center"><input type="radio" name="D5" value="3"></TD>
<TD align="center"><input type="radio" name="D5" value="4"></TD>
<TD align="center"><input type="radio" name="D5" value="5"></TD>
</TR>
<TR>
<TD align="center">Household chores</TD>
<TD align="center"><input type="radio" name="D6" value="1" CHECKED></TD>
<TD align="center"><input type="radio" name="D6" value="2"></TD>
<TD align="center"><input type="radio" name="D6" value="3"></TD>
<TD align="center"><input type="radio" name="D6" value="4"></TD>
<TD align="center"><input type="radio" name="D6" value="5"></TD>
</TR>
<TR>
<TD align="center">Carrying of grocery bags</TD>
<TD align="center"><input type="radio" name="D7" value="1" CHECKED></TD>
<TD align="center"><input type="radio" name="D7" value="2"></TD>
<TD align="center"><input type="radio" name="D7" value="3"></TD>
<TD align="center"><input type="radio" name="D7" value="4"></TD>
<TD align="center"><input type="radio" name="D7" value="5"></TD>
</TR>
<TR>
<TD align="center">Bathing and dressing</TD>
<TD align="center"><input type="radio" name="D8" value="1" CHECKED></TD>
<TD align="center"><input type="radio" name="D8" value="2"></TD>
<TD align="center"><input type="radio" name="D8" value="3"></TD>
<TD align="center"><input type="radio" name="D8" value="4"></TD>
<TD align="center"><input type="radio" name="D8" value="5"></TD>
</TR>
</TABLE>
</TD>
</TR>
<TR>
<TD colspan="2"><HR></TD>
</TR>
<TR>
<TD colspan="2">If you would like to discuss this questionnaire or collaborate in future studies
with us please feel free to leave here your email: </B>
<input type="text" name="email" size="40" maxlength="40">
</TD>
</TR>
<TR>
<TD colspan="2"><HR></TD>
</TR>
<TR>
<TD align="center" colspan="2"><INPUT type="submit" value="SUBMIT THE QUESTIONNAIRE"
name="sques"></TD>
</TR>
<TR>
<TD colspan="2"><HR></TD>
</TR>
</TABLE>
</TD></TR>
<TR><TD align="center">
<IMG src="bottom.jpg" align="center">
</TD></TR>
</TABLE>
</FORM>
</BODY>
</HTML>

```

HTML code of the questionnaire

The PHP script used to validate the online questionnaire form and store the information in the database was the following:

```

<?php
$gen = $_POST["gender"];
$age = $_POST["age"];
$hgt = $_POST["height"];
$wgt = $_POST["weight"];
$occ = $_POST["occupation"];
$ocy = $_POST["otime"];
$Q1 = $_POST["keyb"];
$keyb = $_POST["keybh"];
$Q2 = $_POST["mouse"];

```

```

$mou = $_POST["mouseh"];
$Q3 = $_POST["Q3"];
$Q4 = $_POST["Q4"];
$Q5 = $_POST["Q5"];
$Q6 = $_POST["Q6"];
$Q7 = $_POST["Q7"];
$Q8 = $_POST["Q8"];
$Q9 = $_POST["Q9"];
$Q10 = $_POST["Q10"];
$Q11 = $_POST["Q11"];
$Q12 = $_POST["Q12"];
$cig = $_POST["cigar"];
$Q13 = $_POST["Q13"];
$unt = $_POST["alc"];
$Q14 = $_POST["Q14"];
$Q15 = $_POST["Q15"];
$Q16 = $_POST["Q16"];
$Q17 = $_POST["Q17"];
$Q18 = $_POST["Q18"];
$Q19 = $_POST["Q19"];
$Q20 = $_POST["Q20"];
$Q21 = $_POST["Q21"];
$Q22 = $_POST["Q22"];
$Q23 = $_POST["Q23"];
$Q24 = $_POST["Q24"];
$P1 = $_POST["P1"];
$P2 = $_POST["P2"];
$P3 = $_POST["P3"];
$P4 = $_POST["P4"];
$P5 = $_POST["P5"];
$P6 = $_POST["P6"];
$P7 = $_POST["P7"];
$P8 = $_POST["P8"];
$P9 = $_POST["P9"];
$P10 = $_POST["P10"];
$P11 = $_POST["P11"];
$P12 = $_POST["P12"];
$P13 = $_POST["P13"];
$P14 = $_POST["P14"];
$P15 = $_POST["P15"];
$D1 = $_POST["D1"];
$D2 = $_POST["D2"];
$D3 = $_POST["D3"];
$D4 = $_POST["D4"];
$D5 = $_POST["D5"];
$D6 = $_POST["D6"];
$D7 = $_POST["D7"];
$D8 = $_POST["D8"];
$eml = $_POST["email"];

$ip = $_SERVER['REMOTE_ADDR'];

$go = true;

function check_email_address($email) {
    // First, we check that there's one @ symbol, and that the lengths are right
    if (!ereg("^[^@]{1,64}@[^@]{1,255}$", $email)) {
        // Email invalid because wrong number of characters in one section, or wrong
number of @ symbols.
        return false;
    }
    // Split it into sections to make life easier
    $email_array = explode("@", $email);
    $local_array = explode(".", $email_array[0]);
    for ($i = 0; $i < sizeof($local_array); $i++) {
        if (!ereg("^[A-Za-z0-9!#$%&'*/=?^_`{|}~\-[A-Za-z0-9!#$%&'*/=?^_`{|}~\.-]{0,63})|(\\"[^\\"\\"]){0,62}\\")$", $local_array[$i])) {
            return false;
        }
    }
    if (!ereg("^[?][0-9\.\+]\?$", $email_array[1])) { // Check if domain is IP. If not,
it should be valid domain name
        $domain_array = explode(".", $email_array[1]);
        if (sizeof($domain_array) < 2) {
            return false; // Not enough parts to domain
        }
        for ($i = 0; $i < sizeof($domain_array); $i++) {
            if (!ereg("^[A-Za-z0-9][A-Za-z0-9-]{0,61}[A-Za-z0-9]|([A-Za-z0-9-]{0,63})$", $domain_array[$i])) {
                return false;
            }
        }
    }
}

```

```

    }
    }
    }
    return true;
}
}
?>
<HTML>
<HEAD>
<TITLE>RSI Screening Questionnaire</TITLE>
</HEAD>
</BODY>
<TABLE align="center" border="0" name="tbp">
<TR><TD align="center">
<IMG src="banner.jpg">
</TD></TR>
<TR><TD>
<FONT color="red">
<?php
    if (strlen($gen)==0){
        print "Error - gender required!<br>";
        $go = false;
    }

    if (strlen($age)==0){
        print "Error - age required!<br>";
        $go = false;
    } else {
        if($age<16 || $age>75){
            print "Error - please correct your age!<br>";
            $go = false;
        }
    }

    if (strlen($hgt)==0){
        print "Error - height required!<br>";
        $go = false;
    } else
        if($hgt<145 || $hgt>215){
            print "Error - please correct your height, it should be in centimeters!<br>";
            $go = false;
        }

    if (strlen($wgt)==0){
        print "Error - weight required!<br>";
        $go = false;
    } else
        if($wgt<40 || $wgt>150){
            print "Error - please correct your weight, it should be in kilos!<br>";
            $go = false;
        }

    if (strlen($occ)!=0){
        if (strlen($ocy)==0){
            print "Error - years on occupation required!<br>";
            $go = false;
        }
    } else
        if (strlen($ocy)!=0){
            print "Error - occupation required!<br>";
            $go = false;
        }

    if (strlen($Q1)==0){
        print "Error - answer to question 1 is required!<br>";
        $go = false;
    } else
        if ($Q1=='Y'){
            if (strlen($keyb)==0){
                print "Error - hours spent on keyboard per week required!<br>";
                $go = false;
            } else {
                if ($keyb<0 || $keyb>72){
                    print "Error - invalid number of hours spent on keyboard per
week!<br>";
                    $go = false;
                }
            }
        }
}
}

```

```

if ($Q1=='N')
    $keyb='0';

if (strlen($Q2)==0){
    print "Error - answer to question 2 is required!<br>";
    $go = false;
} else
    if ($Q2=='Y'){
        if (strlen($mou)==0){
            print "Error - hours spent on computer mouse per week required!<br>";
            $go = false;
        } else {
            if ($mou<0 || $mou>72){
                print "Error - invalid number of hours spent on computer mouse
per week!<br>";
                $go = false;
            }
        }
    }

if ($Q2=='N')
    $mou='0';

if (strlen($Q3)==0){
    print "Error - answer to question 3 is required!<br>";
    $go = false;
}

if (strlen($Q4)==0){
    print "Error - answer to question 4 is required!<br>";
    $go = false;
}

if (strlen($Q5)==0){
    print "Error - answer to question 5 is required!<br>";
    $go = false;
}

if (strlen($Q6)==0){
    print "Error - answer to question 6 is required!<br>";
    $go = false;
}

if (strlen($Q7)==0){
    print "Error - answer to question 7 is required!<br>";
    $go = false;
}

if (strlen($Q8)==0){
    print "Error - answer to question 8 is required!<br>";
    $go = false;
}

if (strlen($Q9)==0){
    print "Error - answer to question 9 is required!<br>";
    $go = false;
}

if (strlen($Q10)==0){
    print "Error - answer to question 10 is required!<br>";
    $go = false;
}

if (strlen($Q11)==0){
    print "Error - answer to question 11 is required!<br>";
    $go = false;
}

if (strlen($Q12)==0){
    print "Error - answer to question 12 is required!<br>";
    $go = false;
} else
    if ($Q12=='Y'){
        if (strlen($cig)==0){
            print "Error - number of cigarettes per day required!<br>";
            $go = false;
        } else {
            if ($cig<0 || $cig>40){
                print "Error - invalid number of cigarettes per day!<br>";
            }
        }
    }

```



```

        }
    }
}

if ($Q12=='N')
    $cig='0';

if (strlen($Q13)==0) {
    print "Error - answer to question 13 is required!<br>";
    $go = false;
} else
    if ($Q13=='Y'){
        if (strlen($unt)==0){
            print "Error - number of alcohol units (1/2 pint of beer) per day
required!<br>";
            $go = false;
        } else {
            if ($unt<0 || $unt>40){
                print "Error - invalid number of alcohol units (1/2 pint of
beer) per day!<br>";
                $go = false;
            }
        }
    }

if ($Q13=='N')
    $unt='0';

if (strlen($Q14)==0) {
    print "Error - answer to question 14 is required!<br>";
    $go = false;
}

if (strlen($Q15)==0) {
    print "Error - answer to question 15 is required!<br>";
    $go = false;
}

if (strlen($Q16)==0) {
    print "Error - answer to question 16 is required!<br>";
    $go = false;
}

if (strlen($Q17)==0) {
    print "Error - answer to question 17 is required!<br>";
    $go = false;
}

if (strlen($Q18)==0) {
    print "Error - answer to question 18 is required!<br>";
    $go = false;
}

if (strlen($Q19)==0) {
    print "Error - answer to question 19 is required!<br>";
    $go = false;
}

if (strlen($Q20)==0) {
    print "Error - answer to question 20 is required!<br>";
    $go = false;
}

if (strlen($Q21)==0) {
    print "Error - answer to question 21 is required!<br>";
    $go = false;
}

if (strlen($Q22)==0) {
    print "Error - answer to question 22 is required!<br>";
    $go = false;
}

if (strlen($Q23)==0) {
    print "Error - answer to question 23 is required!<br>";
    $go = false;
}

if (strlen($Q24)==0) {

```

```

        print "Error - answer to question 24 is required!<br>";
        $go = false;
    }

    if (strlen($P1)==0) {
        print "Error - required grading for neck pain!<br>";
        $go = false;
    }

    if (strlen($P2)==0) {
        print "Error - required grading for upper back pain!<br>";
        $go = false;
    }

    if (strlen($P3)==0) {
        print "Error - required grading for lower back pain!<br>";
        $go = false;
    }

    if (strlen($P4)==0) {
        print "Error - required grading for right shoulder pain!<br>";
        $go = false;
    }

    if (strlen($P5)==0) {
        print "Error - required grading for left shoulder pain!<br>";
        $go = false;
    }

    if (strlen($P6)==0) {
        print "Error - required grading for right upper arm pain!<br>";
        $go = false;
    }

    if (strlen($P7)==0) {
        print "Error - required grading for left upper arm pain!<br>";
        $go = false;
    }

    if (strlen($P8)==0) {
        print "Error - required grading for right elbow pain!<br>";
        $go = false;
    }

    if (strlen($P9)==0) {
        print "Error - required grading for left elbow pain!<br>";
        $go = false;
    }

    if (strlen($P10)==0) {
        print "Error - required grading for right forearm pain!<br>";
        $go = false;
    }

    if (strlen($P11)==0) {
        print "Error - required grading for left forearm pain!<br>";
        $go = false;
    }

    if (strlen($P12)==0) {
        print "Error - required grading for right wrist pain!<br>";
        $go = false;
    }

    if (strlen($P13)==0) {
        print "Error - required grading for left wrist pain!<br>";
        $go = false;
    }

    if (strlen($P14)==0) {
        print "Error - required grading for right hand pain!<br>";
        $go = false;
    }

    if (strlen($P15)==0) {
        print "Error - required grading for left hand pain!<br>";
        $go = false;
    }

    if (strlen($D1)==0) {

```

```

        print "Error - required grading for difficulty on writing!<br>";
        $go = false;
    }

    if (strlen($D2)==0){
        print "Error - required grading for difficulty on buttoning the clothes!<br>";
        $go = false;
    }

    if (strlen($D3)==0){
        print "Error - required grading for difficulty on holding a book while reading!<br>";
        $go = false;
    }

    if (strlen($D4)==0){
        print "Error - required grading for difficulty on gripping of a telephone handle!
<br>";
        $go = false;
    }

    if (strlen($D5)==0){
        print "Error - required grading for difficulty on oppening of jars!<br>";
        $go = false;
    }

    if (strlen($D6)==0){
        print "Error - required grading for difficulty on household chores!<br>";
        $go = false;
    }

    if (strlen($D7)==0){
        print "Error - required grading for difficulty on carrying of grocery bags!<br>";
        $go = false;
    }

    if (strlen($D8)==0){
        print "Error - required grading for difficulty on bathing and dressing!<br>";
        $go = false;
    }

    if (strlen($eml) != 0){
        if (!check_email_address($eml))
        {
            print "Error - bad email address!<br>";
            $go = false;
        }
    }

    if($go==true){
        $dat = date('YmdHis',time());

        $link = @mysql_connect('db2.awardspace.com', 'medimaging_rsi', 'phdglam');
        if (!$link) {
            die('Could not connect: ' . mysql_error());
        }

        $db_selected = mysql_select_db('medimaging_rsi', $link);
        if (!$db_selected) {
            die ('Can\'t use the database table : ' . mysql_error());
        }

        $data = mysql_query("SELECT dat FROM trsi WHERE ip='$ip' ORDER BY dat DESC") or
die(mysql_error());

        $info = mysql_fetch_array( $data );

        if (strlen($info['dat'])!=0)
            $diff = (strtotime($dat) - strtotime($info['dat'])) % 60;
        else
            $diff = 30;

        if ($diff > 20)
        {
            // Formulate Query
            // This is the best way to perform a SQL query
            // For more examples, see mysql_real_escape_string()
            $query = sprintf("INSERT INTO `trsi`
('dat`,`gen`,`age`,`hgt`,`wgt`,`occ`,`ocy`,`keyb`,`mou`,`cig`,`unt`,`eml`,`Q1`,`Q2`,`Q3`,`Q4`,`Q5`,`
Q6`,`Q7`,`Q8`,`Q9`,`Q10`,`Q11`,`Q12`,`Q13`,`Q14`,`Q15`,`Q16`,`Q17`,`Q18`,`Q19`,`Q20`,`Q21`,`Q22`,`
Q23`,`Q24`,`P1`,`P2`,`P3`,`P4`,`P5`,`P6`,`P7`,`P8`,`P9`,`P10`,`P11`,`P12`,`P13`,`P14`,`P15`,`D1`,`D

```



```

        print "<BR><BR><BR><BR><BR></FORM></TD></TR></FONT>";
    //}
    } else
        print '<BR><BR><P align="center">You have already submmited your
questionnaire!</P><BR>';
    } else {
        print '<BR><A href="javascript:history.go(-1)" title="Return to the form and
correct the errors"> Go Back and correct errors</A>';
    }
?>

</FONT>
</TD></TR>
<TR><TD align="center">
<IMG src="bottom.jpg" align="center">
</TD></TR>
</TABLE>
</BODY>
</HTML>

```

PHP script for checking questionnaire answers and insert them on the database

Appendix 7 - Occupational conditions incidence questionnaire results

A total of 218 subjects had responded to the questionnaire, which is around 1% of the academic population of the University of Glamorgan. According to the gender 103 were males and 115 females (fig. 1).

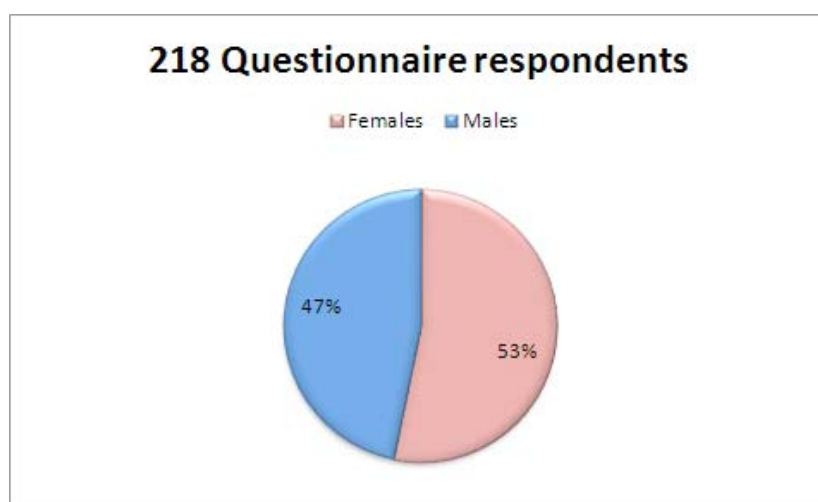


Fig. 1: Total respondents per gender.

Observing the age distribution of the respondents, the majority in both genders were in the age group of 18 to 30 years old (fig. 2).

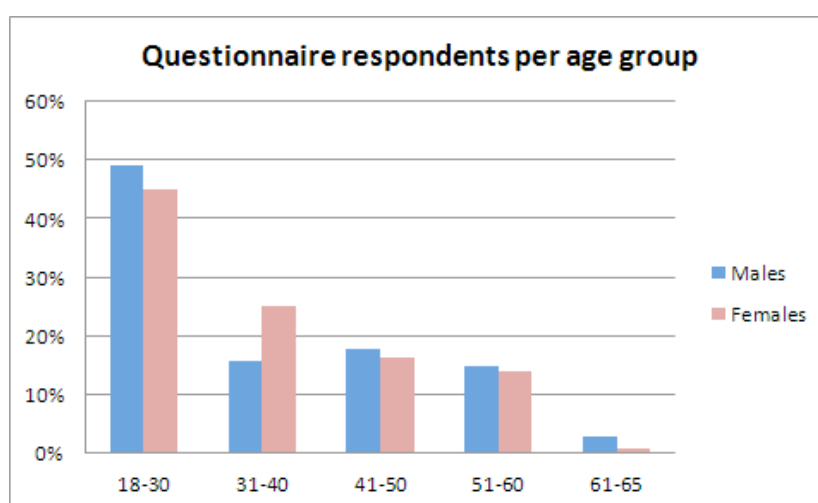


Fig. 2: Age group distribution of the questionnaire respondents per gender.

The fig. 3. shows the Body Mass Index class distribution of the questionnaire respondents per gender. The majority of the respondents of both genders were in the BMI classes normal weight ($18.5 \leq \text{BMI} < 25$) and overweight ($25 \leq \text{BMI} < 30$).

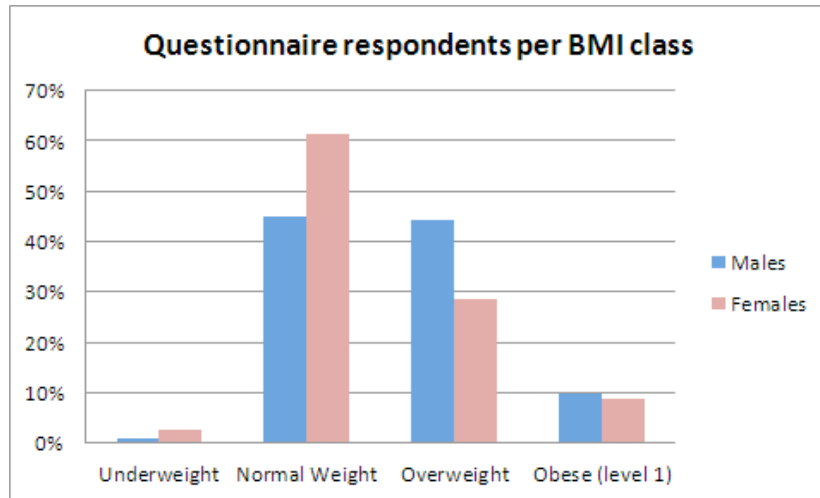


Fig. 3: The Body Mass Index class distribution of the questionnaire respondents per gender.

The respondents of the questionnaire were asked to select as occupation: Administrative/Clerical, Lecturer, Student with occupation and Student. The majority of the male respondents were students, the female respondents were mainly administratives, lecturers and students (fig. 4).

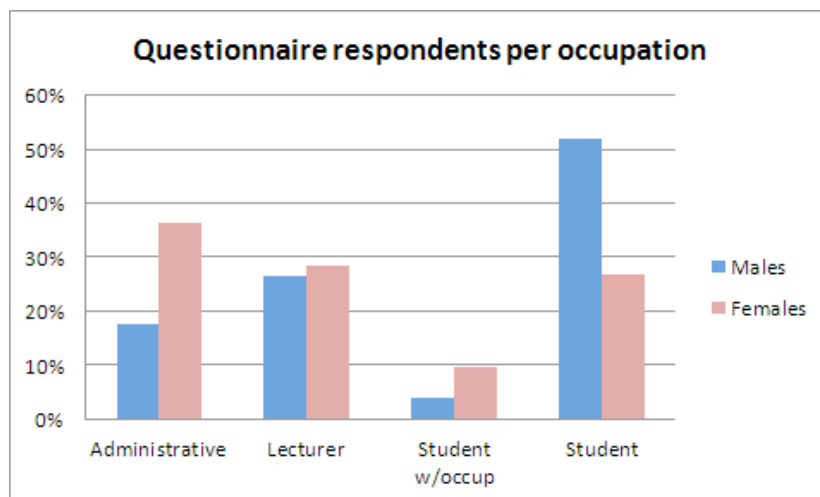


Fig. 4: Occupational distribution of the questionnaire respondents per gender.

The fig. 5 shows the smoking habits of the questionnaire respondents per gender, the majority of both genders respondents are non-smokers.

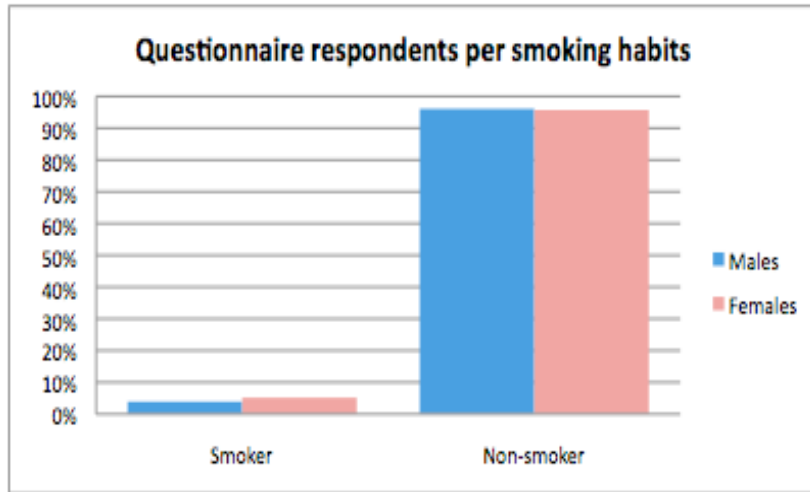


Fig. 5: The smoking habits of the questionnaire respondents per gender.

Observing the alcohol habits of the questionnaire respondents per gender, the number of alcohol consumers is greater in males than females, however is just a difference of 8% (fig. 6).

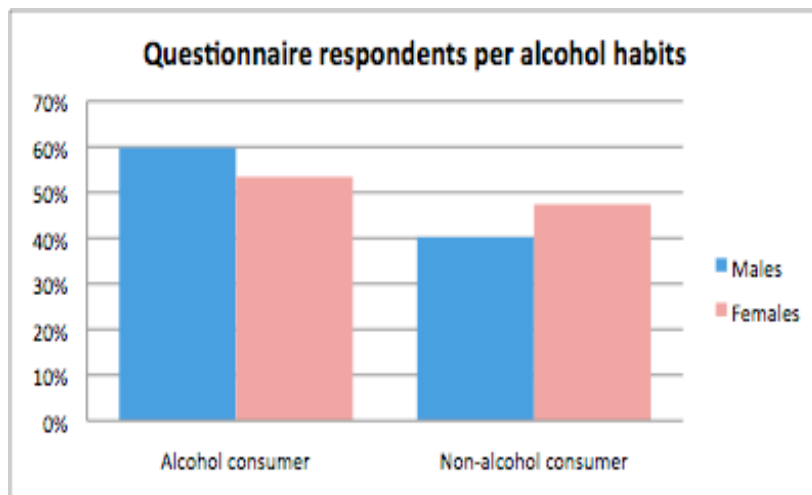


Fig. 6: The alcohol habits of the questionnaire respondents per gender.

The fig. 7 shows the average keyboard exposure time in hours per week of the questionnaire respondents per gender, the majority of both genders spend and average between 20 and 40 hours per week operating a computer keyboard.

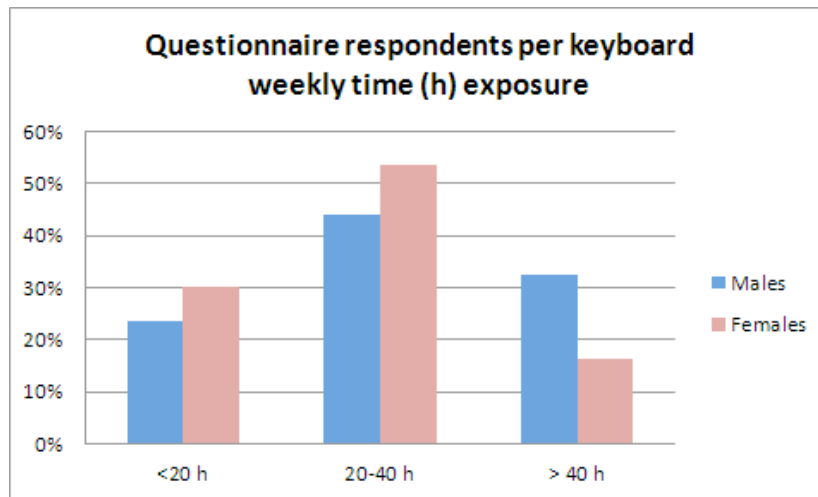


Fig. 7: Exposure average time per week operating a computer keyboard of the questionnaire respondents per gender.

Observing the average mouse exposure time in hours per week of the questionnaire respondents per gender, the majority of both genders spend and average between 20 and 40 hours per week operating a computer mouse.

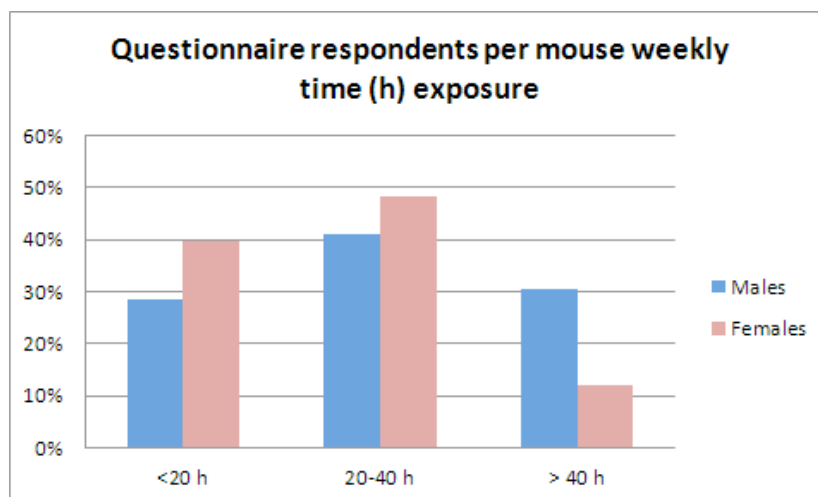


Fig. 8: Exposure average time per week operating a computer mouse of the questionnaire respondents per gender.

From the assessment of the reported conditions answers in the sample population, 36% claim to be free of hand syndromes, 31% argue to have early signs of hand syndromes, 20% reveal signs of hand syndromes and 13% indicated having severe symptoms of hand conditions (fig. 9).

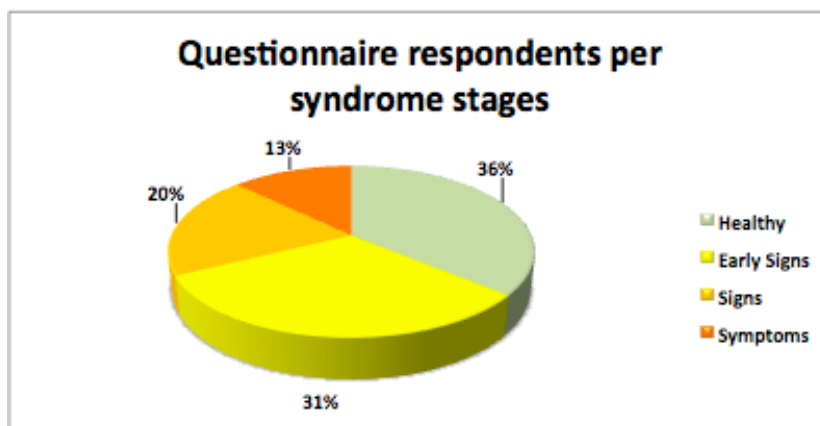


Fig. 9: Distribution of the questionnaire respondents per hand condition stage.

In fig. 10 is possible to observe that women are more affected than men by hand occupational conditions.

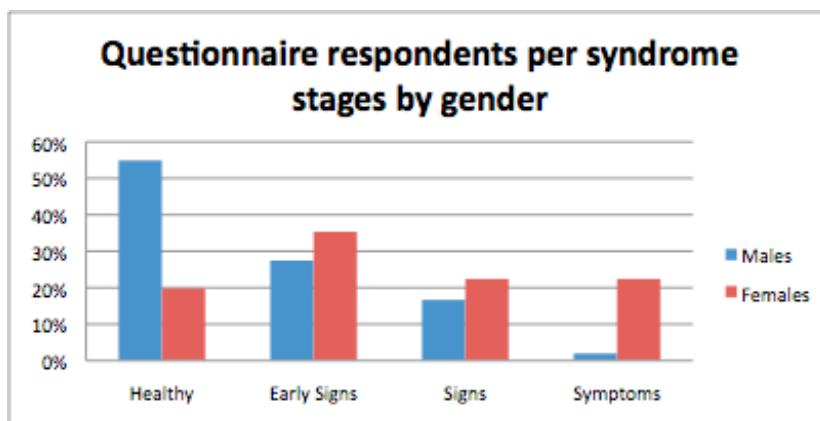


Fig. 10: Distribution of the questionnaire respondents per gender and hand condition stage.

Observing the distribution in age groups of the questionnaire respondents per gender that indicated severe symptoms of hand occupational conditions (fig. 11), the women were more affected in ages between 31 and 40 years old (between 51 and 65 years old were not considered as demonstrative value because of the small sample) and men in ages superior than 60 years old.

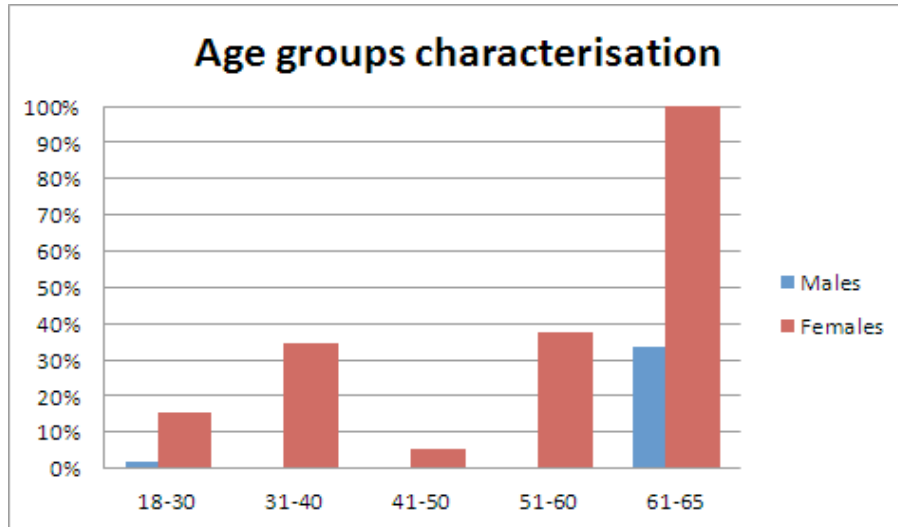


Fig. 11: Age group distribution of the questionnaire respondents per gender that indicated severe symptoms of hand occupational conditions.

In fig. 12 is shown the distribution in BMI classes of the questionnaire respondents per gender that indicated severe symptoms of hand occupational conditions, the women in the normal weight and overweight classes were more affected (BMI classes underweight and obese were not considered as demonstrative value because of the small sample) and men in the overweight class.

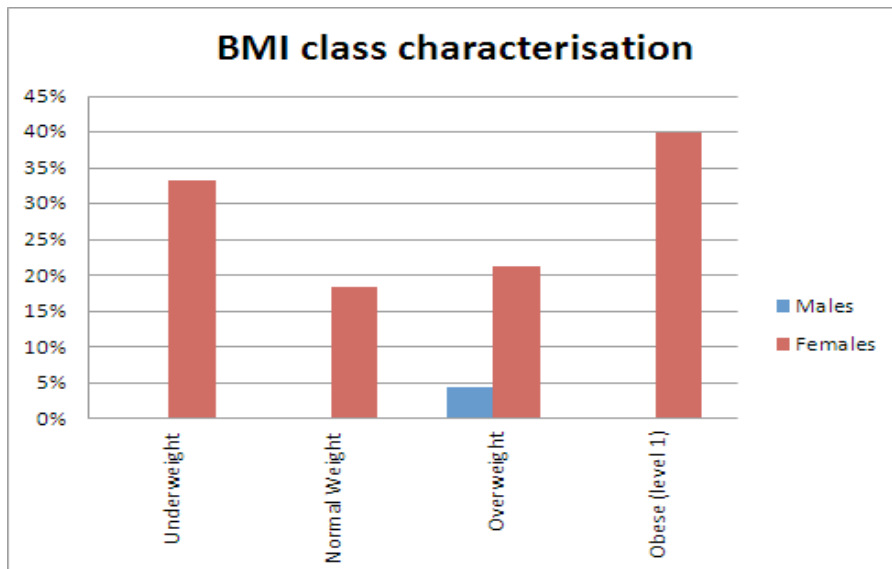


Fig. 12: BMI classes distribution of the questionnaire respondents per gender that indicated severe symptoms of hand occupational conditions.

Observing the distribution in occupations of the questionnaire respondents per gender that indicated severe symptoms of hand occupational conditions (fig. 13), the women an administrative occupation were more affected and men being students with other occupation.

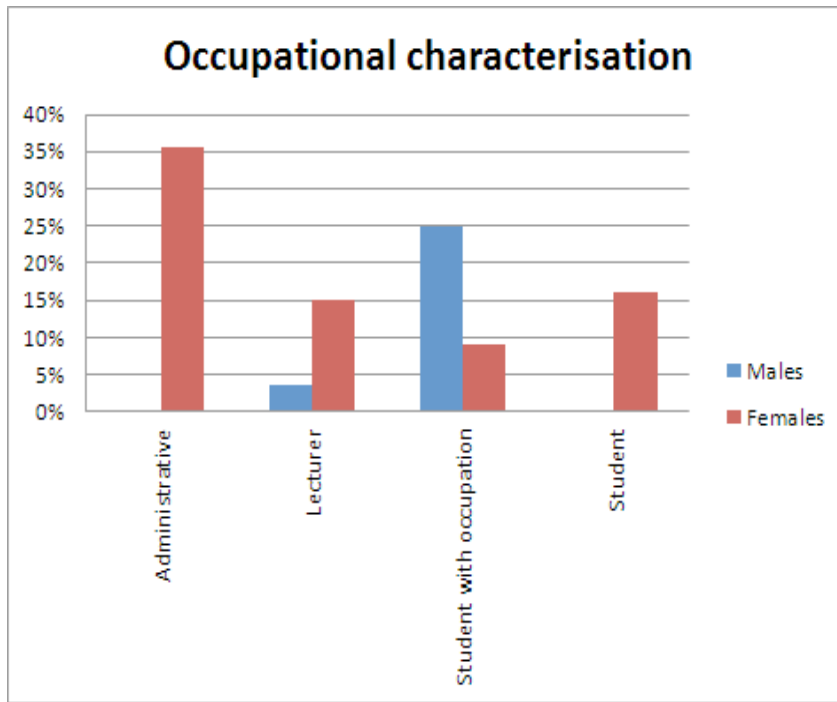


Fig. 13: Occupations distribution of the questionnaire respondents per gender that indicated severe symptoms of hand occupational conditions.

The fig. 14 shows the smoking habits characterisation of the questionnaire respondents per gender that indicated severe symptoms of hand occupational conditions, women that are active smokers are more affected.

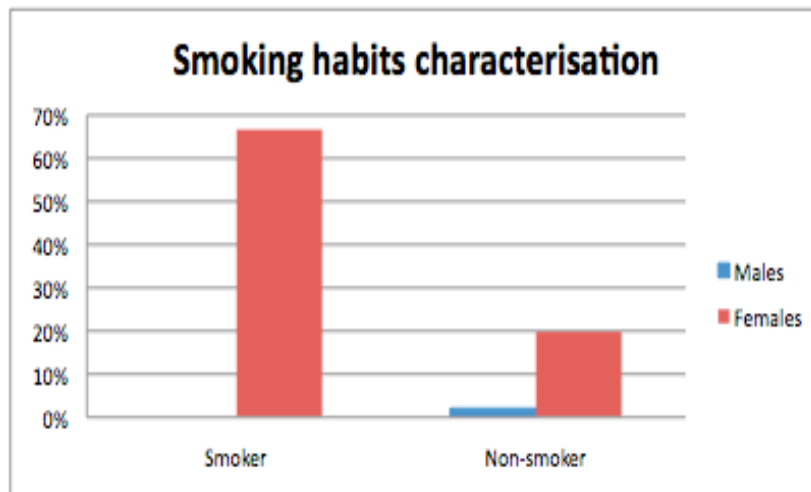


Fig. 14: Smoking habits of the questionnaire respondents per gender that indicated severe symptoms of hand occupational conditions.

Observing the alcohol habits characterisation of the questionnaire respondents per gender that indicated severe symptoms of hand occupational conditions (fig. 15), in women there are no significant difference between consumer and non-consumer, in men the individuals that presented

severe symptoms were alcohol consumers.

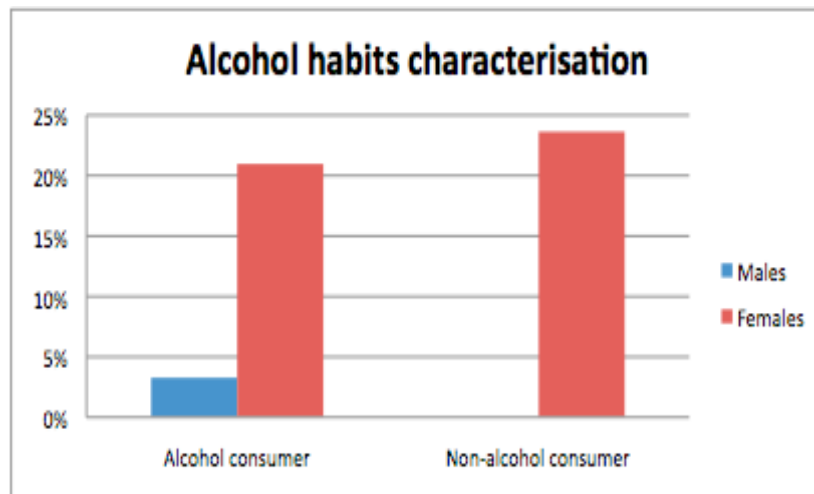


Fig. 15: Alcohol habits of the questionnaire respondents per gender that indicated severe symptoms of hand occupational conditions.

The fig. 16 shows the average keyboard exposure time in hours per week of the questionnaire respondents per gender that indicated severe symptoms of hand occupational conditions, women having more than 40 hours of exposure were more affected.

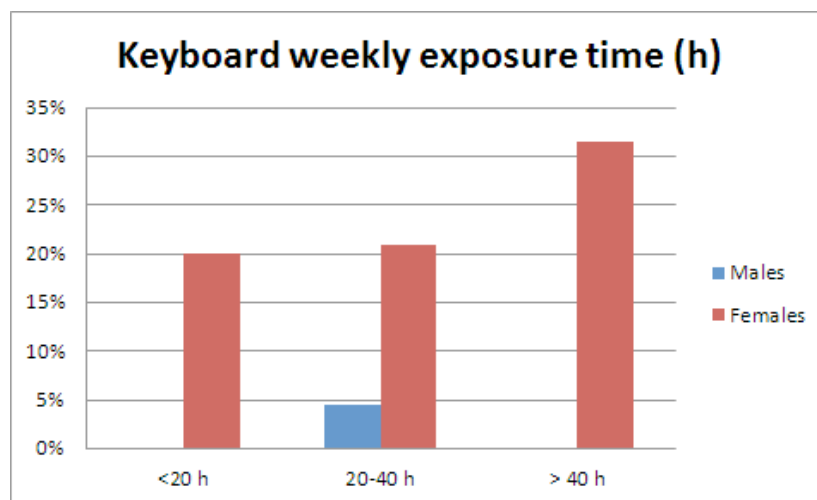


Fig. 16: Exposure average time per week operating a computer keyboard of the questionnaire respondents per gender that indicated severe symptoms of hand occupational conditions.

Observing the average keyboard exposure time in hours per week of the questionnaire respondents per gender that indicated severe symptoms of hand occupational conditions (fig. 17), women having more than 40 hours of exposure were more affected.

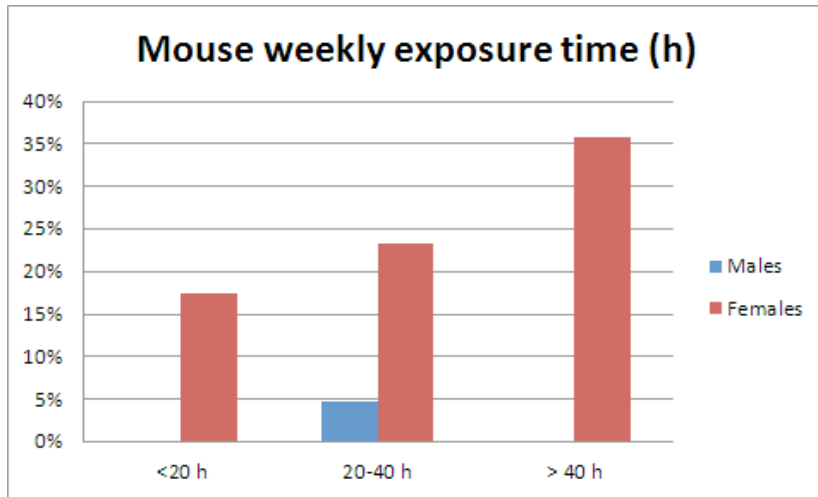


Fig. 17: Exposure average time per week operating a computer mouse of the questionnaire respondents per gender that indicated severe symptoms of hand occupational conditions.



THERMAL PHYSIOLOGY LABORATORY
FACULTY OF ADVANCED TECHNOLOGY
UNIVERSITY OF GLAMORGAN
TREFFOREST, PONTYPRIDD CF37 1DL



CONSENT FORM

Dear Volunteer,

Thank you for agreeing to take part in this study. Your participation is greatly appreciated and the study could not take place without it. The study has obtained ethical approval from the governing body at the University of Glamorgan. We adhere to a strict protocol and therefore require a signed consent form from you. All information gathered will be strictly confidential and only accessed by the researchers responsible for this study. You cannot be recognised by the thermal images and will maintain anonymous..

If you have any queries or would like to discuss any aspect of this study please contact:

- Professor Francis Ring, 01443 483717 (efring@glam.ac.uk), or
- Dr. Peter Plassmann, 01443 483486 (pplassma@glam.ac.uk).

I..... understand that:

1. I will be asked to attend the thermal physiology laboratory to have thermal images taken.
2. I will be required to complete a Euro-QoL form where my body mass index (BMI), age and Euro-QoL score are recorded.
3. I will be required **not** to have eaten a large meal, consumed alcohol, smoked or participated in rigorous activity for two hours prior to thermal imaging.
4. I will be required **not** to apply cosmetics or ointments to the skin and to remove all jewelry and watches prior to thermal imaging.
5. I will be required to rest for twenty minutes prior to thermal imaging in order to obtain thermal equilibrium (allow the body to cool to a pre-set temperature).
6. I will be asked to undress **up to a point I am comfortable with**, in order to achieve clear images.
7. A member of staff from the Medical Imaging Research Group will administer the imaging.
8. I cannot be identified from the image and no personal data (name, d.o.b., etc,) are stored on a computer system.
9. I am free to request the presence of a chaperone throughout the procedure.
10. I am **free to withdraw** from the study at any time

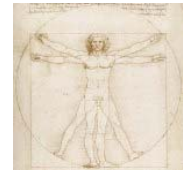
I have read this form and hereby give my consent to participate in this study.

..... Print name Date Signature of volunteer
..... Print name Date Signature of investigator

In the highly unlikely event of any irregularity being detected in the pictures, do you wish us to inform you of this ? Yes / No (*delete as appropriate*)



**MEDICAL IMAGING RESEARCH UNIT
DEPARTMENT OF COMPUTING AND MATHEMATICAL SCIENCES
FACULTY OF ADVANCED TECHNOLOGY
UNIVERSITY OF GLAMORGAN**



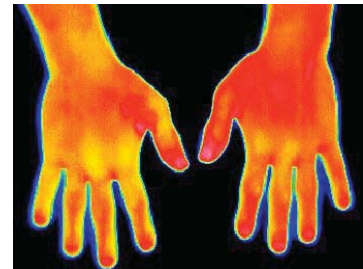
INFORMATION FOR VOLUNTEERS

WHY IS THIS STUDY BEING CARRIED OUT?

This study is the first project to compile relevant reference data for an objective scale of severity of Repetitive Strain Injury (RSI) and Hand Arm Vibration Syndrome (HAVS) in order to aid the diagnosis procedure.

WHAT IS A THERMOGRAM?

A thermogram is a picture of skin temperature, like the one shown on the right. It is made by scanning the natural heat loss from the body surface. It is a harmless, non-invasive procedure and pictures are taken in the same way as conventional photography. Pictures will be used for medical and educational purposes and you cannot be identified from the picture. All information will be stored securely, treated as strictly confidential and full anonymity will be maintained. It is not possible to identify an individual in a thermogram.



WHAT IS RSI?

RSI is an occupational syndrome that causes a loose group of often painful conditions resulting from overuse of a tool or other activity that requires repeated movements. It is a syndrome that affects muscles, tendons and nerves in the hands, arms and upper back. It occurs when muscles in these areas are kept tense for very long periods of time, due to poor posture and/or repetitive motions.

WHAT IS HAVS?

HAVS is a disorder resulting from prolonged exposure to vibration, specifically to the hands and forearms while using vibrating tools. Symptoms include numbness, tingling, and loss of nerve sensitivity. It is a painful and potentially disabling condition of the fingers, hands and arms due to vibration. The fingers become white and swollen when cold and red and pain full when warm up again. Cold weather may aggravate the condition. Picking up small objects becomes difficult as the feeling in the fingers diminishes and there is a loss of strength and grip in the hands. The pain, tingling and numbness in the hands, wrists and arms may interfere with sleep.

WHAT DO I HAVE TO DO?

We ask you to participate in a simple and straightforward process that involves two visits and several pictures being taken of the dorsal hands. The study involves two procedures:

1. A FEW DAYS BEFOREHAND – BEING CLERKED

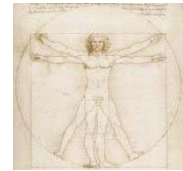
- (a) Filling out a consent form and a simple Euro-QoL questionnaire. Before volunteering, please check this form on our web site (www.MedImaging.org/Projects/IR/Atlas/EuroQol.htm or visit us in J150) to make sure that your score on the form is zero (i.e. you have no problems with mobility, self-care, pain, etc). We will explain to you what a score other than zero means, but will have to exclude you from participating in this study.
- (b) Having your body mass index (BMI) recorded. This is a simple index figure calculated by dividing your weight twice by your height and is used to put you into a group of other volunteers with a similar index.
- (c) Filling out the RSI and HAVS screening questionnaires for pre-staging of the condition in case of complaints of symptoms.

2. ON THE DAY – HAVING THE PICTURES TAKEN

- (d) Not eating a heavy meal, participating in rigorous activity or consuming alcohol or hot drinks or smoking 2 hours prior to the pictures being taken.
- (e) Wearing minimal clothing in order to obtain clear thermograms.
- (f) Removing all jewellery and watches prior to the pictures being taken.
- (g) Refraining from applying cosmetics and ointments to the skin prior to the pictures being taken.
- (h) Resting in a cooled room, minimally dressed for 15 minutes to allow the body to reach the required



**MEDICAL IMAGING RESEARCH UNIT
DEPARTMENT OF COMPUTING AND MATHEMATICAL SCIENCES
FACULTY OF ADVANCED TECHNOLOGY
UNIVERSITY OF GLAMORGAN**



INFORMATION FOR VOLUNTEERS

temperature.

- (i) Taking a series of thermal "photographs" to capture the temperature of the dorsal hands according to the following described procedure:
- 1 before the mechanical stress provocation test;
 - 1 immediately after the mechanical stress provocation test;
 - A series of 1 per minute during 10 minutes after the vascular stress test;

WHAT ARE THE PROVOCATION TESTS?

There are two mechanical stress provocation tests, the keyboard stress test that consists in 5 minutes typing keys shown randomly on a monitor, and secondly the vibrating stress test where a vibrating device is held for 2 minutes with the fingertips of both hands. Each test is conducted on a different day; they can not be performed one after the other because it affects the thermal equilibrium of the hand for a long period of time. These tests are harmless and conform to EU legislation on health and safety. The vascular stress provocation test is a simple and standardised hands cold stress test where the hands (wearing fine rubber gloves) will be immersed for a minute in a bucket filled with water (at 20°C).

HOW LONG WILL IT TAKE?

The process (including resting time) takes approximately 40 minutes per visit. Appointments can be made at your convenience.

WILL I RECEIVE PAYMENT?

Unfortunately funding is limited and you will not be paid. However, you will be contributing to a unique and exciting scientific development and coffee and chocolate cake will be served afterwards! You are also encouraged to ask for some printouts (also available as electronic images per e-mail) A full set of images can be provided on request.

CONTACT:

Ricardo Vardasca, Room J150, Taf Building, University of Glamorgan
01443 48 3601 / rvardasc@glam.ac.uk



**MEDICAL IMAGING RESEARCH UNIT
UNIVERSITY OF GLAMORGAN
FACULTY OF ADVANCED TECHNOLOGY
DEPARTMENT OF COMPUTING AND MATHEMATICAL SCIENCES**



EURO-QOL ASSESSMENT SHEET

Body weight **Age**

Body height

Body mass index

Injuries or surgery within the last 6 months **yes** **no**

Medicaments

Please tick the appropriate field

MOBILITY	
I have no problems in walking about	
I have some problems in walking about	
I am confined to bed	
SELF-CARE	
I have no problems with self-care	
I have some problems washing or dressing myself	
I am unable to wash or dress myself	
USUAL ACTIVITIES (e.g. Work, study, housework family or leisure activities)	
I have no problems with performing my usual activities	
I have some problems with performing my usual activities	
I am unable to perform my usual activities	
PAIN / DISCOMFORT	
I have no pain or discomfort	
I have moderate pain or discomfort	
I have extreme pain or discomfort	
ANXIETY / DEPRESSION	
I am not anxious or depressed	
I am moderate anxious or depressed	
I am extremely anxious or depressed	

Note that this sheet is anonymous. Its sole purpose is to establish volunteers' BMI and to make sure that volunteers satisfy the inclusion criteria for the study (i.e. be subjectively in perfect health, had no injuries/surgery within the last 6 months, take no medication)



Repetitive Strain Injury Screening Questionnaire

(Standard Questionnaire by London Hazards Centre)¹

About you

Name: _____

Do you suffer from swellings, numbness, tingling, pins and needles, stiffness, aches or pain in any of the following parts of your body? (Tick appropriate boxes)

	Swelling	Numbness	Tingling	Stiffness	Aches	Pain
Back						
Neck						
Shoulders						
Arms						
Wrists						
Fingers						
Legs						
Other						

1. Have you visited your doctor about any of these complaints? _____
2. If yes, what diagnosis or treatment did the doctor suggest?

Diagnosis

Treatment

About your job

1. Do you have any of the following types of movement in your job?

Types of movement	Y	N
Repetitive movements of the arms and shoulders		
Repetitive movements of the feet and legs		
Frequent use of awkward wrist positions or bending the wrists		
A twisting, clothes-wringing motion to the hands and wrists		
Keeping parts of you body in a fixed position, with your muscles tense (e.g. holding your arms above your shoulders; holding your elbows out)		
Repeated stretching or reaching movements		
Repeated squeezing, screwing, pressing or twisting movements		



Repetitive Strain Injury Screening Questionnaire

(Standard Questionnaire by London Hazards Centre)¹

2. Is your workstation well designed for the job you do?

Design	Y	N
Can you sit square to do your job?		
Does your chair have good back support?		
Is your chair easily adjustable?		
Is your bench or desk too high or too low?		
Do you have difficulty in reaching the controls, levels, pedals, etc.?		
Do you have to stretch or reach repeatedly in a particular direction to carry out your work?		

3. Does a line management /work process determine the speed of your work or can you control it? _____

4. Is your output measured/is there a monitoring system in operation? _____

5. What work-rate/piece-rate do you have to achieve? _____

6. How often do you take a rest break? _____

7. Can you think of any obvious and immediate improvements that could be made to your job? _____

8. Have you ever raised any of these problems with your boss/management?

9. Do you take painkillers in order to keep on working? _____

10. Are there any other comments you would like to make?

Date: ___/___/_____

Signature: _____



Hand Arm Vibration Syndrome Screening Questionnaire (Standard Questionnaire by UK HSE and NHS)^{1,2}

Name : _____

Ex or current smoker? **Y/N** Occupation: _____

Have you ever used hand-held vibrating tools, machines or hand-fed processes in your job? Y / N

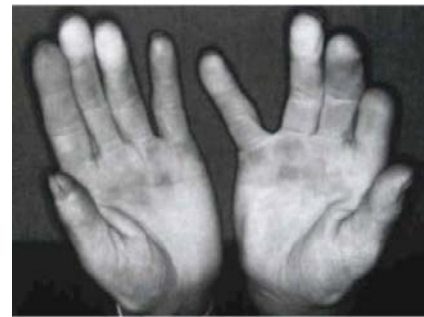
If YES a) list year of first exposure: _____

b) when was the last time you used them? _____
(detail work history later)

1. Do you have any tingling of the fingers lasting more than 20 minutes after using vibrating equipment? **Y / N**
2. Do you have tingling of the fingers at any other time? **Y / N**
3. Do you wake at night with pain, tingling, or numbness in your hand or wrist? **Y / N**
4. Do one or more of your fingers go numb more than 20 minutes after using vibrating equipment? **Y / N**
5. Have your fingers gone white (see photo) * on cold exposure? **Y / N**



*Whiteness means a clear discoloration of the fingers with a sharp edge, usually followed by a red flush.



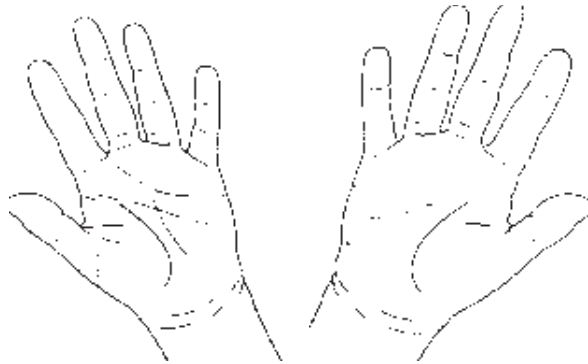


Hand Arm Vibration Syndrome Screening Questionnaire

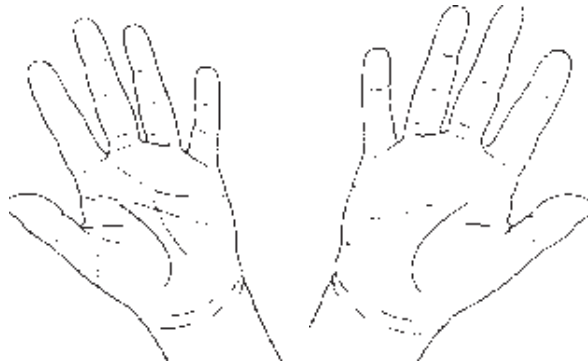
(Standard Questionnaire by UK HSE and NHS)^{1,2}

Mark on the sketch the effected parts.

**a) White colour or
BLANCHING**



**b) TINGLING or
NUMBNESS**



6. If Yes to 5, do you have difficulty re-warming them when leaving the cold? **Y / N**
7. Do your fingers go white at any other time? **Y / N**
8. Are you experiencing any other problems with the muscles or joints of the hands or arms? **Y / N**
9. Do you have difficulty picking up very small objects e.g. screws or buttons or opening tight jars? **Y / N**
10. Have you ever had a neck, arm or hand injury or operation? **Y / N**
If so give details _____
11. Have you ever had any serious diseases of joints, skin, nerves, heart or blood vessels? **Y / N**
If so give details _____
12. Are you on any long-term medication? **Y / N**
If so give details _____

Date: ___/___/_____

Signature: _____

Appendix 13 – The author scientific work: publications and presentations

>Papers Published:

VARDASCA, R., RING, E.F.J., PLASSMANN, P., JONES, C.D., “**Thermal Symmetry on Extremities of Normal Subjects**”, Proceedings of the 1st Research Student Workshop, Faculty of Advanced Technology, University of Glamorgan, March 2007, p14-18.

VARDASCA, R., BAJWA, U., “**Extracting Outlines of Hands from Thermal Images**”, Proceedings of the 2nd Research Student Workshop, Faculty of Advanced Technology, University of Glamorgan, October 2007, p12-16.

VARDASCA, R., “**Template Based Alignment and Interpolation Methods Comparison of Regions of Interest in Thermal Images**”, Proceedings of the 3rd Research Student Workshop, Faculty of Advanced Technology, University of Glamorgan, March 2008, p21-24.

VARDASCA, R., RING, E.F.J., PLASSMANN, P., JONES, C.D., “**Thermal monitoring of hand stress during keyboard typing**”, Proceedings of 9th International conference on Quantitative InfraRed Thermography, July 2-5, 2008, Krakow-Poland, p169-174.

RING, E.F.J., VARDASCA, R., BAJWA, U., “**Monitoring Cooling Agents Applied to the skin of Normal Subjects by Quantitative Thermal Imaging**”, Proceedings of 9th International conference on Quantitative InfraRed Thermography, July 2-5, 2008, Krakow- Poland, p129-134.

VARDASCA, R., BAJWA, U., “**Segmentation and Noise Removal on Thermographic Images of Hands**”, Thermology International, 18/3 (2008), p99-104.

VARDASCA, R., “**Hand Thermogram Standardisation with Barycentric Warp Model**”, Proceedings of the 4th Research Student Workshop, Faculty of Advanced Technology, University of Glamorgan, March 2009, p73-75.

BAJWA, U., VARDASCA, R., RING, E.F.J., PLASSMANN, P., “**Comparison of boundary detection techniques to improve image analysis in medical thermography**”, The Imaging Science Journal, Volume 58, Number 1, February 2010 , p.12-19.

> Abstracts published:

VARDASCA, R., RING, E.F.J., PLASSMANN, P., JONES, C.D., “Thermal Symmetry on Extermities of Normal Subjects”, Thermology International, 2007, 17(2):69

VARDASCA, R., RING, E.F.J., PLASSMANN, P., JONES, C.D., “Thermal Symmetry on Extermities of Healthy Subjects”, Thermology International, 2007, 17(3):114

RING, E.F.J., AMMER, K., PLASSMANN, P., JUNG, A., ZUBER, J., JONES, B., JONES, C.D., WIECEK, B., VARDASCA, R., “Standardisation of Thermal Imaging Systems Used in Medicine”, Thermology International, 2007, 17(3):115

VARDASCA, R., BAJWA, U., “Extracting Outlines of Hands from Thermal Images”, Thermology International, 2007, 17(2):69

VARDASCA, R., RING, E.F.J., PLASSMANN, P., JONES, C.D., "Thermal Symmetry and Temperature Values of Healthy Volunteers on Elbow, Neck, Shoulder and Wrist", Acta Bio- Optica et Informatica Medica, vol.14, nr 1, 2008, p. 16-17

VARDASCA, R., RING, E.F.J., PLASSMANN, P., JONES, C.D., "Thermal Symmetry and Temperature Values of Healthy Volunteers on Elbow, Neck, Shoulder and Wrist", Thermology International, 2008, 18(2):60

VARDASCA, R., BAJWA, U., "Impact of Noise Removal Techniques on Measurement of Medical Thermal Images", Thermology International, 2008, 18(4):153

VARDASCA, R., RING, E.F.J., PLASSMANN, P., JONES, C.D., "Symmetry of temperature distribution in the upper and lower extremities", Acta Bio-Optica et Informatica Medica, vol.15, nr 1, 2009, p. 18

RING, E.F.J., VARDASCA, R., "Thermography and its Clinical Applications: New york 1963", Thermology International, 2009, 19(3): 83

RING, E.F.J., VARDASCA, R., JUNG, A., ZUBER J., RUTKOWSKI, P., BAJWA, U., KALICKI, B., "Detecting Fever in Polish Children by Infrared Thermography", Thermology International, 2009, 19(3): 86

VARDASCA, R., VARDASCA, T., "Automated Comparison of Three Methods for Cold Stress Analysis of Hands", Thermology International, 2009, 19(3): 89

RING, E.F.J., VARDASCA, R., BAJWA, U., "The Effect of Cooling Agents Applied to the Skin in normal Subjects", Thermology International, 2009, 19(3): 93

VARDASCA, R., RING, E.F.J., PLASSMANN, P., JONES, C.D., "Thermal Symmetry of Limbs in Healthy Subjects", Thermology International, 2009, 19(3): 94

VARDASCA, R., "Barycentric Warp Model for Hand Thermal Images Standardisation", Thermology International, 2010, 20(2): 70

VARDASCA, T., VARDASCA, R., "Hand cold stress test methods electronic evaluation and reporting", Thermology International, 2010, 20(2): 70

>Presentations at conferences:

1st Research Students Workshop – University of Glamorgan, Faculty of Advanced Technology – Glamorgan

Business Center, 1st March 2007

- "THERMAL SYMMETRY ON EXTERMITIES OF NORMAL SUBJECTS"

11th National Congress of the Polish Association of Thermology, Zakopane (Poland), 16th – 18th March 2007

- "THERMAL SYMMETRY ON EXTERMITIES OF HEALTHY SUBJECTS"

Workshop Clinical Temperature Measurement & Thermography, Institute of Physics and Engineering in Medicine- Medicenter – Cardiff, 3rd May 2007

- "THERMAL SYMMETRY ON EXTERMITIES OF HEALTHY SUBJECTS"

6th Doctoral Seminar of University of Glamorgan, Glamorgan Business Center, 4th May 2007

- “THERMAL SYMMETRY ON EXTERMITIES OF HEALTHY SUBJECTS”

33rd Annual Meeting of the American Academy of Thermography, Veterinary School – Auburn, Alabama, USA, 7th – 9th June 2007

- “THERMAL SYMMETRY ON EXTERMITIES OF HEALTHY SUBJECTS”

2nd Research Students Workshop – University of Glamorgan, Faculty of Advanced Technology – Glamorgan

Business Center, 1st November 2007

- “EXTRACTING OUTLINES OF HANDS FROM THERMAL IMAGES”

20th Thermological Symposium of the Austrian Society of Thermology, "What is the place for Thermal Imaging in Medicine?", SAS Radisson Hotel, Vienna (Austria), 17 November 2007

- “EXTRACTING OUTLINES OF HANDS FROM THERMAL IMAGES”

Seminar in Thermal Imaging for Medical and Engineering use, Auditorio D1, ESTG – Polytechnic Institute of Leiria, Portugal, 19th December 2007

- “TERMOGRAFIA: UMA FERRAMENTA DE DIAGNÓSTICO E MONITORIZAÇÃO PARA A MEDICINA E ENGENHARIA”

3rd Research Students Workshop – University of Glamorgan, Faculty of Advanced Technology – Glamorgan

Business Center, 6th March 2008

- “TEMPLATE BASED ALIGNMENT AND INTERPOLATION METHODS COMPARISON OF REGIONS OF INTEREST IN THERMAL IMAGES”

12th National Congress of the Polish Association of Thermology, Zakopane(Poland), 28th – 30th March 2008

- “THERMAL SYMMETRY AND TEMPERATURE VALUES OF HEALTHY SUBJECTS IN UPPER JOINTS”
- “INTERPOLATION METHODS COMPARISON IN MEDICAL THERMAL IMAGES”

7th Doctoral and Masters Seminar of University of Glamorgan, Glamorgan Business Center, 15th May 2008

- Paper: “REPETITIVE STRAIN INJURY SCREENING QUESTIONNAIRE AT UNIVERSITY OF GLAMORGAN”

21st Thermological Symposium of the Austrian Society of Thermology, "Recent Advances in Thermology", SAS

Radisson Hotel, Vienna (Austria), 17th November 2008

- “EXTRACTING IMPACT OF NOISE REMOVAL TECHNIQUES ON MEASUREMENT IN MEDICAL THERMAL IMAGES”
- “SYMMETRY OF TEMPERATURE DISTRIBUTION IN THE UPPER AND THE LOWER EXTREMITIES”

Advances in Medical and Forensic Imaging, Royal Photographic Society Conference, The Royal Society, 6, Carlton

House Terrace, London, 23rd February 2009

- “THERMAL IMAGING AS A DIAGNOSTIC AID FOR HAND SYNDROMES”

4th Research Students Workshop – University of Glamorgan, Faculty of Advanced Technology – Glamorgan

Business Center, 12th March 2009

- “HAND THERMOGRAM STANDARDIZATION WITH BARYCENTRIC WARP MODEL”

1st Seminar of Health Informatics, Auditório B1, ESTG – Polytechnic Institute of Leiria, Portugal, 26th May 2009

- “IMAGENS NA MEDICINA”

The 11th European Association of Thermology European Congress of Medical Thermology, 55th Annual Congress of the German Society of Thermography and Regulation Medicine, 22nd Thermological Symposium of the Austrian Society of Thermology, Conference of the German Society of Thermology (DGT), " Temperature Measurement in Humans and Animals.",Wartburg Hotel, Mannheim, Germany, 17th - 20th September 2009

- “Automated Comparison of Three Methods for Cold Stress Analysis of Hands”
- “Thermal Symmetry of Limbs in Healthy Subjects”

4th Research Students Workshop – University of Glamorgan, Faculty of Advanced Technology – Glamorgan Business Center, 12th March 2009

- “HAND THERMOGRAM STANDARDIZATION WITH BARYCENTRIC WARP MODEL”

Seminar on Research in Medical Imaging – Medical Imaging Research Unit, Faculty of Advanced Technology – University of Glamorgan, H144, 23rd February 2010

- “THERMAL IMAGING ASSESSMENTS OF REPETITIVE STRAIN AND VIBRATION INJURY TO THE HANDS”

XI Health School Students meeting, "Primary Health Care", Auditório B1, CAMPUS 2 – Polytechnic Institute of Leiria, Portugal, 12th - 13th March 2010

- “O PASSADO, O PRESENTE E O FUTURO DAS TIC’S NOS CUIDADOS PRIMÁRIOS DE SAÚDE!”

14th National Congress of the Polish Association of Thermology, Zakopane(Poland), 26th – 28th March 2010

- “BARYCENTRIC WARP MODEL FOR HAND THERMAL IMAGES STANDARDISATION”